UCL INSTITUTE OF OPHTHALMOLOGY
LONDON

The Genetic Associations of

Rhegmatogenous Retinal Detachment

and

Ectopia Lentis

Aman Chandra

Institute of Ophthalmology, University College London

Submitted to the University College of London for the Degree of Doctor of Philosophy

February 2014

Supervisors:

Mr David G Charteris

Professor Andrew R Webster

DECLARATION

I, Aman Chandra, confirm that the work presented in this thesis is my own. Where information has been derived from other sources, I confirm that this has been indicated in the thesis.

Aman Chandra

BSc (Hons) MBBS MRCSEd FRCOphth

London, February 2014

ACKNOWLEDGEMENTS

The number of people who have helped me over the period of this work is humbling.

I must firstly thank my supervisors; Mr David Charteris and Professor Andrew Webster for their support throughout this study. They have advised and guided me throughout the many different twists and turns of this work. Along with my supervisors, I am very grateful for the support of the Special Trustees of Moorfields Eye Hospital, Fight for Sight UK and the Royal College of Surgeons of Edinburgh for making this possible.

I was very fortunate to work in numerous units, where many people were involved in supporting me. At St George's, University of London, I must thank Dr Anne Child for allowing me to work in the Sonalee laboratory. Dr Jose Aragon Martin steered me throughout my time there. I was also lucky enough to meet Dr Leon D'Cruz who guided me through the world of protein modelling.

At the MRC Human Genetics Unit in Edinburgh, I was welcomed and instructed by Dr Veronique Vitart and Mirna Kirin, whose work will always amaze me. In London, Dr Valentina Cipriani offered many an hour of patient guidance to me, and I am very grateful for this. I look forward to continuing to work with these statistical masterminds.

Within Moorfields, David Charteris' research team (Margaret and Haydee) not only helped with the study, they also brought smiles to the research oven (room). In this group, I include Phil Banerjee; whose help facilitated many aspects of the thesis, and Danny Mitry; who contributed through the early stages of this study. Both of these gents were particularly valuable sounding boards.

In Professor Andrew Webster's laboratory, I must thank Alice, Eva and Panos for welcoming me, and reassuring me when needed.

I was also very privileged to work with Professor Astrid Limb's "Müllers". I am indebted to the patience of Astrid, Karen, Phillippa and Megan. Many an hour of their time was spent ensuring that I didn't go too far off track. Megan's final help putting this together deserves a special mention.

Towards the end, I had the honour of working with Professor Tony Moore. His attention to detail and phenotyping skills were a privilege to witness.

A special piece of gratitude must go to Dr Gavin Arno. Working with Gavin across two units resulted in him guiding me through a substantial part of this work. I have learned a lot from him, and made a great friend.

My parents instilled in me the thirst for learning, and pushing myself. They must take credit for the result. Janet and Paul must also be thanked for their endless support.

The most important person in all of this is, of course, Liz; my eternal optimism. She has endured my absences, shared my lows, and rejoiced with me in my moments of success. During all of this, she gave us our two boys, Oliver and Henry. They have contributed in their own way to this work; probably more than they will ever know. This really belongs to these three gems in my life and I dedicate it to them.

ABSTRACT

A genetic predisposition to Rhegmatogenous Retinal Detachment (RD) has been suggested for over 40 years. Ectopia Lentis (EL) is known to have a genetic aetiology as part of Marfan Syndrome, other ocular syndromes and when occurring in isolation. This work investigates the genetic aetiology to these conditions in Mendelian and non Mendelian inheritance.

The work in this thesis establishes a clear genotype-phenotype correlation between isolated EL and its most important causative gene: *ADAMTSL4*. This suggests that mutations in this gene result in a more severe phenotype than other genes causing EL. In doing so, a novel clinical grading system for this condition has also been developed. The expression of *ADAMTSL4* and distribution of its protein within ocular tissue has also been investigated and suggests further roles for this protein in ocular development. Modelling of the protein was undertaken and provides insights for future investigations.

Traditional and novel next generation investigative tools have also been employed to examine families with Mendelian inherited phenotypes including RD and EL. The role of a deleted exon in *ADAMTS17* has been identified as playing a role in Weill-Marchesani Like syndrome. A novel ocular phenotype has also been defined in three families demonstrated to be caused by mutations in *ADAMTS18*. This gene has previously been described in few probands with ophthalmic phenotypes, and this work has further delineated the role of this gene. It is becoming clear that members of the ADAMTS family of proteins play a significant role in ocular development.

Finally, over 1300 probands with non-Mendelian RD were recruited and closely phenotyped as part of this work. It has demonstrated novel racial differences in the phenotypes of those affected. This cohort contributed significantly towards the first genome wide association study (GWAS) into RD; and established for the first time the genetic contribution to this condition. Further funding has now been acquired to investigate this cohort further using a novel exome array. Preliminary quality control analysis has been performed; allowing a platform for further detailed analysis to identify putative functional variants associated with RD.

TABLE OF CONTENTS

LIST OF FIGURES

Chapter 1

Chapter 2

Chapter 4

Chapter 5

LIST OF TABLES

ABBREVIATIONS

A:	Adenosine
ABCA4:	ATP-binding cassette, sub-family A (ABC1), member 4
ACTC1:	Actin, alpha cardiac muscle 1
ADAM9:	ADAM metallopeptidase domain 9
ADAMTS:	A Disintegrin And Metalloproteinase with Thrombospondin Motifs
ADAMTSL:	ADAMTS-like
ADVIRC:	Autosomal Dominant Vitreoretinochoriodopathy
AHM:	Anterior hyaloid membrane
AIPL1:	Aryl hydrocarbon receptor interacting protein-like 1
AKAP13:	A-kinase anchor protein 13
AKT3:	V-akt murine thymoma viral oncogene homolog 3
AL:	Axial length
AMD:	Age related macular degeneration
antiVEGF:	Anti Vascular endothelial growth factor
ANTXR2:	Anthrax toxin receptor 2
ANXA9:	Annexin A9
APC:	Adenomatous polyposis coli
ARHGAP22:	Rho GTPase activating protein 22
ARL6:	ADP-ribosylation factor-like 6
ARMS2:	Age related maculopathy 2
ARNT:	Aryl hydrocarbon receptor nuclear translocator
ASD:	Anterior segment dysgenesis
ATOH7:	Atonal homolog 7
AVGR8:	Autogenous Vein Graft Remodelling associated protein 8
B3GALTL:	Beta1, 3-glucosyltransferase
BBS:	Bardet-Biedl syndrome
BCAS3:	Breast carcinoma amplified sequence 3

BCVA:	Best corrected visual acuity
BEST1:	Bestrophin 1
bHLH:	Basic helix–loop–helix
BLAST:	Basic Local Alignment Search Tool
BLID:	BH3-like motif-containing inducer of cell death
BMI:	Body mass index
BMP:	Bone morphogenetic protein
BOSU:	The British Ophthalmic Surveillance Unit
C1QTNF:	C1q and tumor necrosis factor related protein
C2orf71:	Chromosome 2 open reading frame 71
C:	Cytosine
CA4:	Carbonic anhydrase IV
CACNA2D4:	Calcium channel, voltage-dependent, alpha 2/delta subunit 4
CARD10:	Caspase recruitment domain-containing protein 10
CAST:	Cohort allelic sums test
CATT:	Cochran-Armitage Trend Test
CAV:	Caveolin
cbEGF:	Calcium binding Epidermal growth factor
CCDC101:	Coiled-coil domain containing 101
CCT:	Central corneal thickness
CD-CV:	Common Disease – Common Variant
CDH12:	Cadherin-12
CDH23:	Cadherin-related 23
CDHR1:	Cadherin-related family member 1
cDNA:	Complementary Deoxyribose Nucleic acid
CEP290:	Centrosomal protein 290kDa
CERKL:	Ceramide kinase-like
CERS2:	Ceramide Synthase 2

CEU: Ancestry from northern and western Europe (HapMap)

CFH: Complement factor H

CHARMM: Chemistry at HARvard Macromolecular Mechanics

CHEK2: CHK2 checkpoint homolog

CHM: choroideremia

CLRN1: clarin 1

CLU: Clusterin

CMC: Combined Multivariate and Collapsing method

CNGA: cyclic nucleotide gated channel alpha

CNGB: cyclic nucleotide gated channel beta

CNTNAP2: Contactin-associated protein-like 2

CNV: Copy Number Variants

COL11A1: Collagen, type XI, alpha 1

COL11A2: Collagen, type XI, alpha 2

COL18A1: Collagen, type XVIII, alpha 1

COL2A1: Collagen, type II, alpha 1

COL4A4: Collagen, type IV, alpha 4

COL9A1: Collagen, type IX, alpha 1

COL9A2: Collagen, type IX, alpha 2

CRB1: Crumbs homolog 1

CRD: Cysteine rich domain

CREAM: Consortium for Refractive Error and Myopia

CRX: Cone-rod homeobox

CS: Craniosynostosis

CSF: Cerebrospinal fluid

CSPG2: Chondroitin sulfate proteoglycan 2

CT: Computed tomography

CTSK: Cathepsin K

CTSS: Cathepsin S

D: Dislocation

DA: Dislocated anteriorly

dbSNP: Single Nucleotide Polymorphism data base

DCLK1: Doublecortin-like kinase 1

DFNB31: Deafness, autosomal recessive 31

DHDDS: Dehydrodolichyl diphosphate synthase

DLG2: Discs, large homolog 2

DLX1: Distal-less homeobox 1

DM: Diabetes mellitus

DMSO: Dimethyl sulfoxide

DNA: Deoxyribonucleic acid

dNTP: Deoxyribonucleotide triphosphate

DP: Dislocated posteriorly

DR: Diabetic retinopathy

DS: Dioptre Sphere

ECM: Extracellular Matrix

EDTA: Ethylenediaminetetraacetic acid

EFEMP1: EGF containing fibulin-like extracellular matrix protein 1

EFNB: Ephrin-B2

EGF: Epidermal growth factor

EL: Ectopia Lentis

ELetP: Ectopia lentis et Pupillae

ELOVL5: Elongation of long-chain fatty acids family member 5

ENSA: Endosulfine, Alpha

EOG: Electrooculography

EORD: Early onset retina dystrophy

EP: Ectopia Pupillae

ERG:	Electroretinogram
ETDRS:	Early Treatment Diabetic Retinopathy Study
EYS:	Eyes shut homolog
FAM161A:	Family with sequence similarity 161, member A
FBN1:	Fibrillin 1
FCED:	Fuchs corneal endothelial dystrophy
FDM:	Form Deprivation Myopia
FEVR:	Familial Exudative Familial Vitreoretinopathy
FG2:	Denaturation buffer
FG3:	Hydration buffer
FGFR2:	Fibroblast Growth Factor Receptor 2
FOXO1:	Forkhead box O1
FOXC1:	Forkhead box C1
FOXF2:	Forkhead box F2
FRAP1:	FK506 binding protein rapamycin complex-associated protein 1
FSCN2:	Fascin homolog 2, actin-bundling protein, retinal
Fuc:	Fucose
FZD4:	Frizzled family receptor 4
G:	Guanine
GAG:	Glycosaminoglycan
GAPDH:	Glyceraldehyde 3-phosphate dehydrogenase
GAS7:	Growth arrest specific 7
GDF6:	Growth differentiation factor 6
GEL:	Grading in Ectopia Lentis
GJD2:	Gap Junction Protein, Delta-2
GLI3:	GLI-KRUPPEL family zinc finger 3
Glc:	Glucose
GNAT2:	Guanine nucleotide binding protein (G protein), alpha transducing activity polypeptide2

GOLPH3L: Golgi phosphoprotein 3-like

GPR98: G protein-coupled receptor 98

GRAIL: Gene Relationships Among Implicated Loci

GRR: Genotypic relative risk

GRT: Giant retinal tears

GUCA1A: Guanylate cyclase activator 1A

GUCY2D: Guanylate cyclase 2D, membrane

GV: Goldman-Favre

GWAS: Genome Wide Association Studies

HA: Hyaluronan

HAPLN: Hyaluronan and proteoglycan link protein 1

HAS1: Hyaluronan synthase 1

HCCS: Holocytochrome c synthase

HDL: High-density lipoprotein

HES: Hospital Episode Statistic

HGF: Hepatocyte growth factor

HGMD: Human Genome Mutation Database

HLA: Human leukocyte antigen

HORMAD1: HORMA domain-containing 1

HST: Horse shoe tear

HTG: High tension open angle glaucoma

HTRA1: High temperature requirement A1

HWE: Hardy-Weinberg Equilibrium

IBD: Identity by descent

IBS: Identity by state

IDH3B: Isocitrate dehydrogenase 3 (NAD+) beta

IEL: Isolated ectopia lentis

IF: Immunofluorescence

IGV: Integrative Genomic Viewer

IHC: Immunohistochemical

ILM: Inner limiting membrane

IMPDH1: Inosine 5'-monophosphate dehydrogenase 1

IMPG2: Interphotoreceptor matrix proteoglycan 2

IoO: Institute of Ophthalmology

IOP: Intraocular pressure

IPM: Interphotoreceptor matrix

ISCEV: International Society for Clinical Electrophysiology of Vision

IVS: Intervening sequence (intron)

K: Keratometry

kb: Kilobases

KC: Keratoconus

KCNJ13: Potassium inwardly-rectifying channel, subfamily J, member 13

KCNMA1: Potassium large conductance calcium-activated channel, subfamily M, alpha member 1

KCNQ5: Potassium voltage-gated channel, KQT-like subfamily, member 5

KCNV2: Potassium channel, subfamily V, member 2

KLHL7: Kelch-like family member 7

KNO: Knobloch Syndrome

KNO2: Knobloch Syndrome 2

LAMA2: Laminin, alpha 2

LCA5: Leber congenital amaurosis 5

LCPUFA: Long chain polyunsaturated fatty acid synthesis

LCSH: Long continuous stretches of homozygosity

LCT: Lactase

LD: Linkage Disequilibrium

LDB2: LIM domain binding 2

LDS: Loeys–Dietz syndrome

LIM:	Lens induced myopia
LogMAR:	Logarithm of the Minimum Angle of Resolution
LOH:	Loss of heterozygosity
LOXL1:	Lysyl oxidase–like protein 1
LRAT:	Lecithin retinol acyltransferase
LRP5:	Low density lipoprotein receptor-related protein 5
LRRC4C:	Leucine rich repeat containing 4C
LTBP2:	Latent transforming growth factor beta binding protein 2
LUM:	Lumican
LV:	Left ventricular
MAF:	Minor Allele frequency
MAGP-1:	Microfibrillar-associated protein 2
MAP kinase:	Mitogen Activated Protein kinase
MAPT:	Microtubule-associated protein tau
MASS:	Myopia, mitral valve prolapse, borderline aortic root enlargement, skin and skeletal findings
mb:	Megabases
MCL1:	Myeloid cell leukemia sequence 1
MERTK:	C-mer proto-oncogene tyrosine kinase
MET:	Met proto-oncogene
MFN1:	Mitofusin 1
MFRP:	Membrane frizzled-related protein
MFS:	Marfan Syndrome
MIPEP:	Mitochondrial intermediate peptidase
MKKS:	McKusick-Kaufman syndrome
MKS1:	Meckel syndrome, type 1
MMP:	Matrix metalloproteinase
MRC:	Medical Research Council
MRCS:	Microcornea, Rod-cone dystrophy, Cataract, and posterior Staphyloma

MRI:	Magnetic resonance imaging
mRNA:	Messenger Ribonucleic acid
MSX2:	Muscle Segment homeobox, homolog of 2
MYO7A:	Myosin VIIA
MYOC:	Myocilin
MYRIP:	Myosin VIIA and Rab interacting protein
mv:	Microvilli
MVPS:	Mitral valve prolapse syndrome
NAHR:	Non-allelic homologous recombination
nAMD:	Neovascular AMD
NCBI:	National Center for Biotechnology Information
NDP:	Norrie disease
NGS:	Next generation sequencing
NHLBI GO:	National Heart, Lung and Blood Institute Grand Opportunity
NMD:	Nonsense mediated decay
NMR:	Nuclear magnetic resonance
NR2E3:	Nuclear receptor subfamily 2, group E, member 3
NRL:	Neural retina leucine zipper
NSR:	Neurosensory retina
NTG:	Normal tension glaucoma
NUPR1:	Nuclear protein, transcriptional regulator, 1
OAG:	Open-angled glaucoma
OMIM:	Online Mendelian Inheritance in Man
OPTN:	Optineurin
OR:	Odds ratio
ORBIT:	Ocular Biology and Therapeutics
OTX2:	Orthodenticle homeobox 2
PACG:	Primary angle closure glaucoma

PAPLN: Papilin

PAX6: Paired box 6

PBS: Phosphate buffered saline

PCA: Primary component analysis

PCDH15: Protocadherin-related 15

PCR: Polymerise chain reaction

PDA: Patent ductus arteriosus

PDB: Protein Data Bank

PDE6A: Phosphodiesterase 6A, cGMP-specific, rod, alpha

PDE6B: Phosphodiesterase 6B, cGMP-specific, rod, beta

PDE6C: Phosphodiesterase 6C, cGMP-specific, cone, alpha prime

PDE6G: Phosphodiesterase 6G, cGMP-specific, rod, gamma

PDGFRA: Platelet-derived growth factor receptor, alpha

PDR: Proliferative diabetic retinopathy

Phaco: Phacoemulsification

PITPNM3: PITPNM family member 3

PLAC: Protease and Lacunin

PLEKHA7: Pleckstrin homology domain containing, family A member 7

PLXDC2: Plexin domain containing 2

POAG: Primary open angle glaucoma

POR: P450 (cytochrome) oxidoreductase

PPV: Pars plana vitrectomy.

PR: Photoreceptors

PRCD: Progressive rod-cone degeneration

PRDX3: Peroxiredoxin 3 gene

PROM1: Prominin 1

PRPF: Pre-mRNA processing factor

PRPH2: peripherin 2

PRSS56: Protease, serine, 56

PRUNE: Prune exopolyphosphatase

PSARL: Presenilin associated, rhomboid-like

PSMA8: Proteasome (prosome, macropain) subunit, alpha type, 8

PTC: Premature termination codon

PVD: Posterior vitreous detachment

PVR: Proliferative vitreoretinopathy

PXF: Pseudoexfoliation

PXG: Pseudoexfoliation glaucoma

QC: Quality control

QQ-plot: Quantile-Quantile plot

r: Frequency of recombination

RAB23: Member RAS oncogene family

RAB3GAP1: RAB3 GTPase activating protein subunit 1

RASGRF1: Ras protein-specific guanine nucleotide-releasing factor 1

RAX: Retina and anterior neural fold homeobox

RBFOX1: RNA binding protein, fox-1 homolog

RBP3: Retinol binding protein 3, interstitial

RD: Rhegmatogenous Retinal Detachment

RD3: Retinal degeneration 3

RDH: Retinol dehydrogenase

RECQL4: RecQ protein-like 4

RefSeq: Reference Sequence

RFLP: Restriction fragment length polymorphism

RGC: Retinal ganglion cell

RGR: Retinal G protein coupled receptor

RGS9: Regulator of G-protein signaling 9

RHO: Rhodopsin

RIMS1: Regulating synaptic membrane exocytosis 1

RIPA:	Radio immuno precipitation assay
RLBP1:	Retinaldehyde binding protein 1
RNA:	Ribonucleic acid
ROM1:	Retinal outer segment membrane protein 1
RP:	Retinitis Pigmentosa
RP1L1:	Retinitis Pigmentosa 1-like 1
RPE:	Retinal Pigmented Epithelium
RPE65:	Retinal pigment epithelium-specific protein 65kDa
RPGR:	Retinitis Pigmentosa GTPase regulator
RPGRIP1:	Retinitis Pigmentosa GTPase regulator interacting protein 1
rs:	Reference SNP
RS1:	Retinoschisin 1
rtPCR:	Reverse transcription polymerase chain reaction
SAG:	S-antigen; retina and pineal gland
SAP:	Shrimp Alkaline Phosphatase
SCYL1:	SCY1-like 1
SD:	Standard Deviation
SE:	Spherical equivalent
SEM:	Scanning Electron Microscopy
SEMA4A:	Sema domain, immunoglobulin domain (Ig), transmembrane domain (TM) and short cytoplasmic domain, (semaphorin) 4A
SETDB1:	SET domain, bifurcated 1
SFRS15:	SR-related CTD-associated factor 4
SGS:	Sprintzen-Goldberg Syndrome
SHH:	Sonic Hedgehog
SIFT:	Sorting intolerant from tolerant
SIX:	SIX homeobox
SKIV2L:	Superkiller viralicidic activity 2-like
SLC4A11:	Solute carrier family 4, sodium borate transporter, member 11

SMOC1: SPARC related modular calcium binding 1

SNP: Single nucleotide polymorphism

SNRNP200: Small nuclear ribonucleoprotein 200kDa

SNV: Single nucleotide variant

SOCCS: Study Of Colorectal Cancer in Scotland

SOD1: Superoxide dismutase 1, soluble

SOX: SRY (sex determining region Y)-box

SOX2OT: SOX2 overlapping transcript

SPATA7: Spermatogenesis associated 7

SPSS: Statistical Product and Service Solutions

SRBD1: S1 RNA binding domain 1

SS18: Synovial sarcoma translocation, chromosome 18

STL2: Sticklers type 2

STRA6: Stimulated by retinoic acid 6

Sub: Subluxation

SubI: Subluxed Inferiorly

SubIN: Subluxed inferonasally

SubIT: Subluxed inferotemporally

SubN: Subluxed nasally

SubS: Subluxed superiorly

SubSN: Subluxed superonasally

SubST: Subluxed superotemporally

SubT: Subluxed temporally

SULT1A: Sulfotransferase family, cytosolic, 1A, phenol-preferring, member 1

SVD: Snowflake Vitreoretinal Degeneration

T: Thymine

T2D: Type 2 Diabetes

TAF4B: TAF4b RNA polymerase II, TATA box binding protein (TBP)-associated factor

TB: Transforming growth factor binding protein-like

TBS: Tris buffered saline

TCF4: Transcription Factor 4

TEAD1: TEA domain family member 1

TfP: Mitochondrial trifunctional protein

TGF: Transforming growth factor

TGFBR: Transforming growth factor, beta receptor

TIAM1: T-cell lymphoma invasion and metastasis 1

TIMP-3: TIMP metallopeptidase inhibitor 3

Tm: Melting temperature

TMCO1: Transmembrane and coiled-coil domains 1

TOPORS: Topoisomerase I binding, arginine/serine-rich, E3 ubiquitin protein ligase

TRIM: Tripartite Motif-Containing Protein

TSPAN12: Tetraspanin 12

TSR: Thrombospondin type 1 Repeat

TSTA3: Tissue specific transplantation antigen P35B

TTC8: Tetratricopeptide repeat domain 8

TULP1: Tubby like protein 1

TWIST1: Twist basic helix-loop-helix transcription factor 1

U: Uracil

UBC: Ubiquitin C

UCL: University College London

UMD: Universal Mutation Database

UNC119: Unc-119 homolog

USH2A: Usher Syndrome type IIa gene

VCDR: Vertical cup: disc

VEGF: Vascular endothelial growth factor

VMD2: Bestrophin 1

VRE:	Vitreoretinal emergency
VSX2:	Visual system homeobox 2
WDR36:	WD Repeat Domain 36 gene
WML:	Weill-Marchesani-Like syndrome
WMS:	Weill Marchesani syndrome
WT:	Wild type
WTCCC:	Welcome Trust Case Control Consortium
ZBTB38:	Zinc finger and BTB domain containing 38
ZEB1:	Zinc finger E-box binding homeobox 1
ZF:	Zonular filaments
ZIC2:	Zinc finger protein of cerebellum 2
ZMAT4:	Zinc finger, matrin-type 4
ZNF:	Zinc finger protein
ZP4:	Zona pellucida glycoprotein 4

LIST OF PUBLICATIONS ARISING FROM WORK RELATED TO THIS THESIS

1. **Chandra** A, Arno G, Williamson K, Sergionotis PI, Preising MN, Charteris DG, Thompson DA, Holder G, Borman AD, Davangnanam I, Webster AR, Lorenz B, Fitzpatrick DR, Moore AT. Extension of the ocular phenotype features caused by mutations in *ADAMTS18* *JAMA Ophthalmology [In Press]*

2. **Chandra** A, Patel D, Aragon-Martin JA, Pinard A, Collod- Béroud G, Comeglio P, Boileau C, Faivre L, Charteris DG, Child AH, Arno G. The Revised Ghent Nosology; Reclassifying Isolated Ectopia Lentis *Clinical Genetics [In Press]*

3. **Chandra** A, Charteris DG. Molecular pathogenesis and management of ectopia lentis *Eye 2014 Feb; 28(2): 162-8*

4. **Chandra** A, Jones M, Cottrill P, Eastlake K, Limb GA, Charteris DG. The gene expression and protein distribution of ADAMTSL-4 in human iris, choroid and retina *British Journal of Ophthalmology 2013 Sep; 97(9):1208-12*

5. Kirin M., **Chandra** A, Charteris DG, Hayward C, Campbell S, Celap I, Bencic G, Vatavuk Z, Kirac I, Richards AJ, Tenesa A, Snead MP, Fleck BW, Singh J, Harsum S, Maclaren RE, den Hollander AI, Dunlop MG, Hoyng CB, Wright AF, Campbell H, Vitart V, Mitry D. Genome-wide association study identifies genetic risk underlying primary rhegmatogenous retinal detachment *Human Molecular Genetics 2013 Aug; 22(15):3174-85*

6. **Chandra** A, Ekwalla V, Child A, Charteris D. Prevalence of ectopia lentis and retinal detachment in Marfan syndrome *Acta Ophthalmol (Copenh) 2014 Feb; 92(1):e82-3*

7. **Chandra** A, Banerjee PJ, Charteris DG. Grading in ectopia lentis (GEL): a novel classification system *British Journal of Ophthalmology 2013 Jul; 97(7):942-3*

8. **Chandra** A, Aragon-Martin JA, Hughes K, Gati S, Reddy MA, Deshpande C, Cormack G, Child AH, Charteris DG, Arno G. A genotype-phenotype comparison of *ADAMTSL4* and *FBN1* in isolated ectopia lentis *Investigative Ophthalmology & Visual Science 2012 Jul; 53(8):4889-96*

9. **Chandra** A, Aragon-Martin JA, Sharif S, Parulekar M, Child A, Arno G. Craniosynostosis with ectopia lentis and a homozygous 20-base deletion in *ADAMTSL4* *Ophthalmic Genetics 2013 Mar-Jun; 34(1-2):78-82*

10. **Chandra** A, D'Cruz L, Aragon-Martin JA, Charteris DG, Limb GA, Child AH, Arno G. Focus on molecules: ADAMTSL4 *Experimental Eye Research. 2012 Nov; 104:95-6*

UNDER REVIEW AT TIME OF THESIS SUBMISSION:

1. **Chandra** A, Mitry D, Webster AR, Wright A, Campbell H, Charteris DG. Genome wide association studies: Applications and Insights gained in Ophthalmology *Eye*

LIST OF ORAL AND POSTER PRESENTATIONS ARISING FROM WORK RELATED TO THIS THESIS

ORAL PRESENTATIONS:

- The ADAMTS family and the Eye. INVITED SPEAKER. *The 9th International Symposium in Marfan Syndrome and Related Disorders*. Paris: Sep 2014
- Ethnicity in Rhegmatogenous Retinal Detachment: *Royal Australian and New Zealand College of Ophthalmologists Annual Congress*. Tasmania: Nov 2013
- The Lens and the Retina. An undiagnoseable phenotype clarified: *UK Eye Genetics Group 9th Annual Meeting*. London: Jan 2013
- Ectopia Lentis Genetics: *Moorfields / Quinze-Vingts Medical Retina Collaboration meeting*. Paris: Oct 2012
- Genome Wide Genetic Association Study of Primary Retinal Detachment: *International Society for Eye Research (ISER)*. Berlin: July 2012
- A Genotype-Phenotype correlation of ADAMTSL4 and FBN1 in isolated ectopia lentis. *Royal Society of Medicine Ophthalmology section meeting.* London: June 2012
- Research into ectopia lentis. *Marfan Association Patient Day*. London: March 2012
- Update on genetics of ectopia lentis. *British & Eire Association of Vitreo Retinal Surgeons (BEAVRS).* Cantebury: November 2011
- Role of *ADAMTSL4* mutations in isolated ectopia lentis. *Euretina.* London: May 2011
- *ADAMTSL4* mutations in isolated ectopia lentis. *BEAVRS.* Cardiff: November 2011

POSTER PRESENTATIONS:

- Evidence of the role of ADAMTS18 in ocular development. *Association for Research in Vision & Ophthalmology (ARVO).* Seattle: May 2013
- Ocular Manifestation of Marfan Syndrome in UK. *Royal College of Ophthalmologists Annual Congress.* Liverpool. May 2013
- A novel method for Grading Ectopia Lentis (GEL). *American Academy of Ophthalmology Annual Meeting.* Chicago: Nov 2012
- ADAMTS-Like 4 Expression within Human Ocular Tissue. *ARVO.* Ft Lauderdale: 2012
- Novel mutations in *ADAMTSL4* in non consanguineous isolated ectopia lentis. *International Congress of Human Genetics (ICHG).* Montreal: Oct 2011
- Genotype-Phenotype Correlation in *Fibrillin-1* and *ADAMTSL4* Ectopia Lentis. *ARVO.* Fort Lauderdale: May 2011

LIST OF PEER REVIEWED GRANTS ACQUIRED DURING THE COURSE OF THIS WORK

1. FIGHT FOR SIGHT SMALL GRANT AWARD (£14500) 2011

"The genetic associations of primary rhegmatogenous retinal detachment and related predisposing conditions"

David G Charteris, **Aman Chandra (Co-Investigator),** Andrew Webster, Donna Mackay

2. ROYAL COLLEGE OF SURGEONS OF EDINBURGH MAJOR PROJECT GRANT (£49,560) 2012

"Case-control genetic association analysis of primary rhegmatogenous retinal detachment using novel high density exome genotyping."

Aman Chandra (Principal Investigator), Danny Miry, Alan Wright, Harry Campbell, Veronique Vitart, David Yorston, Andrew Webster, David Charteris

ETHICAL APPROVAL ACQUIRED AS PART OF THIS WORK

All projects described in this thesis have been approved by local ethical committees

Approval references

REC reference number: 10/H0703/97

REC reference number: 10/H0311/39

REC reference number: 10/H0106/57-2011ETR3

REC Reference Number: 11/H0703/8

REC Reference Number: 1OlHO7O3l97

CHAPTER 1: INTRODUCTION

1.1. RHEGMATOGENOUS RETINAL DETACHMENT & ECTOPIA LENTIS: A BRIEF HISTORICAL INTRODUCTION

A rhegmatogenous retinal detachment (RD) is the result of a full thickness break in the neurosensory retina resulting in the separation of this neurosensory retina from its underlying pigmented epithelium. The earliest histological observations of RD in humans were described in the nineteenth century[31]. The understanding of this condition in the living human eye was not possible until the development of the ophthalmoscope in 1851[32]. The descriptions by Jules Gonin in 1904 of three cases of RD[33] was the beginning of his research and development of techniques to treat this condition over the next 12 years. Since then, our understanding of the aetiology and treatment of this blinding condition have progressed significantly[34].

The Austrian ophthalmologist Karl Stellwag[35] is credited with coining the term ectopia lentis (EL) in 1856. It describes abnormal movement of the crystalline lens from within its natural position. Inherited EL was first reported later that century by Williams[36], in 1875, by describing a family with EL in two generations. The daughter in that family subsequently developed a RD at the age of 28 years. Since then, the association between the two conditions has been maintained, but rarely studied.

1.2. RHEGMATOGENOUS RETINAL DETACHMENT

1.2.1. ANATOMICAL CONSIDERATIONS

1.2.1.1. RETINA

The retina is a transparent membrane, lining the inner layer of the eyeball. It is thinnest at the ora serrata (100μm) and thickest near the optic disc (560μm), with which it is continuous. Anteriorly, it becomes the epithelium of the iris and ciliary body. It is bounded on its outside by Bruch's membrane of the choroid, and the vitreous body on its inside. The firmest attachments of the retina are at the optic disc and ora serrata.

The retina consists of an outer pigmented and inner neurosensory retina (NSR) layer; derived from neuroectoderm.

1.2.1.1.1. RETINAL PIGMENTED EPITHELIUM

This is a monolayer of hexagonal cells between the choriorcapillaris and the neural retina. These cells have a basal end, resting on the Bruch's membrane and an apical end with microvilli (Figure 1.1). The retinal pigmented epithelium (RPE) is structurally and functionally asymmetric and has numerous functions. These include phagocytosis of the outer segment tips, formation of the blood-retinal barrier (via tight junctions between RPE cells) and secretion of extracellular matrix (ECM) molecules. These latter are secreted both basally (type IV collagen, and laminin) giving rise to Bruch's membrane, and apically; contributing to the interphotoreceptor matrix (IPM)[34]. These cells therefore have a crucial role to play in the maintenance of normal visual function, and number between 4-6 million per human eye.

The neural retina consists of nine layers (Figure 1.2). From most outer (adherent to the RPE) are; photoreceptors (rods and cones), outer limiting membrane (made of zonulae adherens between the radial processes of the Muller cells and the photoreceptors), the bipolar cells: which include the four layers of the outer nuclear layer, outer plexiform layer, inner nuclear layer and the inner plexiform layer. The outer nuclear layer contains the cell bodies of the rods and cones, whilst the inner nuclear layer those of the Muller, amacrine, bipolar and horizontal cells. The outer plexiform layer contains the synaptic connections between the horizontal, bipolar and Muller cells and the photoreceptors. The inner plexiform layer contains such connections between bipolar, amacrine and retinal ganglion cells (RGC). Adjacent to this latter layer lays the retinal ganglion cell layer. This is lined by the nerve fibre layer, containing the nerve fibres of the RGC. The final layer is a basement membrane forming the retinal side of the vitreoretinal surface; known as the inner limiting membrane (ILM)[37].

1.2.1.1.2. PHOTORECEPTORS

These cells are separated into inner and outer segments. The former of these contain the majority of organelles for cell function. The latter contain discs which help these cells play a key role in phototransduction. There are two types of photoreceptors in the human eye; the rods (approximately 110 million per human retina) and the cones (approximately 6.5million per human retina)[34].

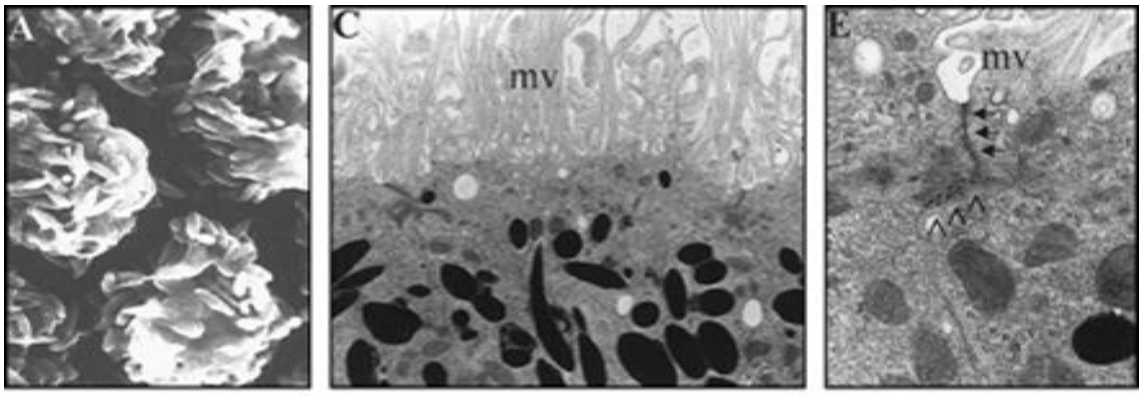

Figure 1.1: Retinal Pigment Epithelium cells intercellular integrity
(adapted from [3])
A: Apical view of RPE cells demonstrating microvilli
B: Transmission Electomicrograph showing tight and adherens junctions and microvilli (mv)
C: Tight junctions demonstrated by high magnification
NSR: neurosensory retina

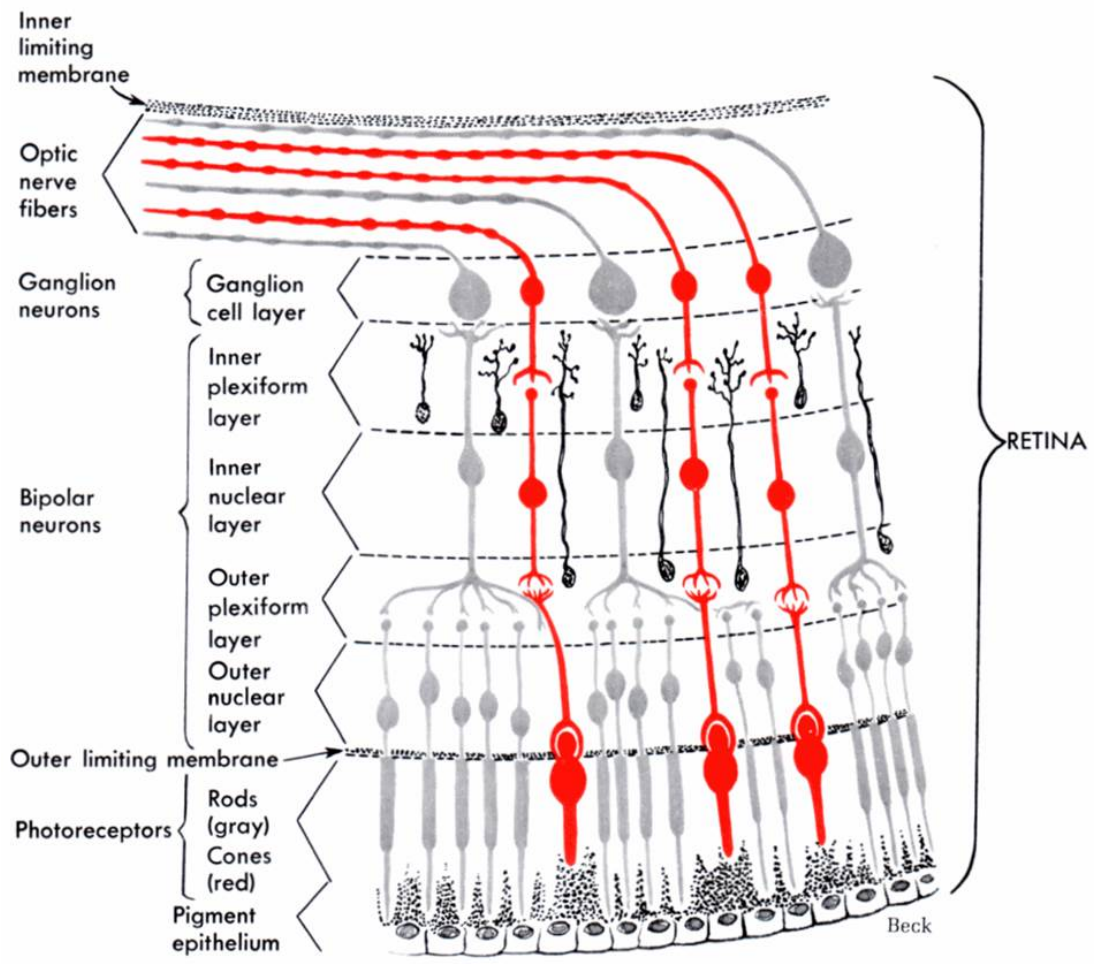

Figure 1.2: The layers of the human retina
Adapted from http://www.arthursclipart.org/medical/

1.2.2. NORMAL ADHESION BETWEEN THE PHOTORECEPTORS AND RETINAL PIGMENT EPITHELIUM

The photoreceptor and RPE layer come together as a consequence of the invagination of the optic vesicle into the double walled optic cup during embryogenesis. The external layer forms the RPE, whilst the inner forms the photoreceptors. They remain continuous at the rim of the optic cup (the future ora serrata) and the stalk connecting the cup to the brain (future optic nerve). As the invagination continues, these layers are continually brought together. In between these two layers exists the IPM (Figure 1.3). This matrix is formed early in embryogenesis, soon after the invagination of the vesicle; certainly by day 45[38]. It has important roles to play in the interaction between the PR and RPE, and also acts as a "buffer" between the two layers. Indeed separating the two layers in embryonic tissue prior to the development of the IPM is more challenging than in older embryos[34]. It is thought to be continually produced by the surrounding cells: the RPE, photoreceptors and Muller cells. It is composed of a hyaluronan (HA) scaffolding and large glycoproteins and proteoglycans. The former contributes towards the adhesion between the PR and RPE.

The other mechanical forces which play a role in the adhesion of the PR and RPE include the hydrostatic and osmotic pressure exerted by aqueous production. Although the RPE has enormous capacity to actively transport fluid across it, there is limited passive posterior movement of this fluid through the NSR and RPE[39], resulting in the NSR pushed against the RPE. The other mechanical forces involve the mechanical interdigitation of the RPE microvilli between the outer segments of the PR. This interaction may be secondary to electrostatic forces[40]; though the real effect of this is likely to be small.

Finally, there are metabolic factors playing a role in maintaining the adhesion between the RPE and PR. It has been demonstrated that oxygenation and active metabolism of the RPE and PR helps maintain the adhesive strength between these two layers[41]. This may play a role in influencing the structure and function of the IPM; thus indirectly affecting the mechanical adhesive properties.

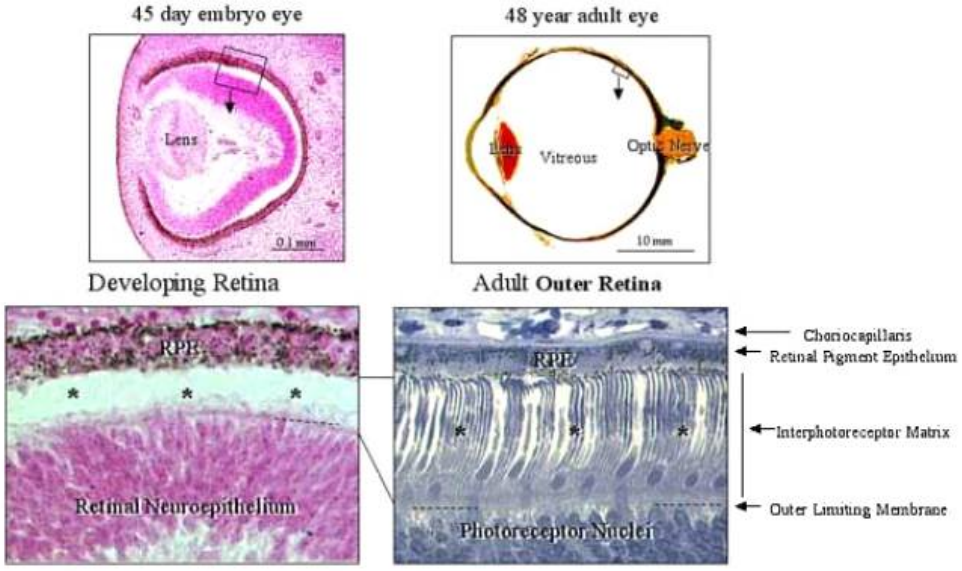

Figure 1.3: Embryonic origin of the Interphotoreceptor Matrix (IPM)
This illustrates the outer eye wall from a 45-day post fertilisation human embryo before the development of photoreceptor cells (*). It is compared with the equivalent region from a 48 year old adult eye, with elongated photoreceptor cells (*); extending from the outer retinal surface. The IPM is between these two layers.
Adapted from http://glycoforum.gr.jp/science/

1.2.3. VITREORETINAL ADHESION

The basement membrane of the Muller cells makes up the principal component of the ILM, with the remaining inner portion is made of vitreous fibrils. It consists of three layers. The innermost layer (lamina rara) is continuous with the vitreous[42]. The middle layer (lamina densa) varies in thickness; being greatest at the posterior pole. The outer layer (lamina rara) is immediately adjacent to the Muller cells, and is irregular in nature. The ILM varies with age, and is at its thickest most posteriorly (up to 1900nm[34]). It ends abruptly at the margin of the optic nerve head; where it becomes continuous with the astrocytes which line the optic nerve head. It is very thin at the fovea (approximately 20nm) with reduced Muller cell processes[43]. The attachment of the vitreous collagen fibres to the ILM differs slightly at different regions of the NSR. At the vitreous base, the collagen fibres are perpendicular to the vitreous base, and therefore insert directly into the lamina rara of the ILM[44] and any crypts between cellular layers. This bond is therefore unbreakable. Elsewhere, however, the collagen fibres run parallel to the retina, and an extracellular "glue" acting as the adhesion[34]. This may be as a result of interactions between macromolecules on the inner surface of the ILM and components on the surface of the vitreous fibrils[5]. The further possible mechanism of an adhesion is the role of type XVIII collagen, which is present in the human ILM[45]. Type XVIII collagen is a heparan sulphate proteoglycan and opticin (see Section 1.2.4) which binds to heparan sulphate[46]. The opticin on vitreous collagen fibrils therefore may bind to the type XVIII collagen and act as a potential adhesive mechanism (Figure 1.4). Evidence for an important role of type XVIII collagen in vitreoretinal adhesions comes from the abnormal vitreoretinal adhesions seen in *COL18A1* knockout mice[47].

1.2.4. BIOCHEMICAL STRUCTURE OF THE VITREOUS

The vitreous is a highly specialised hydrated ECM and is the largest structure in the eye. It has a volume of approximately 4ml (weighing approximately 4g) (Figure 1.5), with a water content of over 98%. As with other ECM, it is composed of fibrillar proteins and charged carbohydrates (glycosamineglycans, GAGs). The main fibrillar component is collagen fibrils, and the major GAG is HA.

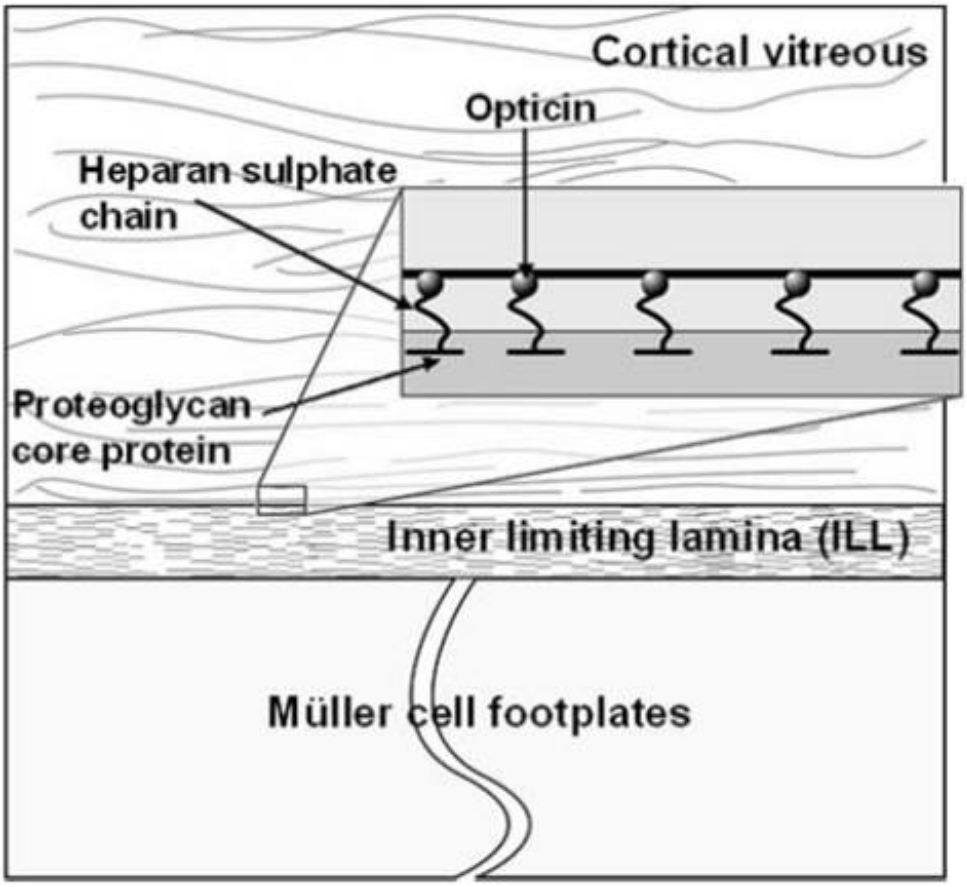

Figure 1.4: Postbasal vitreoretinal junction. Weakening of the adhesion at this interface predisposes to posterior vitreous detachment. Vitreoretinal adhesion may be dependent upon intermediary molecules acting as a 'molecular glue' and linking the corticol vitreous collagen fibrils to components of ILM. It is possible that opticin, because it binds to both vitreous collagen fibrils and HA in the ILM, contributes towards this 'molecular glue'. *Adapted from* [5]

Figure 1.5:
Adherent vitreous (arrow) evident on dissection from human eye

1.2.4.1. COLLAGENS

The human eye has a collagen concentration of approximately 300µg/ml [5], which is probably continually produced throughout life[48]. They are formed of three polypeptide chains, making a triple-helical shape. They consist of a highly conserved repeating triplet sequence, whereby glycine is every third amino acid. The collagen proteins also contain non-collagenous regions, usually at the end of the molecules. Within the vitreous, the collagen is of mixed composition, made of Type II, IX and V/XI collagen.

1.2.4.1.1. Type II Collagen

This is the most abundant of the collagen types in vitreous; accounting for approximately 75%[49]. The molecules undergo extracellular modification allowing them to form fibrils. It is known that alternative splicing of exon 2 results in two forms of procollagen; with type IIA predominating. This may explain the "ocular only" variant of Stickler's, caused by mutation in exon 2 (see Section 1.2.10.4.1).

1.2.4.1.2. Type IX Collagen

This makes up approximately 25% of the vitreous collagen, and cannot form fibrils alone. It is a heterodimer of three distinct polypeptide chains, and is synthesised with a chondroitin sulphate chain attached[49].

1.2.4.1.3. Type V/XI Collagen

These two types of collagen are found in most tissues independently. The vitreous however contains a hybrid molecule (thus termed type V/XI). This hybrid may play a role in initiation of collagen fibril formation in the vitreous[5]. Linkage to *COLXIA1* and *A2* have been associated with Stickler's syndrome[50]; although the latter of these does not have an abnormal ocular phenotype.

1.2.4.1.4. Type VI Collagen

This is found in very small concentrations in the vitreous, and may play a role in linking together collagen and HA[5].

1.2.4.2. NON-COLLAGENOUS PROTEINS

1.2.4.2.1. Fibrillin

Although fibrillin is found in the vitreous, the role of this protein is unclear in this tissue. This is discussed at further length in section 1.3.1.

1.2.4.2.2. Opticin

This is a member of the small leucine-rich repeat proteins family. It exists as a dimer in solution[51], and may play a role in binding GAGs.

1.2.4.3. GLYCOSAMINOGLYCANS and PROTEOGLYCANS

The predominant GAG in the vitreous is HA. It is a linear GAG, which is unsulphated[5]. It is at its highest concentration in the posterior cortex, and its concentration increases till the age of 20 years, after which is it stable[52]. It is a high molecular size polymer with electrostatic interactive properties. Its biophysic and hydrodynamic properties and size allow it to contribute to the structure and functional organisation of the vitreous[53]. It also acts as a template for the assembly of other vitreous macromolecules.

Other GAGs in the vitreous are proteoglycans; they are attached to a protein core. These include chondroitin sulphate. The main Chondroitin Sulphates is versican. It is suggested that it may play a role in acting as a molecular bridge between cell surfaces and the ECM[53]. It may therefore play a part in vitreous adhesion to the ILM. Mutations in the encoding gene (previously known as *CSPG2*) have been shown to cause the vitreoretinopathy Wagner syndrome[54].

Finally heparan sulphate is a major proteoglycan component of basement membranes. This includes the ILM on the surface of the retina. Although it is found in vitreous development, it has very low concentrations in post natal vitreous.

1.2.5. FUNCTION OF THE VITREOUS

The vitreous body acts as a barrier against movement of solutes. Diffusion rates of low molecular weight solutes through the vitreous are slow[55], and unaffected by disease states[56]. Bulk flow of high molecular weight substances is even lower[57]. It is also

thought that the vitreous body may protect the retina, and may act to absorb external forces and reduce mechanical deformation of the globe[56]. However such mechanical functions are of limited importance; illustrated by the normal function of eyes which have undergone vitrectomy.

1.2.6. MORPHOLOGY OF THE VITREOUS

The vitreous is divided into three regions; the central vitreous, the vitreous base and the vitreous cortex. Within the central vitreous, collagen fibres are at their lowest concentration, and run in a posterior-anterior fashion. These fibres run into the vitreous base anteriorly and the cortex posteriorly. Collagen fibres run perpendicular to the vitreous base, and are interwoven closely. The cortex is a thin layer which surrounds the central vitreous, and has a high concentration of collagen. The fibres run parallel to the ILM. Anteriorly this layer runs across the vitreous base and along the posterior surface of the lens (anterior hyaloid).

1.2.7. REGIONS OF FIRM VITREOUS ADHESIONS

The vitreous is attached to adjacent structures, with varying strengths. It is most firmly attached to the 6mm circumferential band known as the vitreous base, where the collagen fibres of the vitreous attach perpendicularly (tangentially elsewhere) (Figure 1.6). The vitreous fibres attach to the basement membrane of the non-pigmented epithelium of the posterior pars plana and the peripheral ILM[58].

1.2.7.1. VITREOUS BASE ANOMALIES

Within the vitreous base, there are several anatomical variations, which may have varying strengths of vitreous attachments; thus being regions with a tendency for retinal holes or breaks.

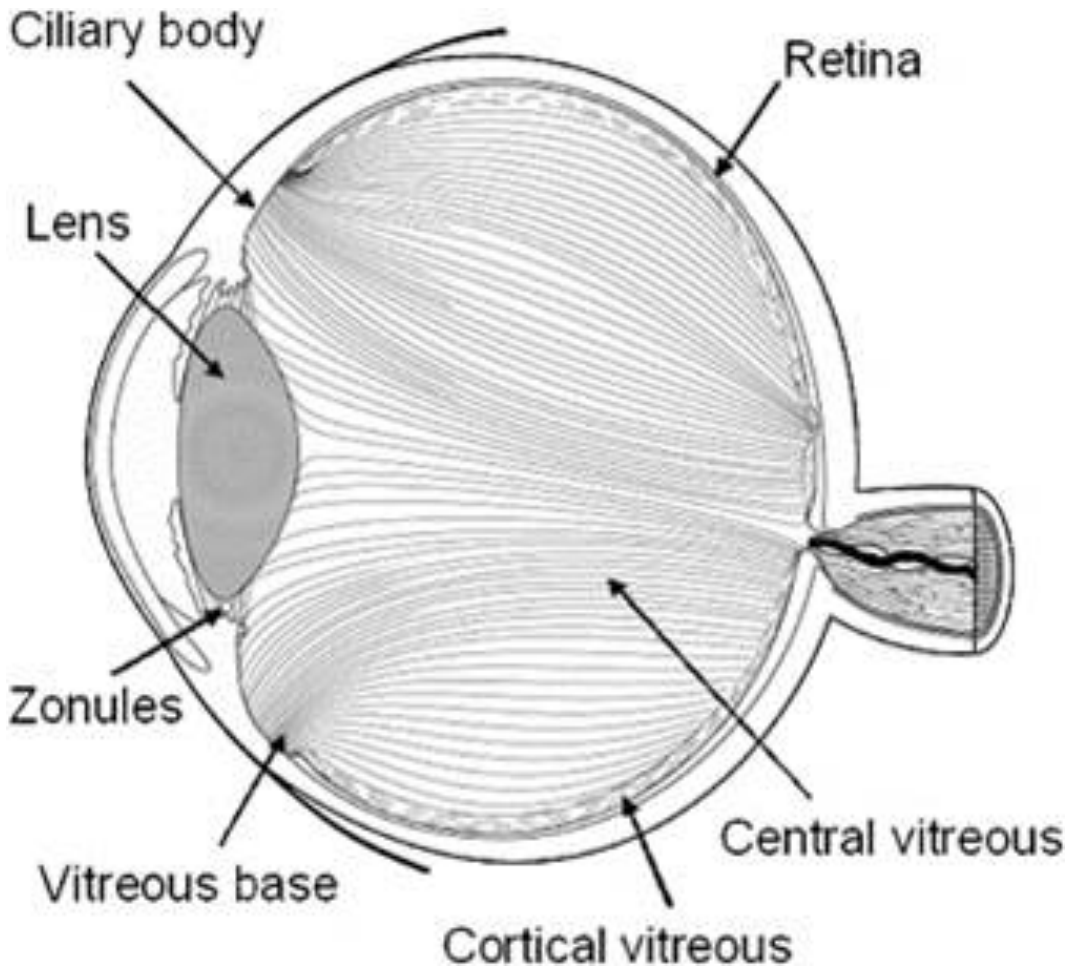

Figure 1.6:
Orientation of collagen fibres attachment at different structures within the posterior segment of the human eye
Adapted from [5]

1.2.7.1.1. Ora bays

Ora bays are indentations which are either separated from the pars plana (enclosed bay) or partially separated (partially enclosed bay). It is reported that these bays may be present in less than 5% of eyes, with a very small rate of associated retinal tears being present[59].

1.2.7.1.2. Meridonal complexes and folds

Meridonal folds are radial linear elevations of the peripheral retina, associated with dentate processes. Histologically, these are associated with thickened retina, hyperplasia or RPE and rarely retinal breaks[60]. Complexes are combinations of folds and ciliary processes and ora bays.

1.2.7.1.3. Retinal tufts

These are internal projections of retinal tissue associated with the vitreous base. They are either non cystic; which are fibroglial tissue in continuation with the vitreous, or cystic; which histologically consist of disorganised retinal layers and a loss of photoreceptors[61]. Both types have very low risks of developing tears.

1.2.7.1.4. White with/without pressure

These lesions were first described in 1952[62], and may represent tangential light upon dense collagen fibres[34]. Although some have suggested an increased risk of giant tears in fellow eyes with these lesions at the vitreous base[63], others afford no prognostic risk to these lesions[64].

1.2.7.2. LATTICE DEGENERATION

The most important peripheral retinal degeneration associated with abnormal vitreous adhesion is lattice degeneration. First reported in 1920[65], it is usually described as demarcated, circumferentially orientated areas of retinal thinning with excessive vitreoretinal attachments at its edges and overlying vitreous liquefaction. There may be associated pigmentary changes, thinned punched out areas, overlying retinal vessels, fine white lines and retinal holes[66, 67]. It is present in up to 10% of the population, with a higher incidence in myopic patients[66, 67]. Retinal tears may occur on the posterior or lateral margins of these lesions, although reported in less than 2% of eyes followed for over 3 years[68]. It is suggested, nonetheless, that up to 30% of patients with acute RDs and retinal breaks had lattice degeneration[69]. Round holes, which frequently are associated with lattice degeneration may result in RD, although there is no evidence that eyes with these lesions are more likely to develop a RD after a posterior vitreous detachment[70]. Nevertheless, these degenerative features are important factors in the risk of developing RD.

1.2.7.3. OPTIC NERVE & FOVEA

Further regions of firm attachment include the optic nerve margin. This may be exacerbated by the cellular proliferation from the optic nerve head; and the formation of an epipapillary membrane. An irregular 3-4mm diameter ring around the fovea is also a site of strong vitreoretinal adhesion[71], being a source of many vitreomacular disorders.

1.2.7.4. BLOOD VESSELS

Along the retinal blood vessels, vitreous appears to have strong attachments, and may be the cause of haemorrhage occasionally seen in the presence of posterior vitreous detachments[5]. Furthermore, the ILM thins and may be absent over major vessels[72], leading to potential incarceration of the vitreous, thus becoming continuous with the perivascular tissue.

1.2.7.5. LENS

The other regions of firm adhesion include most anteriorly; at the lens. The attachment to the lens (Wiegert's ligament) is particularly strong (see Section 1.4).

1.2.8. AGEING VITREOUS

1.2.8.1. BIOCHEMICAL CHANGES

As the human vitreous ages, it undergoes a process of liquefaction. It occurs as pockets of fluid in the central vitreous cavity, which enlarge and eventually coalesce. There is a steady increase in this occurrence from the age of 40 years, with more than half of the vitreous liquid by the age of 80 years old[52]. The process involves aggregation of collagen fibrils; leaving areas of the vitreous without fibres, thus converted to liquid[73, 74]. This is accompanied by the appearance of macroscopic fibres centrally. Bishop *et al*[74] showed that there was a loss of type IX collagen as the vitreous aged. The chondroitin sulphate side chains act as "spacers", and their loss may precipitate aggregation of collagen fibres; in particular the type II fibres. Furthermore, HA acts to separate the collagen fibrils, and digestion of HA results in reduction of the collagen network[75]. It is suggested that free radicals may alter the HA and/or collagen structure; resulting in a dissociation between HA and collagen[76]. The results are thought to be collagen aggregation with HA pooling in liquefied lacunae.

1.2.8.2. VITREOUS BASE CHANGES

As the eye ages, the posterior border of the vitreous base extends. At birth, the posterior border is at the ora serrata. With age, the collagen fibres of the vitreous base intertwine with the internal limiting membrane. The extension is thought to be due to synthesis of new "vitreous" collagen, creating further unbreakable bonds. This progression in thought to be more prominent in men[77].If there are any abnormalities in this new border, there may be a predisposition towards break formation.

1.2.8.3. POSTERIOR VITREOUS DETACHMENT

Posterior vitreous detachment (PVD) is a process by which the cortical vitreous separates from the ILM, as far as the vitreous base, and may occur in up to 25% of the population in their lifetime[78]. It is a result of both the liquefaction and weakening of the interaction between vitreous and ILM. This is as a result of the dense posterior vitreous cortex rupturing, thus allowing liquefied vitreous from lacunae to pass into the subhyaloid space. Its prevalence increases with age, and has been shown to occur more frequently and at a younger age in myopia[79, 80].

Sebag[81] first described the irregular PVD; whereby the liquefaction exceeded the weakening of the vitreoretinal adhesion. In this situation, during PVD, tears in the retina may occur, leading to subsequent RD.

1.2.9. PATHOGENESIS OF RHEGMATOGENOUS RETINAL DETACHMENT

A Rhegmatogenous Retinal Detachment has been defined as a full thickness break in the NSR associated with liquefied vitreous migrating through this break extending over two disc diameters[62]. The term rhegmatogenous retinal detachment is therefore actually a misnomer, as it describes the separation of the NSR from the underlying RPE; thus re-creating the potential space between the original layers of the embryonic optic cup.

RD arises from a full thickness break in the NSR. A retinal break occurs when there is a misbalance between the level of vitreous liquefaction and the weakening of the vitreoretinal adhesion. Therefore, breaks tend to occur at areas of firmer vitreoretinal adhesion. This is usually around blood vessels, around vitreoretinal degenerations (particularly lattice degeneration) and at the posterior margin of the vitreous base. The resultant break is usually a horseshoe shape (always pointing towards the optic disc, and the vitreous attached to the anteriorly positioned operculum. However, with further traction, the operculum may avulse, leaving a round hole[82]. It has been reported from long term studies that retinal tears may occur in 22% of eyes with PVD[83]. Post mortem studies have suggested that the prevalence of retinal tears is between 3% to 27%[84, 85]. However most eyes with a retinal break do not develop into a RD; as the metabolic pump of the RPE and the osmotic pressure of the choroid are usually sufficient to keep the RPE and NSR attached.

Three factors need to be present for a primary RD to occur. There needs to be tractional forces, a retinal break, and liquefied vitreous gel to separate the NSR from the underlying RPE[34]. Gravitational forces[34], and even slight rotatory eye movements can have important tractional effects to propagate the RD.

Beyond horseshoe tears and round holes, other notable retinal breaks include dialysis and giant retinal tears (GRT). The former are circumferential tears along the ora serrata, with vitreous attached to the posterior margin. It has been suggested that most are

secondary to trauma[86], others postulate a potential genetic predisposition[87]. Giant retinal tears are circumferential tears extending more than 90°[88].They are responsible for approximately 0.5% of cases of RD[63]. They are more common in males, and may be associated with trauma, complicated intraocular surgeries or hereditary vitreoretinopathies (such as Stickler's syndrome) [89], though most are idiopathic.

1.2.9.1. RISK FACTORS IN THE AETIOLOGY OF RHEGMATOGENOUS RETINAL DETACHMENT

The annual risk of RD is between 6.3 and 17.9 per 100,000[90]. There is growing evidence that the numbers of RD are increasing. Within England, the reported number of RD (based on Hospital Episode Statistics[91]: HES) grew from 3519 in 1998-9 to 7,827 in 2011-12 (Figure 1.7). Whether this is related to the increase in risk factors (such as the increase in myopia[92]) is uncertain. There are numerous such risk factors.

1.2.9.1.1. Myopia

The greatest risk factor for is myopia. It is suggested that eyes with a spherical error of between -1DS and -3DS have a fourfold lifetime risk of developing RD, with this risk increasing to over tenfold in those with a refractive error >10DS [93, 94]. Myopia predisposes to RD through increased vitreous liquefaction, earlier posterior vitreous detachment and a higher incidence of vitreo-retinal degeneration[82]. The biological explanation behind this phenomenon is unclear. It is suggested that altered Muller cell function may affect the vitreoretinal adhesions[79]. It is possible that myopia is associated with a developmental change to the vitreous structure itself[95].

1.2.9.1.2. Non Penetrating Trauma

Non penetrating trauma is also a significant risk factor in the development of RD, being present in up to 12.2% of cases [96, 97]. Blunt trauma may cause compression in an antero-posterior direction; resulting in tractional forces on the retina; resulting in breaks in the NSR[82].

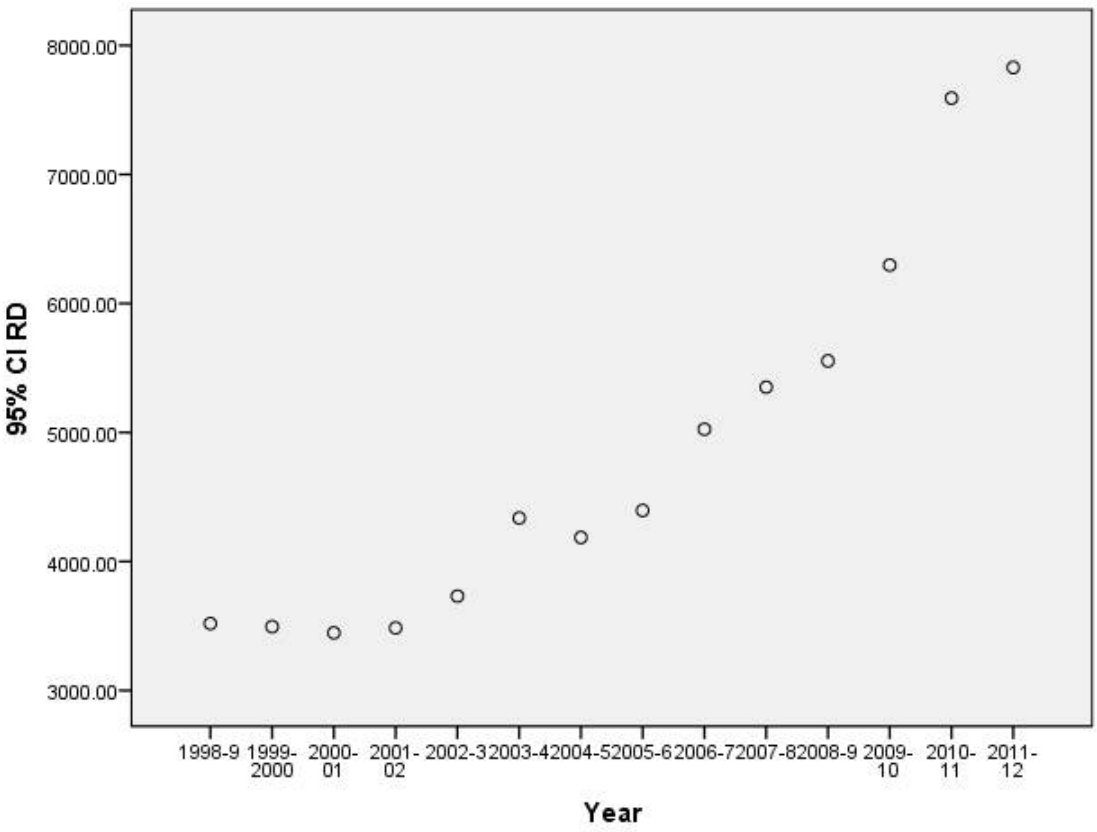

Figure 1.7: Incidence of RD in the UK (data acquired from Hospital Episodes Statistics (HES) of England)

1.2.9.1.3. Previous Cataract Surgery

Previous cataract surgery has been noted in up to 24% of cases of RD [97], with 17% of these having had vitreous loss during surgery. This may be secondary to increased rates of PVD after cataract surgery[98]. This may be associated with reduced concentrations of HA[82]. Recent data however suggests that this risk is reducing, with main operative risk factors being young age, male gender and peri-operative vitreous loss[99].

1.2.9.1.4. Socioeconomic Class

Higher socioeconomic class [100], has been associated with increased rates of RD. Whether myopia, also known to aggregate with affluence, is a contributing effect is unclear.

1.2.9.1.5. Gender

Male gender seems to be associated with RD [101]. This is perhaps related to myopia and the posterior extension of the vitreous base; both of which are more common in men[77, 101].

1.2.9.1.6. Race

Finally, there appears to be racial differences in RD. The incidence of RD in black patients is reported as being significantly lower than Caucasians [102] [103] [104]. This is not explained by predisposing risk factors, which are not thought to differ between races [85]. Indians appear to have a lower prevalence of RD compared to Chinese and Malay [105]. These differences have yet to be explained.

1.2.10. GENETICS OF RHEGMATOGENOUS RETINAL DETACHMENT AND ASSOCIATED CONDITION

There is evidence of a genetic predisposition to many of the risk factors and features of RD. These are discussed below.

1.2.10.1. LATTICE DEGENERATION

Lattice degeneration has a prevalence of between 6 to 9.5% [106] and is implicated in between 7 and 29% of RD cases[97, 107-109], being the most prevalent vitreoretinal

degeneration predisposing to RD [67]. A hereditary factor in the aetiology of lattice has been proposed for over four decades [66, 110-112]. Although autosomal dominant[110, 111] and recessive[112] modes have been suggested, Mukarami[113] investigated 100 patients with lattice without RD, and suggested that its inheritance was complex; with a three-fold higher prevalence of lattice degeneration in first degree relatives. In 2012, Meguro and colleagues [114] published a genome wide association study (GWAS) suggesting an association with *COL4A4* in a Japanese population. The role of this protein in the retina is unclear.

1.2.10.2. GIANT RETINAL TEARS & RETINAL DIALYSIS

Retinal dialysis and GRT account for approximately 6% and 1.3% of all RD cases [97]. Retina dialysis are suggested to be traumatic [115] with authors suggesting that a genetic predisposition is unlikely[86]. In a series of over 500 cases, Hagler found that less than 2% of cases had a relevant family history[116].

GRT may be caused by trauma in some cases. However a recent review at Moorfields Eye Hospital (unpublished) suggests that trauma accounted for 22% of GRT over five years at this unit. It must be considered that hereditary vitreoretinopathies also have a high rate of GRT in presentation of RD[117].

Furthermore, the high prevalence of bilaterality in GRT[63] and dialysis[87], the concentration of cases in sibships [87]and evidence from twin studies [118, 119] do suggest a genetic aetiology to GRT and dialysis.

1.2.10.3. MYOPIA

The genetics of myopia is an extensive topic, and is briefly described below.

Myopia is the most common ocular “disorder” [120], with an estimated 2.5billion people expected to be affected by 2030[121]. The main principal components, axial length and corneal curvature both shown to have high heritability; one study demonstrating this to be 0.95 for the former and 0.67 for the latter [122]. Guggenheim and colleagues [123] recently suggested that genetic components of these ocular endophenotypes were related, with a shared genetic scaling involved in ocular development.

Family aggregation studies have suggested a higher prevalence of myopia in children with myopic parents compared with those without[124]. Yap and colleagues[125] suggested that the prevalence of myopia in 7 year olds without myopic parents was 7.3%, compared to 45% when both parents were so. Twin studies have estimated the monozygotic heritability as high as 0.9[126]. The increased risk to siblings of a person with high myopia (λs) has been reported between 4.9[127] to 20 [128] for high myopia. Wojciechowski *et al*. [129] described this to range between 1.9 and 2.52 for low myopia.

To date there are at least 16 loci, distributed among 13 chromosomes, listed on the OMIM database (http:// www.ncbi.nlm.nih.gov/omim) (MYP2–MYP17) for non-syndromic high myopia, common myopia or ocular refraction. At least seven loci for refractive phenotypes (MYP1, MYP3, MYP6, MYP11, MYP12, MYP14 and MYP17) have been successfully replicated in independent linkage datasets and identified as being associated with myopia. However, recent association studies have greatly advanced the understanding of the genetic aetiology of myopia.

In a large twin based GWAS of refractive error in a European population, several polymorphisms at 15q25 near the *RASGRF1* gene were found to be associated with ocular refraction[130]. In a companion paper, Solouki et al reported another European GWAS with a polymorphism (rs634990) at 15q14 significantly associated with refractive error [131]. More recent reports have replicated loci at 15q14 that underscore a risk for high myopia, in particular an association with axial length[132] and a further GWAS for high myopia in a French population have refined a risk locus at MYP10 implicating a role for microRNA variation in predisposition to high myopia[133].

The recent expansion of collaborative GWAS have illustrated many novel loci and biological pathways involved in myopia aetiology, which are discussed further in section 4.1.9.1.

1.2.10.4. MONOGENIC CONDITIONS ASSOCIATED WITH RHEGMATOGENOUS RETINAL DETACHMENT: VITREORETINOPATHIES

1.2.10.4.1. Stickler Syndrome

The most common cause of inherited RD is Stickler syndrome[117]; first described in 1965 as a connective tissue disorder comprising of articular, auditory, facial and ocular features[134]. It is now regarded as the most common manifestation of the spectrum of type II/XI collagenopathies; which include Kniest dysplasia, metatropic dysplasia, achondrogenesis type II and spondyloepiphyseal dysplasia congentia. Stickler syndrome is at the milder end of the spectrum regarding systemic manifestations[135].

The diagnostic criteria for Stickler syndrome is[50] a congenital vitreous anomaly with three of the following clinical features:

1. Midline cleft palate
2. Audiometrically confirmed sensorineural hearing loss
3. Abnormal Beighton score[136] for joint hypermobility
4. RD or paravascular pigmented lattice degeneration.

Although myopia, characteristic lamellar corticol cataract, angle anomalies and megalophthalmos exist, the main clinical characteristic is the vitreous phenotype. It is believed that the vitreous phenotype is demonstrative of the underlying genetic mutation[117].

The most common subtype of Stickler syndrome is type 1; associated with skeletal, ocular and auditory features. The myopia is usually non-progressive, and congenital. These patients are at high risk of developing a GRT[117]. It is a highly penetrant autosomal dominant condition caused by mutations in *COL2A1*on chromosome 12q13. Frame shift, nonsense, missense and splice site mutations have been reported[137], though the former two are the most common; resulting in haploinsufficiency[117] . It is suggested that these patients have a membranous vitreous in the retrolenticular area extending to the periphery (Figure 1.8a). Interestingly, mutations in exon 2 of *COL2A1* gene have been reported to cause an ocular only phenotype[138], whilst it has also been

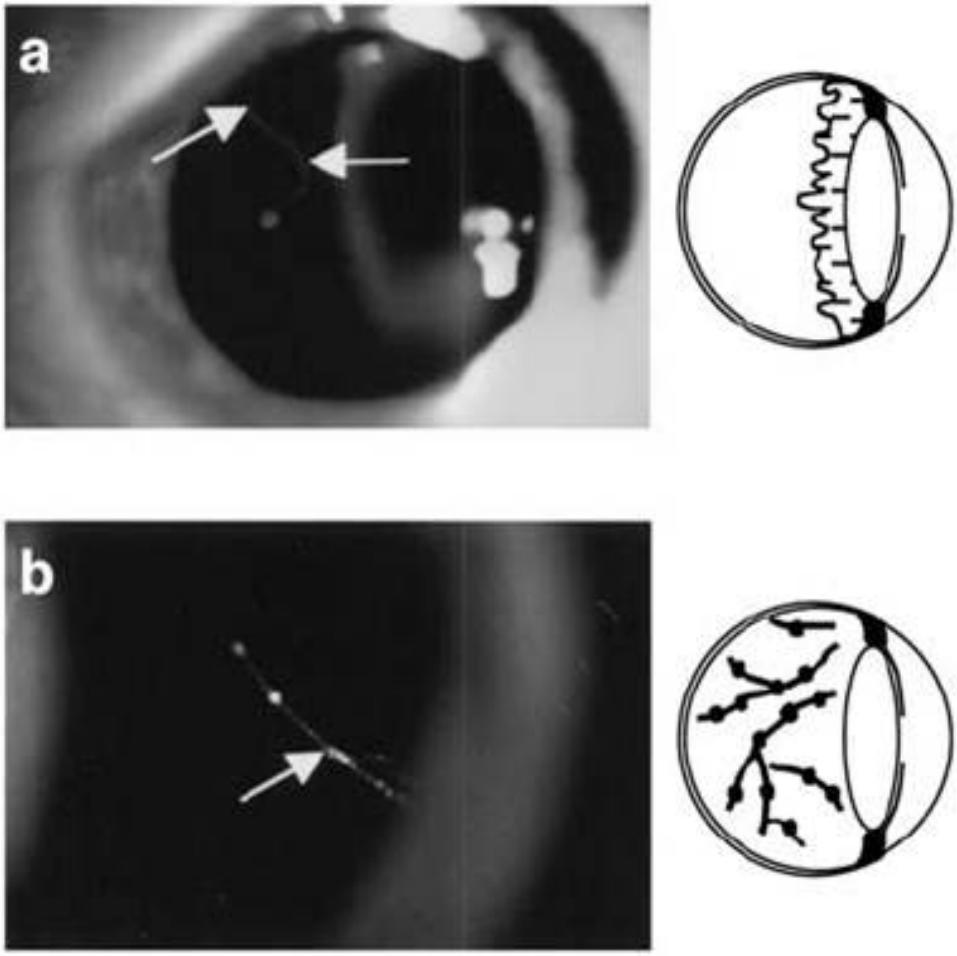

Figure 1.8: Vitreous phenotypes in Stickler's syndrome

(a) 'Membranous' congenital vitreous. Note vestigial gel occupying retrolental space and bordered by a distinct folded membrane (arrows).

(b) 'Beaded' congenital vitreous anomaly seen in cases of COL11A1 mutations. Note irregularly thickened fibre bundles giving 'string of pearls or beaded' appearance (arrow).

Adapted from [28]

suggested that certain missense mutations may not lead to the characteristic vitreous phenotype[135]. There does perhaps therefore exist a genotype-phenotype correlation. Mechanisms such as alternatively spliced exons, alternative transcripts, effects of different amino acids or compound heterozygosity have been proposed as mechanisms for phenotypic variability[117]

Stickler type 2 is also an autosomal dominant condition caused by mutations in *COL11A1* on 1p21. Pedigrees with these mutations manifest a beaded congenital vitreous anomaly (Figure 1.8b) associated with arthropathy and cleft palate[139].

This genotype- phenotype correlation based on vitreous phenotype is controversial[140], with conversion between vitreous phenotypes being described[141].

Type 3 Sticklers is caused by mutations in *COL11A2*, which is not present in the vitreous, and therefore does not manifest an ocular phenotype. Type 4 Sticklers is inherited recessively, by mutations in *COL9A1*[142] and *COL9A2*[143]. The vitreous phenotype is unclear from the few reports.

Heterozygous splice site mutations in *COL11A1* mutations have also been described to cause Marshall syndrome[144]. This condition has similar features to Sticklers; myopia, early cataracts, vitreous liquefaction and retinal breaks. However, these patients' skeletal features are in stark contrast to Sticklers; characterised by short stature, hypoplastic nasal bones and round faces. Certain mutations have been reported to cause overlapping syndromes[145]; adding to controversy over the differentiation of the conditions.

1.2.10.4.2. Chromosome 5q Retinopathies

Wagner Syndrome was first described in 1938. It used to be considered allelic to Stickler syndrome and is characterised by an optically empty vitreous with pre-retinal condensations to the periphery, progressive chorioretinal degeneration, pseudostrabismus, and progressive reduction in the ERG; with b wave preservation[146, 147]. Other clinical features include cataracts and anterior segment dysgenesis. RD is reported in up to 75% of patients[148]. In 2005 Miyamoto and colleagues[54] described a heterozygous mutation in *CSPG2* on 5q13 causing Wagner syndrome in a consanguineous Japanese family. This gene encodes versican; a macromolecule in the

vitreous as described above. Mutations in this gene have since been described in European families[149].

Allelic to Wagner is a condition first described in 1994 by Stone[150]; Erosive vitreoretinopathy. The features in this family resembled Wagner syndrome; marked vitreous syneresis, tractional and RD, diffuse rod-cone dystrophy (with ensuing nyctalopia). The most marked feature was the progressive "erosion" of the RPE; resulting in visualisation of the choroidal vessels. High myopia was not evident. The same group subsequently illustrated the allelic nature of this condition with Wagner, by mapping two families to the similar region (on 5q13-14)[151]. This was confirmed when four families with Wagner and one with Erosive retinopathy were found to share the same causative mutation on Exon 7 of *CSPG2* (c.4004-5T-->C).

1.2.10.4.3. Snowflake Vitreoretinal Degeneration

Snowflake Vitreoretinal Degeneration (SVD) was first described by Schepens in 1974[152] and is characterised by a fibrillar vitreous degeneration; which may be so dense as to obscure the retina. Patients have an absent cup from the optic nerve and parapapillary sheathing with radial perivascular degeneration. The name of the condition comes from minute crystals that have been observed in the inner retina[152]. It is the only vitreoretinopathy associated with a corneal manifestation; guttatae similar to Fuch's Endothelial dystrophy. Patients have been reported to have elevated dark adaptation and reduction of the scotopic b-wave in dim light[153]. Myopia is low, with no lattice degeneration reported. The rate of RD is reported to be 20% in those affected[154]. In 2008 a missense mutation in *KCNJ13* was reported to cause snowflake retinopathy[155]. Although the mutation described has since been demonstrated to disrupt the function of the encoded potassium channel in toads[156], a confirmation of the role of this gene in SVD is awaited. The protein is found in the apical processes of the retinal pigment epithelium[157] and it is hard to explain all the phenotypes of SVD with mutations in this gene. Interestingly, a homozygous nonsense mutation in the same gene has since been described in two families with Leber congenital amaurosis[158].

1.2.10.4.4. Goldmann-Favre

Goldman-Favre (GV) is an autosomal recessive vitreoretinopathy caused by mutations in *NR2E3* on 15q22[159]. It is allelic with enhanced S-cone syndrome; characterised by pigmentary clumps along the arcades, cystoid macular oedema, variable myopia and absent rod and enhanced S-cone function on ERG. If there is associated vitreoretinal degeneration; these are termed GV[160]. RD in this condition is rare.

1.2.10.4.5. Autosomal Dominant Vitreoretinochoriodopathy

Autosomal Dominant Vitreoretinochoriodopathy (ADVIRC) is a dominant condition cause by mutations in *VMD2* on 11q13[161], the same gene in which mutations result in Best disease. It is characterised by an annular ring of chorioretinal hypopigmentation anterior to the vortex veins to the ora serrata; for 360°[162]. These patients have a depressed Arden ratio on ERG (as those with Best disease) and some have fibrillar degeneration. To date, one case has been reported to be associated with RD[163].

1.2.10.4.6. Familial Exudative Familial Vitreoretinopathy

Familial Exudative Familial Vitreoretinopathy (FEVR) is a rare condition which is characterised by abnormal retinal vascularization during childhood, which may lead to retinal traction and detachment; as well as exudative RD[164]. The X-linked form of the disorder has been linked to the Norrie disease gene in 1993[165]. Mutations in other genes, such as *TSPAN12*[166], *FZD4* and *LRP5* [167] have since been reported.

1.2.10.4.7. Knobloch Syndrome

Knobloch Syndrome (KNO) was first described in 1971[168] and is characterised by high myopia, vitreoretinal changes, occipital encephalocoeles and rhegmatogenous retinal detachment. It has been reported in at least 23 families since. It is a recessive condition caused by mutations in *COL18A1*; encoding type XVIII collagen. This is found in the ILM, and thought to play a role in vitreoretinal adhesion. KNO is discussed at length in section 3.5.2.

1.2.10.4.8. Marfan Syndrome

Marfan Syndrome (MFS: OMIM 154700) is caused by mutations in *Fibrillin-1* (*FBN1)* is associated with EL and an increased risk of RD. It is discussed at length in chapter 2.

1.2.10.5. GENETIC PREDIPOSITION TO NON-SYNDROMIC RD

Further to syndromic Mendelian vitreoretinopathies, a genetic predisposition for non-syndromic, complex inherited RD was first proposed over 40 years ago[169]. Large population studies have suggested that a positive first degree relative family history of RD ranged between 1-8.2%[96, 170]. Go and colleagues reported autosomal dominant RD in two families with no features of sticklers with an R453T mutation in *COL2A1*[171]. More recently Edwards and colleagues describe a large family with autosomal dominant RD and no ocular or systemic features of Sticklers, with the pathogenic C192A mutation in exon 2 of *COL2A1* [172]. Go and colleagues have also demonstrated that familial occurrence of RD was a risk factor in its development[173]. They suggested a risk ratio of 2.6 for cumulative lifetime risk of RD in first degree relatives of those with RD compared with those without. Siblings in particular had a 3-fold risk; even when age, sex and myopia are controlled for. Very recently, Mitry and colleagues suggested that the sibling recurrence risk (λs) for RD was 2.1, and the parent-offspring risk as 2.9[174]. The precise genetic risk of non-syndromic RD is, however, not well defined.

The common consideration in both syndromic and non syndromic conditions is the role of mutations affecting structural proteins, such as collagen. These proteins play in an integral part of the vitreous and retina, and abnormalities can therefore contribute to pathological vitreoretinal adhesions and thus breaks in the NSR. It is possible that such a common gene may play a role in Mendelian and non-Mendelian RD.

1.3. ECTOPIA LENTIS

1.3.1. ANATOMY AND AETIOLOGY OF ECTOPIA LENTIS

The human crystalline lens develops around the 5th week of gestation as a product of and separating from the surface ectoderm. It is held in its natural position behind the iris by the zonular filaments (ZF). These form a circular structure between the equatorial lens and the ciliary body through a triangular shape (Figure 1.9) with the apex of the

Figure 1.9: Anterior view of the ciliary process with zonules attaching to the lens. Zonules form columns (a) on either side of the ciliary processes (b), which meet on a single site (c) as they attach to the lens. These two columns form a triangle having its base on the ciliary body and its apex on the lens. The zonules form a tent-like structure (d) as they become attached to the lens capsule. The equatorial surface of the lens is folded (e) by the attachment of
the zonule. The iris is pulled upward, showing its posterior surface with the radial folds (f) and the circular furrows (g). *Adapted from[14]*

triangle on the equatorial margin of the lens covering an area of up to 55nm[175] which is rich in fibrillin fibres[176]. Their integrity is crucial to the maintenance of the lens' position. They were first described as being part of the family of microfibrils in 1971[177] and the most important macromolecular component of ZF are fibrillins.

The three distinct fibrillins are fibrillin-1, -2 and -3, which are encoded by *FBN1* (OMIM 134797), *FBN2* (OMIM 612570) and *FBN3* (OMIM 608529) respectively. *FBN1* is a 237kb gene consisting of 65 exons located at 15q21.1[178]. It encodes fibrillin-1, the most abundant macromolecule in ZF. This protein consists of 47 epidermal growth factor domains (EGF), 43 of which are calcium binding (cbEGF) and two cysteine rich domains (Transforming growth factor binding protein-like (TB) domain)[179]. The latter of these are only found in LTBP/fibrillin family of proteins, and their specific function is unclear, although they may play a role in integrin binding[180] or TGF interaction[181]. cbEGF domains, in particular, form intradomain disulphide bonds and also contain a calcium binding consensus sequence. When calcium binds to these bonds, the molecule strengthens and is more resistant to degradation. It is these structures which are crucial to the ECM function of these proteins. It is proposed that fibrillin-1 provides force-bearing structural support, whereas fibrillin-2 acts mostly in the early process of fibre assembly[182].

The structure of the fibrillin microfibril is of a "beads on a string" (Figure 1.10) of 10-15nm diameter with beads 50nm apart[23]. The bead like structures are mostly encoded for by exon 24 of *FBN1*[183]. Mutations in this exon lead to severe MFS. Other constituents of ZF include elastin, proteoglycans and GAGs. The most important associated glycoprotein is MAGP-1, which probably plays a role in cross linking the microfibrils[23].

Heterozygous mutations in *FBN1* lead to haploinsufficiency of fibrillin-1. This results in disrupted microfibrillar architecture in the ECM[184]. Mutations in this gene result in classical MFS, neonatal MFS, autosomal dominant ascending aortic aneurysms, familial arachnodactyly, Shprintzen–Goldberg syndrome (OMIM 182212) and severe progressive kyphoscoliosis, the "MASS" phenotype (Myopia, Mitral valve prolapse, borderline Aortic root enlargement, Skin and Skeletal findings), mitral valve prolapse syndrome (MVPS) and autosomal dominant isolated EL. There may be significant overlap between these conditions.

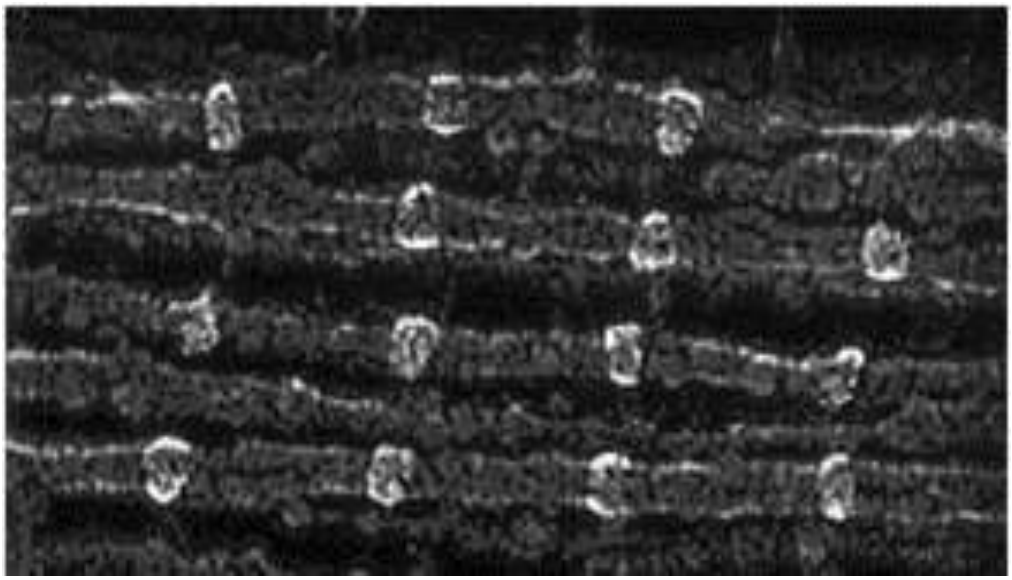

Figure 1.10: Election microscopy image of ciliary zonules fibrillin-1.
Adapted from [23]

As fibrillin is a significant element of the ciliary zonules, it is unsurprising that EL manifest in up to 60% of MFS cases[185]. The diagnosis of MFS is based on the Ghent criteria[186], of which EL is a major feature.

Although over 800 mutations in *FBN1* have been described[187], analysis suggests that a significantly higher proportion of missense mutations involving cysteine residues (responsible for the disulphide bonds which are critical to the structural properties of fibrillin-1) and mutations at the 5' end are causative in EL[187, 188], in particular within the first 15 exons. These exons encode the N-terminus of fibrillin-1. This portion of the protein is thought to be integral to homodimer formation of the fibrillin-1 molecules, which eventually lead to polymers of fibrillin-1 and thus microfibrils[189], although most of this has been inferred from mutational analysis rather than direct proteonomics.

The effect of mutations in *FBN1* on lens structures is demonstrated by evidence of abnormal distribution and structure of microfibrillary bundles in the capsule of MFS patients, particularly at the site of zonule attachment[176, 190], conjunctiva[191] and zonules themselves[192].

Fibrillin-1 is also found throughout other ocular tissue[193]. In the anterior segment, beyond the zonules and peripheral lens capsule, it is present in the ciliary body and processes, the connective tissues of the iris, the corneal epithelium and the endothelium of Schlemm's canal. Disruption to fibrillin-1 (as seen in MFS) would unsurprisingly lead to clinical manifestations related to these structures. The cornea is thought to be less steep ("lower K values"), have thinner central thickness and reduced hysteresis in patients with MFS [194-197], leading to some authors suggesting that corneal phenotype being used as a minor criteria in the diagnosis of MFS[198]. It is probable that these features are secondary to corneal maldevelopment as a consequence of *FBN1* mutations.

Furthermore, histological examination of the anterior chamber angle in eyes from patients with MFS have revealed structural abnormalities[199]. This may explain a mechanism behind raised intraocular pressure, and the higher prevalence of open angle glaucoma in MFS compared to the general population[200, 201]. However, it must be considered that although fibrillin-1 is not in the optic nerve tissue itself, it is present in the lamina cribrosa. This is known to act as a biomechanical structure in response to

intraocular pressure[202, 203]. The structure of the lamina cribrosa in MFS has not been investigated, but it is conceivable that there may be alterations in lamina cribrosa structure as a consequence of fibrillin-1 defects. This may result in an increased susceptibility of the optic nerve to intraocular pressure; as is seen in other forms of glaucoma[204]. Alternatively, a structural defect in the lamina cribrosa may result in more compliance of the optic nerve. Either theory is yet to be proven, and may be worth pursuing as a line of investigation in the future.

Within the posterior segment, fibrillin-1 is known to be present in the lamina cribrosa, choroid, sclera and Bruch's membrane[193]. The most common ocular manifestation of MFS is myopia. The cause of this is two-fold. It may be secondary to EL, specifically anterior movement of the lens, thus making the refractive index more myopic in that eye. Secondly, it is thought that those with MFS have a greater axial length[185]. It is possible that this is secondary to defects in the sclera, resulting in increased axial growth. It is likely to be the latter, as anterior displacement of the lens is not commonly found in MFS, and is more of a feature of homocystinuria[205], another condition associated with EL. Furthermore, it has recently been suggested that corneal flattening may counter the effect of axial growth, resulting in myopia not as extreme as would be expected with the axial lengths found in MFS[206].

1.4. RHEGMATOGENOUS RETINAL DETACHMENT & ECTOPIA LENTIS

It is also proposed that retinal tears and RDs are more common in MFS[185, 207]. This data is not robustly replicated, and is therefore a subject of a national prospective epidemiological study through the British Ophthalmic Surveillance Unit (BOSU)[208], led by our research team at Moorfields Eye Hospital. The explanation behind these may be simply secondary to the increased prevalence of axial myopia seen in MFS. Certainly in a large series, those MFS patients with RD had greater axial length (AL) than those MFS patients without[185]. The relationship between axial myopia and retina tears and RD has been discussed previously in this thesis. Whether the increased incidence of RD in MFS is independent of axial myopia is as yet uncertain. A further risk factor in the development of RD includes lattice degeneration. Lattice degeneration has been described in 27.5% of eyes with EL and MFS in a report from Moorfields Eye Hospital[209]. Although this is greater than the general population[66], it is approximately the same prevalence seen within high myopes[210].

Alternatively there may be changes in the vitreous predisposing to RD. Microfibrils are thought to be a constituent of vitreous[211]. Furthermore, fibrillin-1 is thought to exist in conjunction with other macromolecules in the vitreous body[212] and there is thought to be increased central and posterior vitreous liquefaction in MFS[213].

Changes in vitreous structure, and particularly increased adhesions to the retina predispose to RDs in other vitreoretinopathies. This concept of MFS being a vitreoretinopathy is not certain, and it is not classically considered as one[160]. The role of an abnormal vitreous in MFS predisposing towards the development of RD is therefore controversial.

The more probable cause of increased rates of RD may be related to the EL seen in MFS. Certainly it appears that RD is more common in MFS patients with EL[185, 214-216]. The zonules themselves are regarded, embryonically, as tertiary vitreous; being attached to the pars plicata and plana. The posterior zonule insertion is in close relation to the anterior hyaloid's attachment to the lens capsule. The anterior vitreous adheres to the capsule just centrally to the insertion of the posterior lens zonules (Figure 1.11 and 1.12), though this distance varies with age. This attachment to the lens is called Wiegerts ligament[217] (Figure 1.13). This attachment is very close to the posterior zonules in children, and regresses as time proceeds (Figure 1.11). This attachment may be seen on the slit lamp; known as Egger's line[218]. This ligament delineates Berger's space; which is a potential space within the Wiegert's ligament, and continuous with Cloquet's canal (Figure 1.13).

Disruption of the zonules, and therefore movement of the lens with Wiegerts ligament is therefore likely to induce vitreoretinal traction[73]. It is therefore unsurprising that this traction may lead to breaks in the neural retina and potential RD. The relationship between the ectopic lens and the vitreous has been demonstrated with biomicroscopic studies[219].

A further role the zonules may play in traction is evidenced by zonular traction tufts. These were first described in 1969 as thickened zonules posteriorly displaced towards the anterior retina[220]. These were shown to consist of retinal thickening and degeneration at the base, glial tissue within the tuft, and attachment of the zonular tufts at the apex. They are found in up to 15% of autopsy cases, and are bilateral in 15% of

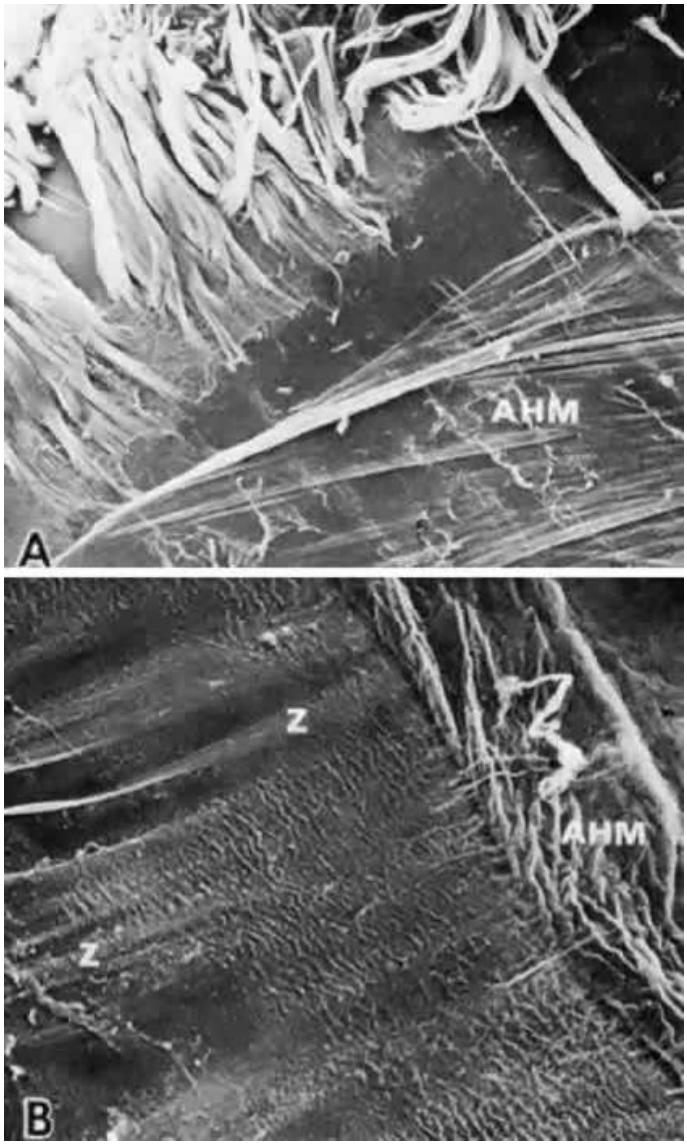

Figure 1.11: Posterior zonular bundles and the anterior hyaloid membrane (AHM). **A.** Irregular retraction of the AHM from the posterior zonular insertion in a 3-year-old patient. Note layering of posterior zonular bundles (SEM, × 90). **B.** Complete retraction of the AHM to the end of the posterior zonular fibers (Z) in a 71-year-old patient (SEM, × 400). *Adapted from http://www.oculist.net/downaton502/prof/ebook/duanes/pages/v7/v7c014.html*

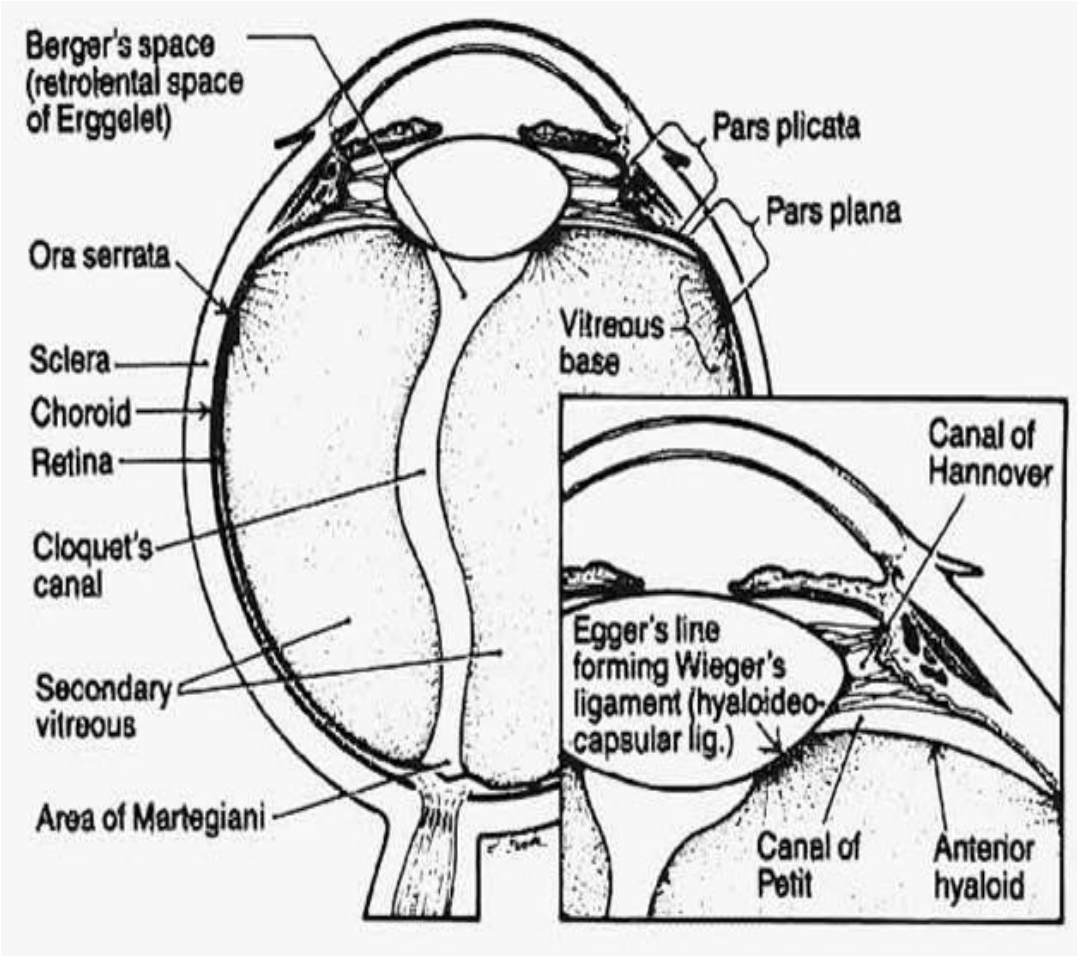

Figure 1.12: Anterior attachments of the vitreous
Adapted from http://www.oculist.net/

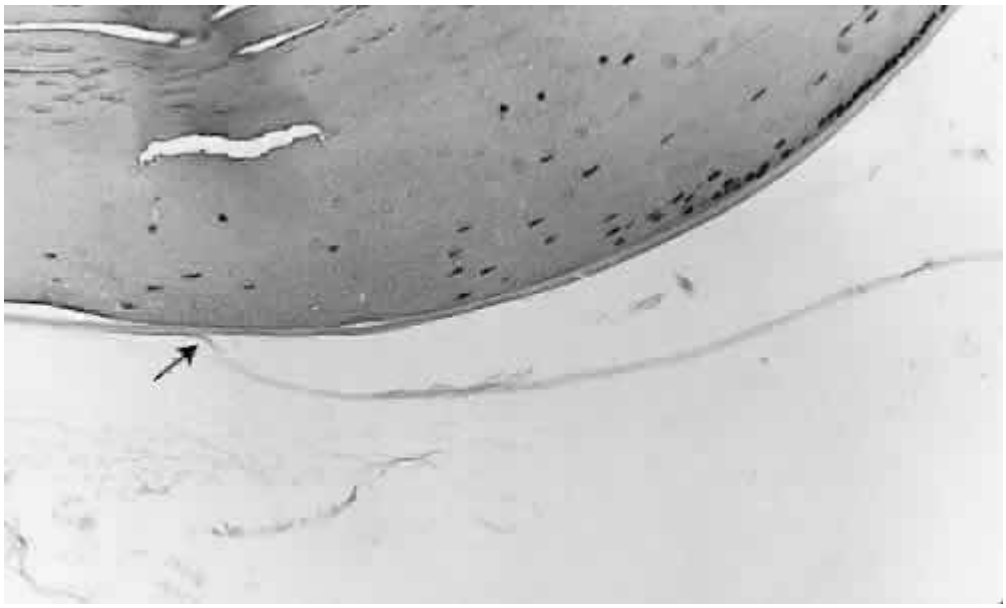

Figure 1.13: Junction of the anterior hyaloid membrane and the lens capsule: site of Wieger's "ligament" (*arrow*) (haematoxylin and eosin, × 220).
Adapted from http://www.oculist.net

the time. Tractional breaks associated with these are rare. However in the case of zonular loss, it is unknown whether the presence of these tufts increase the risk of RD.

This relationship between RD and EL is further corroborated by considering other conditions associated with non-traumatic EL. These include homocystinuria, (OMIM 236200)[221] (cystathionine beta-synthase gene), in which EL is the most common ocular feature. RD is a recognised complication of this metabolic disease, certainly if untreated[205, 222]. Furthermore, a more specific ocular phenotype includes Knobloch syndrome 1(OMIM 267750)[223] (*COL18A1* gene) and Knobloch syndrome 2 (OMIM 608454)[1] (*ADAMTS18* gene). Both these conditions are classically characterised by EL and RD (amongst other ocular phenotypes and occipital bone defect[224]). The cause of the RD in this rare condition may be a distinct vitreoretinopathy, or related to the EL. Other rare conditions associated with EL include Weill-Marchesani syndrome (WMS) [225] (*FBN1* and *ADAMTS10* genes), Weill-Marchesani like syndrome (WML) (OMIM 613195)[226] (*ADAMTS17* gene) and mutations in latent transforming growth factor-beta binding protein gene (*LTBP2*) (OMIM: 602091)[227]. These are discussed further in chapter 3. They are rare, and the incidence of RD in these conditions is inconclusive.

These conditions are characterised by defects in extracellular proteins; resulting in disrupted ECM. There are similarities therefore with defects resulting in inherited RD. It is possible that a common gene or pathway may be involved in both, unifying the phenotypes.

1.5. AIMS OF THESIS

The aims of this work are to investigate the genetic predisposition of Rhegmatogenous Retinal Detachment and Ectopia Lentis. These two closely related conditions have different genetic aetiologies. Working with numerous teams across four laboratories, three universities and one hospital, I have aimed in this thesis to investigate the genetic predisposition to these conditions. This involves techniques to investigate both Mendelian and non-Mendelian inheritance. Furthermore, I aimed to establish expression patterns within the eye of a gene and its protein which is common throughout this thesis. By furthering the understanding of both conditions independently; it may be possible to understand them in the context of each other.

CHAPTER 2: ECTOPIA LENTIS: GENOTYPE AND PHENOTYPE

Publications arising from work related to this chapter

(i) **Chandra** A, Aragon-Martin JA, Hughes K, Gati S, Reddy MA, Deshpande C, Cormack G, Child AH, Charteris DG, Arno G. A

A genotype-phenotype comparison of *ADAMTSL4* and *FBN1* in isolated ectopia lentis.

Invest Ophthalmol Vis Sci. 2012 Jul 24;53(8):4889-96

(ii) **Chandra** A. Patel D, Aragon-Martin JA., Pinard A., Collod- Béroud G., Comeglio P., Boileau C., Faivre L., Charteris DG., Child AH. Arno G.

The Revised Ghent Nosology; Reclassifying Isolated Ectopia Lentis.

Clinical Genetics [In press]

(iii) **Chandra** A, Ekwalla V, Child A, Charteris D.

Prevalence of ectopia lentis and retinal detachment in Marfan syndrome.

Acta Ophthalmol (Copenh) 2014 Feb; 92(1):e82-3

(iv) **Chandra** A, Banerjee PJ, Charteris DG.

Grading in ectopia lentis (GEL): a novel classification system.

British Journal of Ophthalmology 2013 Jul;97(7):942-3.

(v) **Chandra** A, Aragon-Martin JA, Sharif S, Parulekar M, Child A, Arno G

Craniosynostosis with ectopia lentis and a homozygous 20-base deletion in *ADAMTSL4*.

Ophthalmic Genet. 2013 Mar-Jun;34(1-2):78-82

2.1. INTRODUCTION

The most common cause of inherited Ectopia Lentis (EL) is considered to be MFS. As discussed in the general introduction, this condition is thought to be associated with an increased risk of Rhegmatogenous Retinal Detachment (RD)[185, 207]. However, the current rate of these two related ocular manifestations (RD and EL) in MFS was not clear. To answer this, we undertook a questionnaire survey (Appendix I) of 567 members of the Marfan Trust (UK) diagnosed with MFS.

185 (32.6%) completed questionnaires were returned (Male: 49%, Female: 51%; P=0.22). The mean age of this cohort was 47 years (M=48, F=47).

28 (15.1%) of respondents reported having had a RD between 1965 and 2011 (M: 17(61%), F: 11(39%)). The mean age of developing RD was 33 years, occurring earlier in women (25 years) than men (33 years) (P=0.019). 21% of those with RD had had previous lens surgery. 44% of those who had had RD surgery were affected bilaterally, whilst 13 (46%) had recurrence of RD.

56 MFS patients (30.2%) reported having had EL between 1955 and 2011. The mean age for EL diagnosis was 32 years (range 4-64, male mean age: 32 years; female mean age: 16 years (P=0.549)). 75% of those who had had surgery had bilateral lens surgery.

This survey lacked genetic data. It would be interesting to know if certain mutations in *FBN1* predispose to RD or any other manifestations of MFS.

It seems that RD occurred later than previous large studies[185]. It is of interest that women seem to have developed this earlier than men, and is a novel finding not described in MFS, other syndromic nor non-syndromic RD. Further differences from non syndromic RD include the high rate of bilateral RD, and recurrent RD. These figures agree with previous reports, suggesting recurrence to occur in 30-42% of MFS cases[207]. It appears that management of RD in MFS is more complicated with lower success rates than non syndromic RD.

21% of patients in our cohort who had had RD had previously had lens surgery, and it appears that EL surgery continues to be a risk for developing RD.

With regard to EL, we report it to have been bilateral in 75% of affected patients, perhaps because this questionnaire collected historical data; suggesting that over time, bilateral EL is more common. Although there is no statistical significance between the age of diagnosis of EL and gender, the trend of women being affected younger may need further confirmation.

Although there are limitations to questionnaire studies, including whether this cohort is representative, I believe that this work does provide further valuable insights. Clearer data can only be ascertained from large prospective epidemiological studies.

Beyond MFS, the most common inherited cause for EL, is isolated ectopia lentis (IEL). This condition describes, as the name implies, ectopia lentis with no other ocular or systemic features of other syndromes. These patients do not fulfil the Ghent criteria for MFS [186] (Appendix II) or resemble other syndromes. In many older series, this may represent misdiagnosis of these syndromes (MFS, Weill-Marchesani, Weill-Marchesani Like, Knobloch 1 & 2, Homocystinuria). Since the advent of modern molecular genetics, it is possible now to more definitely exclude most other causes.

2.1.1. AUTOSOMAL DOMINANT ISOLATED ECTOPIA LENTIS

Traditionally it is reported that IEL can be inherited in an autosomal dominant manner (OMIM 129600), most commonly caused by novel mutations in *FBN1* not described in patients with classical MFS[228]. There are many reports of pedigrees in which the classical features of MFS are not reported, but EL segregates in an autosomal dominant fashion[188, 229, 230]. However, these patients are likely to represent part of a phenotypic spectrum of MFS[231], and the exclusion of MFS in these patients must be undertaken carefully and in view of the most recent Ghent criteria for MFS[186]. For example, Edwards and colleagues presented a family with autosomal dominant EL with some mild skeletal features but no cardiological features of MFS[232], hence diagnosing IEL. However, the mutation they found in *FBN1* (R240C) was subsequently described in a family with classical MFS[233]. Because of the previous report of this mutation in MFS, the diagnosis would alter in this family to MFS, according to the most recent Ghent criteria[186]. Furthermore, it has been demonstrated with long term follow up that patients with IEL secondary to *FBN1* mutations may progress to develop cardiovascular features of MFS[234, 235]. It is therefore recommended that these patients have long term cardiology follow up[186].

2.1.2. AUTOSOMAL RECESSIVE ISOLATED ECTOPIA LENTIS

IEL can also be inherited in an autosomal recessive pattern (OMIM 225100). This has been established for over 70 years[236, 237]. Al Salem and colleagues[238], in 1990, were the first to describe detailed ocular phenotypes of two consanguineous families from Iraq and Jordan with recessive IEL. They were all diagnosed before the age of 10, and had no features of systemic syndromes. By a combination of linkage and fine mapping in the Jordanian family, Ahram and colleagues[2] 19 years later described a homozygous nonsense mutation in *ADAMTSL4* on 1q21.2. This gene encodes ADAMTS-Like 4 (A Disintegrin And Metalloproteinase with ThromboSpondin motifs Like -4). This was the first report of a genetic cause for autosomal recessive IEL. A splice site mutation in this gene was subsequently confirmed in a consanguineous family from Turkey[10]. It has since been described in sporadic, unrelated patients throughout Europe[7, 9]. Of further interest, the most common mutation in this gene as well as two novel missense mutations also appear to cause autosomal recessive ectopia lentis et pupillae[8, 30]. This does suggest that this gene may perhaps be involved in ocular development. Finally, RD was documented as a complication of numerous patients in these cohorts[8, 30, 238].

2.1.2.1. *ADAMTSL4*

The *ADAMTSL4* gene (OMIM 610113) is a member of the *ADAMTSL* (A Disintegrin And Metalloproteinase with Thrombospondin motifs Like) gene family. It is found on chromosome 1q21 and encodes the 1074 amino acid ADAMTS-Like 4 protein (NP_061905). *ADAMTSL4* consists of 17 coding exons and two untranslated exons, which span 11.5 kb of genomic sequence. ADAMTS-Like 4 is one of the family of 7 ADAMTS-Like proteins, themselves part of the Thrombospondin type 1 repeat (TSR) (see Section 5.1) superfamily of proteins. These 7 proteins are divided into two distinct clades, of which ADAMTS-Like 4 and ADAMTS-Like 6 form part of one clade, differing from ADAMTS-Like 1, ADAMTS-Like 3 and ADAMTS-Like 7 by lacking immunoglobulin repeat regions[21]. The function and disease associations of these proteins are as yet unclear, and thus comparisons between structure and function remain challenging. ADAMTS proteins (A Disintegrin And Metalloproteinase with ThromboSpondin motifs) comprise a protease domain and an ancillary domain, the latter of which determines substrate recognition and function in tissue specificity. ADAMTS-Like proteins are structurally similar to the ADAMTS ancillary domain,

including at least one TSR module. Although the TSR repeats are very closely related, ADAMTS-Like proteins lack the proteolytic domains found in ADAMTS proteins. This homology with the ancillary domain may suggest an inhibitory or enhancer relationship between the ADAMTS-Like and ADAMTS proteins. Alternatively this relationship may be of a competitive nature, or represent the formation of complexes between these proteins. However, these roles have not yet been clearly defined. ADAMTS-Like 4 contains seven Thrombospondin type 1 repeat domains, six of which are clustered towards the C terminus. These domains are found in numerous mammalian proteins and are thought to have a role in anchoring ADAMTS-like proteins to the extracellular matrix (ECM)[239]. Other domains present in the full-length protein are an ADAMTS spacer 1 domain, an ADAMTS cysteine rich module and a PLAC (Protease and Lacunin) domain.

The ADAMTS proteases are involved in maturation of procollagen (ADAMTS2, ADAMTS3, ADAMTS14) and von Willebrand factor (ADAMTS13). Additionally, they play a role in proteoglycanase activity as well as in ECM proteolysis relating to morphogenesis, angiogenesis, ovulation, cancer, and arthritis. ADAMTS-Like proteins lack the disintegrin-like domain thought to be essential in the protease domain and are therefore catalytically inactive. On this basis, it is suggested that they may have an architectural or regulatory role within the ECM, or a possible regulatory role of ADAMTS proteases.

The ocular localisation of ADAMTS-Like 4 and its encoding mRNA in ocular tissue is discussed in Chapter 5.

2.2. AIMS

The aim of this chapter is to investigate the genotype-phenotype relationship of the two most important genes causing isolated ectopia lentis (*FBN1* and *ADAMTSL4*). It is hoped to further understanding of the role mutations in ADAMTS-Like 4 may play in ocular phenotype. Furthermore, a novel clinical grading system for ectopia lentis was devised and verified.

2.3. METHODS

2.3.1. PHENOTYPING

Consecutive patients diagnosed with IEL (present or previously operated upon), were identified and invited to participate in the study. IEL was diagnosed by exclusion of other systemic and ocular conditions associated with EL. In particular MFS was excluded by assessing against the current Ghent criteria[186].

Ophthalmic examination included visual acuity measurement, slit lamp examination, Goldmann applanation tonometry for intraocular pressure measurement, gonioscopy, dilated examination of lens and fundus, fundal photography, spectral domain optical coherence tomography, corneal pachymetry and topography analysis (Pentacam high-resolution rotating Scheimpflug imaging system [Pentacam HR, Oculus, Wetzlar, Germany]), and axial length measurement (IOL Master [Carl Zeiss Meditex, Jena, Germany]). Statistical analysis (descriptive analysis and Mann–Whitney U test where appropriate) was performed by using SPSS for Windows version 19.0 (SPSS Inc., Chicago, IL). Systemic examination included measurement of arm span, upper and lower segment height, skeletal examination (palate, scoliosis, pectus deformity, and acromegaly), and Beighton score analysis of joint hypermobility[136] (Appendix III).

If not previously done, echocardiography was performed by my colleague Dr Anne Child at the cardiological genetics department at St George's Hospital, London. Two-dimensional echocardiography was performed with either the Philips iE33 or Vivid 7 (GE Medical Systems, Milwaukee, WI). Standard cardiac views were obtained and analysed according to protocols specified by the European Society of Echocardiography[240] and the American Society of Echocardiography[241]. Left ventricular (LV) wall thickness, left atrial diameter, LV diameter, LV mass, transverse aortic root dimension, and diastolic function were measured.

2.3.2. PHLEBOTOMY

After informed consent, 10ml of venous blood was extracted from patients and stored at -30^0C until ready for transportation to the Sonalee Laboratory at St George's University of London where the genetic analysis was performed on DNA from these samples, under the supervision of Dr Jose Aragon Martin and Dr Gavin Arno.

2.3.3. DNA EXTRACTION

The FlexiGene DNA kit (Qiagen, Hilden, Germany) was used to extract DNA. Firstly, lypholised Qiagen protease was suspended with 50µl of hydration buffer (FG3). This was then divided into aliquots and stored at -20^{0}C.

Blood was rapidly thawed in a 37^{0}C water bath before DNA extraction. During this process, denaturation buffer (FG2) was mixed with the reconstituted protease. For each DNA sample, 1ml of FG2 was mixed with 10µl of the protease solution.

5ml of lysis buffer FG1was mixed with 2ml of whole blood, mixed and centrifuged for 5 minutes at 2000 x g (Thermo Scientific Heraeus Multifuge X3R Centrifuge). This causes lysis of red blood cells. The supernatant was discarded leaving a small pellet of leucocytes. 1ml of Protease/FG2 mixture was then added resulting in proteolysis. The mixture was vortexed till completely homogenised. This sample was then incubated at 65^{0}C for 10 minutes in a water bath.

1ml of 100% isopropanol was added and mixed with the sample. This leads to precipitation of DNA out of solution; which is at this stage visible. The mixture was then centrifuged for 3 minutes at 2000 x g. The supernatant was discarded, leaving a pellet of DNA. 1 ml of 70% ethanol was added to clean the sample. After vortex mixing, the mixture was centrifuged for 3 minutes at 2000 x g. The supernatant was discarded and the pellet of DNA was left to air dry, before 200µl of FG3 (hydration buffer) was added and the mixture then incubated in a water bath at 65^{0}C for 1 hour to aid hydration of the DNA.

2.3.4. DNA QUANTIFICATION

This DNA solution was then quantified; in terms of DNA concentrations and purity. Spectrophotometric analysis (Thermo Scientific NanoDrop 2000 – Thermo Fisher Scientific Inc.) was utilised. This method is based upon absorption of ultraviolet light (260nm) by nucleic acids. Using Beer-Lambert law for absorption of light, the spectrophotometer relates the light absorption to the concentration of nucleic acids. Purity is measured by comparing the absorption of 260nm and 280nm light (260:280). This ratio is used as the most common contaminants (proteins) absorb 280nm. The 260:280 has a high sensitivity for nucleic acids, and is little influenced by protein contamination; secondary to the higher extinction coefficient nucleic acids have at 360nm and 280nm

compared to proteins. Protein contamination therefore contributes little error to DNA quantity estimation.

Based on the concentrations, an aliquot of nucleic acids at concentration 50ng/µl were prepared. This is calculated with the below equation:

$$C1V1 = C2V2$$

(C1 = Concentration of Stock DNA sample, V1 = Volume to be extracted from stock, C2 = 50ng/µl (required concentrations for PCR), V2 = 50µl (final volume of working DNA solution))

2.3.5. PRIMER DESIGN

Primers were designed using Primer3[242] software. Polymerase Chain Reaction (PCR) primers ideally had GC content between 50-60%, minimally self-complimentary, and between 18-28 nucleotides. PCR primers ideal annealing temperature were aimed to be similar ($<5^0$C difference). Primers with significant similarity to other nucleotide sequence through the genome were dismissed (checked on NCBI BLAST website: http://blast.ncbi.nlm.nih.gov/). Primers were designed to produce Amplimer lengths of up to 1000 nucleotides. Optimisation included assessing optimal melting temperatures (Tm) and requirement of DMSO (Dimethyl sulphoxide). Primers did not produce secondary structures.

2.3.6. *ADAMTSL4* AMPLIFICATION METHODS

In designing primers, *ADAMTSL4* complimentary DNA (cDNA) sequence according to GenBank (RefSeq NM_019,032.4) was used, with the A of the ATG translation initiation codon as nucleotide 1. The initiation codon is identified as codon 1.

Primers, product size and annealing temperatures for *ADAMTSL4* sequencing are in Appendix IV:

PCR is a method of amplifying small fragments of DNA [243]. PCR was performed using Platinum ® Taq DNA Polymerase (Invitrogen, USA).

The reaction mix for each primer pair was prepared on ice. A master mix was prepared for the number of reactions to be undertaken. Per exon per DNA sample, 2µl of 10x PCR

buffer was added to 1.2µl of 25mM $MgCl_2$., 2µl of 2mM Deoxyribonucleotide triphosphate (dNTP), 11.3µl H_2O and 1.6µL Dimethyl sulfoxide 8% (DMSO). 0.4µl of forward and reverse primer (10mM) were then added. Finally 0.1µl Taq polymerase (5U/µl) was taken from the freezer and added. The protocol used for each primer is elaborated in Appendix V.

This mixture was added to 1µl of DNA in the well of a 96 well plate. The samples were mixed thoroughly before PCR cycling. The cycles were as below:

1. 95^0C initial denaturation (2 min)
2. 95^0C denaturation (1 min),
3. Annealing temperature (dependant on the primer set) 1 min (57^0C)
4. 72^0C elongation (1 min).
5. 72^0C for 10 minutes for final elongation of the PCR products.
6. 4^0C for 10 minutes for termination.

2-4: Repeated 40 cycles

At this juncture, a 2% agarose electrophoresis gel was prepared. This included 250ml of Tris Boric Acid EDTA solution mixed with 5g of Agarose. This solution was warmed in a microwave to melt the agarose, after which, 25µl of ethidium bromide was added to this liquid gel. Ethidium bromide is an intercalating agent which fluoresces brightly when exposed to ultraviolet light. This mixture was poured into an electrophoresis tray to cool.

2.3.7. *FBN 1* AMPLIFICATION METHOD

FBN1 is a 65 exon gene covering approximately 237.4kb on 15q21.1. In designing primers, *FBN1* cDNA sequence according to GenBank (RefSeq NM_000,138.3, provided in the public domain by http://www.ncbi.nlm.nih.gov/gene) was used, with the A of the ATG translation initiation codon as nucleotide 1. The initiation codon is identified as codon 1.

Primers used for PCR and sequencing this gene are in Appendix VI. The PCR mix for the different exons is documented in Appendix VII. The cycles used are in table 1.

PROTOCOL 1			PROTOCOL 2		
1	95^0C	5 mins	1	95^0C	5 mins
2	95^0C	30Secs	2	95^0C	30Secs
3	58^0C	30Secs	3	54^0C	30Secs
4	56^0C	30Secs	4	52^0C	30Secs
5	54^0C	30Secs	5	50^0C	30Secs
6	72^0C	30Sec	6	72^0C	30Sec
7	72^0C	5 mins	7	72^0C	5 mins

Table 1 PCR cycle for amplification of *FBN1*

Protocol 1, Steps 2-6 were repeated 35 times for Exons 1, 4, 6, 8-19, 22-26, 29-30, 32-34, 36-37, 39-42, 44-46, 48, 50-51, 53-56, 58-65.

Protocol 1, Steps 2-6 were repeated 40 times for Exons 2, 3, 5, 7, 15, 21, 27, 35, 38, 43, 47, 49, 57

Protocol 2, steps 2-6 were repeated 40 times for Exons 20, 28, 31, 52.

2.3.8. AGAROSE GEL ELECTROPHORESIS

After PCR cycling for either gene, 2µl of PCR product was mixed with the loading dye. This consisted of 30% glycerol, 0.25% bromophenol blue and Xylene cyanol and dionised water. The mixture was then loaded into individual wells within the gel. Adjacent to each Exon PCR products was loaded a DNA size ladder (Bioline Hyperladder IV, London, UK). The electrophoresis was run for 20 minutes at 220V constant voltage. The separated fragments were visualised on a transilluminator (UV light of wavelength 210nm) (BioRad) and photographs were taken with an orange filtered camera.

2.3.9. PURIFICATION OF PCR PRODUCTS

After electrophoresis, and the correct sized fragments were verified by agarose gel electrophoresis, the products underwent enzymatic clean-up to eliminate unincorporated primers and dNTPs. This was done using Exonuclease-1 (EXO) and Shrimp Alkaline Phosphatase (SAP) (ThermoFisher Scientific, Walton, Massachusetts, USA). Exonuclease-1 degrades single stranded DNA in a 3' to 5' direction, releasing deoxyribonucleoside 5'-monophosphates in a stepwise manner. This releases dNTPs from the unincorporated primers. SAP catalyses the release of 5'- and 3'-phosphate groups from extra nucleotides. The mixture was as below:

SAP (1U/µl) (240µl), Dilution Buffer (120µl), Exonuclease-1 (20U/µl: 6µl) were combined and 3.2µl of this mixture was added to each PCR product. The resultant mixture was incubated at 37^0C for 1 hour, followed by 80^0C for 15 minutes. The products were then stored at -20^0C.

2.3.10. SEQUENCING

The cleaned products were sequenced using Big Dye Terminator Cycle Sequencing Kit (containing Taq DNA Polymerase, dNTPs, ddNTPs-Dye terminators, MgCl2 buffer)(Applied Biosystems). The protocol used for the sequencing reaction is tabled below (Table 2):

Constituent	Volume
Big Dye 3.1 (1X)	1µl
Primer (1µM)	1µl (Forward) or 1µl (Reverse)
PCR Product	1µl
dH_2O	6µl
TOTAL	10µl

Temperature (0C)	Time	Number of cycles
95	4m	1
95	10s	30
57	15s	
60	4m	
4	10m	1

Table 2: BIG DYE mixture and Cycle for sequencing

The Qiagen DyeEx purification plates were centrifuged in order to remove the storage buffer from the sephadex gel column. The sequence reaction was then transferred to the column and centrifuged again (1000 x G at 3 mins – Thermo Scientific HEaeus Multifuge X3R Centrifuge). The elutant was the purified sequencing product. It was then incubated at 85^0C for 20 minutes for evaporation. 12µl of Formamide was then added to resuspend the samples. The samples were heated for 4 minutes at 95^0C; to denature the samples. The samples were then sequenced employing an ABI 3130XL genetic analyser using standard protocols.

The results were read using FinchTV (Version 4.0) (Geospiza, Inc.; Seattle, WA, USA; http://www.geospiza.com).

Mutations were then verified. In silico websites were used to verify the pathogenicity of mutations. These included SIFT[244], Polyphen[245]. Furthermore, we confirmed absence of these mutations in 160 unrelated chromosome controls. We also confirmed their absence from population databases, such as the Exome Variant Server[246], Genebank dbSNP library[247] or 1000 Genome[248].

2.3.11. GRADING SYSTEM

During the recruitment and analysis of this study, it became apparent that no unified clinical grading system existed for EL.

A novel grading in ectopia lentis (GEL) classification system was thus created to encompass the full possibilities of lens movement. This was to be judged on pharmacologically dilated pupils. Primarily, subluxation (Sub) was defined as movement of the lens within the iris-lens diaphragm, whilst dislocation (D) was defined as complete movement either anteriorly (DA) into the anterior chamber or posteriorly (DP) into the vitreous cavity. Subluxation was categorised by direction and extent of lens movement as follows:

Direction was described as such: superiorly (SubS), superonasally (SubSN), nasally (SubN), inferonasally (SubIN), inferiorly (SubI), inferotemporally (SubIT), temporally (SubT) and superotemporally (SubST).

Extent was coded as to whether the lenticular edge had passed the central pupillary axis or not; graded as 2 or 1 respectively.

For example a left eye lens which has moved superotemporally beyond the pupillary axis is graded SubST2 (Figure 2.1) , a right eye lens which has moved inferonasally but not beyond the pupillary axis is graded SubIN1 (Figure 2.2). See Table 3.

55 clinical images of EL were acquired from hospital databases, and 11% of these patients were clinically validated. Such a proportion has previously been used[249]. Two ophthalmologists assessed these images and patients independently at two separate time points 8 weeks apart. One non-ophthalmic physician also assessed the images. All involved used the GEL classification to grade the EL. Cohen's Kappa coefficient was calculated for inter and intra observer reliability.

2.4. RESULTS

Eighteen unrelated consecutive patients diagnosed with IEL were recruited. One patient was found to have a *FBN1* mutation which has been previously reported in classical MFS (see below). Although no cardiac and skeletal features of MFS were present, this patient was re-diagnosed as MFS according to the revised Ghent criteria[186]. A further patient, on ophthalmic examination, was clarified to have ectopia lentis et pupillae (ELetP). Detailed ocular phenotyping was therefore undertaken in 16 unrelated patients with IEL, and one patient with ELetP (Figure 2.3a). Two patients were bilaterally phakic (Figure 2.3b), and one patient was aphakic secondary to posterior lens dislocations. All other patients had had ocular surgery in the past for EL: two via an anterior segment approach, and the remainder via a posterior approach.

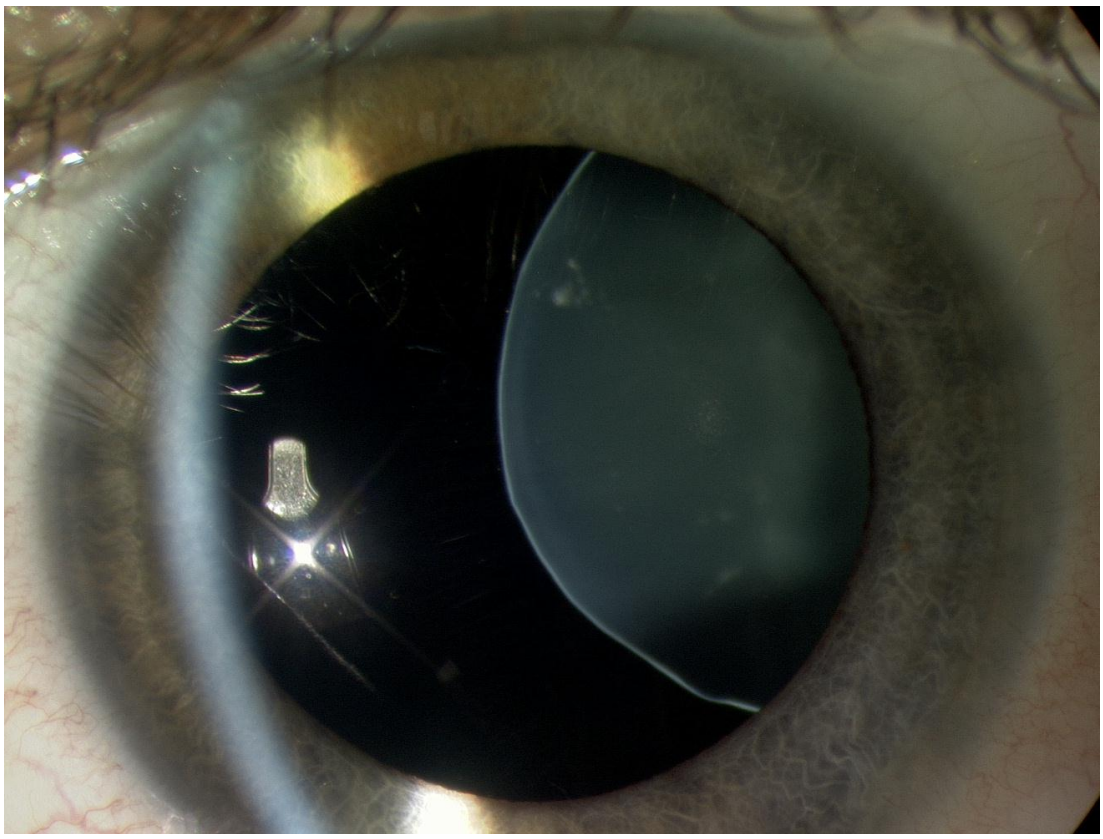

Figure 2.1: SubST2 (Left Eye)

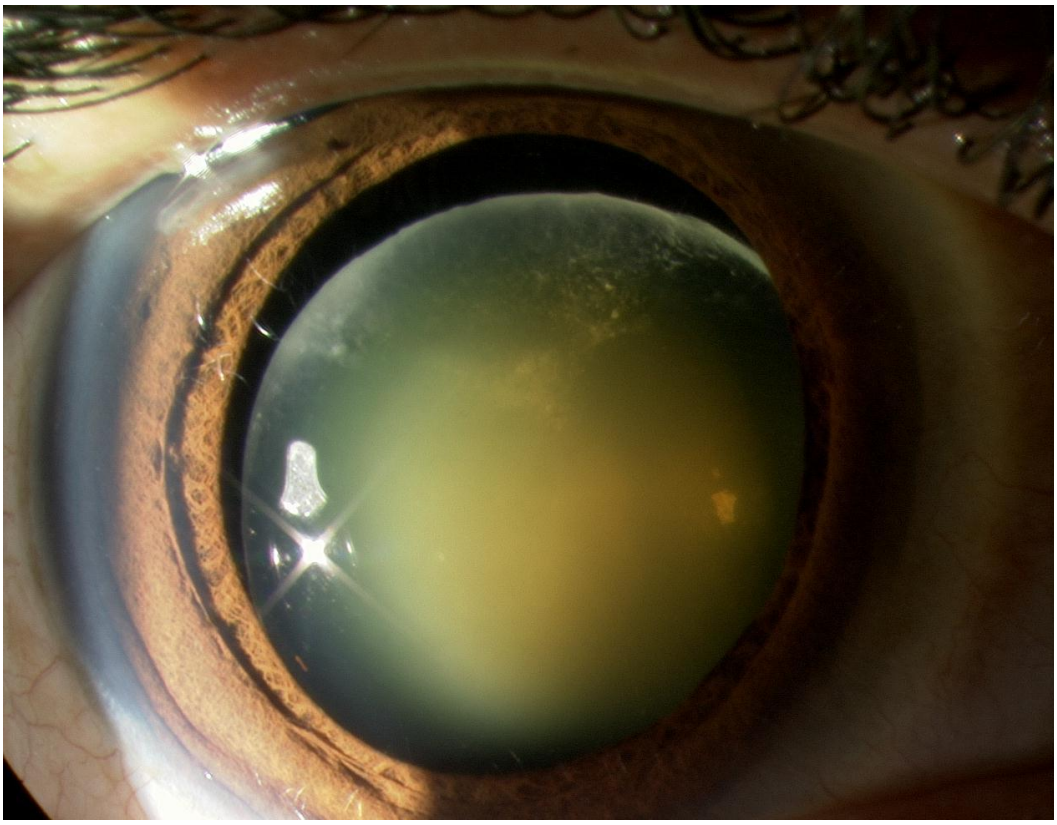

Figure 2.2: SubIN1 (Right Eye)

MOVEMENT	DIRECTION	EXTENT	CODE
Dislocation	Anterior	-	DA
	Posterior	-	DP
Subluxation	Superiorly	1	SubS1
		2	SubS2
	Superior Nasal	1	SubSN1
		2	SubSN2
	Nasal	1	SubN1
		2	SubN2
	Inferonasal	1	SubIN1
		2	SubIN2
	Inferior	1	SubI1
		2	SubI2
	Inferior temporal	1	SubIT1
		2	SubIT2
	Temporal	1	SubT1
		2	SubT2
	Superotemporal	1	SubST1
		2	SubST2

Table 3: GEL Classification system

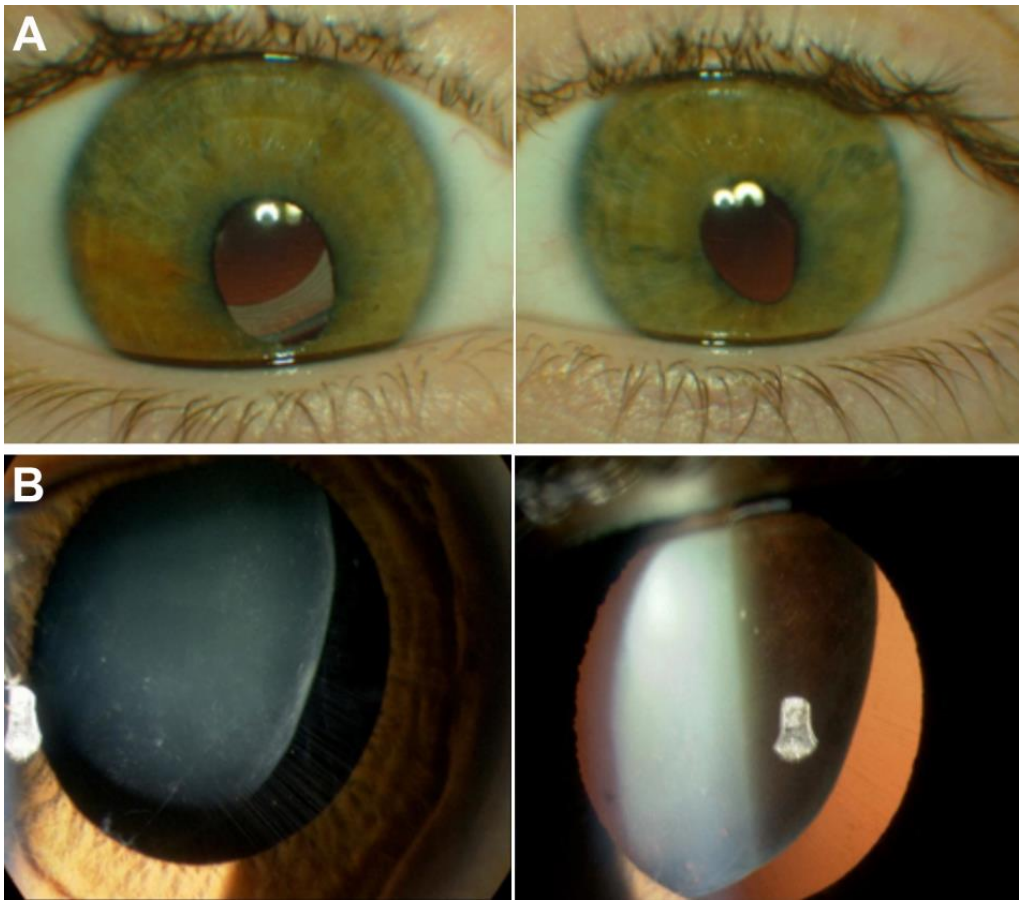

Figure 2.3: Clinical image of ectopia lentis.
(A): Patient with Ectopia Lentis & Pupillae
(B) Isolated ectopia lentis in a patient with a homozygous c.767_786del20 (p.Gln256Profs*38) mutation in *ADAMTSL4*.

2.4.1. GENETICS

2.4.1.1. *FBN1*

Four patients (25%) were discovered to have heterozygous mutations in *FBN1* (Table 4, Figure 2.4) which have not previously been reported in MFS. Three of these: c.2473C>T (p.Pro825Ser) (Figure 2.4a), c.3464A>G (p.Asp1155Gly) (Figure 2.4b), c.4259 G>A (p.Cys1420Tyr) (Figure 2.4c), are missense mutations. The first affects a consensus amino acid in a cbEGF-like domain whilst the second results in a change of a cysteine residue within a cbEGF-like domain. In silico analysis (SIFT[244], PolyPhen[245]) revealed these mutations to be pathogenic. The third affects a non-consensus amino acid in a cbEGF-like domain of fibrillin-1, and has previously been reported in a patient with a fibrillinopathy not fulfilling the Ghent criteria[250]. The fourth is an intronic mutation (c.1327+1 G>A) (Figure 2.4d) in IVS10 predicted to abolish a splice donor site[251]. A further patient (a female diagnosed with IEL at 46 years of age with no cardiovascular features of MFS), was found to have a missense mutation in *FBN1* (c.3344A>G (p.Asp1115Gly)) (Figure 2.4e), which has previously been reported in classical MFS[252]. Her diagnosis was therefore altered to MFS and she was not included for analysis in this study. The final study group thus consisted of seventeen patients.

2.4.1.2. *ADAMTSL4*

Nine patients (53%) were found to have mutations in *ADAMTSL4* which were thought to be causative. Six (66.7%) were homozygous for a nonsense 20 base pair deletion (c.767_786del20 (p.Gln256Profs*38)) (Figure 2.5). This mutation results in a frameshift leading to a premature termination codon (PTC) after 38 codons of altered reading frame.

The remaining three patients were presumed compound heterozygotes for *ADAMTSL4* mutations. These included four novel mutations (Table 5 & 6) in exons 5 and 6 for IEL, and exon 14 for ELetP (Figure 2.6). The patient with ELetP was presumed compound heterozygous for two mutations; the 20 base pair deletion (above) and a novel mutation: c.2270dupG (p.Gly758Trpfs*59). Segregation analysis was not possible for the compound heterozygous mutations. The mutations were thus termed “presumed heterozygous”, as it was not possible to determine whether mutations were in cis- or trans-. All mutations are nonsense, resulting in a PTC. One additional patient

PATIENT	FH	Consanguinity	Origin	Genetic Mutation			
				Nucleotide	Amino acid	Exon	Zygosity
1	No	No	White British	c.2473C>T	p.Pro825Ser	20	HETEROZYGOUS
2	No	No	White British	c.3464A>G	p.Asp1155Gly	28	HETEROZYGOUS
3	No	No	White Polish	c.4259 G>A	p.Cys1420Tyr	34	HETEROZYGOUS
4	No	No	White British	c.1327+1 G>A	splice site mutation	10	HETEROZYGOUS

Table 4: Genetic information of patients with IEL and *FBN1* mutations

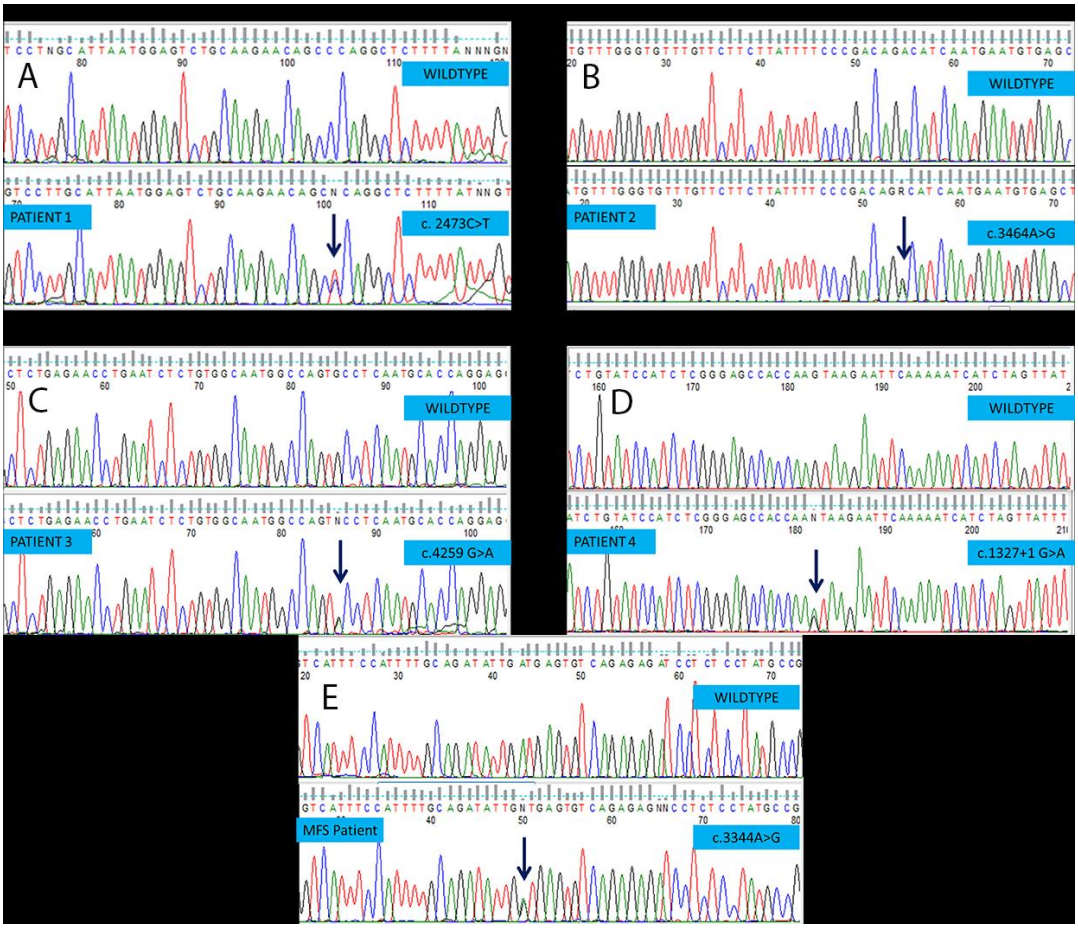

Figure 2.4:*FBN1* mutations in ectopia lentis.
A-D: Mutations found in isolated ectopia lentis caused by *FBN1* mutations.
E: Mutation previously described in MFS, found in patient with apparent IEL.

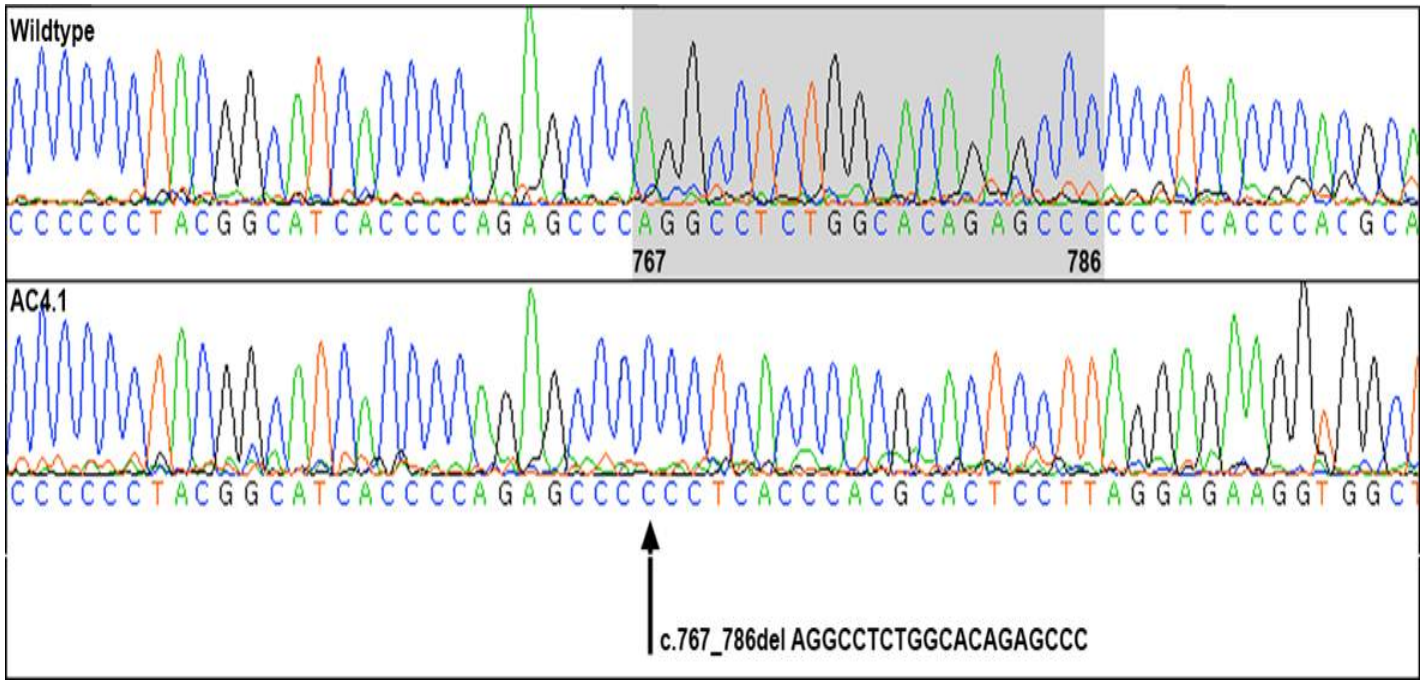

Figure 2.5: Homozygous 20 base-pair mutation (c.767_786del20 (p.Gln256Profs*38)) in *ADAMTSL4* found in six of our cohort. This mutation has been described throughout Europe[7-9].

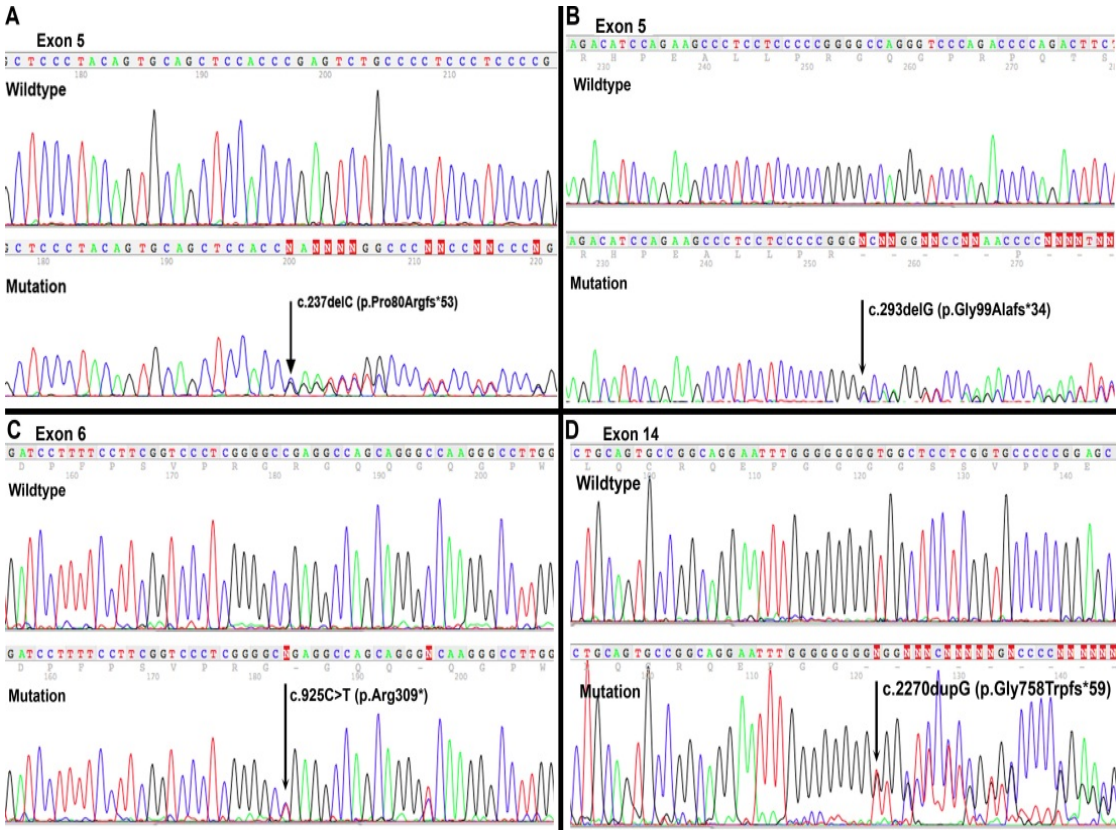

Figure 2.6: Sequence chromatographs showing novel mutations in *ADAMTSL4*

PATIENT	FH	Consanguinity	Origin	Genetic Mutation			
				Nucleotide	Amino acid	Exon	Zygosity
8	No	No	White British	c.767_786del20	p.Gln256Profs*38	6	HETEROZYGOUS
9	No	No	White British	c.767_786del20	p.Gln256Profs*38	6	HOMOZYGOUS
10	No	No	White British	c.767_786del20	p.Gln256Profs*38	6	HOMOZYGOUS
11	No	No	White British	c.767_786del20	p.Gln256Profs*38	6	HOMOZYGOUS
12	No	No	White British	c.293delG c.925 C>T	p.Gly99Alafs*34 p.Arg309*	5 6	PRESUMED COMPOUND HETEROZYGOUS
13	No	No	White British	c.237delC c.767_786del20	p.Pro80Argfs*53 p.Gln256Profs*38	5 6	PRESUMED COMPOUND HETEROZYGOUS
14	No	No	White British	c.767_786del20	p.Gln256Profs*38	6	HOMOZYGOUS
15	No	No	White British	c.767_786del20	p.Gln256Profs*38	6	HOMOZYGOUS
16	No	No	White British	c.767_786del20	p.Gln256Profs*38	6	HOMOZYGOUS
17	No	No	White British	c.767_786del20 c.2270dupG	p.Gln256Profs*38 p.Gly758Trpfs*59	6 14	PRESUMED COMPOUND HETEROZYGOUS

Table 5: Genetic information of patients with IEL and *ADAMTSL4* mutations

Patient 8: Heterozygous mutation not thought to be causative

EXON/ INTRON	MUTATION	REFERENCE
Exon 11	11:c.1785T/G	Ahram *et al* (2009)[2]
Intron 4	IVS4-1G>A/	Greene *et al* (2010)[10]
Exon 5	**c.293delG**	Chandra (2012)[27]
	c.237delC	Chandra (2012)[27]
Exon 6	c.767_786del	Aragon Martin (2010)[7] Neuhann (2010)[9] Christensen (2010)[8]
	c.826_836del	Aragon Martin (2010)[7]
	c.926G>A	Aragon Martin (2010)[7]
	c.925 C>T	Chandra (2012)[27]
Exon 12	c.2008C>T	Aragon Martin (2010)[7]
	c.1960C>T	Aragon Martin (2010)[7]
Exon 14	**c.2270dupG**	Chandra (2012)[27], Sharifi (2013)[30]
	c.2254C>T	Sharifi (2013)[30]
Exon 19	c.3153C>A	Aragon Martin (2010)[7]
	c.3161A>G	Aragon Martin (2010)[7]

Table 6: Published mutations in *ADAMTSL4* causing EL. (Mutations in bold first described by this work)

(patient 8) was found to only have a heterozygous c.767_786del20 mutation. No other mutations were found in *ADAMTSL4* or *FBN1*. This mutation does not cause EL in heterozygous carriers. This patient was thus placed in the "unknown cause" group.

Unknown: Four patients (25%) were not found to have any causative mutations in *FBN1* or *ADAMTSL4*, including the patient described above with a heterozygous *ADAMTSL4* mutation. Two patients had affected family members. Case 5 (male) has reportedly 2 affected brothers. Case 6 has an affected maternal aunt. These suggest non-autosomal dominant inheritance. Family members are not available for analysis.

The *FBN1* and *ADAMTSL4* mutations described here were not observed in the control group. Furthermore, they are not reported in the Genbank dbSNP library[247], 1000 Genomes[248] or in the Exome Variant Server[246].

2.4.2. CARDIOVASCULAR FINDINGS

All patients were normotensive (<140/90mmHg) and none were found to have abnormal indices of left ventricular or atrial dimensions, aortic root dimension or left ventricular function. There were no differences between groups.

2.4.3. MUSCULOSKELETAL FINDINGS

Two patients had normal range Beighton joint hypermobility scores of 2/9. All others scored 0. No patients had any skeletal features of connective tissue disorder or MFS.

2.4.4. OPHTHALMOLOGICAL PHENOTYPE

16 patients with IEL and one with ELetP (Figure 3a) were examined. Ophthalmic parameters were measured for each individual eye, and a mean calculated per patient (Table 7). The mean values for all patients with were then used in statistical analysis.

2.4.4.1. AGE OF DIAGNOSIS

For the purpose of analysis, patients who reported the diagnosis of congenital EL were allocated the age of onset of 0.5 years. The median age of diagnosis of EL was 35 years old (range 15-46) in *FBN1* group, 8.5 years (range 3-47) in the *unknown* group and 2 years (range 0.5-46) in the *ADAMTSL4* group. 9 out of the 10 in the *ADAMTSL4* group were diagnosed in childhood. One patient (patient 13, Table 5) was diagnosed at 46

years old. Two explanations may account for this late diagnosis. Firstly the patient was found to have a novel mutation in exon 5, and it is possible that this mutation somehow protects from an early manifestation of EL. However, she admits to poor vision most of her life, and at diagnosis was found to have significant EL. It is more likely that her vision was affected by EL at an earlier age, which was not diagnosed. Excluding this outlier, the median age of diagnosis of EL in the *ADAMTSL4* group was 2 years (range 0.5-9). Comparing the mutation groups revealed that patients with *ADAMTSL4* mutations were affected by IEL at a significantly younger age than those with *FBN1* mutations (Figure 2.7a) (2 years v 35 years, P<0.01).

2.4.4.2. AXIAL LENGTH

Patients 16 and 17 (ELetP) were examined at 8 years and 11 years of age. All others were assessed as adults (>18years old). We excluded axial length of the children in the analysis, as AL in this age range is not comparable to adults[253]. Mean axial length was 22.74mm (95%CI: 21.3-24.2) for the *FBN1* group, 27.54mm (95%CI: 24.2-30.9) in the *ADAMTSL4* group and 24.55mm (95%CI: 18.8-30.3) for the unknown group. Comparing the two mutation groups (Figure 2.7b) revealed that patients with *ADAMTSL4* mutations had significantly longer axial lengths (P<0.01). If the axial length of the children with IEL are included, analysis still reveals the difference to be significant (P=0.01).

2.4.4.3. VISUAL ACUITY

Mean ETDRS letters score was 59 (95%CI: 17-101) for the *FBN1* group, 58 (95%CI: 44-73) for the *ADAMTSL4* group and 72 (95%CI: 60-83) for the *unknown* group. The differences were not significant.

2.4.4.4. CORNEAL THICKNESS

Mean corneal thickness was 410.2µm (95%CI: -26-846) for the *FBN1* group, 566.1 (95%CI: 515.3 – 616.8) for the *ADAMTSL4* group and 561.1µm (95%CI: 552.4 – 569.8) in the *unknown* group (Not significant).

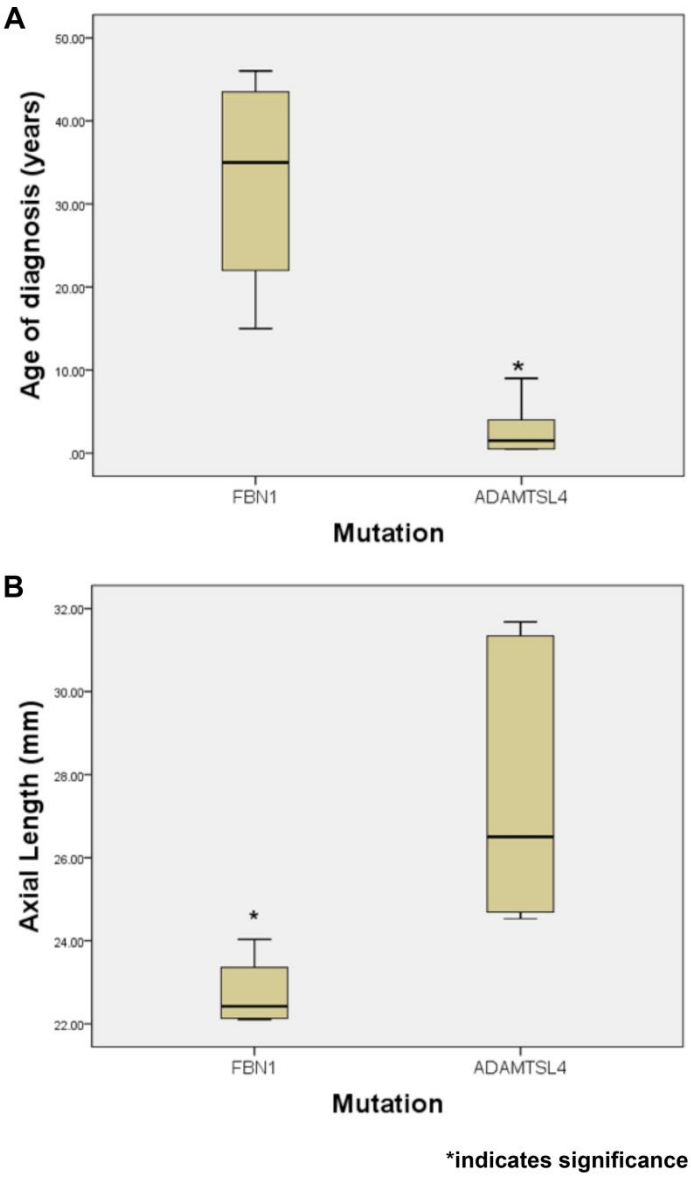

Figure 2.7: Features of ectopia lentis.
(A): Age of diagnosis (years) of isolated ectopia lentis in patients found to have *FBN1* or *ADAMTSL4* mutations.
(B): Axial length (mm) in patients diagnosed with isolated ectopia lentis secondary to *FBN1* or *ADAMTSL4* mutations.

2.4.4.5. CORNEAL POWER

Mean corneal refractive power was 40.9D (95%CI: 40.0-41.8) in the *FBN1* group, 41.5D (95%CI: 39.7-43.3) in the *ADAMTSL4* group and 41.7D (95% CI: 39.6 -43.8) in the *unknown* group (Not significant).

2.4.4.6. FOVEAL THICKNESS

Mean foveal thickness was 352.5µm (95%CI: -73.2 – 778.2) for the *FBN1* group, 302.4µm (95%CI: 251.8 – 353.0) for the *ADAMTSL4* group and 359.5µm (95%CI: 306.5 – 412.5) in the *unknown* group (Not significant).

2.4.4.7. INTRA OCULAR PRESSURE

Mean intraocular pressure (IOP) was 16.9mmHg (95%CI: 13.7-20.1) in the *FBN1* group, 16.6mmHg (95%CI: 13.7-19.6) in the *ADAMTSL4* group and 18mmHg (95%CI: 12.9-23.1) in the *unknown* group (Not significant).

2.4.4.8. OPTIC DISC FEATURES

Mean cup: disc was 0.25 (95%CI: 0.02-0.48) in the *FBN1* group, 0.2 (95%CI: 0.1-0.3) in the *ADAMTSL4* group and 0.36 (95%CI: 0.16-0.56) in the *unknown* group (Not significant).

No difference was observed in any features of the optic nerve head.

2.4.4.9. OTHER OPHTHALMIC FEATURES

No pattern was noted with regard to the direction of lens subluxation or dislocation. Furthermore, gonioscopy did not reveal any unusual anterior segment drainage strands. All angles were open ($>45^0$) at the time of examination. No significant pattern was observed for other associated ophthalmic conditions. A summary of the ophthalmic phenotype of this cohort is in table 7.

PATIENT	Age (yrs)	Sex	Genetic Mutation	Age of Diagnosis (yrs)	Axial Length (mm)	Vision (ETDRS letters)	Direction of subluxation	Surgery	Other Ophthalmic disorderds
1	55	M	*FBN1*	46	24.03	46.50	Nasal	PPV	Nil
2	70	M	*FBN1*	29	22.16	84.50	Inferior	PPV	Nil
3	18	F	*FBN1*	15	22.68	77.50	Temporal	Nil	Nil
4	64	F	*FBN1*	41	22.10	28.50	Inferior	PPV	Narrow angles
5	58	M	*U*	47	24.15	79.50	Nasal	PPV	Nil
6	27	M	*U*	3	29.16	68.00	Inferior	PPV	Exophoria
7	13	F	*U*	11	20.32	76.50	Inferior	PPV	Nil
8	57	M	*ADAMTSL4*	6	24.60	64.00	Temporal	PPV	Nil
9	45	F	*ADAMTSL4*	2	27.12	84.50	Temporal	PPV	Exophoria
10	62	F	*ADAMTSL4*	9	31.34	67.00	Posterior	Nil	Staphyloma
11	31	F	*ADAMTSL4*	C	24.53	54.50	Posterior	PPV	Exotropia
12	20	M	*ADAMTSL4*	C	25.89	68.50	Posterior	PPV	RD
13	46	F	*ADAMTSL4*	46	21.49	77.5	Nasal	Phaco	Nil
14	38	F	*ADAMTSL4*	1	31.68	41.50	Superior	PPV	Staphyloma
15	19	M	*ADAMTSL4*	4	24.69	46.00	Temporal	Nil	Nil
16	8	M	*ADAMTSL4*	2	22.73	45	Inferonasal	Nil	Nil
17	11	F	*ADAMTSL4*	2	20.99	71.5	Superior	Phaco	ELetP

Table7: Ocular phenotype of IEL patients

U: No mutation found, C: Congenital PPV: Pars Plana vitrectomy, Phaco: Phacoemulsification, RD: Rhegmatogenous Retinal Detachment, ELetP: Ectopia lentis et pupillae

2.4.5. CRANIOSYNOSTOSIS and ECTOPIA LENTIS

In addition to this cohort, DNA was analysed from a further patient referred to our group from another ophthalmic unit. Although this patient was not part of this initial study, the phenotype was recorded and genetic analysis was undertaken.

2.4.5.1. PHENOTYPE

The proband was one of non-identical triplets born at 30 weeks gestation by elective caesarean section due to maternal hypertension, after assisted pregnancy using parental ova and sperm. She weighed 2lb 10ozs at birth, and was healthy. She had a patent ductus arteriosus (PDA), which was closed using indomethacin. She was noted to have two haemangiomas. Her two sisters also had PDA and one had a haemangioma.

At 10 weeks of age she was noted to have right coronal craniosynostosis (CS), with secondary facial asymmetry, requiring fronto-orbital advancement. Compared to her sisters, the proband's early developmental milestones were slightly delayed, with speech at 18 months, and walking at 2 years. On examination at age 10 she had slight facial asymmetry with right eye higher than left. She has no other features to suggest MFS. Further examination revealed a normal echocardiogram.

She presented with shimmering of the irides at 10 months of age, which was noted by her parents. Relevant family history included a blind grandfather, of unknown aetiology. Examination revealed high myopia (spherical equivalence: Right Eye -12.5dioptres, Left eye -15dioptres). She had a right exotropia (>45 degrees) associated with hypertropia and a full range of ocular movement. Posterior segment examination revealed attached vitreous with no retinal degenerations or breaks. Both lenses were subluxed temporally, affecting visual acuity. She underwent a right lensectomy in October 2004, with a subsequent contralateral lensectomy in March 2005 both of which were uneventful. She is now bilaterally aphakic with a best corrected LogMAR visual acuity of 1.8 (right eye) and 0.1 (left eye). Most recent examination revealed intraocular pressures of 14mmHg (Right) and 16mmHg (Left). Retinal examination revealed no abnormalities. In particular there was no evidence of myopic fundal degeneration.

Neither parents nor siblings exhibited any of these systemic or ophthalmic phenotypes.

2.4.5.2. GENETIC SCREENING

Chromosomes: normal 46xx.

The common genetic causes of craniosynostosis: *FGFR2* exon 8 and exon 10 and *FGFR3* exon 6 were ruled out by the North East Thames Regional Genetics Service (Great Ormond Street Hospital). *FBN1* full gene analysis was undertaken by our laboratory. No mutation was identified in *FBN1*.

ADAMTSL4 analysis was undertaken, which revealed the 20 base pair deletion (c.767_786del20, p.Gln256Profs*38) found in our larger cohort of IEL above (Figure 2.5).

2.4.6. GRADING ECTOPIA LENTIS CLASSIFICATION SYSTEM

55 clinical images were obtained from Moorfields Eye Hospital databases. Inter ophthalmologist correlation was high on both occasions (κ=0.91 and 0.93, P<0.0001). Analysis between time points of the same ophthalmic observer revealed good correlation (κ =0.89, 0.82, P<0.0001). Interpretation of images by non-ophthalmic observer and ophthalmologists revealed κ = 0.77 (P<0.0001). 5 patients whose images had also been assessed (11%) were examined clinically and graded by two ophthalmologists. The grades of these clinical examination and photographical assessment were compared, and demonstrated complete correlation (κ = 1).

2.5. DISCUSSIONS

The incidence and aetiology of retinal detachment in MFS is unclear. Whether it is secondary to disruption of fibrillin-1 directly, thus causing a vitreoretinopathy is unlikely. It is most probable that it is related to the EL seen in MFS or the associated axial myopia. A method of investigating this is to examine a genotype-phenotype correlation between the two most important genetic causes of EL: *FBN1* (causing a fibrillinopathy) and *ADAMTSL4*. In doing so, it is hoped to understand the risks of RD development in this condition and the closely related MFS.

18 patients with EL were recruited. All patients underwent cardiovascular and skeletal examinations which excluded other associated conditions in 17 patients. We found five patients with causative *FBN1* mutations, nine patients with causative mutations in

ADAMTSL4, three patients with no known mutations and one patient in whom a heterozygous mutation was found in *ADAMTSL4* which could not fully explain the recessive inheritance of this condition.

2.5.1. *FBN1* MUTATIONS

Four of the five mutations found in *FBN1* all affected the calcium-binding epidermal growth factor –like ((cb) EGF-like) domains. One affected a consensus amino acid in a (cb) EGF-like domain, whilst the second resulted in a change of a cysteine residue within a cbEGF-like domain. Mutations affecting these residues are thought to result in EL at a younger age[187], and this particular individual was the youngest to be affected in our cohort. In silico analysis revealed these mutations to be pathogenic. The third affected a non-consensus amino acid in a cbEGF-like domain of fibrillin-1 and has previously been reported in a patient with a fibrillinopathy not fulfilling the Ghent criteria[186]. The fourth (c.3344A>G (p.Asp1115Gly) missense mutation results in a substitution of a glycine for an aspartic acid at codon 1115 in the cbEGF-like #13 domain of the fibrillin-1 protein. This mutation has previously been reported in a patient affected by classic MFS and affects one of the conserved amino acids in this type of domain throughout the protein.

The cbEGF domain is thought to be crucial towards the function of fibrillin-1 (Figure 2.8). Most of the understandings of these domains have been based on mutational findings[187], though there has been some cellular work investigating these and closely related *FBN1* domains[254]. It is hypothesised that disease causing mutations, particularly EL causing mutations, may lead to post-translational folding defects in the protein[255, 256]. Misfolded fibrillin-1 may accumulate in the endoplasmic reticulum[256]; thus leading to haploinsufficiency thought to be causative in MFS phenotype. In particular there is thought to be a predominance of mutations affecting cysteine residues in these domains[257], particularly missense mutations[187]. Four of our mutations affected these domains. Consistently, they were all found in the first 15 exons (5’ end), confirming reports that these exons harbour more EL causing mutations, thus suggesting that the N-terminus of the protein (encoded by this end of the gene) is also particularly significant in the aetiology of EL[258]. It has even been suggested that there is an inverse relationship between mutations in the distal part of the gene (3’ end) and EL[250].

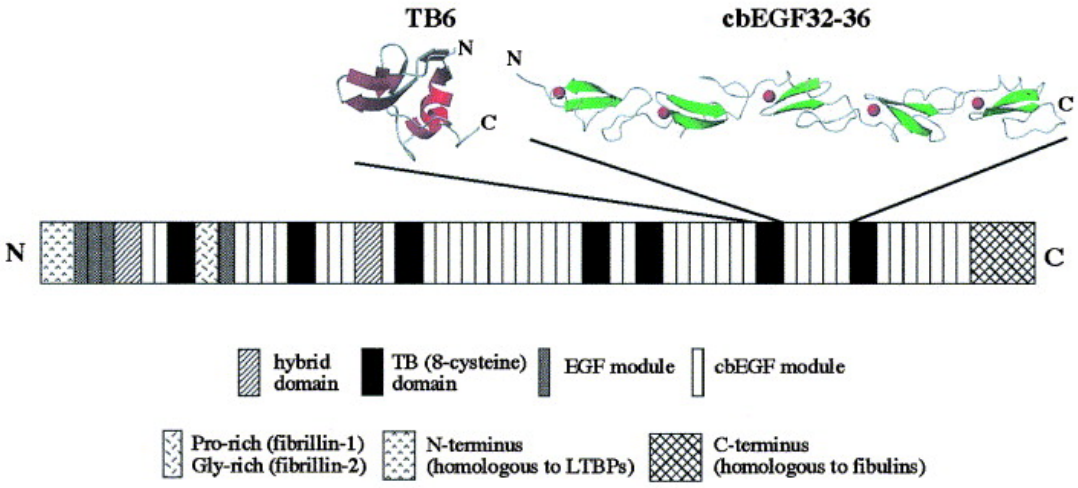

Figure 2.8: Domain organisation of fibrillin-1. A schematic drawing of the structure of cbEGF32-36, modelled on the structure of cbEGF32-33 is indicated. Calcium ions are shown as red spheres. *Adapted from* [11]

The fifth *FBN1* mutations found was intronic (c.1327þ1 G>A) in IVS10; predicted to abolish a splice donor site. The prevalence of splice site mutations in *FBN1* is unclear. It has been shown that missense mutations of *FBN1* are the most commonly found in patients with EL, followed by splice site mutations and in-frame mutations[187]. PTC mutations are thought to be significantly lower in proportion in those patients with EL[187]. Conversely, PTC mutations appear to have a striking correlation with skeletal features of MFS. This suggests different structural disruptions to fibrillin-1 have alternative effects on different organs.

One female patient was found to have a heterozygous mutation in *FBN1*, which had previously been described in a patient with classical MFS[252], in particular the cardiovascular phenotype. The diagnosis of MFS depends on the Ghent criteria which were updated in 2010. This patient would be one of the 15% of patients who represent diagnostic differences between the previous and new Ghent criteria[259]. This patient, with no skeletal or cardiovascular features of MFS would previously have been diagnosed as IEL. There are previous reports of patients described as "isolated" EL caused by *FBN1* mutations[228], whom would now be termed MFS because of their mutation profile. Such diagnostic changes are important for patients, their families and those involved in their care. An up to date understanding and awareness of *FBN1* mutations causing disease[260] is therefore critical.

Further to this we investigated all published reports of IEL or incomplete Marfan syndrome published between January 1993 and January 2013 to clarify whether the new Ghent criteria would alter published reports. The NCBI database was searched using the terms "FBN", "Marfan", "eye", "Marfan related", "Lens" and "ectopia lentis". Papers describing patients as having EL were highlighted. Within each paper, individuals with EL and a *FBN1* mutation who did not fulfil the Ghent criteria for MFS appropriate for the era of the paper were analysed.

There are 102 different mutations described in 181 individuals, representing 128 probands, reported in 44 papers over this twenty year period. 16 of the patients reported did not have their ages published. 53 patients of the remaining were under the age of 20 years. The 2010 Ghent criteria[186] state that true "isolated" EL cannot be diagnosed in individuals younger than 20 years, because of rapid cardiovascular development before this stage. Immediately this suggests that at least 29.3% of patients published with IEL were incorrectly so according to the modern Ghent criteria.

We investigated these mutations on the Universal Mutation Database (UMD)[260], Human Genome Mutation Database (HGMD)[261], NCBI, and an internal database of over 300 mutations in *FBN1* at the Sonalee Laboratory at St George's University of London. We searched for evidence that these mutations were reported in patients with MFS. This would immediately therefore change the diagnosis of a patient with such a mutation and EL to MFS. Our results therefore represent an absolute minimum proportion of mutations causing MFS, as complete clinical data is not available for all mutations. A mutation was ascribed the title "MFS mutation" only if there was absolute certainty from available literature that this was true.

Out of 181patients described as having EL caused by *FBN1* mutations, 64 (35%) would now have their diagnosis altered to MFS based on Ghent criteria[186]. However, when concentrating on probands alone, 70 (54.7%) would now have their diagnosis altered.

Analysing the mutations themselves, 51 out of 102 (50%) have been described in patients with MFS. The different types of mutations described are in table 8.

MUTATION TYPE	Number (%)
Missense	75 (73.5%)
Splice site	11 (10.8%) (2 proven to cause exon skipping)
Insertion/ Deletion	10 (.8%) (1 causing PTC)
Nonsense	6 (5.9%)

Table 8: Mutations in *FBN1* causing EL reported in literature (1993-2013)

When analysing the most common type of mutations (missense), 69.3% (52 out of 75) involved a cysteine (39 replacing and 13 creating a cysteine). This is comparable to the 61% suggested in the largest study of pathogenic *FBN1* mutations[187], which suggested that missense mutations involving cysteine residues were significantly associated with EL. Of their cohort, 81.6% of the cysteine involving missense mutations replaced this residue, with the rest creating it. Comparison of those mutations creating or replacing cysteine residues in our findings amongst the MFS mutations and "non MFS mutations" is of interest. In the MFS mutations, 60.7% of the cysteine involving missense mutations resulted in this residue being replaced. In the "non MFS" mutations, this was 92% (P=0.0385). PTC mutations, which Faivre et al[187] described as being significantly less common in EL, accounted for only 6.9% (7 mutations) of the mutations.

The most widely reported mutations are demonstrated in the Figure 2.9:

These data present interesting findings. The most widely reported mutations are all missense, with 60% involving cysteine residues.

Of these, the four most reported have all been described in MFS. This illustrates again the predominance of MFS mutations in EL. The mutations in blue (R62C, C2017R, E2447K, Y63C, G1594V, N164S, S634P, C652Y, E2250G) may be considered "EL" mutations of *FBN1*. This must be interpreted with caution, as these reports include up to only 2 independent probands.

This work describes the major changes that have occurred as a consequence of the 2010 Ghent criteria. Over 50% of probands not fulfilling the criteria for MFS now would be, based on their *FBN1* mutation. It is worrying that the guidelines are still occasionally being ignored since the 2010 watershed of the new Ghent criteria; with patients being described as isolated EL with *FBN1* mutations already shown to cause MFS[262, 263]. A further point of interest is those papers which describe patients with MFS, with truly novel *FBN1* mutations and not enough clinical criteria to fulfil this diagnosis[264]. Clearly the Ghent criteria of 2010 need to be more widely publicised and clarified.

These findings suggest that EL caused by mutations in *FBN1* is actually part of a spectrum of fibrillinopathies with MFS. This also demonstrates the importance of having an up to date database of *FBN1* mutations known to cause MFS.

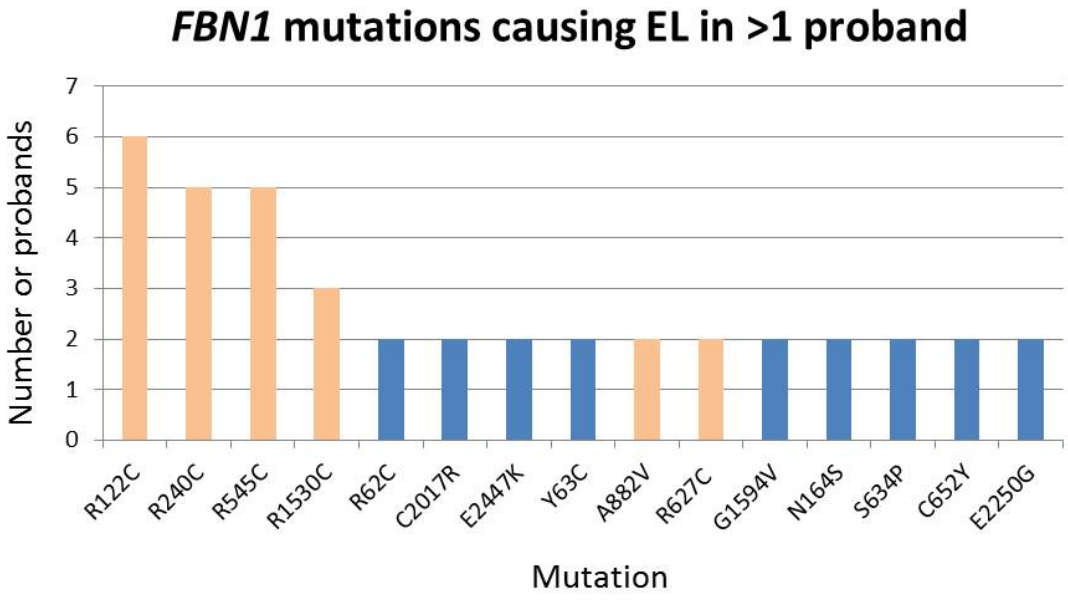

Figure 2.9: *FBN1* mutations causing ectopia lentis reported in the literature in >1 proband (1993-2013). Mutations described also in MFS.

The only such database to date is the UMD database [252]. This was however last updated in 2003.

To highlight that those with *FBN1* mutations causing EL are in a spectrum with MFS, it can be argued that the term "*FBN1* associated isolated ectopia lentis" or "Autosomal dominant isolated ectopia lentis" (OMIM 129600) should be dismissed. Loeys et al [186] suggest the phrase "Ectopia Lentis Syndrome" be used, to illustrate that other systems may become involved. However, this is somewhat inaccurate, as not all of these patients will develop other complications. Alternative phrases, such as "incomplete Marfan Syndrome", "Lenticular fibrillinopathy" or simply "dominant ectopia lentis" should be used to demonstrate that these patients are not necessary "isolated". Truly "Isolated Ectopia Lentis" should be reserved for those with autosomal recessive EL. To date, *ADAMTSL4* is the only gene that has been shown to cause this condition.

It must be acknowledged that some of the work in this thesis contradicts this theory, in that current terminology is used. Four patients with *FBN1* related EL were termed "isolated" in this work[27]. Furthermore, one of our cohort with a *FBN1* mutation was 18 years of age at the time of analysis (Patient 3). Although her mutation was not described in classical MFS, technically MFS cannot be excluded. However, since this work, she has become 20 years old, and still has no cardiovascular signs of MFS. She will however receive lifelong cardiovascular follow up, as will all patients with a *FBN1* mutation.

2.5.2. *ADAMTSL4* MUTATIONS

We found 9 patients with IEL and recessive mutations in *ADAMTSL4* which were thought to be causative. Six of these were the same homozygous 20 base pair deletion (termed a "micro-deletion"[265]) in exon 6. This mutation was first described simultaneously by our group in the UK[7], in Germany[9] and in Norway[8]. Neuhann and colleagues[9] described 8 individuals from 7 families originating from the south of Germany. The location for the mutation is notable for the "deduplication" of the octamer CAGAGCCC (Figure 2.10). One can see that after the deletion, the same octamer (separated in the wild type sequence by 12 bp AGGCCTCTGGCA) as at the beginning of the mutation continues. These are thought to have a potential causative role in

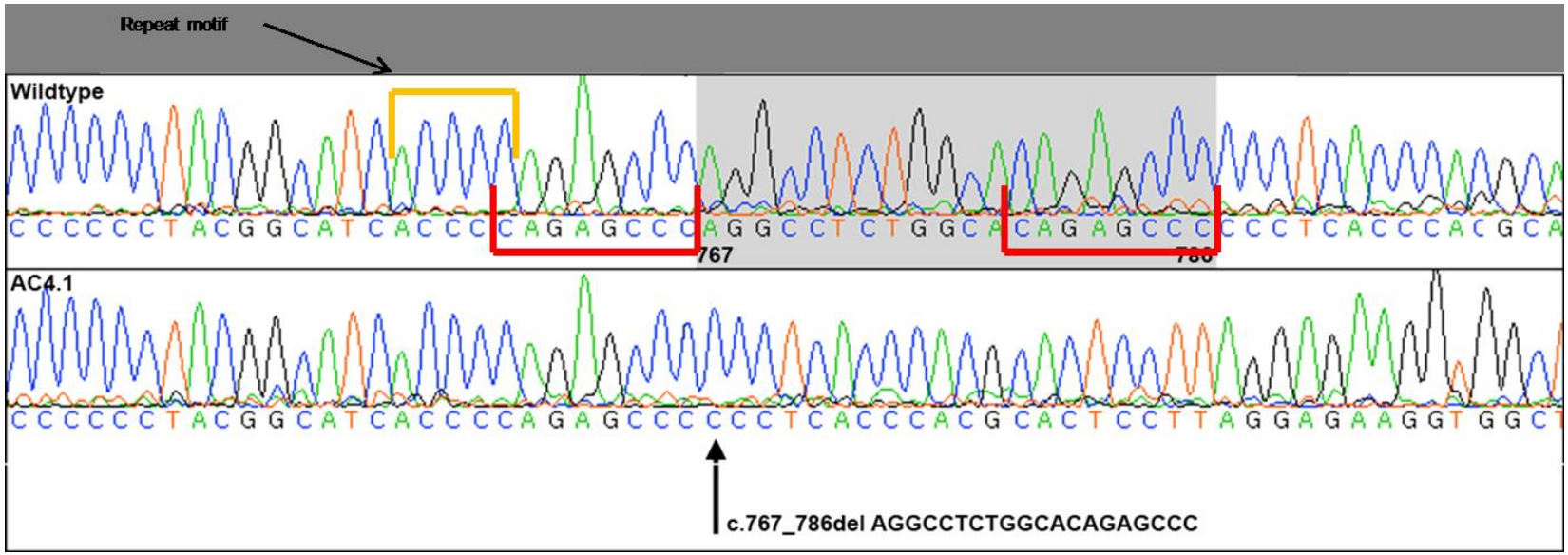

Figure 2.10: *ADAMTSL4* Exon 6 deletion (c.767_786del20) illustrating repeat octamer (Red) and the repeat ACCCC motif preceding this mutation (Yellow)

the occurrence of microdeletions. Viguera et al. [266] suggest that during DNA replication, DNA polymerase pauses. During this pause, disassociation between the primer and template strands may occur. The primer strand may then "slip" along to the adjacent direct repeat sequence, thus deleting the intermediary nucleotides. Such deduplications occur in up to 66% of microdeletions [267]. However, the frequency of these are thought to be inversely related to the size of the microdeletion, occurring in less than 3% of deletions >6bp [265]. In this gene, the size of the microdeletion would suggest that the occurrence of this deduplication would be therefore particularly unusual. In an analysis of 8399 microdeletions, Ball and colleagues[265] discovered certain repetitive motifs were more significantly associated +/- 2base pair of the deletions. Interestingly, the motif sequence ACCCC (termed the "Immunoglobulin heavy chain class switch repeat") was one of the more significantly associated repeat ($P=2.24x10^{-6}$). This is present 7 base pairs upstream of this micro deletion (Figure 2.10). This particular dataset investigated microdeletions of up to 20bp; however, the vast majority of the deletions studied were less than 6 base pairs. The inference of their data to this mutation is therefore limited. Furthermore, the frequency of deletions of greater than 6 base pairs are thought to represent less than 3% of all microdeletions[261, 265].

Nonsense mutations represent at least 11% of all described gene lesions causing human inherited disease[261]. Therefore homozygous large micro deletions (</=20bp) resulting in PTC are very rare. For this mutation to be frequently found throughout Europe suggest a Founder mutation, with a moderate allele frequency. Discovering it in 3 heterozygotes out of 190 controls, Christensen suggested an allele frequency of 0.0079 with a homozygous individual in approximately 1 in 16000 individuals[8]. Extrapolating this to the UK, one would expect over 3500 individuals with this mutation.

With regard to a founder effect, all patients with the 20bp deletion described by Neuhann shared the identical SNP haplotype "C-A-T-ins4" (SNPs rs41317515, rs9659061, rs12124948, rs66703603). The marker TSL4CA "209 allele" (CA is repeated 14 times) was found in all their cases, and 37% of the control cohort. This, they therefore suggest, implies a founder effect. The next nearest marker ((D1S498, 770kb distance to *ADAMTSL4*) showed some variation amongst the *ADAMTSL4* cases –suggesting that the original founder mutation is at least 150 generations old. This mutation has been found in 15 unrelated families across Europe, adding further evidence that this mutation has this ancient founder effect.

This microdeletion results in a PTC, after 110 nucleotides, in exon 6. The result of this would be either protein truncation or nonsense mediated decay (NMD) as a consequence of mRNA being read as erroneous. Christensen and colleagues[8] investigated *ADAMTSL4* mRNA from patients with the 20bp deletion, and suggested a truncated product was produced. They however did not show their original data demonstrating this, and it has not been since replicated. It is also been suggested that nonsense mutations which result in PTC more than 55 nucleotides from the Exon-Exon boundary are more likely to result in NMD[268]. This mutation results in a PTC which is 232 nucleotides from the end of exon 6. We believe that, at present, it is difficult to determine which (NMD or protein truncation) would be the case in this 20 base pair deletion[269].

Most other mutations published in *ADAMTSL4* with EL would result in the loss of the C-terminal six TSR-1 domains which may suggest an important role for these in the protein's function. Our group at St George's had previously described a mutation in exon 19[7] which only affect the PLAC domain. If this transcript would survive NMD, it would suggest that this domain is critical for ADAMTS-Like function.

Four novel nonsense mutations were discovered in exons 5, 6 and 14. The mutations in the first were both deletions. One (c.237delC) had the same motif as the 20bp deletion (ACCCC) preceding it (Figure 2.11a). The second exon 5 deletion (c.293delG) had the oligonucleotide C_5G two base pairs upstream form the deletion (Figure 2.11b). The insertion in exon 14 (c.2270dupG) had the oligonucleotide G_6 immediately upstream to it (Figure 2.11d). Both of these sequences have been shown to be most frequently in the vicinity of micro deletions and insertions respectively[265]. The final mutation was a substitution resulting in a nonsense mutation.

The effect of these mutations is again unclear. c.237delC(p.Pro80Argfs*53) results in a frameshift and a PTC after 53 codons. The resultant PTC is 19 nucleotides from the end of the exon. c.293delG results in a frameshift and a PTC after 34 codons. This is then 34 nucleotides from the exon-exon boundary and suggests that the mRNA is less likely to undergo NMD[268], thus resulting in a truncated protein. The insertion mutation (c.2270dupG) produces a PTC after 59 codons; 108 nucleotides from the end of the exon. The final mutation, a substitution in Exon 6 (.925C>T) changes an arginine to a PTC immediately. This PTC is 108 nucleotides from the end of the exon. These final two mutations may therefore result in NMD. This uncertainty in understanding the

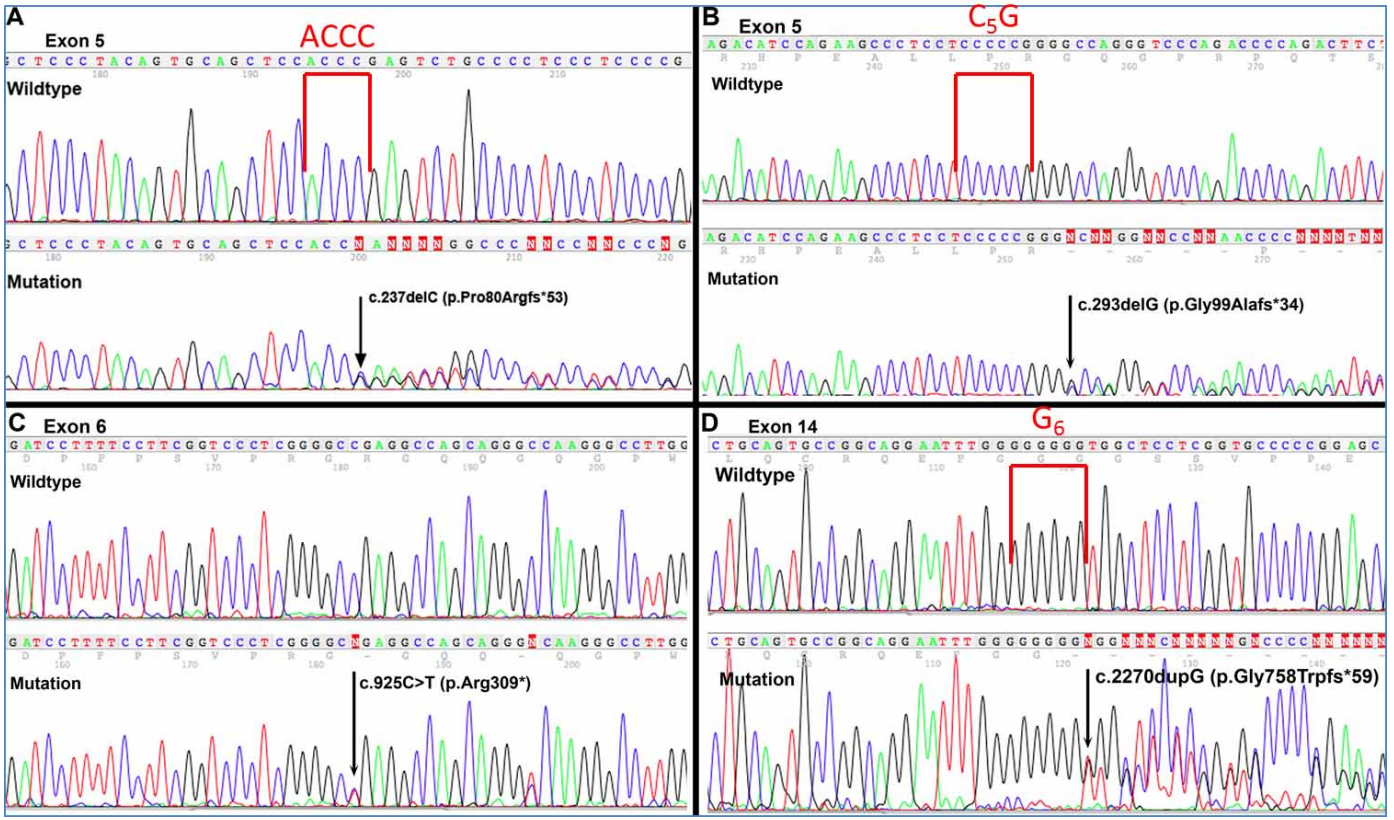

Figure 2.11: Novel mutations in *ADAMTS4*, and repeat preceding motifs (A, B, D)

effect on the protein of mutations in this gene, add further controversy to the role of this protein in the eye, manifesting in EL.

To date, there have therefore been two missense mutations and 12 nonsense mutations described in the literature in *ADAMTSL4* (Table 6). It is thought that these nonsense mutations which are more likely to result in NMD as described above) tend to result in recessive disorders[270].

The phenotype analysis was enlightening. It is useful to put these findings in the context of the phenotype of MFS. We analysed the corneal features. It is suggested that in MFS, the cornea is thinner and of lower curvature [194, 198]. It is unclear why this is the case. The majority of the corneal microstructure is stroma. The stroma, of neural crest origin, consists of collagen I, with some collagen V and proteoglycans[271]. Fibrillin-1 is thought to be present in the corneal epithelium[193], but evidence from other parts of the cornea is lacking. The contribution of corneal epithelium to corneal pathology is limited. The only direct evidence of fibrillin-1 modulating corneal phenotype comes from an association study, which suggested that *FBN1* may contribute to central corneal thickness[272]. Nonetheless differences between the corneal phenotype of MFS and controls continue to be described. Iordanidou and colleagues[195] described highly reflective ECM of the stroma and brightly reflective particles among the endothelial cells in patients with MFS, though this finding is yet to be replicated or explained further. It would be interesting to understand if the EL seen in MFS relates to corneal features. Kara and colleagues[197] recently suggested that corneal hysteresis and corneal resistance factors were significantly lower in MFS patients with EL than without. Konradsen[196], in addition to confirming that MFS patients had lower K values and central corneal thickness, also suggested that within MFS; those with EL demonstrated greater astigmatism. Finally, there have also been reports that corneal guttata are present more commonly in MFS patients with zonular deficiencies[273].

We investigated corneal curvature and central corneal thickness in our cohort. It is particularly interesting that all patients (by definition with EL) had corneal curvature (K) values of <42D, a suggested cut off for MFS[198]. Some may caution in interpreting this data as most of the patients in this series had had lens surgery by vitrectomy. The effect on corneal curvature of this is unclear[274, 275]. Most data however suggests that any induced astigmatism after this surgery resolves to baseline[276, 277], suggesting that our data is likely to be a true reflection of the

patients' true curvature. Our data therefore suggests that EL itself may influence corneal curvature.

When comparing central corneal thickness (CCT), we found no differences between the two groups. It is suggested that peripheral corneal thinning (due to altered fibrillin-1 between the corneal epithelium and Bowmans layer) combined with ocular elongation, may lead to central corneal thinning[194] in MFS. Sultan and colleagues[194] also suggest that this feature is correlated with EL. These findings are however not consistently described. Indeed, although these two corneal features (curvature and CCT) were in the 1993 Ghent criteria[278], they were removed from the most recent version[186]. The effect in IEL is even less well understood, with Zhao and colleagues[230] finding normal CCT in a family with dominant EL secondary to a *FBN1* mutation. Our findings add more controversy to the debate of the effect of *FBN1* mutations and EL on CCT.

The further findings were of particular interest. The age of onset of EL is important not only for understanding the aetiology, but also of clinical relevance for patients. It has been long established, in MFS, that missense mutations affecting cysteine residues resulted in a younger age of onset of EL than other missense mutations[187]. This is thought to be because of the important role that cysteine residues and disulphide bonds play in the structural integrity of the suspensory zonules[14]. The youngest patient in our *FBN1* cohort (Patient 3) was the only one to have a mutation affecting such a residue (p.Cys1420Tyr), in line with the cysteine residue theory.

However, the cohort with *ADAMTSL4* mutations was affected at a significantly younger age, compared to those with *FBN1* mutations. This is significant, as we believe that this demonstrates that ADAMTS-Like 4 may play an independent role in ocular development, unrelated to fibrillin-1 function. It is becoming apparent that mutations in other genes in the ADAMTS family are resulting in early onset ocular malformations. There is evidence for a possible interactive role between many of the ADAMTS proteins and fibrillin-1[279], and this remains a likely possibility in view of the very similar ocular phenotypes seen from mutations in these genes and *FBN1*. However, unlike ocular manifestations secondary to *FBN1* mutations, all those with mutations in genes of the *ADAMTS* family who have been published to date and with relevant information available are affected before the age of 20[1, 2, 7, 9, 10, 22, 27, 226, 280,

281]. The young age of onset of these ocular phenotypes suggests a developmental role for these proteins.

The data suggests that children affected with IEL, thought to be recessively inherited, should have *ADAMTSL4* mutation analysis as the primary candidate.

Investigating the axial length data in this cohort was highly relevant. As discussed in the introduction, patients with MFS are thought to have increased axial lengths. One would therefore imagine a similar finding in patients with EL secondary to *FBN1* mutations. However, our data suggests that the axial lengths are greater in those patients with *ADAMTSL4* mutations than *FBN1* mutations. This may be related to the age of onset of the EL. It is established that the rate of AL growth is greatest before the age of 10 years[282]. The molecular basis of axial length growth in humans and animals have been the subject of studies for over 3 decades (see Brown *et al*.[283] and Meng *et al* [284]). Highly relevant is the finding in 15 Japanese children that axial length growth increases in the presence of non-traumatic EL[285]. This study showed that even after lens extraction, AL continues to grow at a greater rate and for longer than normal. Interestingly, they found no difference in their cohort of 15 patients between those with IEL (n=5) and MFS (n=10). There are no definite theories as to why AL grows more rapidly in EL at a young age. It is possible that this may be secondary to two significant mechanisms: Form deprivation myopia (FDM) and lens induced myopia (LIM); both which are closely related. Animal models have shown that blurring vision during critical periods in globe growth have important effects on the axial length[286, 287]. It is probable that any of the signalling molecules, including dopamine, acetylcholine, vasoactive intestinal peptide, glucagon, retinoic acid, crystallin, seratonin and melatonin, nitric oxide or other growth factors may be influential; be this at the neural retina, RPE, choroid or sclera[286, 288-290]. It is clear, that this mechanism plays an important role in human development as well, whichever the cause of FDM[291]. It has been shown that severing the optic nerve in chicks does not inhibit axial length elongation by FDM, and if only part of the field is deprived, axial elongation occurs only in the corresponding retina[292]. These features strongly suggest that FDM is controlled by local retinal mechanisms.

The aetiology is different between FDM and LIM[293]. LIM is controlled by visual pathway signals; illustrated by the findings that optic nerve severing in chicks limits the effect of negative lenses on the induced myopia[294]. The effect of the parasympathetic

innervation to axial growth has also been investigated. Nickla and colleagues showed that lesions to the parasympathetic innervation via the VII cranial nerve, to the ciliary and the cervical ganglion disrupted axial elongation in response to occlusion, but had no effect on lens induced myopia[293]. The underlying implications of this are not fully understood, but does emphasise the fact that different mechanisms control these phenomenon.

In the clinical setting, FDM is more commonly found in cases of corneal scarring or lid obstruction. LIM is more commonly found in the instances of anisometropia. What effect an ectopic lens may have has not been demonstrated. It is more likely that blurring from ectopic lens edge, cataractous lens or effective aphakia from significant subluxation, would lead to LIM rather than FDM. It is interesting to consider that in the papers describing phenotype data in ectopia lentis et pupillae, axial myopia is a prominent feature[295-297]. It is possible to envisage that ectopia pupillae (EP) would result in more FDM over the fovea than lens effect. Conversely, recent animal[298] and clinical studies[299] have suggested that peripheral rather than foveal blurring may have more impact on axial myopia development. The importance of LIM may still be greater than FDM in these cases.

It has been suggested that FDM in one eye may affect the contralateral AL[300]. However, this study examined guinea pigs which had pre-existing anisometropia prior to form deprivation. Drawing conclusions from this paper is thus challenging.

Our results indicating long axial length in patients with *ADAMTSL4* mutations suggest that these patients may be more susceptible to RD than those with *FBN1* mutations. Indeed, there are reports of RD in the few papers describing *ADAMTSL4* mutations[2, 8, 30]. Whether this is secondary to the early onset EL, the apparent increased axial myopia or secondary to an effect of ADAMTS-Like 4 itself is unclear. Whichever the underlying cause, it is our suspicion that patients with *ADAMTSL4* mutations are more predisposed to RD than those with *FBN1* mutations.

Finally, one should consider what effect mutations in *ADAMTSL4* might have on other organs. The protein is thought to be expressed widely[2]. We found one patient who had had EL and a coronal craniosynostosis [301] with the 20bp deletion (c.767_786del 20). It is worth considering this case in particular.

Craniosynostosis (CS) can be classified according to the sutures involved (in order of frequency sagittal, coronal, metoptic and lambdoidal). Although it can be inherited as part of over 180 syndromes, 85% of cases are nonsydromic with no identifiable mutation[302]. Coronal CS has an incidence of approximately 1 in 10,000 live births, with up to 75% of cases being female and approximately 10% of cases reporting a positive family history[303]. The most common mutations associated with CS are found in fibroblast growth factor receptor genes 1-3 (*FGFR* 1-3)[304] and the transcription factor *TWIST1*[305]. *FGFR* has been shown to be involved in modulating osteoblast activity in bone ossification[306], and disruptions to this are thought to be the molecular basis for CS[302]. Other genetic mutations described have been *MSX2, EFNB1, RAB23, POR, GLI3, RECQL4* and *FBN1*.

Sprintzen-Goldberg Syndrome (SGS) (OMIM 182212), also known as marfanoid craniosynostosis syndrome, has been described over 40 times and is characterised by craniosynostosis, distinctive craniofacial features, marfanoid skeletal changes, and neurologic and brain anomalies. Marfanoid cardiovascular features include valve incompetence, but not aortic root dilatation. Mutations in *FBN1* have been identified in SGS[307, 308]. Sood and colleagues[307] first reported a patient with typical features of MFS, including EL, associated with features of SGS with a heterozygous missense mutation in exon 29 (p.Cys1223Ty) of *FBN1*. They first proposed that the elastin-microfibrillar pathway may affect early patterning events in the cranium. Ades and colleagues[308] subsequently described two patients with CS and EL, one of whom fulfilled the Ghent criteria, who had *FBN1* mutations in exon 26. Hiraki[309] presented a 19 month child with CS who had a deletion of *FBN1*. In spite of these reports, the role of *FBN1* in CS is still to be clearly defined.

Loeys-Dietz Syndrome (LDS) causes ascending aortic aneurysm with associated abnormalities in the cardiovascular, skeletal, craniofacial and neurocognitive systems. CS is known to be a feature. Mutations in the genes which encode the transmembrane receptor of TGFβ (*TGFBR1* & *TGFBR2*) cause LDS. This enforces the hypothesis that abnormal transforming growth factor beta (TGFβ) signalling pathway may cause vascular and craniofacial phenotypes. Mutations in *TGFBR2* have also been found in patients fulfilling the Ghent criteria for MFS[310]. LDS, SGS and MFS therefore are considered related conditions, part of a spectrum.

Craniosynostosis and EL have been described in sporadic cases with an unknown mode of inheritance (OMIM 603595)[311-315]. None of the most common mutation hotspots for craniosynostosis yielded a mutation in our patient: (*FGFR2* & *FGFR3*). In addition, no mutation was identified in *FBN1* or *TGFBR2* known to cause MFS or EL and LDS respectively. We therefore investigated other genes associated with EL, and discovered the deletion mutation in *ADAMTSL4*. Christensen et al[8] mention a patient with ectopia lentis et pupillae who had craniosynostosis corrected caused by the same mutation. Our patient did not have pupil involvement. Taken together, these findings raise interesting questions. The first explanation is that these patients represent identification of a mutation causing EL and craniosynostosis syndrome. This case may be the first example of pleiotropic effects of *ADAMTSL4* with regulatory or environmental influences affecting different phenotypes; our patient was one of non-identical triplets conceived by in vitro fertilisation of parental ova and sperm, who were delivered at 30 weeks. It has been suggested that infertility treatment may itself be associated with craniosynostosis[316]. However, that study was based on only 10 affected patients, and must be interpreted with caution. Furthermore, a subsequent multi-national study found no association between maternal subfertility, or treatments for infertility and infantile craniosynostosis[317]. Such an association is therefore controversial. Furthermore, the report by Christensen and colleagues[8] did not mention infertility.

Alternatively, one must consider that this nonsense mutation is the most commonly reported in *ADAMTSL4*, with no other patients presenting with CS. It may be therefore that this patient manifested two rare conditions, only one of which (EL) which we have discovered the causative mutation. It is difficult to be certain without further reports being published.

2.5.3. GRADING IN ECTOPIA LENTIS (GEL)

Our novel grading system (GEL) revealed very high correlation between both ophthalmic and non-ophthalmic observers. The correlation between inter and intra ophthalmologists are excellent[318, 319]. Although the correlation between ophthalmologists and non-ophthalmic physician is lower, this level may still be regarded as excellent[318] or substantial[319].

The number of cases used in our validity testing compares favourably with other novel ophthalmic clinical assessment tools[320], and our levels of inter observer correlation

equally compared favourably with previous ophthalmic systems[321]. The system also was highly repeatable at different time points.

Previous grading systems have been suggested[322, 323] but their reproducibility has not been validated. Waiswol and Kasahara[323] described a four point grading system for EL and reported a correlation between visual outcomes after surgery for EL with less severe subluxation. Furthermore they suggest fewer complications in patients with less complex subluxations. Their grading system was based on undilated pupils; which may differ from the appearance preoperatively. GEL is undertaken under pharmacological dilatation, which may help standardise the assessment. The GEL system allows more detailed description of lens movement; for which maximal pupillary dilation would be optimal.

It must be acknowledged that the GEL system does not account for subluxation where the lens is rotated. In practice, to confirm that this is the plane of movement, the observer requires a detailed slit lamp examination. Therefore by excluding rotation from the classification system simplifies its use, and does not limit GEL to ophthalmic specialists.

This system was devised during the recruitment of cohort for the genotype-phenotype work. It was therefore not employed in that work. It would be of interest to validate it in further cohorts, and perhaps further delineate any genotype-phenotype correlation.

In summary work presented in this chapter has defined for the first time a genotype-phenotype relationship between the two most important genes in IEL; highlighting the importance of *ADAMTSL4*. The role of *FBN1* in this condition is likely to be less important than previously considered. A novel clinical grading system has been suggested, and may provide the basis for clearer phenotyping of this condition in the future.

GENE	OCULAR PHENOTYPE	REFERENCE
ADAMTSL4	Isolated Ectopia Lentis (OMIM 225100)	Ahram (2009)[2] Greene (2010)[10] Aragon Martin(2010)[7] Neuhann(2010)[9] Chandra (2012)[27]
	Ectopia lentis et pupillae (OMIM 225200)	Christensen(2010)[8] Chandra (2012)[27] Sharifi (2013)[30]
	Ectopia Lentis and craniosynostosis (OMIM 603595)	Chandra (2012)[27]
ADAMTS10	Weill-Marchesani (OMIM 277600)	Dagoneau (2004)[280] Kutz (2008)[281] Morales(2009)[226]
ADAMTS17	Weill-Marcahasni-Like (microsherophakia and short stature) (OMIM 613915)	Morales (2009)[226] Khan (2012)[324]
ADAMTS18	Knobloch 2 syndrome (OMIM 608454)	Aldahmesh (2011) [1]
	Early onset retinal dystrophy	Peluso (2013)[22]

Table 9: Ocular manifestations of recessive mutations in the *ADAMTS* genes

CHAPTER 3: FAMILIAL INVESTIGATIONS OF RHEGMATOGENOUS RETINAL DETACHMENT AND ECTOPIA LENTIS

Publications arising from work related to this chapter:

(i) **Chandra** A., Arno G., Williamson K., Sergionotis PI., Preising MN., Charteris DG., Thompson DA., Holder G., Borman AD., Davangnanam I., Webster AR., Lorenz B., Fitzpatrick DR., Moore AT.

Extension of the ocular phenotype features caused by mutations in *ADAMTS18*

JAMA Ophthalmology [In Press]

3.1. INTRODUCTION

Investigating families with Mendelian traits not only informs us about the pathogenesis within the family, and in potentially other families with similar monogenic conditions; it also is believed to help reveal genes in multifactorial diseases. For example autosomal dominant mutations in *MAPT* lead to frontotemporal dementia[325], and yet normal variation in this gene can alter mRNA levels resulting in sporadic progressive supranuclear palsy[326]. As Jonathan Cohen suggested in 2010, these "Goldilocks alleles" can offer direct insights into the mechanisms of complex diseases[327]. Furthermore, the traditional distinction of Mendelian and complex inheritance for inherited diseases has for a long time now been blurred[328]. However such compartmentalisation of conditions does help with focussing methods of investigation.

Towards this, families were sought in whom RD or EL were inherited. As previously discussed, both of these conditions are thought to be related[185, 214-216], though rarely investigated in conjunction. For such families, those in whom a clear diagnosis was not made were highlighted and recruited. Attention was particularly drawn to families with RD and EL.

3.2. AIMS

The aims of this chapter are to investigate families in whom RD and/or its associated condition, EL, are inherited. Those families in whom a formal clinical and genetic diagnosis had not been made were recruited in order to undertake genetic investigations.

3.3. METHODS

Methods employed in this work include PCR, Sanger Sequencing, SNP genotyping with homozygosity mapping, next generation sequencing, RNA extraction, and reverse transcriptase PCR.

Phenotype examination, phlebotomy, DNA extraction and quantification, primer design were completed as described in section 2.3. PCR was performed also as described in chapter 2. Platinum ® Taq DNA Polymerase (Invitrogen, USA), BioTaq (Bioline) DNA polymerase or MyTaq DNA Polymerase (Biolabo) were used. DMSO was occasionally added to increase reaction efficiency. $MgCL_2$ concentration was altered on occasion to improve the reaction.

The sequence of the PCR products was read using Sanger's chain termination method[329]. BigDye terminator v3.1 (ABI, California, USA) was used as described in section 2.3.10.

Genes sequenced in these studies included *FBN1* and *ADAMTSL4* which have been described in chapter 2. The sequencing of the 26 exons *ADAMTS10* was undertaken by our collaborators; Professor Valérie Cormier-Daire, Department of Genetics, INSERM U781, Hôpital Necker, Université Paris Descartes, Sorbonne Paris Cité, France.

Genes amplified as part of this chapter included:

23 exons of *ADAMTS18,* 26 exons of *PAPLN*, 35 exons of *LTBP2* and 22 exons of *ADAMTS17.* Primers are given in the appendices VII-XI and reaction conditions are as follows.

For *ADAMTS18*

STEP	Temp (^{0}C)
1. Denaturation (180s)	95
2. Denaturation (30s)	95
3. Annealing (60s)	60
4. Elongation (90s)	72
5. Final elongation (5min)	72
6. Termination (>10min)	4

Repeat Cycle of steps 2-4: 40 times.

For *PAPILIN and LTBP2*

STEP	Temp (^{0}C)
1. Denaturation (180s)	95
2. Denaturation (30s)	95
3. Annealing (60s)	65 (except Exon 19 of *PAPILIN* (66.5^{0}C)
4. Elongation (60s)	72
5. Final elongation (5min)	75
6. Termination (>10min)	4

Repeat cycle of steps 2-4 40 times

For *ADAMTS17*

For Exons 1, 3-14, 16-22:

STEP	Temp (^{0}C)
1. Denaturation (180s)	95
2. Denaturation (30s)	95
3. Annealing (30s)	56 (except Exon 21: 64^{0}C)
4. Elongation (30s)	72
5. Final elongation (5min)	72
6. Termination (>10min)	4

Repeat cycle of steps 2-4 40 times

3.3.1. EXOME SEQUENCING

Although traditional methods of gene discovery for Mendelian conditions, including linkage and candidate gene screening are thought to have identified loci for up to a half of all known such disorders[330], the recent revolution of next generation sequencing (NGS) has changed the genetic landscape. Since 2005, the availability of NGS has become widespread. Combining this technology with highly targeted capture has allowed an exponential growth of sequencing the coding region; the "Exome". Since the first report of this combination being fruitful in investigation of human disease in 2009[331], and the first discovery of a causative mutation in Mendelian disease in 2010[332], this has led to over 600 papers describing the success of exome sequencing between Jan 2010 and Dec 2012[18].The steps involved in whole exome sequencing are illustrated in the Figure 3.1.

In summary, DNA is randomly sheared (into sizes 100-300bp), typically using ultrasound (Step A). Adapter ligation then occurs which are complimentary to primers in the hybridisation step (B). After washing, NGS is undertaken. Amplification occurs by primers bound to a surface of a "flow cell". The termination method uses fluorescently modified nucleotides used for sequencing. This dye labelled

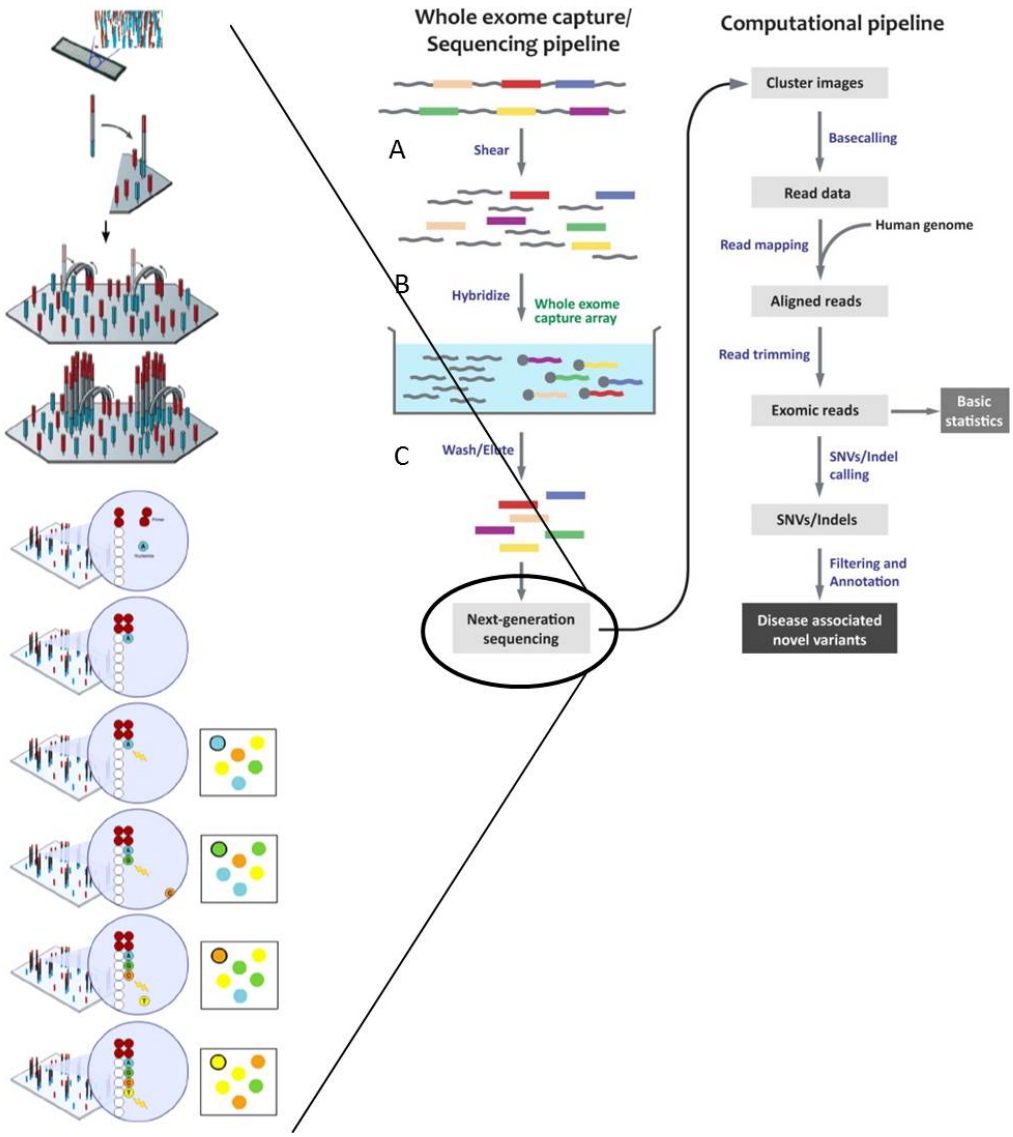

Figure 3.1: Schematic diagram illustrating the steps of next generation sequencing (*Adapted from* [18] and [29])

nucleotide (complementary to the base) leads to termination of DNA synthesis. This is then imaged, before removal of this incorporated base for a repeat cycle.

After calling the bases, the data is read and aligned to a reference genome. A major challenge in interpreting the data from these experiments involves shortlisting candidate variants from the background vast number of variants which are seen. On average there would be 20,000 single nucleotide variants (SNV) identified from the exome of a European individual[333]. The model used for filtering out those variants is dependent on mode of inheritance, population structure, and whether the search is for *de novo* mutations. An initial step would involve using online databases, such as dbSNP[247], exome variant server[246] or 1000 genomes project[248], or internal databases of unaffected controls. Minor allele frequencies of 1% and 0.1% are thought to provide power for autosomal recessive and dominant traits respectively[333]. Subsequently filtering on predicted deleterious nature of the mutation is often utilised; therefore focussing on frameshift, nonsense, splice site and non-synonymous missense mutations. Subsequent exclusion techniques included biological effect of genes and distribution within ocular tissue.

3.3.2. HOMOZYGOSITY MAPPING

Although as mentioned previously linkage analysis may seem less favourable in the new era of NGS, a very productive method of this was used in this chapter. In consanguineous families, exploiting large runs of homozygosity has been the cornerstone of understanding recessive disorders.

Homozygosity refers to both alleles of a genetic sequence being identical. Long regions of apparent homozygosity may represent deletion polymorphisms, loss of heterozygosity (LOH), segmental uniparental disomy, or autozygosity[334, 335]. It is this latter cause which is exploited when investigating genetic causes of autosomal recessive conditions in consanguineous families. Autozygosity mapping is based on the assumption that regions either side of a disease allele are likely to be identical by descent in a consanguineous family[336]. This is demonstrated in Figure 3.2. Although regions of homozygosity (sometimes termed loss of heterozygosity) can be found in outbred populations (usually up to 1.5Mb)[337, 338], long continuous stretches of homozygosity (LCSH – usually over 2Mb) on multiple chromosomes are regarded as indicative of parental blood

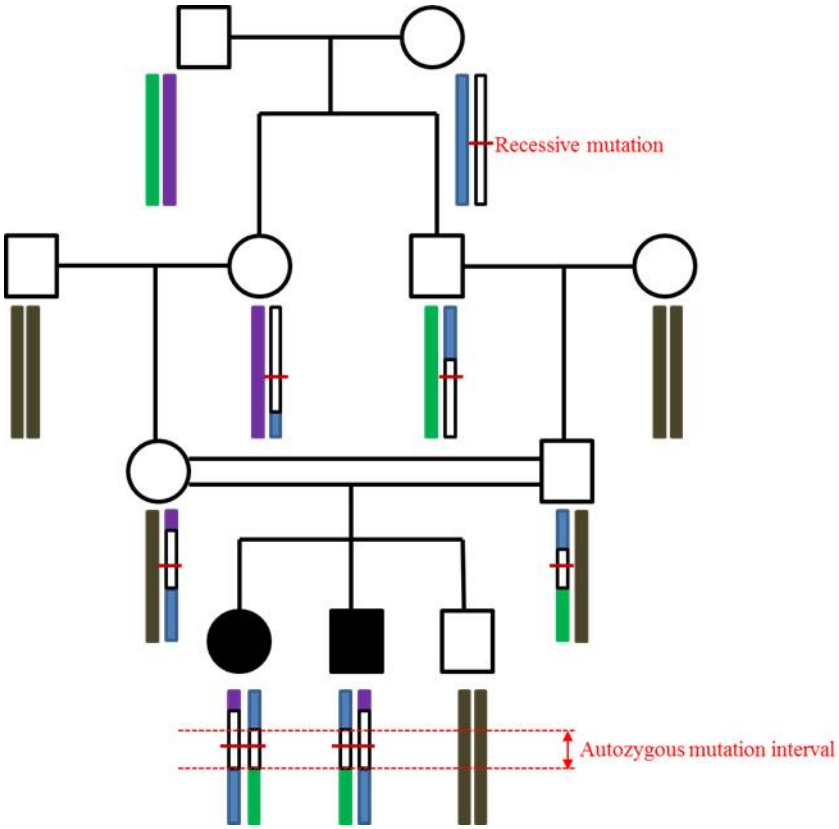

Figure 3.2: Homozygous region around a mutation in a consanguineous family. This region is autozygous, as it is identical by descent (IBD).

relationship[338-340]. A very conservative threshold of 5mb has been suggested for the term of LCSH[338] to suggest parental consanguinity. See Figure 3.2.

Consanguinity increases the probability of IBD (as demonstrated in Figure 3.2), thus the risk of autosomal recessive diseases. It is estimated that an offspring of first cousin parents have up to a 2% increased risk, compared to non-consanguineous parents, of having an autosomal recessive disorder; an approximately 1.1% increased risk of infantile mortality and up to 4% risk of pre-reproductive age mortality[341]. Ocular disease is particularly common amongst consanguineous families, as these conditions do not tend to be lethal.

Investigating regions on the genome, for linkage or for regions of homozygosity, involves genotyping markers on DNA throughout the genome. Traditional polymorphism based markers involved blood group analysis, electrophoretic mobility of variants of serum proteins and HLA tissue types[342]. From approximately 1975, the use of restriction fragment length polymorphisms (RFLP) became widespread, initially viewed by Southern blotting. From the 1990's the use of short tandem repeats (microsatellites) become particularly powerful for linkage, as numerous alleles may be present in a family. Some of the early examples of these being used to determine aetiology of human disease include ophthalmic conditions [343, 344]. The advent of the Human Genome Project[345] (see Section 4.1.3) enabled the mapping of the more common polymorphisms; SNPs. Assessing for linkage with SNPs became common in the early part of this century. Further details of SNPs and their importance are discussed in chapter 3. Their use in assessing for regions of homozygosity grew as SNP genotyping array technologies improved.

3.3.3. GENOTYPING

Microarray hybridisation technology was developed in the 1990s, allowing many hybridisation assays to occur simultaneously. Microarrays consist of many thousands of probes (oligonucleotides) fixed to a glass or other surface. Fluorescently labelled denatured DNA (from the test sample) is then hybridized to the probe molecules on the microarray. The bound fluorescence is then viewed with a scanner, and the signal emitted is then analysed according to intensity. Genome-wide SNP microarrays are available from two large companies; Affymetrix and Illumina. Affymetrix chip technology involves synthesis of oligonucleotide probes on the glass microarray, in situ.

For some cases in this study, Affymetrix SNP 6.0 was used. This incorporates 1.8 million markers, which includes 906600 SNPs and 946000 oligonucleotide probes designed to detect copy number variants. The distance between each marker is approximately1.6kb (http://ubioinfo.cicancer.org/TUTORIAL_3_CFontanillo_EuGESMA.pdf).

Illumina use pre-synthesized oligonucleotides. These are more than 70 nucleotides long, with a 50nucleotide gene-specific probe and approximately 22-25 nucleotide "address" code. These are coupled to silica microspheres (beads) which are 3μm diameter. Each of these beads acts as the array, and houses more than 100,000 identical oligonucleotides. The beads are spread across a microarray and immobilised within wells. After whole genome replication and fragmentation of target DNA, hybridisation to the probes occurs. Scanning of the fluorescent labels thus allow interpretation of the genotypes of interest. See Figure 3.3.

During this work, the Illumina CytoSNP-12 v2.1 was used in three families at St George's University of London. This chip incorporates over 250,000 SNPs across the genome.

For either chip, 500ng of DNA from each individual was sent for genotyping (St George's University of London: Illumina CytoSNP12, St Mary's Hospital Academic Medicine Department, University of Manchester: Affymetrix SNP 6.0). Excel sheets of SNP genotypes indicating regions of homozygosity were received from either department.

3.3.3.1. ANALYSIS OF GENOTYPE DATA

Illumina Genotype data is called using Illumina GenomeStudio, before being exported onto Excel ©. On Excel ©, a macro formula function was created to search for homozygous calls. Runs of consecutive homozygous calls were presumed to represent regions of loss of heterozygosity. If multiple affected members of one family were investigated, the macro would search for regions which were shared amongst them, and these were annotated.

Regions of homozygosity were then annotated on www. http://genome.ucsc.edu/cgi-bin/hgGateway to identify genes within these regions.

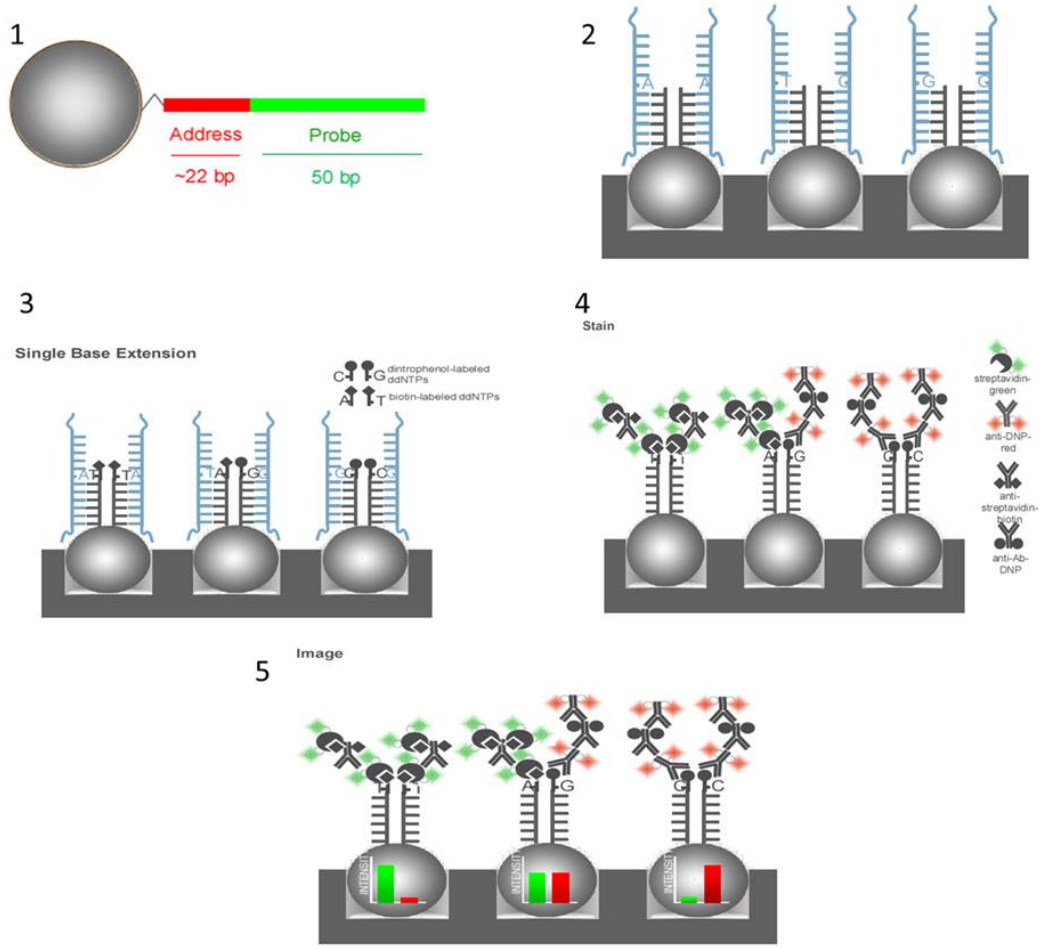

Figure 3.3: Schematic diagram illustrating the steps of bead technology.
1: Bead with oligonucleotide attached.
2-3: Hybridisation and single base extension along probe.
4-5: Staining of nucleotide of interest and imaging of fluorescent labels.

3.3.4. RNA EXTRACTION AND cDNA AMPLIFICATION

DNA sequencing was revolutionised by Sanger's "chain terminating" method in 1977[329]. However, even with the great strides that have been made in the interval 35 years, confirming that variations found by this method are pathogenic require definitive segregation analysis and/ or investigation of downstream cellular effects of such variations. It has been noted that up to 50% of point mutations which cause human disease affect the process of splicing[346]. Genomic DNA sequencing cannot inform us about the effect on the mRNA sequence, and thus impacts on splicing; such as the creation of pseudoexons or exonic deletion. Although there are bioinformatics methods of analysing mutations affecting the spliceosome[347] and experimental studies using in vitro or in vivo minigene approaches, the most accurate method involves investigating the mRNA itself. Handling RNA comes with significant challenges; due to the continual state of flux that RNA is in, the short half-life and differential rate of expression in different tissues. However, in cases where a certain genomic mutation cannot be found, one has to consider mutations elsewhere, perhaps in the intron or co-transcription factors; affecting the transcriptome. In this work, such techniques were used to amplify *ADAMTS17* in investigating family 6.

3.3.4.1. RNA EXTRACTION

RNA is unstable, therefore extracting and using this nuclear material involves more precautions than with DNA. The QIAamp RNA Blood Mini Kit (Qiagen ®) protocol was employed.

Prior to starting; all surfaces are cleaned with RNAse AWAY (Cole-Parmer©, USA). Buffer RPE was diluted in 4 volumes of 100% ethanol. 10µl of β-Mercaptoethanol, a potent reducing agent, was added to 1ml of Buffer RLT.

1ml of freshly extracted blood was mixed with 5mls of buffer EL. This was then incubated for 15 minutes on ice, with intermittent vortexing. The mixture was then centrifuged at 400xg for 10 mins at 4°C. The supernatant was discarded. 2mls of Buffer EL was added to the cell pellet, and vortexed. This was again centrifuged at 400xg for 10 minutes at 4·C before discarding the supernatant. 600µl of buffer RLT was then added to the leucocyte pellet and vortexed. This lysate was then added to the QIAshredder spin column and centrifuged at maximum speed (14,000xg) for 2 minutes.

The spin column was discarded, and the homogenised lysate was retained. 600µL of 70% ethanol was then added to this lysate and mixed. This mixture was added to a fresh QIAamp spin column and centrifuged into a 2ml collection tube for 15s at maximum speed (>8000 x g). This residue then underwent on-column DNase digestion with RNas-free DNase as such: 350µl of buffer RW1 was added to the QIAamp spin column with the residue in place. This was centrigfuged for 15s at maximum speed (>8000 x g). 80µl of buffer RDD and DNase solution (70µl RDD with 10µl DNase) was added directly to the QIAmp spin column, and allowed to work for 15 minutes at room temperature. 350µl of buffer RW1 was then added to the spin column and centrifuged for 15s at >8000 x g. The QIAamp spin column was placed in a fresh 2ml collection tube and 500µl of buffer RPE was added, before centrifuge at maximum speed for 15s. The flow through was discarded, and 500µL of buffer RPE was added to the spin column before a further centrifuge at full speed for 3 minutes. The spin column was then placed into a 1.5ml microcentrifuge tube and 40µl of RNase-free water was pipetted directly onto the membrane. A final centrifugation for 1 minute at maximum speed was undertaken. This final step was repeated with the flow-through being pipetted directly back onto the membrane before centrifuge.

The RNA sample in the collection tube (RNA solution) was quantified (concentration and purity) using spectrophotometric analysis (spectrophotometric analysis (Thermo Scientific NanoDrop 2000 – Thermo Fisher Scientific Inc.: see Section 2.3.4). Most abundant extracted RNA is ribosomal and messenger RNA. A simple test of integrity is to then run 2-5µL of this total RNA on a 1% Agarose Gel. Two of the four (28S and 18S) subunits of RNA can be demonstrated on the 1% Gel. Any genomic DNA contamination would manifest as larger products on the Agarose gel (Figure 3.4).

8µL was then used in cDNA synthesis and the rest stored at -40^0C.

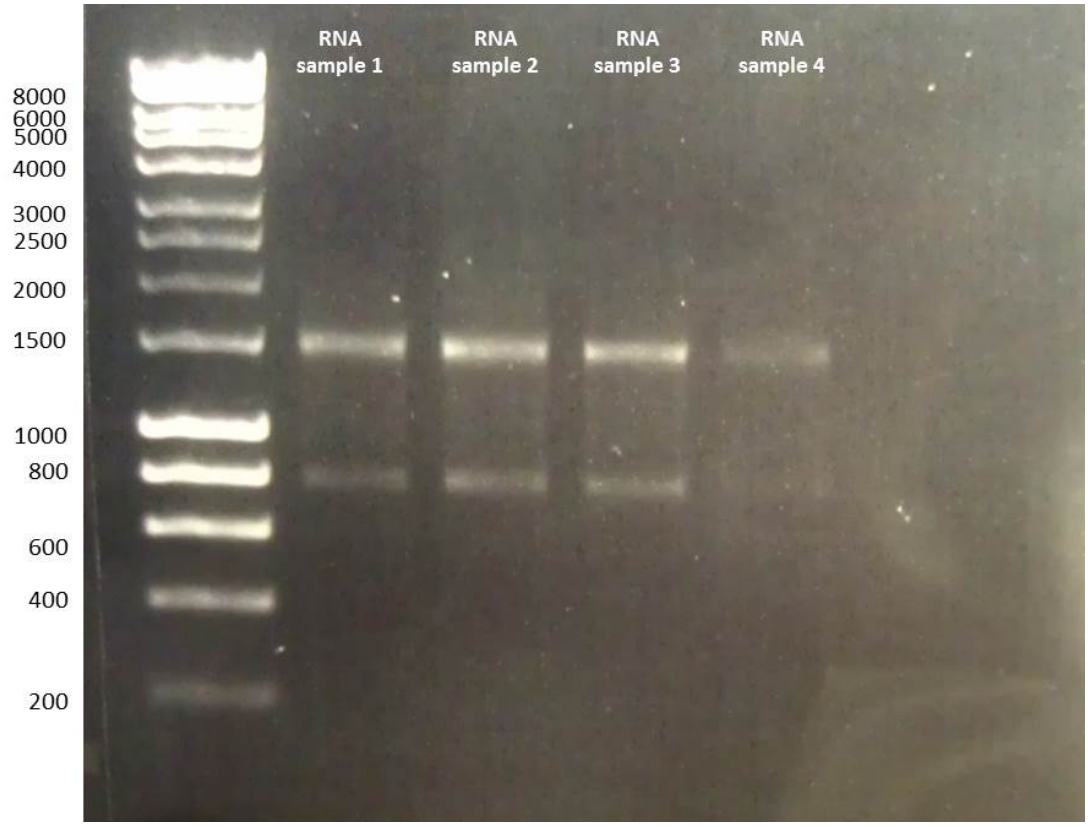

Figure 3.4: 1% Agarose gel of RNA demonstrating two bands representing 2 subunits of ribosomal RNA. No large band is seen, confirming no contamination by genomic DNA.

3.3.4.2. RT-PCR

RNA underwent two-step reverse transcription PCR. In this process, cDNA is first synthesised by rt-PCR from the RNA. This cDNA was then either stored (4°C) or used in PCR using primers of choice.

cDNA synthesis itself has two stages:

Two mixtures (SOLUTION A) were prepared as below, totalling 10µL:

RNA	8µL
Random Hexamer (50ng/µl)	1µl
dNTP (10mM)	1µL

These two samples were incubated at 65°C for 10 minutes. This is to denature the total RNA. The sample is then placed on ice immediately for 2 minutes to reduce RNA degradation and premature cDNA synthesis. During this period, solutions as below are prepared.

	+	- (Enzyme free)
5x RT buffer	4µL	4µL
RNAse inhibitor (10units/µl)	1µl	1
Reverse Transcriptase	0.25µl	-
RNAse-free water	4.75µL	5µl
TOTAL	10µl	10µl

All steps are done on ice: Solution A (10µL) was added to each of these above which included a negative control.

Both samples are then incubated for 4 hours at 37°C, before a termination step for 15 minutes at 70°C. PCR was then undertaken for β-actin using primers spanning exon/exon boundaries, to confirm cDNA presence. Subsequently primers were used to amplify *ADAMTS17* from this cDNA are demonstrated in appendix XII.

3.4. RESULTS

3.4.1. FAMILY 1-3

3.4.1.1. FAMILY 1

See Figure 3.5A for pedigree.

3.4.1.1.1. CLINICAL

This patient (IV:1) was examined by colleagues in Gießen, Germany (Dr Markus Preising and Professor Birgit Lorenz). This male child was born at full term via normal vaginal delivery to first cousin parents. He was noted to have reduced vision at 6 months old. At one year old his binocular vision was recorded as 0.1 LogMAR. He was noted to have ectopia pupillae. Pigmentary changes were noted throughout the retina. Electroretinogram (ERG) illustrated a reduced amplitude of the combined rod and cone specific responses. The amplitude of rod responses was however maintained. Photopic cone amplitude was markedly diminished, and remained so, at the next four examinations over six years. Whether these changes are stationary or progressive is not clear. Most convincingly there was significant micro-cornea (horizontal corneal diameter 8.5cm OU). At last appointment (7 years old: 2006) visual acuity was LogMAR (1.25LogMAR (right eye)and 1.43 (left eye). Axial length at 3 years of age was 23.04mm bilaterally and the patient was emmetropic. The provisional diagnosis for this child was cone-dystrophy of unknown origin associated with EP and microcornea. There was no lenticular pathology.

No one else in the family was affected, in particular both parents (III:1 and III:2).

3.4.1.2. FAMILY 2

See Figure 3.5B for pedigree.

3.4.1.2.1. CLINICAL

Family 2 are of Pakistani origin. The proband (AII:1) was born in 1981 to parents who were first cousins once removed. He was born full term, via normal vaginal delivery. He presented at the age of two years with bilateral cataracts. These were extracted and it was noted that he had weak zonules. He was also noted to have a significant exoptropia, and underwent medial rectus resection and lateral rectus recession in the same year as

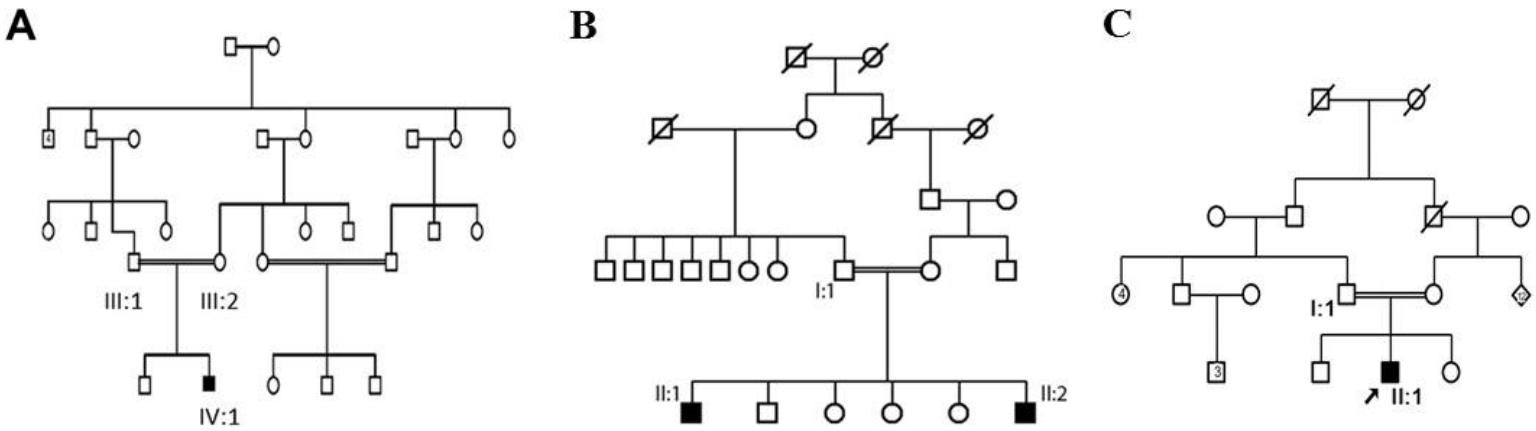

Figure 3.5: Pedigrees of Family 1-3.

A: Family 1: Proband (IV:1) is indicated by the black arrow.
His parents (III:1 and III:2) are first cousins.
B: Family 2: The proband (AII:1) and his brother (AII:2) were affected.
His parents are first cousins once removed.
C: Family 3: The proband's (II:1) parents are first cousins

the cataract surgery. He was found to have an unusual tessellated fundal appearance (Figure 3.6), associated with a nystagmus. In 1984, there was concern of neurological delay, and he therefore had urine homocystine levels measured which excluded homocystinuria. By 1990, his visual acuity was noted to be 1.0 (LogMAR). Paediatric electrodiagnostic analysis in 1992 suggested that there was unlikely to be gross retinal dysfunction. By 1993, he was noted to have micro-cornea (8mm horizontally bilaterally) (Figure 3.7). A pattern ERG was attempted, but the nystagmus prevented a detectable response. A full field ERG was undertaken in 2003. Rod specific ERG b-wave amplitude was 60μV on the right and 45μV on the left; both accompanied by latency delays. Maximal response a- and b-wave amplitudes were 135 and 155μV on the right and 125 and 140μV on the left. A-wave latency delays were noted. 30Hz flicker was of abnormal implicit time from both eyes, with amplitudes of 15μV bilaterally. Photopic single flash ERG demonstrated profound a-wave latency delay with additional abnormal b-wave implicit time. Overall, this demonstrated subnormal cone and rod function with profound delays, worse in the former. Axial lengths were 26.06mm (in right eye) and 25.86mm (in left eye). His best visual acuity in 2012 was 0.9 LogMAR (6/48). He had no other medical history, and required no medication. His parents were unaffected.

His brother (AII:2) was born in 1988 at full term by normal vaginal delivery. He presented at the age of three years with bilateral ectopia lentis (EL). He was hypermetropic with a refractive error of +6.5DS bilaterally. His best visual acuity was regarded as 0.78 LogMAR (6/36) bilaterally. Central macula pigmentation was noted at this stage. He was registered partially sighted. He was noted over the years of attending the eye clinic that he was of Marfanoid appearance. In 1999, he suffered an RD in the right eye. His lens was extracted at the time of initial repair of the RD. He underwent three operations, which resulted in this eye being left with silicone oil in situ. His retina was detached under the oil. He was noted to have unusual peripapillary atrophy in the left eye at that stage. In 2006, he suffered a RD in this left eye, and at surgery, the vitreoretinal interface was described as unusual. After two operations, his retina has remained attached. He is aphakic, and has aphakic glaucoma. His axial lengths were 21.7mm (right eye) and 29.5mm (left eye; posterior Staphyloma). He was also noted to have microcornea (8mm). Systemic examination revealed arachnodactyly (Figure 3.8C).

Systemic examination has excluded connective tissue disorders such as MFS.

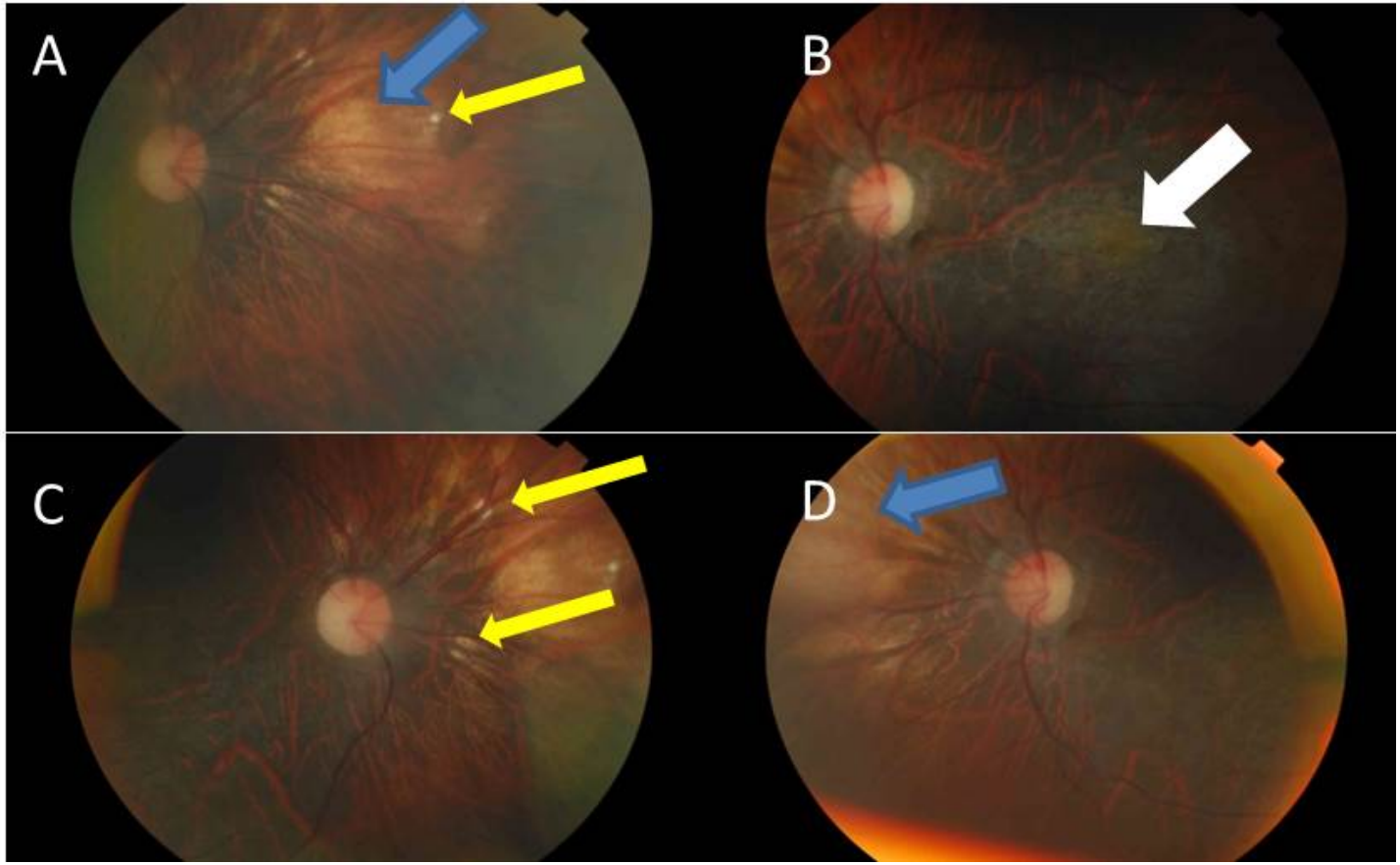

Figure 3.6: Fundal photography of AII:1. A & C: Right eye. B & D: Left eye. Blue arrows indicate periparillary atrophy. Yellow arrows indicate punched out chorioretinal lesions. Maculopathy is visible in B (white arrow).

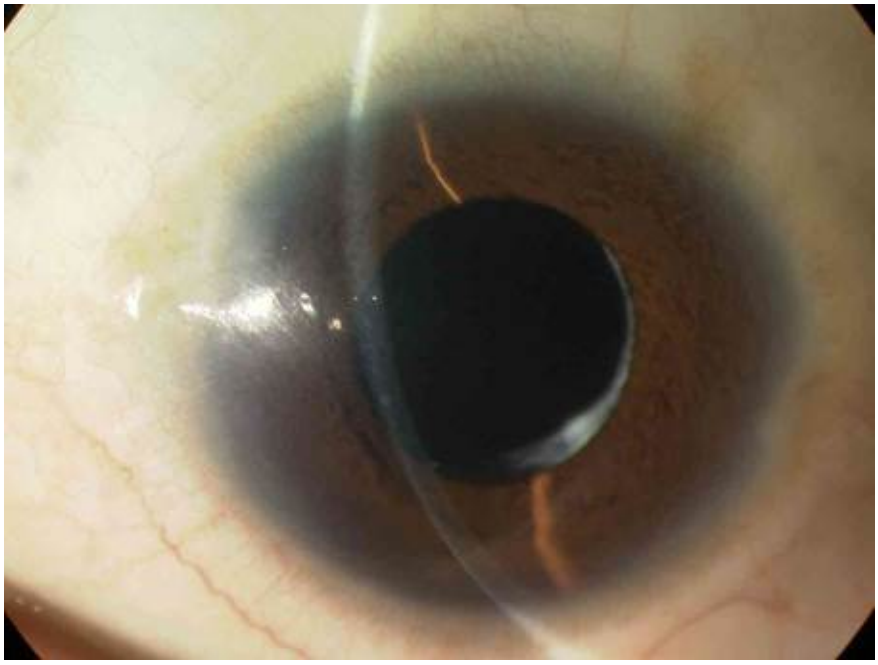

Figure 3.7: Anterior segment photography of AII:1 illustrating microcornea

.

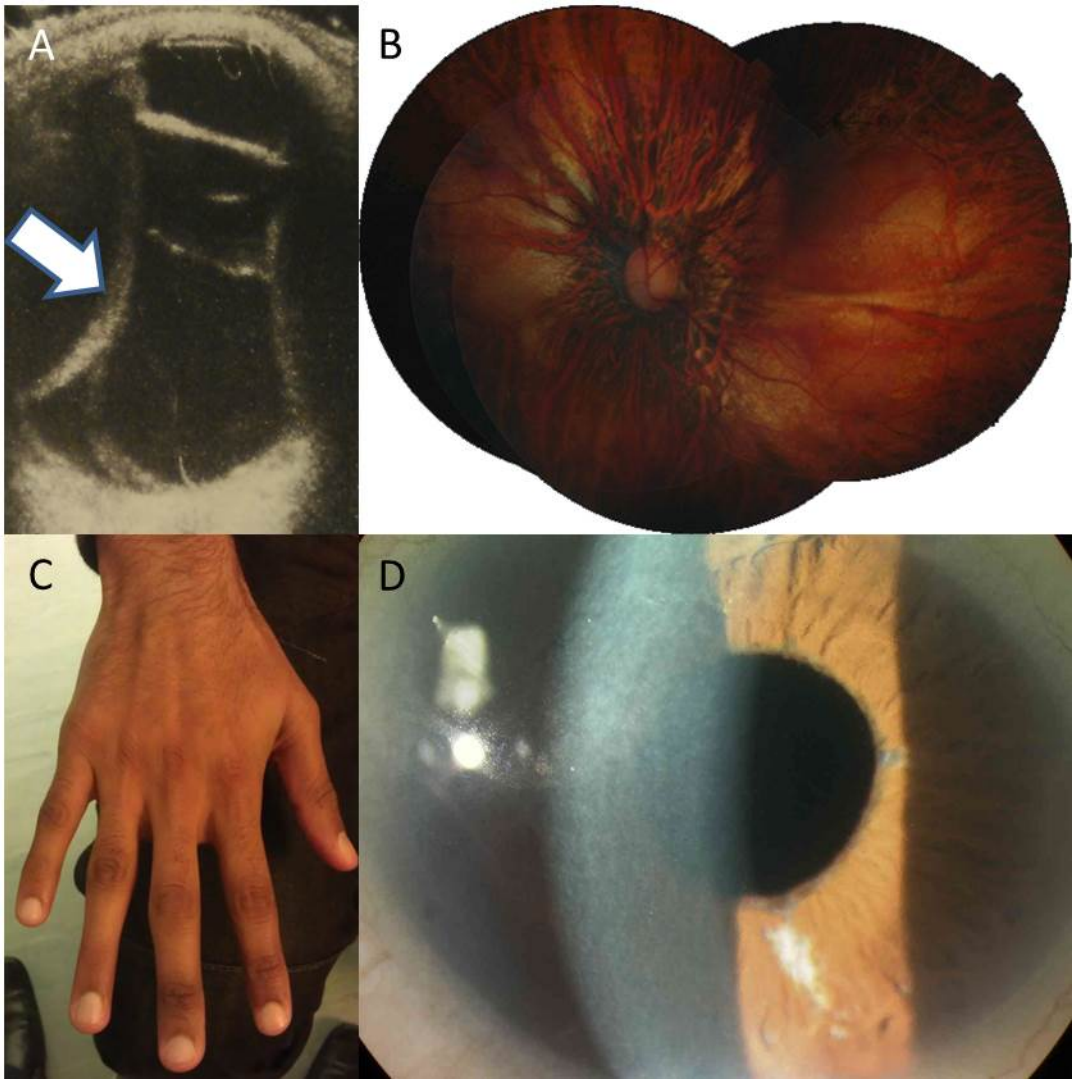

Figure 3.8: Clinical features of AII:2. A: Ocular ultrasound demonstrating almost total retinal detachment (arrow). B: Left fundal photograph demonstrating widespread peripapillary atrophy. C: Arachnodactyly
D: Microcornea and normal appearing iris

Post-contrast computed tomography (CT) of the brain and orbits demonstrated imaging features common to both siblings (Figure 3.9 a-f). The sella turcica was expanded with displacement of pituitary tissue and infundibulum inferiorly and posteriorly respectively within the pituitary fossa. Meckel's caves (location of the Gasserian ganglion of the Trigeminal nerves) were also observed to be large and predominantly of cerebrospinal fluid (CSF) density. This CSF density was seen to extend to and through foramina Ovale (through which the Mandibular nerves exit the skull). The overall appearances were suggestive of dural ectasia and herniation similar to that seen in raised CSF pressure states (e.g. Idiopathic Intracranial Hypertension) neurocutaneous syndromes, (e.g. Neurofibromatosis type I) or connective tissue disorders (such as MFS).

3.4.1.3. FAMILY 3

See pedigree (Figure 3.5C)

3.4.1.3.1. CLINICAL

The male proband (BII:1) is of Pakistani origin born to first cousin parents. At two years of age he was noted to have myopic astigmatism. With correction, there was no improvement by the age of six years of age and he was referred for an opinion on punctate lens opacities and a myopic tessellated fundus (Figure 3.10). At this time his visual acuity was logMAR 0.2 in his right eye and 0.3 in the left. Spherical equivalence was noted to be -5DS bilaterally. Microcornea was noted.

By eight years of age his visual acuity had deteriorated (Right eye 0.4 LogMAR and Left eye 0.34 logMAR). His myopia has also increased -7.50 DS (right) and -9.50DS (left) (spherical equivalent). Electroretinography revealed cone dysfunction with normal rod function.

A ISCEV[348] ERG aged 13 years showed progression to a cone rod dystrophy. His myopic refraction had further progressed to -14DS spherical equivalence bilaterally. He was noted to have central cataracts, smooth irides and microcornea (7.5mm horizontal bilaterally: Figure 3.10A).

At the age of 15 years old, he developed a total RD in the right eye, secondary to a giant retinal tear. A year later, he presented with the same condition in his contralateral eye. The RD was successfully repaired in each eye.

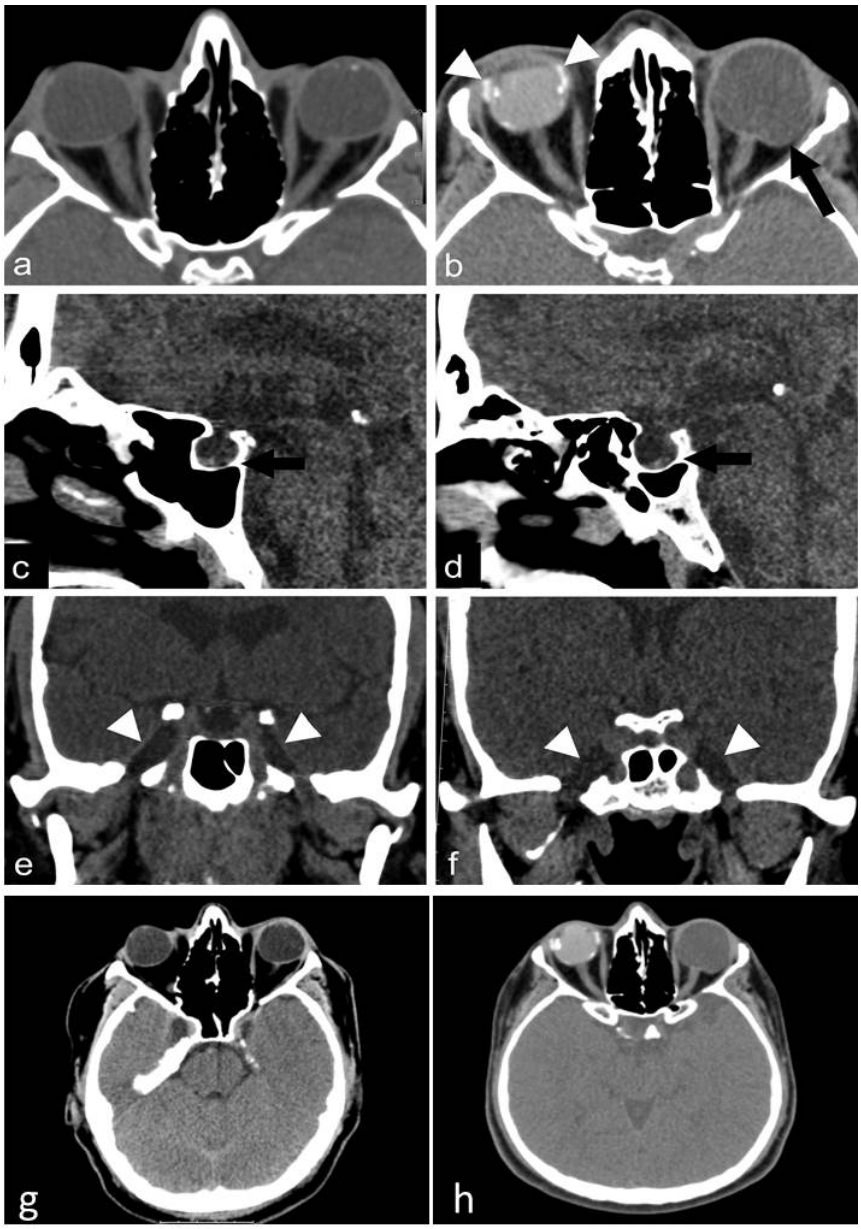

Figure 3.9: Computerised Tomography of AII:1 and AII:2. Post-contrast Computed Tomography (CT) of the 2 siblings: panels a,c,e and b,d,f belong to each sibling respectively. Axial reconstructions through the orbits (a & b) demonstrating aphakic and elongated orbits. In panel (b), there is a posterolateral ocular staphyloma (white arrow) and evidence of previous scleral banding and silicone oil tamponade (white arrowheads). Sagittal reconstructions through the pituitary fossa (c & d) demonstrating enlargement of the fossa which is predominantly CSF filled and displacement of the pituitary gland and infundibulum inferiorly and posteriorly respectively (white arrows). Coronal reconstructions through Meckel's caves and foramina Ovale (e & f) demonstrating bilateral CSF filled enlarged Meckel's caves and herniation of this through foramina Ovale (white arrowheads). g & h: Axial sections of skull, demonstrating no occipital defect. (Thanks to Dr Indran Davagnanam (Dept of radiology, Moorfields Eye Hospital) for images and report).

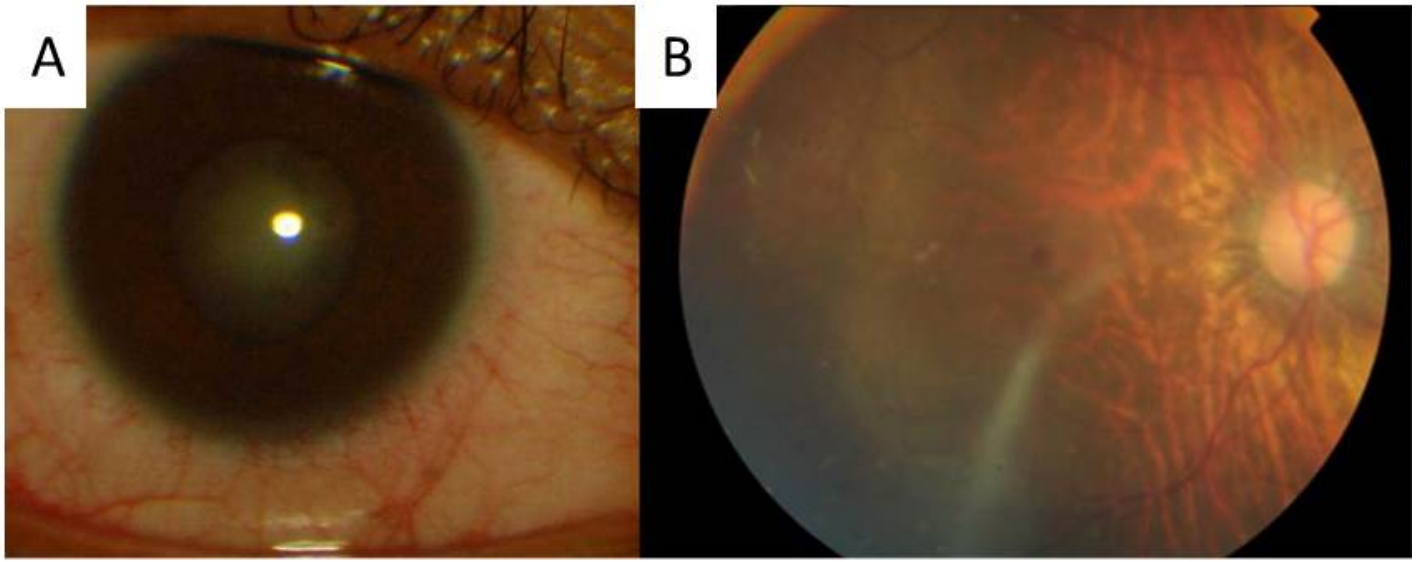

Figure 3.10: Phenotype of BII:1. (A) microcornea and punctate cataract
(B) tessellated fundus

Axial lengths were 27.7mm (right) and 29.0mm (left). Magnetic resonance imaging (MRI) imaging revealed no occipital defect. No other family members were affected.

3.4.1.4. GENETIC

3.4.1.4.1. Family 1

The proband had an unusual phenotype consisting of microcornea, ectopia pupillae and cone dystrophy, which has not previously been described. The pedigree suggested this to be inherited in an autosomal recessive manner. With the consanguinity in the family, it was more likely that this would be due to autozygosity; thus homozygous mutations.

The EP in this child was initially considered as an incomplete iris coloboma. The MRC Human Genetics Unit, University of Edinburgh (Dr K. Williamson and Dr D Fitzpatrick) were investigating this case using classic trio based exome sequencing (III:1, III:2, IV:1) as part of the UK10K exome sequencing cohort[349]. This was undertaken at the Wellcome Trust Sanger Institute (Cambridge, UK) using the Agilent SureSelect All Exon 50 mb kit. Excluding variants with a minor allele frequency >0.005, they then focussed on homozygous non-synonymous and pathogenic changes. In fact there was only one homozygous nonsense mutation. This was c.1067T>A [p.L356*] on exon 7 of *ADAMTS18*, a 23 exon gene on chromosome 16q23.1 covering 153kb of genomic sequence. This was confirmed with Sanger Sequencing, and found to be heterozygous in both parents (Figure 3.11). No other family members were available for investigation.

3.4.1.4.2. Family 2

The diagnosis in these two affected brothers was unclear, so investigations were undertaken to elucidate the cause of the phenotype. Because of the consanguinity in the family, it was assumed that the inheritance would be autosomal recessive. The proband (AII:1) was analysed using the Affymetrix Genome Wide Human SNP array 6.0[350]. Regions of homozygosity are demonstrated in table 10.

To help define the causative mutation, DNA from this proband underwent high throughput sequencing for 106 genes known to cause retinal dystrophies at St Mary's Hospital, University of Manchester [4].

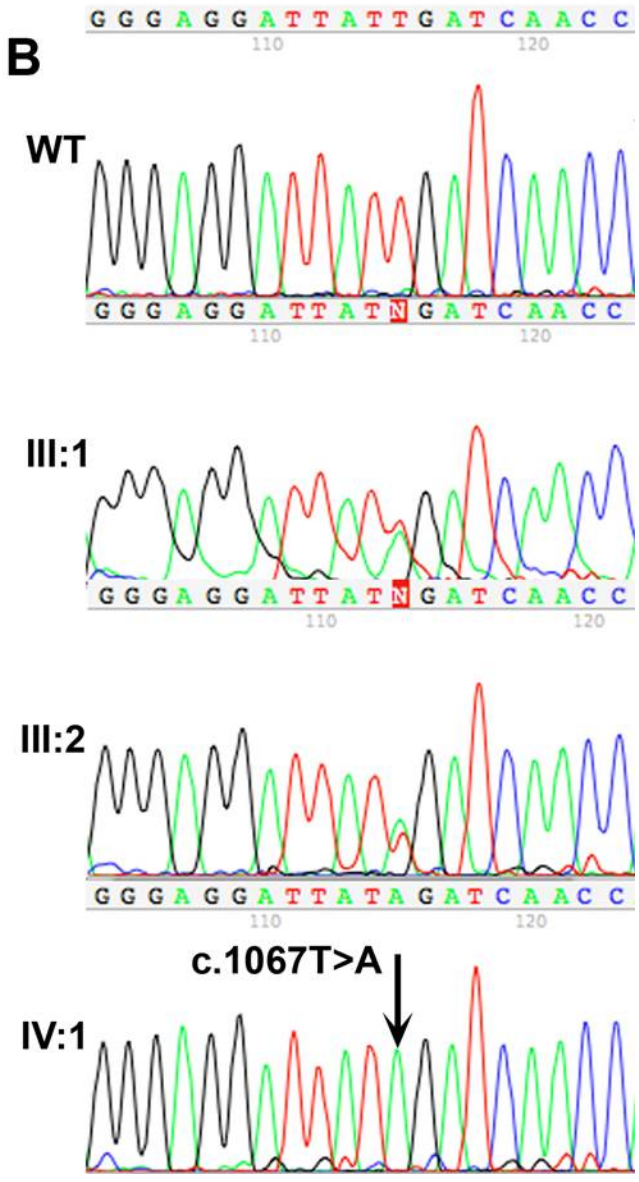

Figure 3.11: Chromatograph demonstrating the *ADAMTS18* mutation c.1067T>A [p.L356*] in family 1. It is in the heterozygous state in both parents (III:1 and III:2). The wild type (WT) is also shown.

Chromosome	Autozygosity size (mb)
19:6,059,840-14,742,924	8.683
20: 1,681,609-9,950,715	8.269
16: 72,334,370-79,228,734	6.895
22: 33,056,621-38,877,740	5.821
22: 44,069,626-46,165,101	5.095
19: 52,108,930-54,054,786	1.945
12: 128,059,453-129,656,359	1.597
20: 60,398,804-61,406,884	1.008

Table 10: Regions of homozygosity for AII:1 (presumed to be autozygous)

The genes screened at the University of Manchester are defined in table 11.

No pathogenic mutations were discovered. The homozygosity data was therefore revisited. In the region on chromosome 16q23.1 one candidate gene stood out; *ADAMTS18* (Figure 3.12).

This gene was sequenced in the two affected brothers (AII:1, AII:2),their father (AI:1) and 40 control chromosomes from the same ethnic group as the patients. One homozygous missense mutation was discovered (c.2159G>C (p.C720S)) (Figure 3.13).

3.4.1.4.3. Family 3

Because of the similar phenotype to Family 2, *ADAMTS18* was sequenced in DNA from the proband (BII:1) and his father (BI:1) using the same methods as described for Family 2. One homozygous mutation in exon 13, (c.1952G>A [p.R651Q]). was discovered from the proband which was in the heterozygous state in the father (Figure 3.14).

All three mutations are predicted to be pathogenic according to in silico analysis (SIFT[244], PolyPhen[245], Mutation Taster[351]). The two missense mutations were absent from 40 ethnically matched controls chromosomes and are not present in online databases (1000 Genomes[248], Exome Variant Server[246], Genbank dbSNP library[247]). The amino acid residues affected by the mutations are conserved amongst vertebrates.

3.4.2. FAMILY 4

See Figure 3.15 for pedigree.

3.4.2.1. CLINICAL

This family are of Romanian gypsy origin. The proband (CII:1) was noted to have poor vision by the age of 2 years old. He has had developmental delay diagnosed by the age of four years old. By the age of 15 years he was seen at Moorfields Eye Hospital and a horizontal jerk nystagmus was evident bilaterally. Visual acuity was LogMAR 0.7 (right and left) at 50 centimetres.

CA4	*PROM1*	*RLBP1*	*ELOVL4*	*BBS2*	*OTX2*
CERKL	*PRPF3*	*ROM1*	*CNGA3*	*BBS4*	*DHDDS*
CNGA1	*PRPF31*	*RP2*	*CNGB3*	*BBS5*	*PITPNM3*
CNGB1	*PRPF8*	*RPE65*	*GNAT2*	*BBS7*	*MKS1*
CRB1	*PRPH2*	*RPGR*	*PDE6C*	*GPR98*	*PRPF6*
CRX	*RGR*	*SAG*	*RS1*	*PCDH15*	UNC119
EYS	*RGS9*	*SEMA4A*	*FZD4*	*USH2A*	
FSCN2	*RHO*	*TOPORS*	*LRP5*	*CDH23*	
GUCA1B	*KCNV2*	*TTC8*	*NDP*	*MYO7A*	
IDH3B	*RIMS1*	*TULP1*	*GUCA1A*	*USH1C*	
IMPDH1	*RPGRIP1*	*CEP290*	*TIMP3*	*USH1G*	
KLHL7	*UNC119*	*AIPL1*	*EFEMP1*	*FAM161A*	
MERTK	*C1QTNF5*	*GUCY2D*	*RDH5*	*C2orf71*	
NR2E3	*BEST1*	*LCA5*	*TEAD1*	*IMPG2*	
NRL	*ABCA4*	*LRAT*	*RAX2*	*PDE6G*	
RP1	*CHM*	*RD3*	*CLRN1*	*SNRNP200*	
RP9	*BBS9*	*RDH12*	*ARL6*	*RBP3*	
PDE6A	*MKKS*	*SPATA7*	*BBS1*	*ZNF513*	
PDE6B	*TRIM32*	*ADAM9*	*BBS10*	*CDHR1*	
PRCD	*DFNB31*	*CACNA2D4*	*BBS12*	*RP1L1*	

Table 11: Genes screened by next generation sequencing by the University of Manchester [4]

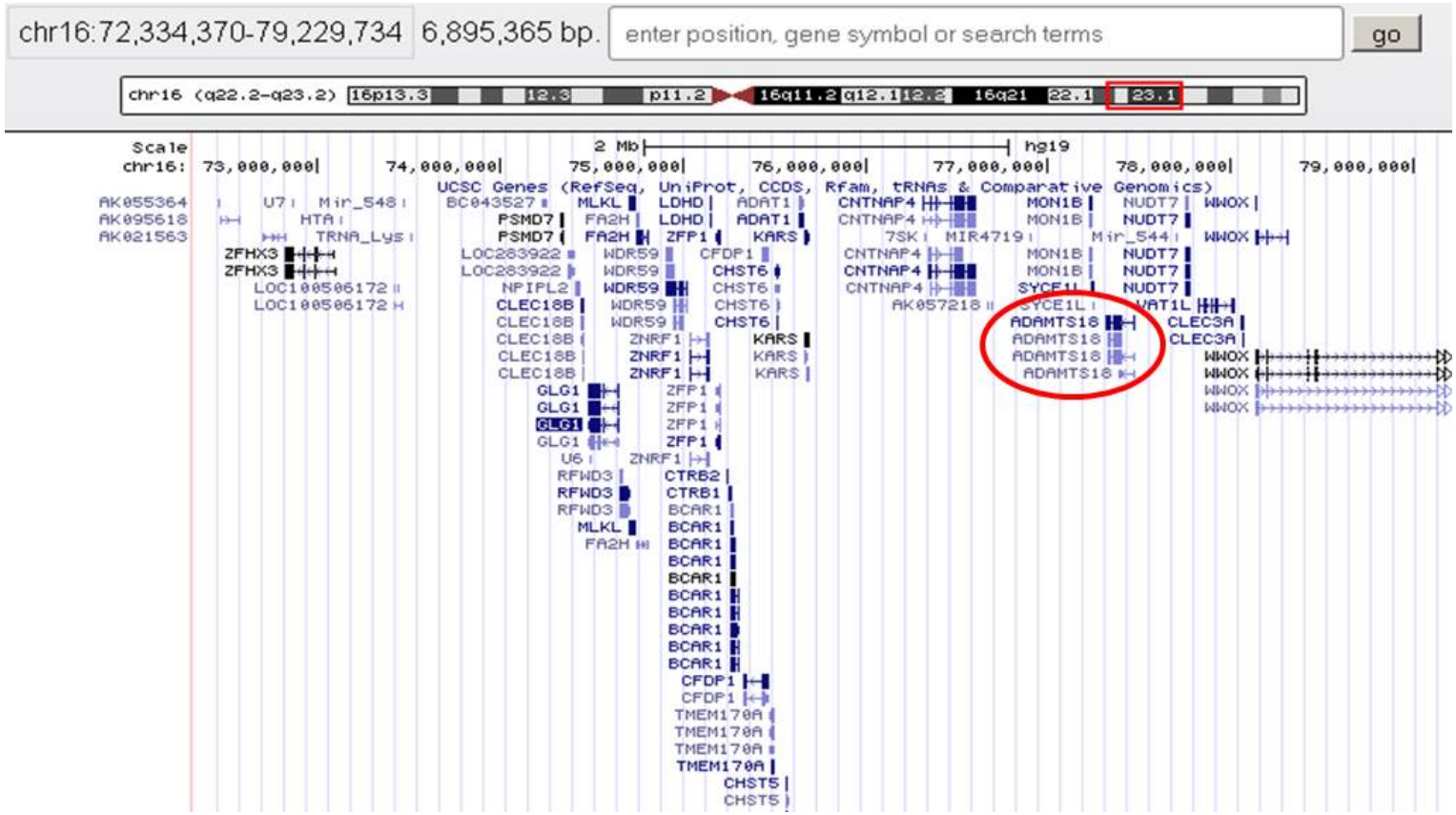

Figure 3.12: Genes within 16:72,334,370-79,229,734. Encircled is *ADAMTS18*.
Image from www.http://genome.ucsc.edu

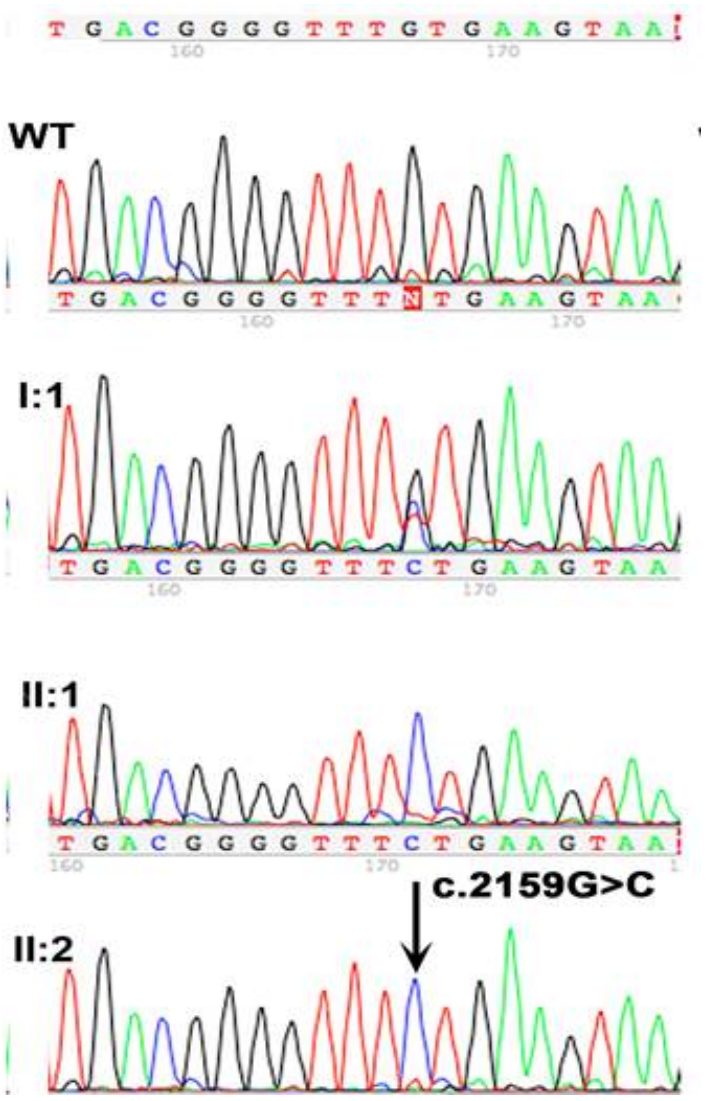

Figure 3.13: Chromatograph demonstrating the *ADAMTS18* mutation (c.2159G>C) in affected members of Family 2: II:1 and II:2. It is absent in the wild type (WT), and heterozygous in the unaffected father (I:1)

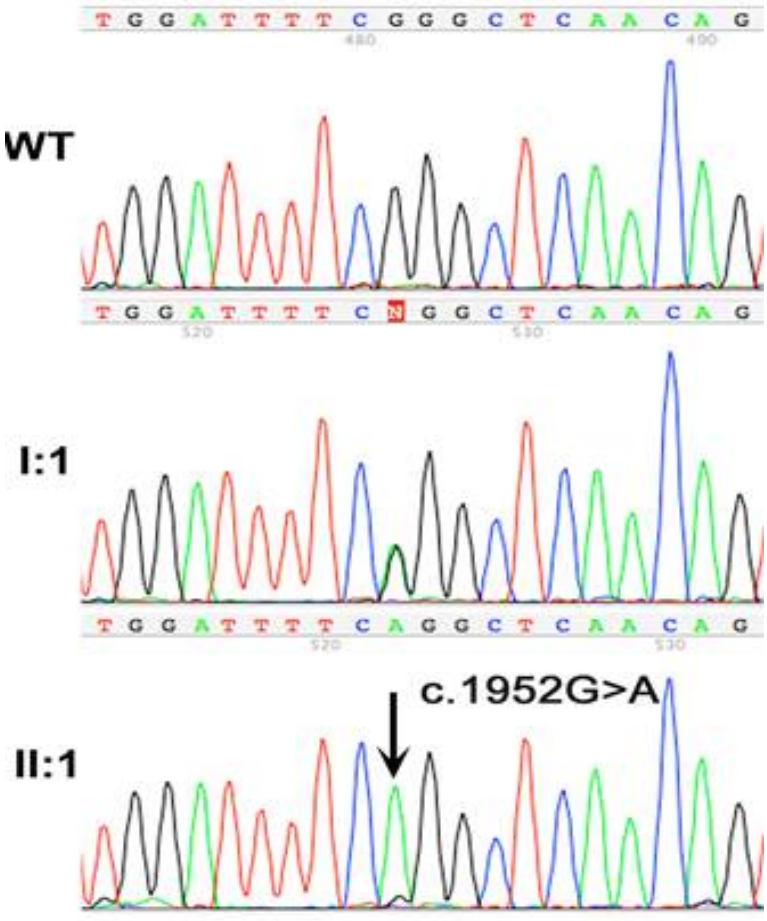

Figure 3.14: Chromatograph demonstrating the *ADAMTS18* mutation (c.1952G>A) in affected family 3. It is absent in wild type (WT) and in the heterozygous state in the unaffected father (I:1)

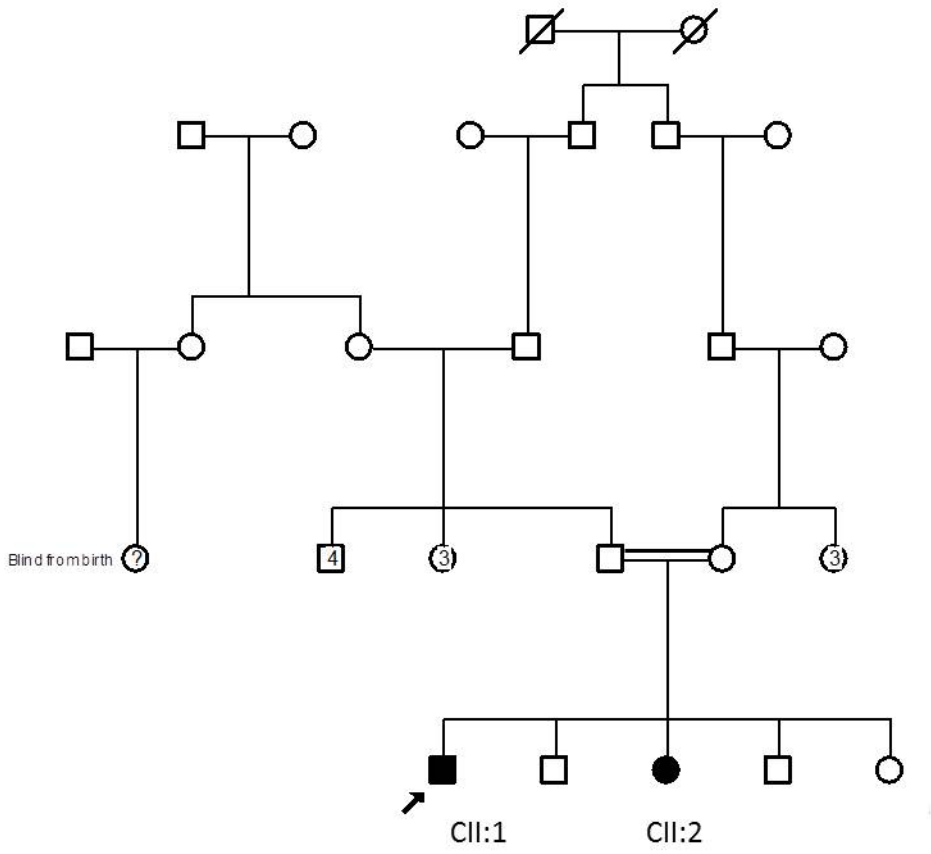

Figure 3.15: Pedigree of Family 4

Anterior segment examination revealed microcornea bilaterally (horizontal corneal diameter 8mm bilaterally at 16 years of age – Figure 3.16A & D) and bilateral EL. Both lenses were displaced superotemporally. He had characteristic lens opacities (Figure 3.16B & E). Fundal examination demonstrated bilateral chorioretinal atrophy. Electordiagnostic examination (aged 15 years) revealed a small amplitude cone specific ERG with a delay to peak. Rod photoreceptor function was normal. This was interpreted as a cone dystrophy. Axial lengths were noted, at 16 years old, to be 26.01mm (right eye) and 26.02mm (left eye). He is registered partially sighted. Examination revealed a fibrillar vitreous, similar to seen in vitreoretinopathies[117]. Skull imaging revealed an occipital bone midline defect above the external protuberance with herniation of brain; suggesting an encephaloceole.

His sister (CII:2) was noted to have EL at a very early age. She has also characteristic lens opacities (Figure 3.17). No developmental delay was noted. She had a similar fundal appearance to her brother; characteristic chorioretinal, particularly peripapillary atrophy. Axial lengths, at 10 years old, were noted to be 29.3 (right eye) and 29.1 (left eye), indicating high myopia. Skull imaging revealed an unusual appearance over the occipital protuberance which may be consistent with an encephaloceole.

3.4.2.2. GENETIC

The very similar phenotype to family 2 led to screening *ADAMTS18*. This revealed no mutations. Therefore, because of the consanguinity in this family, autozygosity mapping was arranged for CII:1. DNA was hybridised to the Illumina CytoSNP-12 v2.1. Regions of homozygosity are shown in table 12.

There were numerous regions over 5mb on different chromosomes. Of particular interest in the region on chromosome 21 which harbours more than 30 genes, including *COL18A1*. An image of this region from www.ucsc.edu is demonstrated in figure 3.18, with *COL18A1* in particular gene of interest highlighted.

The gene *COL18A1* is known to cause Knobloch syndrome 1; a condition with strikingly similar phenotype to our proband. This gene is currently undergoing screening at the UCL Institute of Neurology, and it is expected that a homozygous mutation will be harboured within this gene.

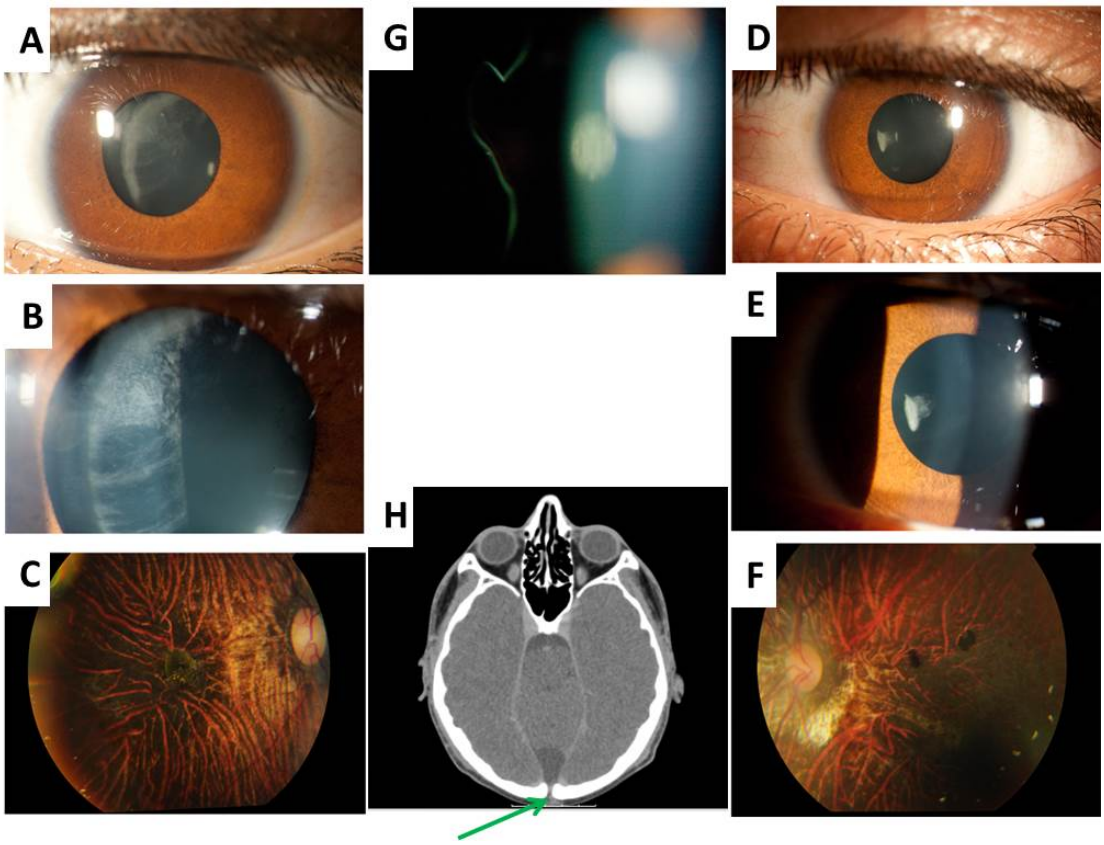

Figure 3.16: Clinical features of CII:1. **A&D:** Right & Left anterior segment demonstrating featureless iris. **B&E:** Right and Left characteristic lenticular opacities. **C&F:** Right and Left fundal photograph. **G:** Fibrillar vitreous
H: Axial CT demonstrating occipital defect (arrow).

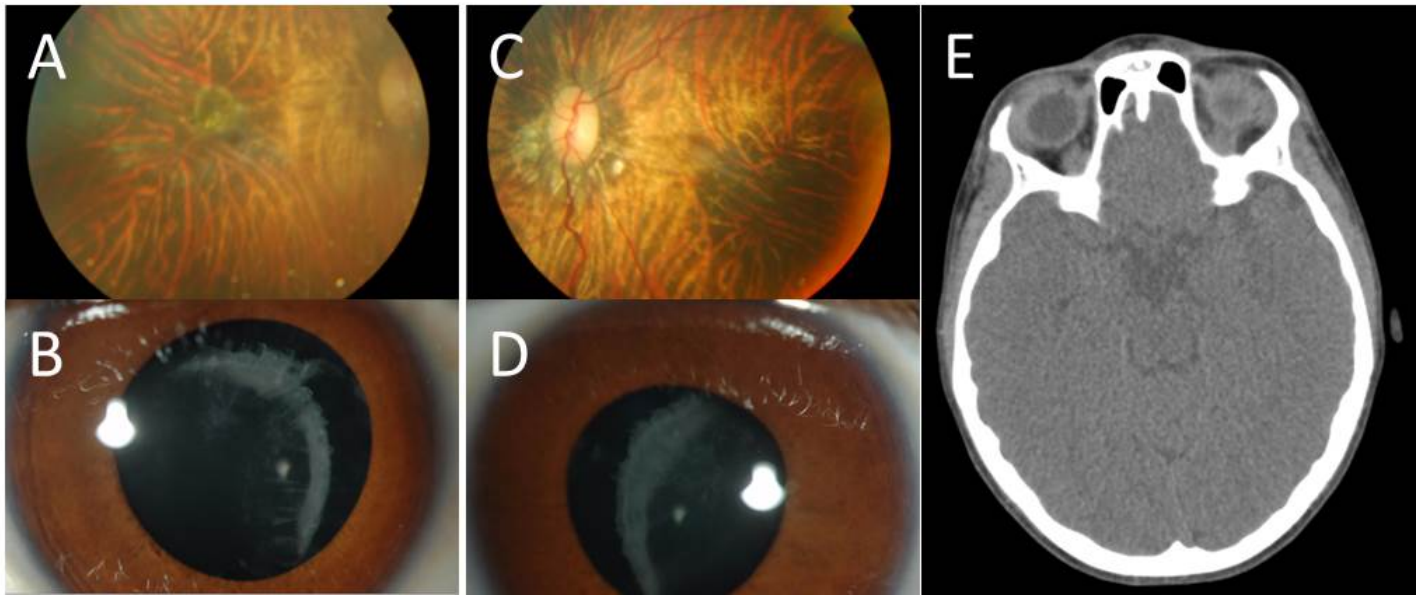

Figure 3.17: Clinical images of CII:2. **A & C** Fundal images of right and left eye. **B & D:** Anterior segment images illustrating characteristic cataract and ectopia lentis. **E:** Axial Computerised Tomography of brain

Chromosome	Nucleotide	Size (bases)
17	21,714,456-55,220,949	33,506,493
1	223,614,061-241,720,543	18,106,482
1	4,833,498-14,126,651	9,293,153
44	9,972,163-18,787,232	8,815,069
2	138,870,442-158,283,430	19,412,988
2	99,264,217-107,778,931	8,514,714
1	156,209,857-165,195,664	8,985,807
11	57,992,068-77,730,725	19,738,657
21	31,194,195-48,098,824	16,904,629

Table 12: Regions of autozygosity greater than 8mb for BII:1

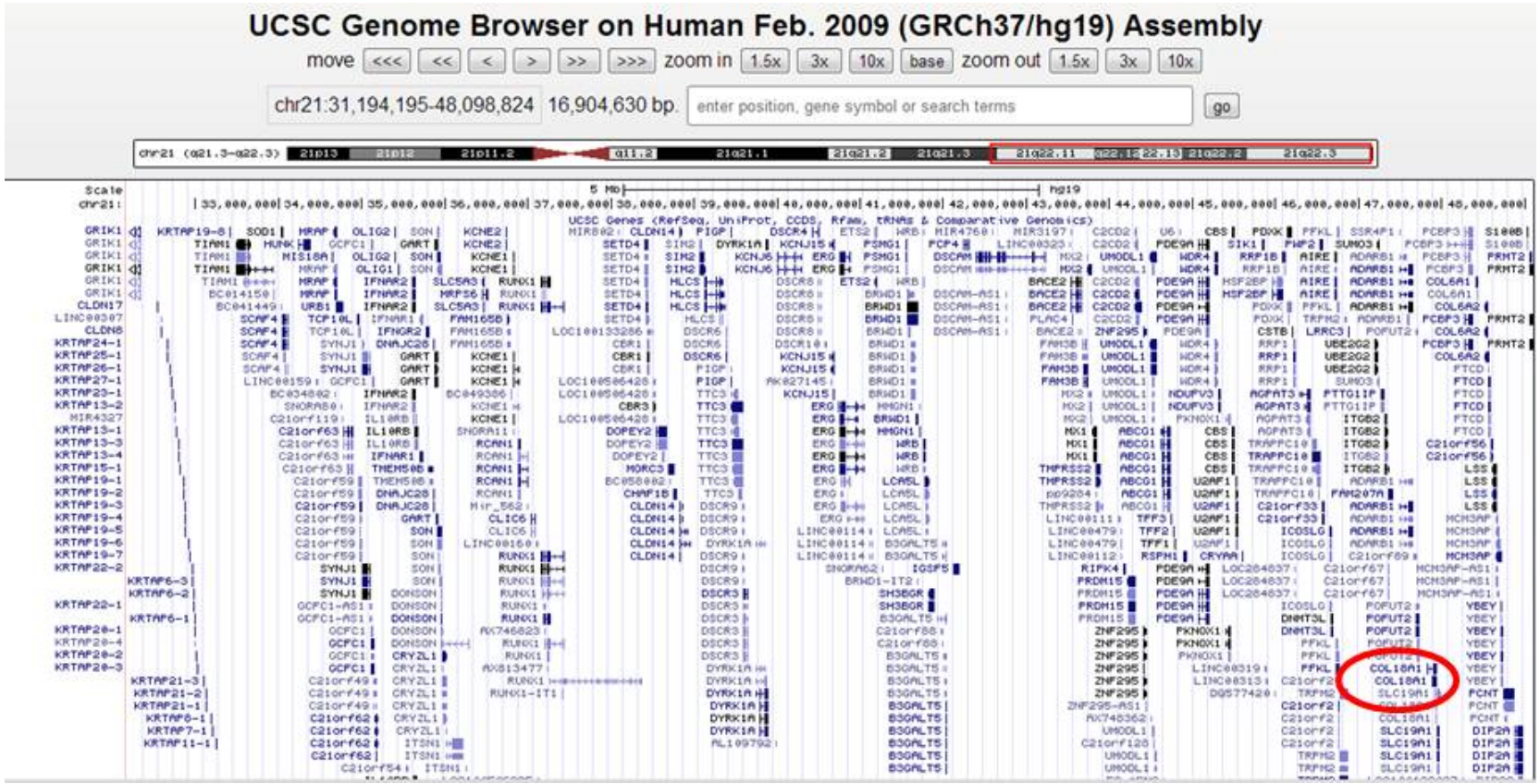

Figure 3.18: Genes harboured in region of LOH in chromosome 21 (from www.usc.edu). *COL18A1* is circled.

3.4.3. FAMILY 5

See figure 3.19 for pedigree.

3.4.3.1. CLINICAL

This is a family of six brothers and two sisters. Four of the brothers have a characteristic phenotype of RD and EL during childhood.

The proband DII:1 presented to Moorfields Eye Hospital by the age of seven years, having already lost the vision in the right eye secondary to failed RD surgery with lens extraction. At the age of 14 years old, he was noted to have a RD in his left eye, premature cataract and EL. The RD was secondary to a giant retinal tear. He was noted to have extensive superior circumferential lattice degeneration in this eye. This was repaired with pars plana vitrectomy and silicone oil injection. After removal of this silicon oil, his retina has remained attached. He is aphakic, with poor vision in the functioning left eye. He has also developed aphakic glaucoma. He is noted to have microcornea (8mm horizontal diameter) (Figure 3.20A). Although he is reported to be having been a high myope as a child, this may have been primarily lenticular, as his axial length at age 22 years was 21. 3mm.

Systemic examination reveals some Marfanoid features, including arachnodactyly (Figure 3.20B), large arm span: height (179cm tall with arm span 183.5cm) and an arched palate. Beighton hypermobility score[136] was 4/9. However, echocardiography features were completely normal, contributing towards an exclusion of clinical MFS (personal communication Dr A Child, St George's Hospital, London). MRI imaging of the brain revealed no occipital defect (Figure 3.21).

DII:2 developed a total RD in the left eye at eight years of age. The surgery to repair this failed, and he was left with a phthisical eye. Later that year, he was noted to have EL and a total RD in the contralateral (right) eye. This was repaired at Moorfields Eye Hospital with a lensectomy, vitrectomy and oil injection. He has also developed aphakic and silicone oil associated glaucoma in this eye. He has microcornea (Figure 3.20C) and axial length in this functioning right eye of 22.51mm. Systemically, he is noted to have Marfanoid features, including arachnodactyly (Figure 3.20D). Cardiovascular examination was unremarkable.

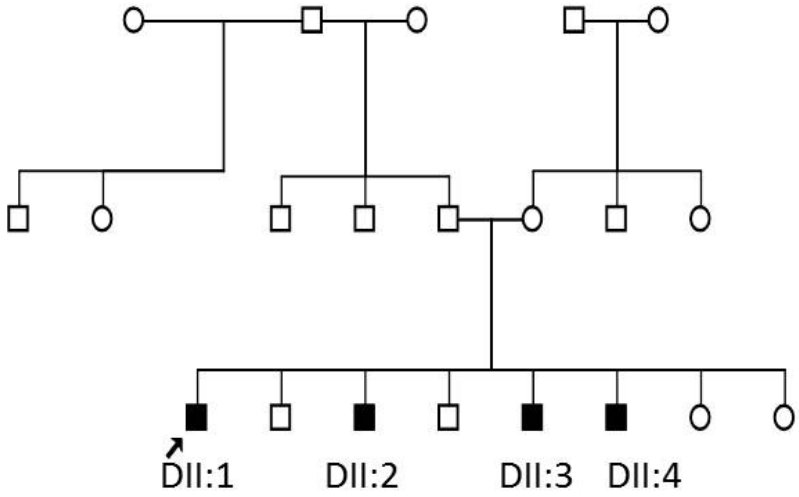

Figure 3.19: Pedigree of family 5

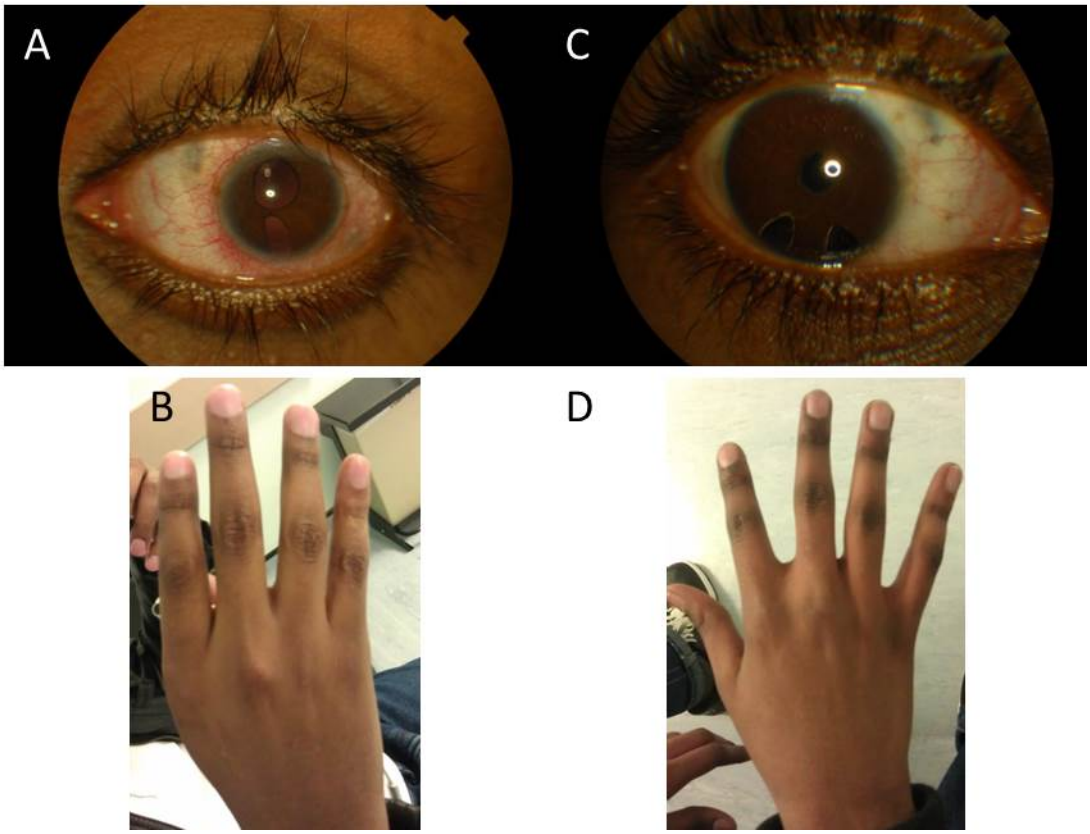

Figure 3.20: Clinical images of Family 5
A&C: Anterior segment images (A: DII:1, B:DII:2) illustrating microcornea. **B&C:** Arachnodactyly (B: DII:1, D: DII:2).

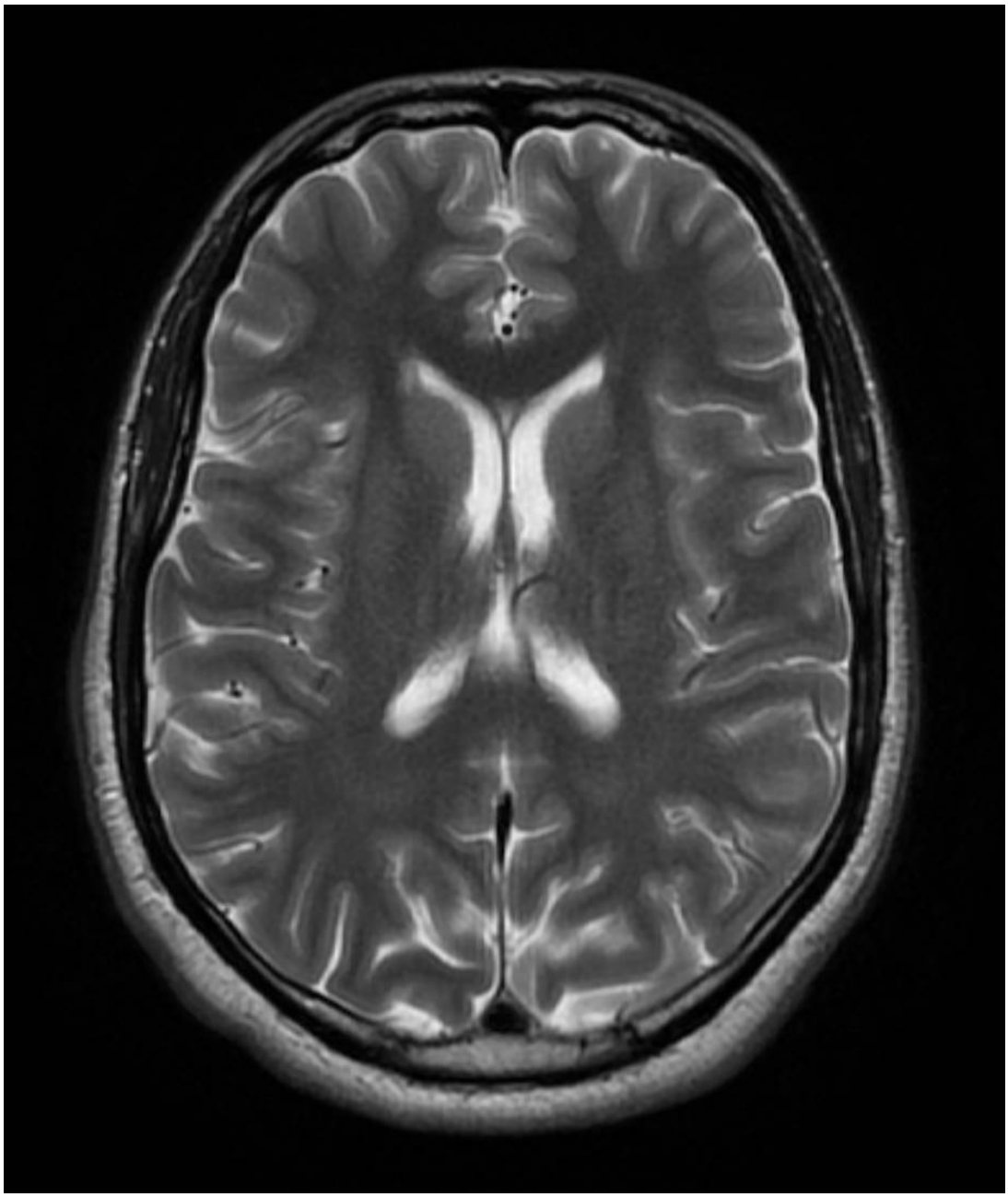

Figure 3.21: Axial MRI of DII.1 skull, demonstrating no occipital skull defect. (Thanks to Dr Indran Davagnanam (Dept of radiology, Moorfields Eye Hospital) for images and report).

DII:3 was diagnosed with a right RD at the age of four years. At the time bilateral EL was also noted and extensive nerve layer myelination. The right eye was repaired with pars plana vitrectomy and lensectomy. Later that year the same operation was undertaken on his left eye for RD with EL. He had silicone oil injected into both eyes, but required further surgery to the left eye at the age of 11 years. He has also developed aphakic silicone oil associated glaucoma.

DIII:4 was diagnosed with significant EL bilaterally at the age of three years. He underwent bilateral vitreolensectomies. He was stable until the age of five years, when a total RD was noted on the right. In this boy it will be difficult to know if this was a primary RD or secondary to the vitrectomy for the lens removal. In view of the family history it is likely that he may have developed an RD independently. He required silicone oil injection in this eye. A further operation was required at the age of seven years to remove emulsified silicone oil from this eye. At most recent visit, his vision was LogMAR 1.0 (right) and 0.74 (left).

3.4.3.2. GENETICS

DNA was only available from the proband (DII:1), thus limiting the analysis. The other affected members are children, and parental consent for investigations was not possible. In view of the similar features to family 2 (particularly AII:2) *ADAMTS18* was sequenced in the proband. This revealed no pathogenic mutations.

Because of the EL and Marfanoid features, *FBN1* was sequenced. One heterozygous missense variant was discovered (c.8300A>G (p.N2767S)) (Figure 3.22).

In parallel to this experiment, DNA from DII:1 was hybridised to the Illumina CytoSNP-12 v2.1 and homozygous regions identified. Homozygosity mapping for DII:1 revealed large regions of autozygosity (Table 13).

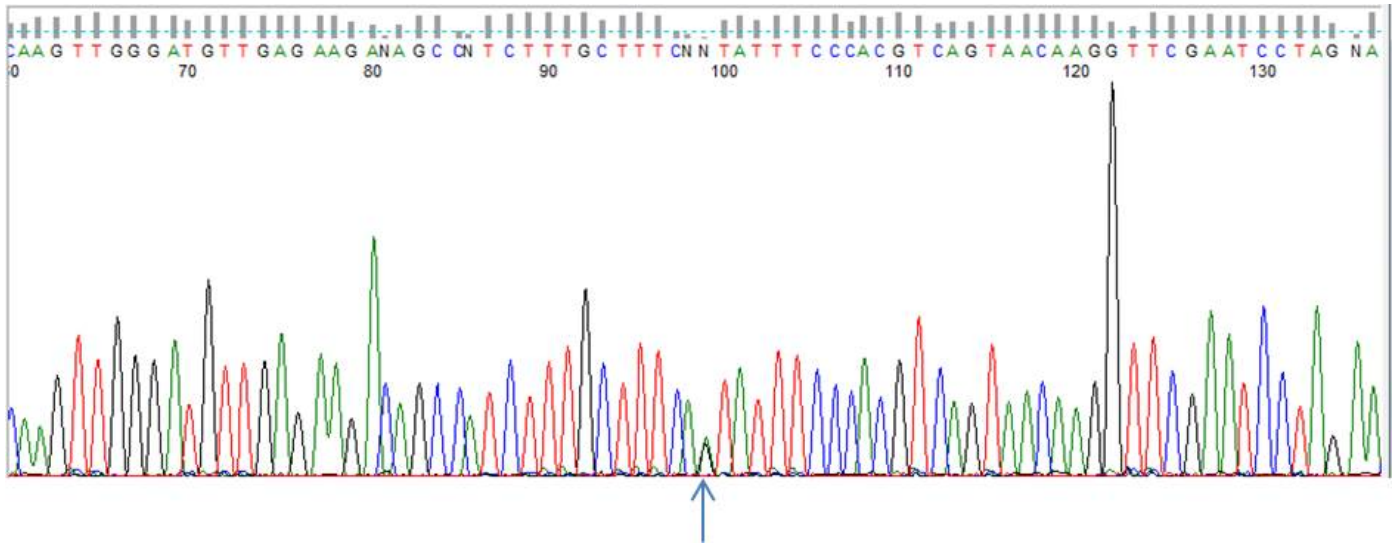

Figure 3.22: Chromatograph of *FBN1* sequence, arrow demonstrating the heterozygous variant (c.8300A>G (p.N2767S)) in DII:1

Chromosome	Nucleotide location	Size (Mb) Total homozygosity (55.3Mb)
5	5: 38463799-58831872	20.3
5	5:116069685-127108252	11.0
7	7: 4809660-13889107	9.1
14	14: 71194774-76774194	5.6
19	19: 1192769-3311830	2.1
7	7:155768061- 157637962	1.9
22	22: 17903914-19135603	1.2
9	9:139711726-141044489	1.3
18	18: 2122221-3254795	1.1

Table 13: Regions of homozygosity from D:II:1.

Secondary to the homozygosity mapping, two genes were identified of interest within these regions; *PAPLN* and *LTBP2*. The former is a 25 exon gene covering 37.1kb and the latter a 36 exon gene covering 8.6kb, both on 14q:24.

Sequencing *Papilin* revealed no pathogenic variants. *LTBP2* sequencing revealed one homozygous missense single nucleotide variant on exon 3: (c.785C>T (p.Pro262Leu) (Figure 3.23).

Segregation analysis has not been possible in this family.

These four families share many ocular phenotypes, and yet only two of the families have yet had a confirmed genetic cause identified. The ocular phenotypes of the families still under investigation is demonstrated in table 14.

3.4.4. FAMILY 6

See Figure 3.24 for pedigree.

3.4.4.1. CLINICAL

A 14-year old male proband (EVI:1) of Sri Lankan origin, born of a consanguineous marriage, was noted to have elevated intra ocular pressures of 23mmHg and 26mmHg in the right and left eyes respectively. He was found to have bilateral lens subluxation, with phacodonesis. Best-corrected visual acuity was 6/9. The child was born through a breech delivery at full term and had normal developmental milestones, with no hearing or developmental problems. He had no abnormal cardiac signs. His hands and feet were normal, although his toes were slightly short and his joints were slightly hypermobile. His father had been seen previously (see below)

This child was tall (75th percentile for his age). He had high myopia (-10.0 DS: right eye, -12.0 DS left eye), but short axial lengths (21.7mm right eye and 22.0mm left eye), suggesting lenticular myopia. His anterior chamber depths were 1.7mm in the right and 1.3mm in the left. B-scan ultrasonography showed microspherophakia (small spherical crystalline lens). The lens thickness (normal: <4mm) was 4.35mm in the right eye and 4.35mm in the left eye. Gonioscopic examination showed closed angles. After 4 years of follow-up, his intraocular pressure was maintained with medication.

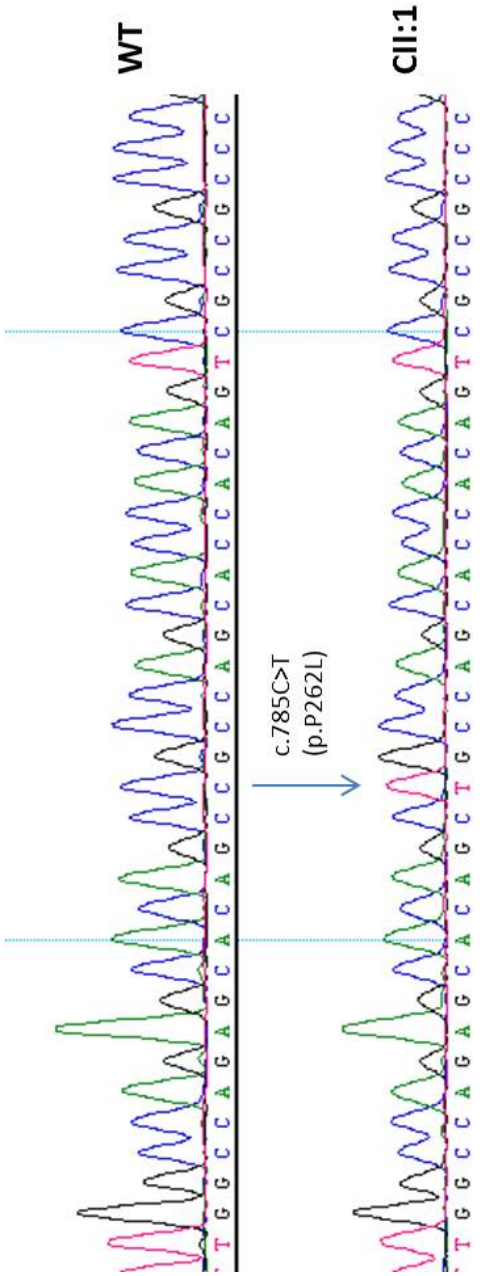

Figure 3.23: Chromatograph demonstrating homozygous variant c.785C>T (p.P262L) in exon 3 of *LTBP2* in DII:1

PHENOTYPE	Family 4	Family 3
Ectopia Lentis	✓	✓
Microcornea	✓	✓
Childhood cataract	✓	✓
Featureless Iris	?	✓
RD/ Vitreoretinopathy	✓	✓
Cone dystrophy	?	✓
Myopia	0	✓
Hypermetropia	✓	0

Table 14: Ocular phenotypes of affected members in families with unknown genetic aetiology.

✓: Present.; 0: Absent; ?Unknown

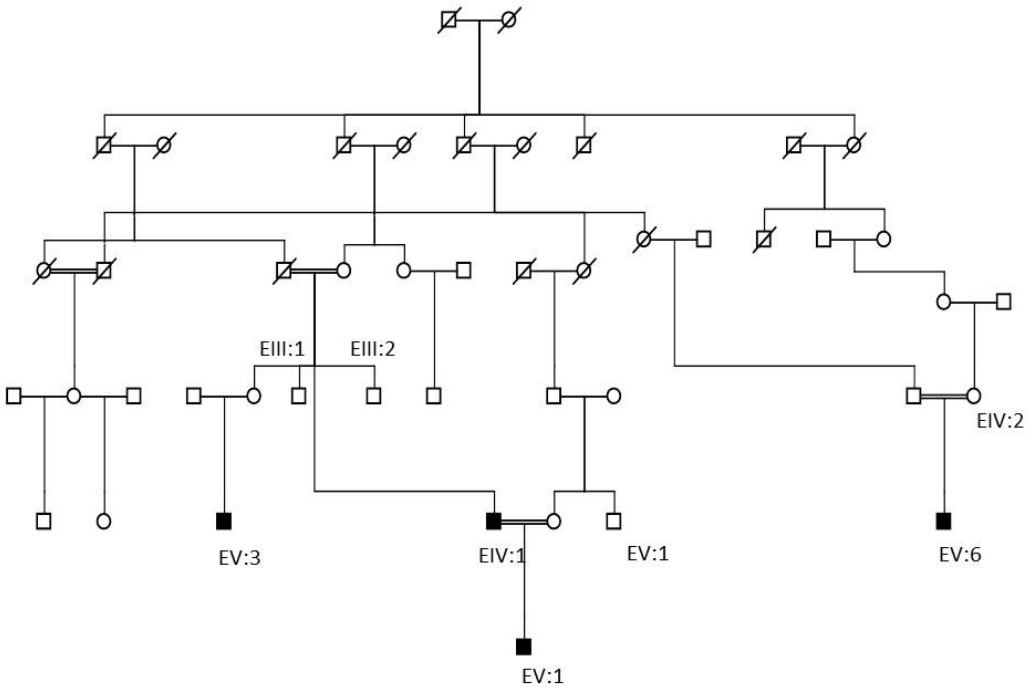

Figure 3.24: Pedigree of Family 6
The teenage proband (EVI:1) is indicated with a filled-in square (male). His mother (EV:1) is second cousin once removed to his father (EIV:1), and his paternal grandparents (EIII:1 and EIII:2) were first cousins. Individual EV:6, who is second cousin once removed to EIV:1, also has bilateral ectopia lentis

He had been reviewed by a clinical geneticist who ruled out MFS. WMS had been diagnosed clinically in his father. It is probable that the proband has WML, with ocular features but no brachydactyly or joint stiffness.

The proband's father (EV:1) is a patient under the care of Moorfields Eye Hospital. He had evidence of EL, both lenses were subluxed infero-temporally at a young age. He had no evidence of angle-closure. EV:1 had classical WMS habitus: He has short toes and fingers (brachydactyly) (Figure 3.25) with broad feet.

His height was 172cm (25th centile for his age), and he had no cardiac problems. This gentleman was also born of a consanguineous marriage. The diagnosis of WMS was made in Sri Lanka. His second cousin once removed (EV:6) also diagnosed with WMS, had bilateral lens subluxation and advanced glaucoma. This gentleman's eye examination at last follow up was LogMAR 0.6(Right eye) and 0.2(Left eye). He had been diagnosed and treated at Moorfields Eye Hospital with open angle glaucoma. He was myopic with a refractive error of -12.0DS in the right eye (axial length of 23.76mm, lens thickness 5.4mm) and -13.0DS in the left eye (axial length of 23.61mm, lens thickness 5.62mm).

No affected individual in this family suffered from RD. It is interesting that axial lengths were not as long as the myopia would have suggested.

3.4.4.2. GENETICS

DNA samples from EIV:1 and EVI:1 underwent Sanger sequencing of 65 exons of *FBN1* revealing no pathogenic variants. Subsequently, *ADAMTSL4* was sequenced in both samples, which equally did not reveal any mutations. Collaborating with Professor Valérie Cormier-Daire (Department of Genetics, Paris Descartes University Hôpital, France), *ADAMTS10* was screened, as the father had been diagnosed with WMS. No pathogenic mutation was discovered in this gene. Three samples (EV:3, EV:6 and EIV:1) were hybridised to the Illumina Cyto12 SNP chip to assess for regions of homozygosity.

Figure 3.25: Hand of FV:1; demonstrating bradydactyly

At this juncture, more saliva samples (DNA-Oragene, Genotech, Ontatrio, Canada) were collected from EIV:1 and EIV:2 and EV:6 in the post from Sri Lanka, as the laboratory stock of DNA had been depleted. DNA was not extractable from the saliva sample from EIV:2.

To our attention came the gene *ADAMTS17*. Three homozygous mutations in this gene were published in WML [226]. Subsequently, we sequenced two samples (EIV:1, EIV:1); the proband and his father, which were received by post.

Exons 1-14, and 16-22 were sequenced and no pathogenic mutations were found. However, we were consistently unable to sequence exon 15 in EVI:1; though the primers and conditions had been optimised, and successful in control DNA. This was also challenging in EIV:1, and eventually, it was completed. No pathogenic mutations in exon 15 were found, and in fact one heterozygous variant (c.A2090G (p.K697R)) was found (Figure 3.26).

This variant was not present on dbSNP[247], Exome Variant server [246] or 1000 genomes project[248]. There are however at least seven SNPs recorded in the 70bases around this one, and a SNP 2 bases downstream (rs200441121) and 2 SNPs upstream (TMP_ESP_15_100636611) and rs141443664, three and five bases away respectively. This suggests that this may be a polymorphic region. The variant is thought to benign according to Polyphen[245]. Nevertheless, it was thought this condition was inherited recessively. This variant was thus dismissed.

At around this time, the results from the homozygosity mapping were available. Using Genome Studio (Illumina: http://www.illumina.com/software/genomestudio_software.ilmn) the genotypes were called and exported to Microsoft Excel. Using an Excel macro formula, homozygous calls for SNPs were matched between the three affected individuals to assess which regions of homozygosity were shared. By far the largest region was on 15q25 (Figure 3.27).

In the region on 15q25, there are over 80 genes. One particular gene stood out: *ADAMTS17*. This posed significant problems, as it was believed that one of the affected patients had a heterozygous variant in *ADAMTS17* which should not have been possible

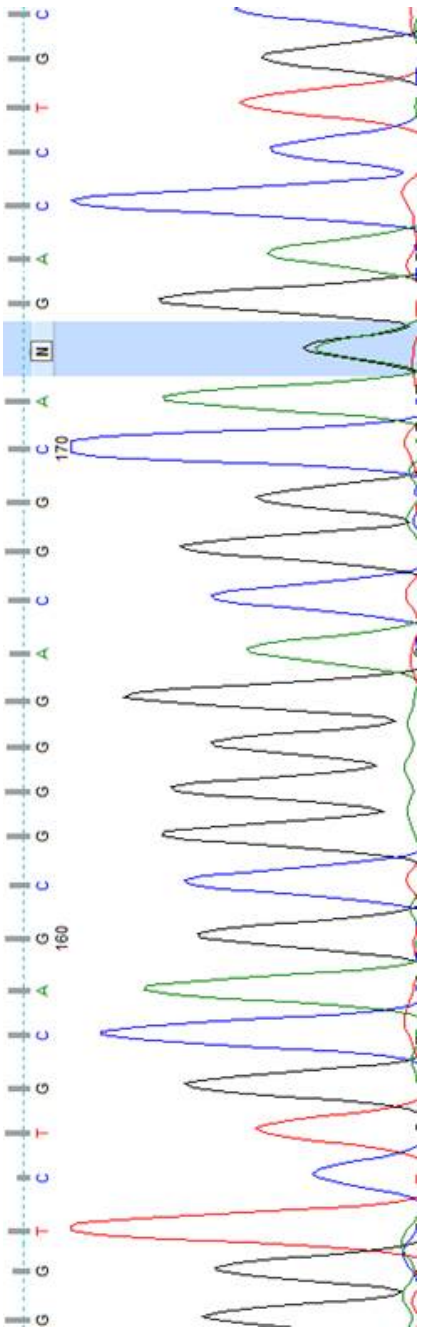

Figure 3.26: Heterozygous variant in *ADAMTS17* for EIV:1

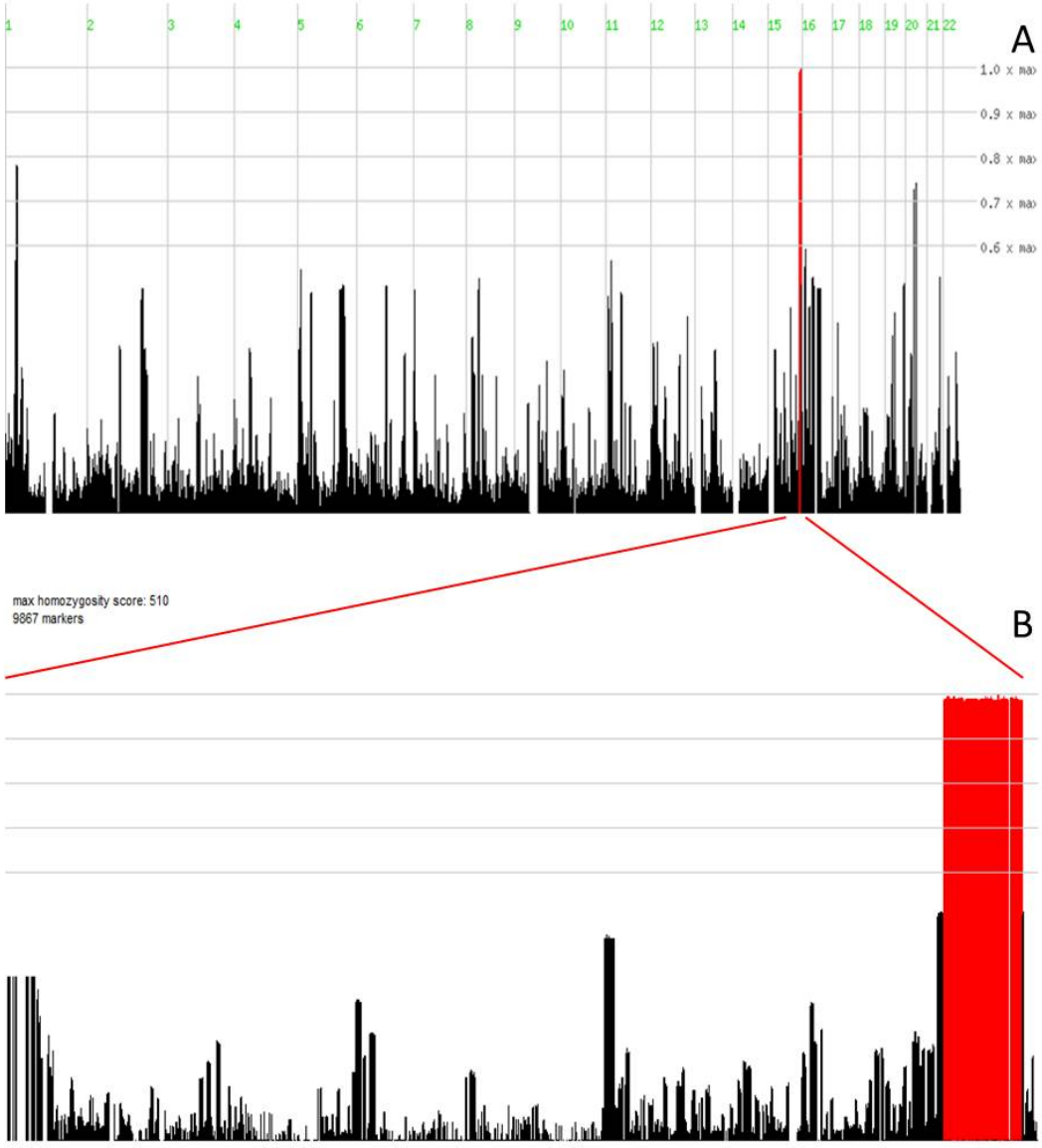

Figure 3.27: A: Regions of homozygosity shared between FV:3, FV:6 and FIV:1. B: Largest region on chromosome 15 magnified: Height of bar indicates the amount of homozygosity.

in a region of homozygosity. Exon 15 from *ADAMTS17* was therefore re-sequenced to check the variant again. This was again challenging, but eventually managed. We believed that the variant was now homozygous (Figure 3.28), suggesting a sequencing error previously.

At this point it was believed that the previous heterozygous change was inaccurate. There was therefore evidence of shared homozygosity including *ADAMTS17*. All other genes in the shared regions were considered, and no candidates were thought to be convincing based on a priori knowledge.

ADAMTS17 was thus the most likely gene causing the phenotype in this family, based on 3 families published with a very similar phenotype to EVI:1 (WMS-Like). Having screened all the exons in the genomic DNA, we considered whether a deep intronic change in *ADAMTS17* may be responsible.

It is thought that deep intronic changes, if affecting splicing, more commonly activate cryptic splice sites and in doing so, create a "pseudo exon"[352]. Repetitive sequences, such as Alu sequences are found throughout the genome, and may act as potential cryptic 3' splice sites[353]. Numerous examples of this have demonstrated the presence of pseudo-exons causing disease phenotype[354, 355]. It is on this theory which led to attempts to amplify *ADAMTS17* mRNA from leucocytes; to establish if a post transcriptional extra exon had been created, or a skipping of an exon; which would not have been detectable from genomic DNA. rtPCR was then performed to produce cDNA, which was then used for PCR.

Morales and colleagues [226] had amplified exons 11-13 from leucocytes. Using their primers (GACACATCCTGCAAGACCAA and AGGCTTATCGTCAACCAC), amplification was possible from control cDNA (Figure 3.29).

Primers were then designed to cover the whole of the *ADAMTS17* gene as described in the methods. However, experiments to amplify this gene failed repeatedly. Long range PCR with primer 1F (GCTGGAGGGCTTCACTC) and 22R (GACTGCGTGTCACGAGTCG) was also attempted. This also was not successful.

Concurrently, we had taken a fresh DNA sample from EIV:1 from blood extraction, as he was in the UK.

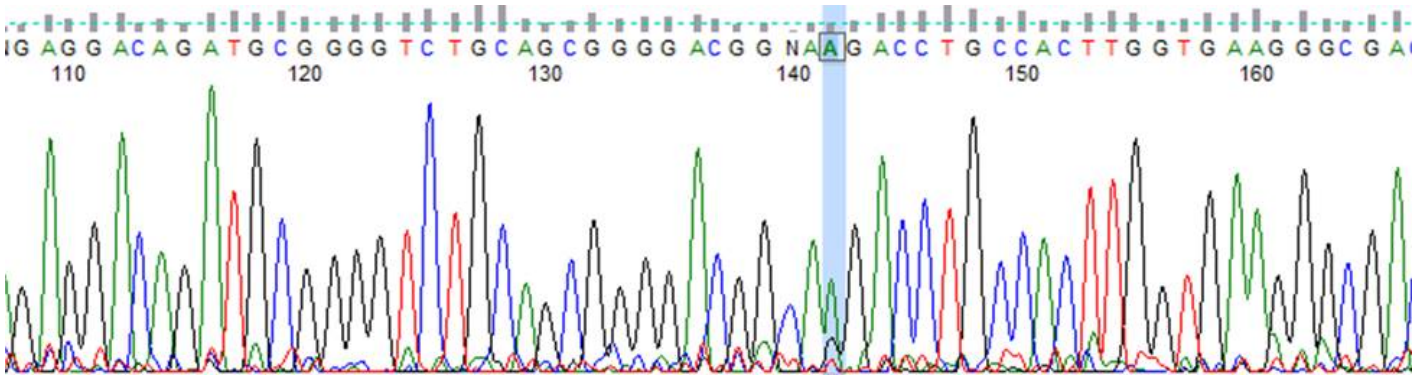

Figure 3.28: Sequencing of Exon 15 in FIV:1. The previously described heterozygous variant (highlighted) appears now to be homozygous: There appears to be a shoulder of the proceeding G: This was thought to be an artefact. Bi-directional sequencing was not available to confirm, as this was the only successful sequence

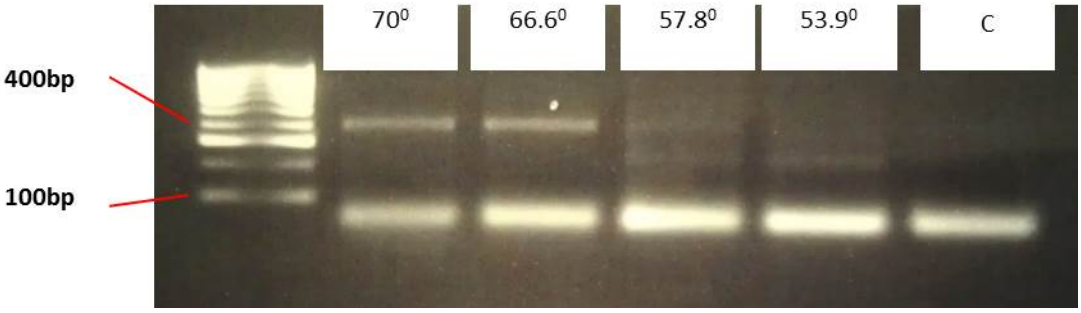

Figure 3.29: Amplification of cDNA of Exon 11-13 (*ADAMTS17*) in control DNA

The genetic cause of this phenotype had to be re-considered. This fresh sample along with EV:6 underwent exome capture next generation sequencing to determine if an alternative gene in the regions of shared homozygosity harboured a pathogenic mutation. The data was returned in .bam files and Excel spread sheet. When comparing all homozygous variants which were present in in both samples, non-synonymous and with a frequency <1% in the 1000 genomes, revealed no genes in the regions of homozygosity, and no convincing candidate genes.

When the exome data for *ADAMTS17* was analysed it became apparent that Exon 15 was not covered in either samples (Figure 3.30), but was covered by the same exome experiment on other samples.

This suggested that Exon 15 was not amplified in either of the affected individuals. Using fresh DNA samples from EIV:1, EV:6 and a positive control, exons 14, 15 and 16 were reamplified with PCR. Exons 14 and 16 were amplified, whilst 15 was not in EIV:1 and EV:6 (Figure 3.31).

This clarified that Exon 15 was not amplified from either of the affected patients. The previous sequencing of exon 15, must have been from a mislabelled sample., as this saliva sample had come with EIV:2 in the post from Sri Lanka. We were unable to extract DNA from the sample labelled EIV:2 to confirm this mislabelling.

3.5. DISCUSSIONS

3.5.1. *ADAMTS18*

Family 2 was the first family we discovered with an inherited previously undescribed phenotype including EL and RD. The affected pair were from a consanguineous family, and it was therefore assumed that the causative mutation would be homozygous. In such families, the chance of either parent carrying a mutation is not entirely independent. In these families, runs of homozygosity secondary to autozygosity are therefore more common[340]. In addition, the rarer the phenotype, the more likely that the causative mutation is autozygous[340]. Therefore, autozygosity mapping was deemed a prudent approach.

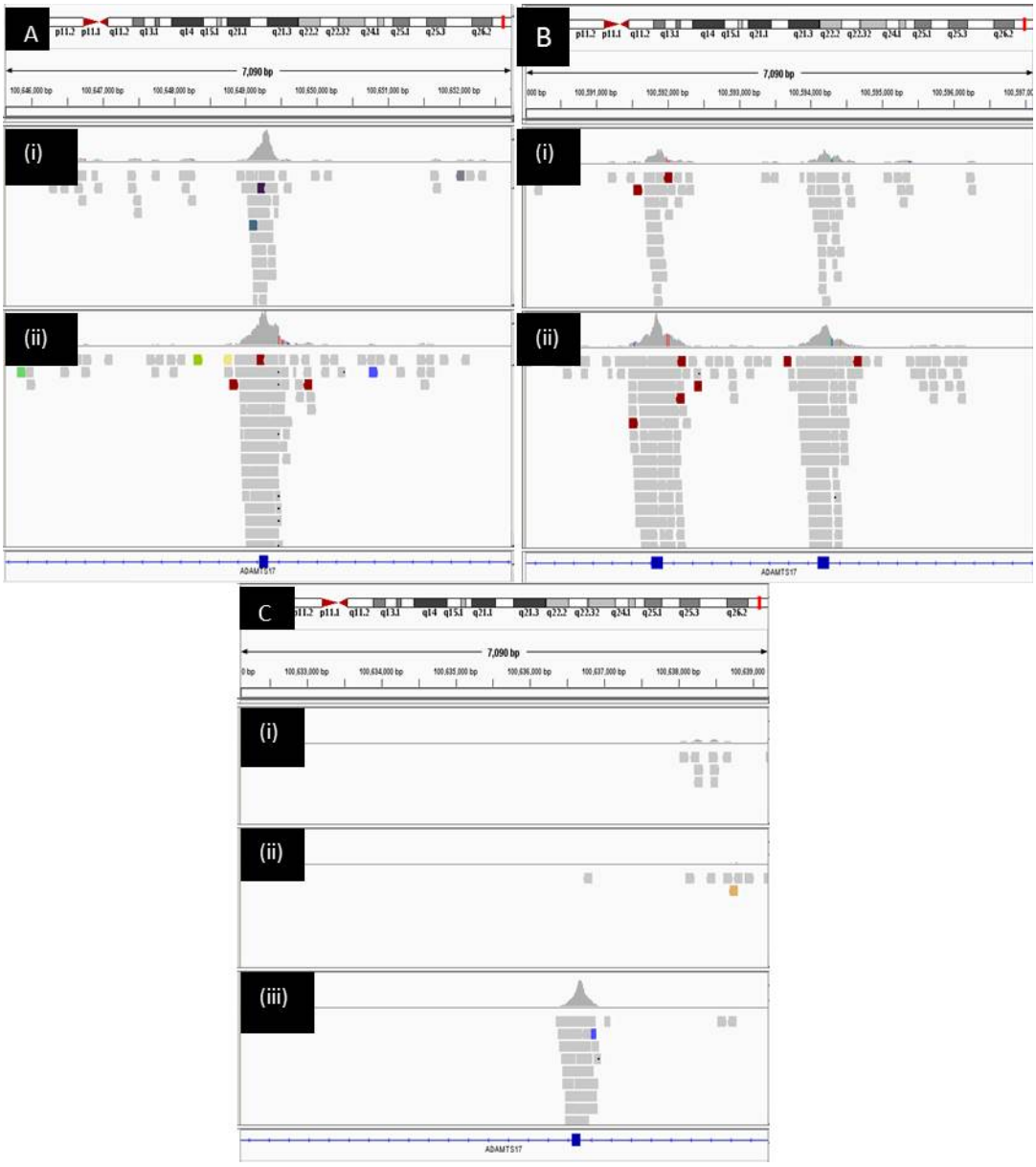

Figure 3.30: View from Integrative Genomic Viewer (IGV). Results from Next generation Exome Sequencing. *ADAMTS17:* **A**: Exon 14. (i) EIV:1 (ii) EV:6. **B:** Exon 16 and 17. (i) EIV:1 (ii) EV:6. **C.** Exon 15. (i) EIV:1, (ii) EV6 (iii) Control

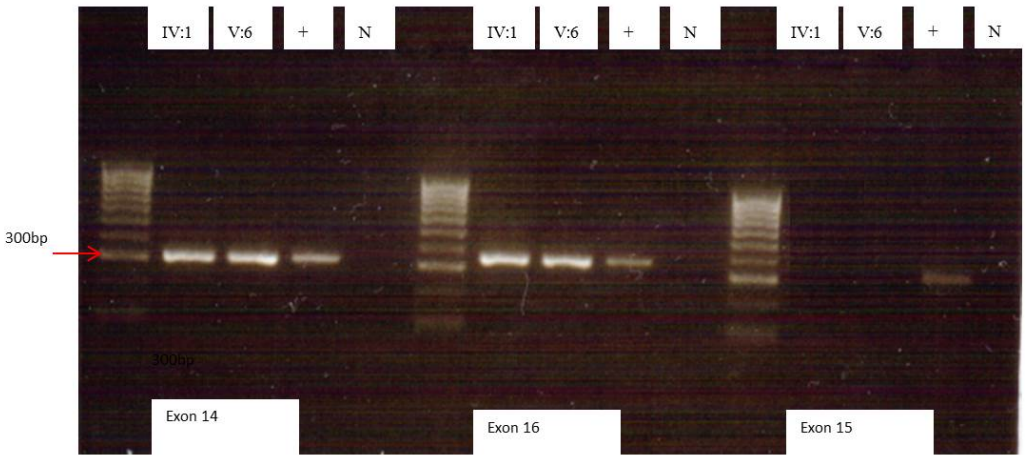

Figure 3.31: PCR 2% Agarose Gel of *ADAMTS17*, exon 14, 15 and 16.
+: Positive control**. N:** Negative control. Expected amplicon size: Exon 14: 315bp, Exon 16: 361bp, Exon 15: 331bp.

In addition, high throughput sequencing of 106 genes which are known to cause retinal dystrophies excluded known mutations. Autozygosity analysis and Sanger sequencing demonstrated a causative missense mutation in *ADAMTS18.* Because of the strikingly similar phenotype between Family 2 and 3, *ADAMTS18* was investigated in the latter family; leading to a discovery of a further pathogenic missense mutation. Family 1 were analysed in another unit for novel causes of coloboma by trio-based exome sequencing. The proband was found to have a homozygous nonsense mutation in *ADAMTS18.*

ADAMTS18 (OMIM 607512) is a 23 exon gene on chromosome 16q23.1 covering 153kb of genomic sequence. It encodes ADAMTS18, one of the 19 ADAM metallopeptidase with Thrombospondin type 1 motif proteins. As previously described, they are a family of enzymes with a wide range of biological processes, including cell migration, coagulation, angiogenesis and ECM regulation[21].

ADAMTS18 was first identified and described in 2002, which suggested it to be widely distributed within the body[17]. One of the first suggested roles stemmed from the findings that the region 16q was frequently deleted in cancer cells (http://amba.charite.de/~ksch/cghsuper/index.htm), and *ADAMTS18* was then demonstrated to be a tumour suppression gene[356, 357]. It is thought that somatic methylation of promotor regions of this gene (as a consequence of early tumour genesis) leads to silencing, and thus promoting carcinoma in a wide range of tissue. Conversely, Wei and colleagues[358] showed that somatic mutations within the gene promoted migration, growth and metastasis of melanoma cells. They suggest that mutations are mostly found near the C-terminus, altering the substrate specificity of the protease. A conclusion to these seemingly contradicting functions has not been reached. However, it seems probable that the roles ADAMTS18 may have on modulating the ECM are likely to play a part in the impact on tumour biology.

For ADAMTS proteins, cleavage of the C-terminus is an important post translation step. However, for *ADAMTS18,* thrombin, in vascular endothelial cells, can induce this cleavage. It is interesting that this cleaved C-terminus of ADAMTS18 may fragment platelets and thus prevent thrombus formation[359, 360] and thus potentially reduce carotid artery thrombosis[361]. This demonstrates that the C-terminus of ADAMTS18 has its own role, independent of the N-terminus protease domain; a unique feature amongst ADAMTS proteins.

Genome wide association studies have suggested a role for *ADAMTS18* in advanced age. These include contributing to bone mineral density[362, 363], and tentatively for influencing white matter integrity [364]. However, an exact mechanism has yet to be suggested for either of these.

A role in ophthalmic disease was first suggested by Aldahmesh and colleagues in 2011[1]. They describe an eight year old girl from Saudi Arabia of consanguineous parents. This child was reported as having classical Knobloch syndrome. In addition to the classical features, this child also was described as having progressive retinal degeneration; though ophthalmic phenotype data in this paper is limited. The condition in this child was termed Knobloch Syndrome 2 as this was the first to describe a novel genetic cause for KNO. Aldahmesh and colleagues demonstrated the orthologue of ADAMTS18 to be present in developing lens and retina of the mouse. The role of this protein in the development of Knobloch syndrome is unclear.

3.5.2. KNOBLOCH SYNDROME

Knobloch Syndrome (OMIM 267750, 608454) (KNO) is a very rare autosomal recessively inherited condition. Its prevalence is unknown and has been reported in 63 individuals representing 23 families to date. It was first described in 1971 in a family in whom all those affected had high myopia, vitreoretinal changes, occipital encephalocoeles and RD[168]. The former three have been maintained as cardinal features of the syndrome. Since the initial description, other features have been sporadically described. Reported extraocular features include abnormal lymphatic vessels in the lung[365], unusual palmar creases[366], neuronal migration defect [367], cerebral and cerebellar atrophy[368] duplex kidneys[369], acute lymphoblastic leukaemia[370] and epilepsy [371]. Described ocular features include early onset cataract, EL, retinal dystrophy[1], fibrillar vitreous condensations[224, 370] retinal pigmentary changes with nycloptia, glaucoma, nystagmus and phthisis[372], corneal dystrophy[368] and chorioretinal atrophy[224, 370]. It has been suggested that the ophthalmic phenotype may itself predict the presence of the syndrome[224].

KNO is therefore characterised by high myopia, vitreoretinopathy and occipital defects. There are similarities with other vitreoretinopathies. Stickler 1 (OMIM108300), Stickler 2 (OMIM 604841) and Marshall Syndrome (OMIM 154780) all manifest with axial myopia and cataract with a high propensity of RD. Autosomal recessively inherited

syndromes such as Walker-Warburg Syndrome[373] and vitreoretinopathies such as Stickler IV (OMIM 614134), Stickler V (OMIM 614284), Goldman Favre syndrome (allelic with enhanced S-cone syndrome: OMIM 268100) can be particularly challenging to differentiate from KNO. The most similar families with autosomal recessive vitreoretinopathies are from Switzerland[374] (later mapped to 22q13[375]), Italy[376] and of Hispanic origin[377]. The latter two of these reports may well have been undiagnosed KNO.

Homozygous mutations in *COL18A1* were first described as causative of KNO in 2000[378] and further families have since been reported. [367, 370, 379-381]. *COL18A1* is found on 21q22.3 and spans 108.5kb. The encoded protein COL18A1 is a non-fibrillar collagen found in three isoforms, each differing in the N-terminus (Figure 3.32). Their production depends on two separate promoters. Exon 1 and 2 encode the shortest variant, whilst Exon 3 encodes the longer two. The middle length variant is a consequence of alternative splicing of exon 3, leading to the removal of the frizzled domain (Figure 3.32)[24]. The long isoforms are found to localise in liver, whilst the shorter in basement membranes and muscles[382]. Figure 3.33 demonstrates that the protein contains 11 non-collagenous domains and 10 triple-helical collagen domains and similar in structure to COL15. It is of interest that these two collagens contain Thrombospondin regions; similar to members of the TSR superfamily; including ADAMTS18.

As with its distribution, the function of this protein is expansive[24]. Particularly of interest is the role of the C-terminus fragment of this protein; endostatin. Endostatin is a 183 amino acid product of enzymatic cleavage from the N-terminus of COL18A1 by cathepsin, elastase and matrix metalloproteinases (MMP) -3, -7, -9, -13, -14 and -20[383]. It acts via Integrinα5β1 and VEGF membrane receptors to maintain the integrity of basement membranes[384], inhibit angiogenesis[385] and inhibit the Wnt/β-catenin signalling[386]. Of further interest is the role it may play in inhibiting tumour growth; to such an extent that is has been used in clinical trials, and indeed been approved as a treatment for non-small cell lung cancer[387]. Whether this effect is via a similar mechanism to that of the role of ADAMTS18 in tumour biology is unknown, and may be worth investigating in view of the proposed similar ocular phenotype of mutations in these genes.

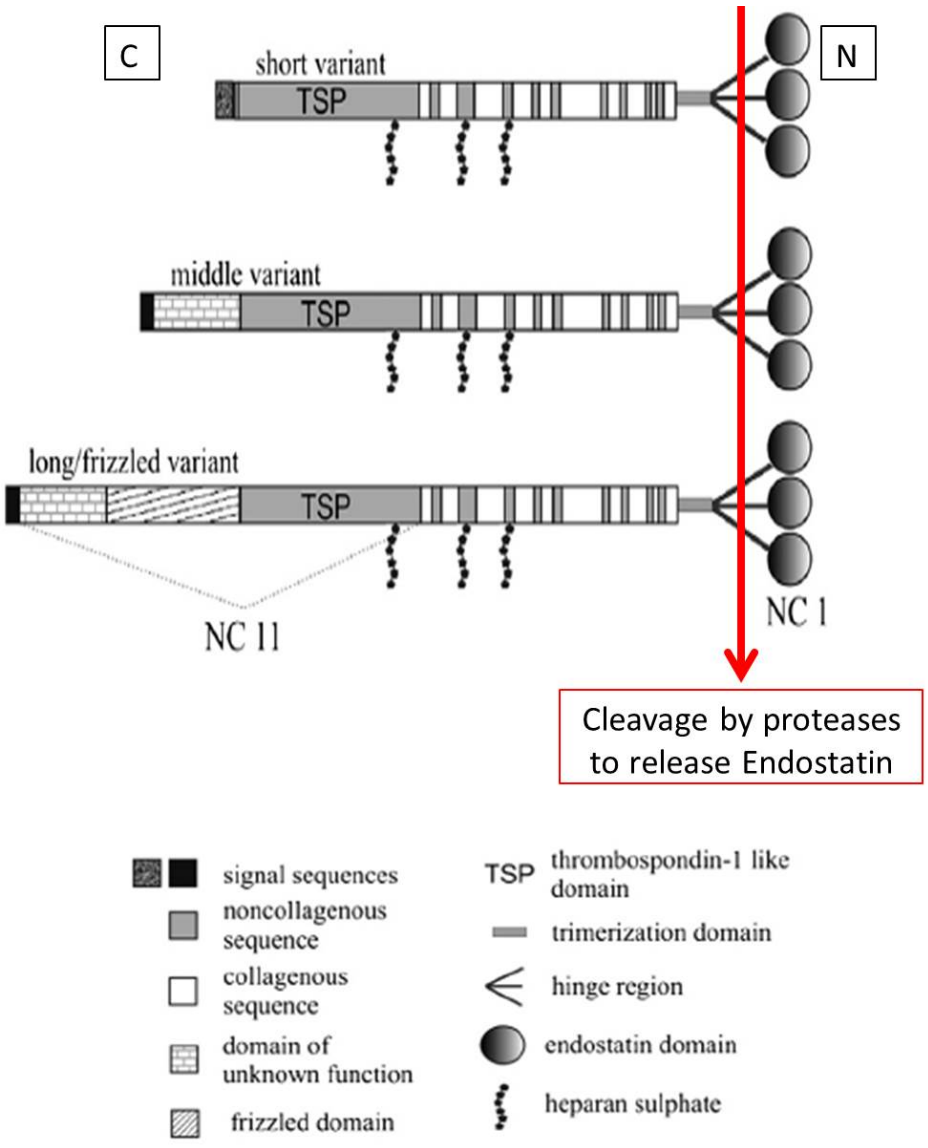

Figure 3.32: Three isoforms of COL18A1. *Adapted from*[24]

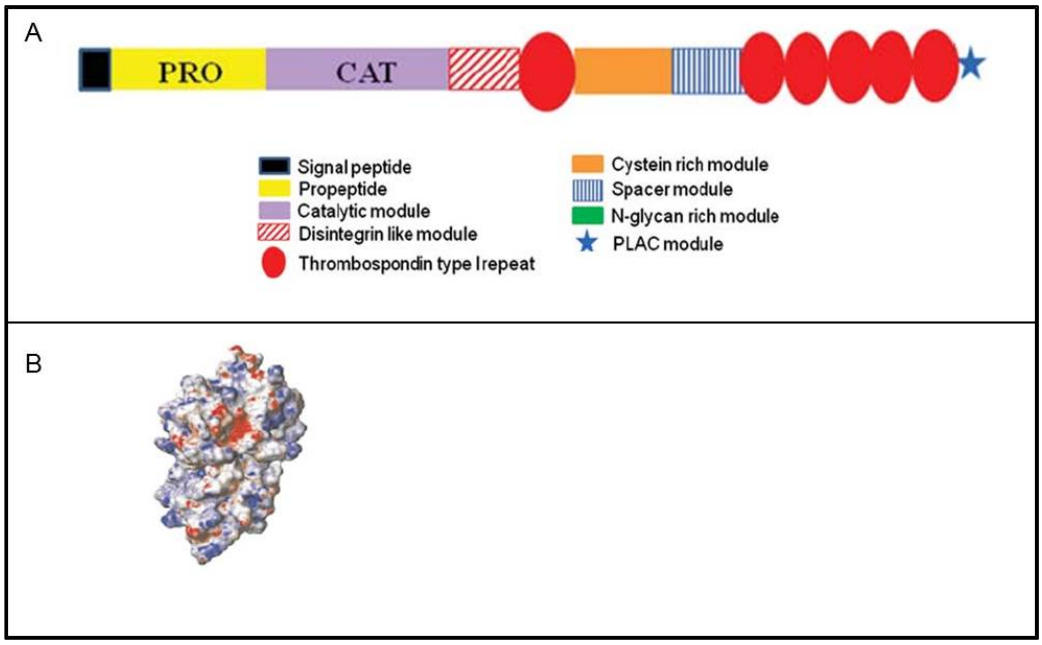

Figure 3.33: ADAMTS18. A: Schematic image of ADAMTS18 demonstrating domains. B: Homology modelling of molecular surface of the catalytic domains. Front view showing the active site
Adapted from [16] and [17].

A further similarity lies in the fact that, although functional cleavage products are reported for many proteins, ADAMTS18 is the only one of its family to manifest this phenomenon.

Within the eye, it is expressed widely, including in various basement membranes, the internal wall of Schlemm's canal and trabecular meshwork, epithelial layers of the iris and the muscle cells of the ciliary body and iris [388]. With this widespread distribution, it is unsurprising that mutations may result in a diverse phenotype described above in KNO.

Although in patients who have had endostatin measured, there are reports of reduced levels in KNO[389, 390], normal levels were described in a patient with a splice site mutation (IVS1-2A>T)[371]. This suggests that the whole protein may be required for ocular development, rather than a specific role of the cleaved C-terminus product.

KNO is characterised by an occipital defect. It is unclear whether this is a consequence of disrupted bone development or is a manifestation of abnormal neuronal cell migration, suggested by knockout animals[391]. The lack of a skull defect in the knockout mouse[47], do suggest that the former may be more plausible. Although Khan and colleagues[224] have suggested that occipital defects are not necessary for the diagnosis of KNO; they base this on only four reports, none of whom had had skull imaging. It is appropriate to still consider that occipital defects as a cardinal feature of the condition.

The role of COL18A1 causing particular ocular features is worth exploring. Although it is present in the lens, it is unclear as to why peri-nuclear cataracts seem to predominate (when described)[224]. Why EL is described in KNO is also not clear. This may be as a result of basement membrane disruption of the capsule; particularly at the insertion of the zonules. This speculation has not been confirmed.

High myopia is cardinal to the diagnosis of KNO and again the cause of this is undetermined. Other collagen genes[392] and other vitreoretinopathies have been associated with myopia. However, the role of COL18A1 in myopia is not clearly understood. It does not seem to play a role in non-syndromic myopia[393, 394]. It seems unlikely to be a consequence of lenticular changes (leading to form deprivation) as not all cases of KNO manifest such lenticular changes. Fukai and colleagues suggest

that disruption of the vitreoretinal interface is a precursor of myopia in *col18-/-* mice[47]. It has been established that COL18A1 is found in the human ILM[45]. They suggest that the ILM, being buffered by vitreous is uniquely vulnerable to loss of COL18A1 compared to other basement membranes. The vitreous, consisting mostly of collagens II, IX and XI is significantly different to the ECM surrounding other basement membranes. The vitreous adheres to the ILM and breakdown of this adhesion results in vitreous detachment. Disruption of a major component of the ILM (COL18A1) may result in abnormal vitreoretinal adhesions. This theory is certainly plausible, and would explain the high prevalence of RD in KNO, but not the high myopia.

In 2004, Menzel and colleagues[379] excluded linkage to *COL18A1* in 2 brothers with KNO, from non-consanguineous parents. They suggested an unmapped locus causing KNO and termed this Knobloch Syndrome 2 (KNO2). Seven years later, Aldahmesh and colleagues suggested *ADAMTS18* mutations as the cause of KNO2. Interestingly the term Knobloch Syndrome 3 was coined for a family in whom linkage suggested the region 17q11.2[372]. It was later determined by high density SNP mapping, as opposed to using microsatellites as in the original study, that this family actually had a mutation in *COL18A1*[395], discounting the suggestion of KNO3. There therefore only exists KNO1 (caused by mutations in *COL18A1*) and KNO2 (*ADAMTS18*). The latter has however only been described in one patient. Due to a lack of cardinal features; particularly an occipital defect, our patients have not been diagnosed with KNO.

After years of speculation, it appears however that Family 4 are likely to have the diagnosis of Knobloch syndrome. Their high myopia, EL, vitreoretinopathy and occipital bone defect are consistent with the cardinal features of this condition. In addition, both affected patients have microcornea and an early onset retinal dystrophy. These features are shared with our two families who had mutations in *ADAMTS18*. However, on homozygosity mapping, it appears that *COL18A1* is the likely candidate, and DNA from this proband has been submitted for screening of the gene at the UCL Institute of Neurology.

The diagnosis being made in this family has helped the understanding of the proband's (CII:1)) neuro-developmental delay. Epilepsy in KNO was first described in a four year old in 2002[371]. Keren and colleagues[367] reported pachygyria of the frontal lobes and agenesis of the septum pellucidum in a patient with KNO. They were the first to

describe neurodevelopmental delay in KNO, which they suggest may be associated with loss of the medium and long isoforms of COL18A1. Pais an-Ruiz and colleagues[368] have also described Knobloch in an Indian family with epilepsy, ataxia and neurological decline. Both groups suggest that mutations affecting the C-terminus of the protein are more likely to result in neurological manifestations. It is at this end of the protein where the TSR domains are found. Other proteins with this domain have been implicated in neuronal growth[26], and this important domain may have a role to play in this. It would be of interest to know if a mutation in *COL18A1* is found in this family, if it affects this end of the protein.

The exact role that ADAMTS18 may have in this condition or in our expanded phenotypic description is unknown. A second patient with a homozygous mutation in *ADAMTS18* was published in January 2013[22]. This patient was diagnosed with an early onset retina dystrophy (EORD). In particular this patient had no features of KNO, which led the authors to suggest that this gene produces multiple effects on the eye. It is of interest that our three families with mutations in *ADAMTS18* had phenotypic features which overlapped with both KNO and EORD (Table 15). This confirms that the phenotypes described are likely to be relevant but also poses questions as to the real effect of ADAMTS18 on ocular tissue and development. Peluso and colleagues[22] attempted to explain this with *ADAMTS18* knock-down Medaka fish. They suggested that fish depleted of ADAMTS18 had disrupted central nervous system development. In particular the telencephalon, the telencephalic ventricles and the optic tectum in the mesencephalon were all affected. This phenotype was rescued by injection of wild type human *ADAMTS18* RNA, but not with *ADAMTS18* RNA containing their missense mutation. Interestingly, they demonstrated no ocular phenotype in this knock down model. However, using the light induced photoreceptor damage model, reduction of the retinal outer segment, and a reduction of rhodopsin-positive retinal areas in the knock down fish compared to the wild type after prolonged light exposure was demonstrated. Although they demonstrated the expression of *ADAMTS18* from human retinal cDNA libraries, they did not demonstrate the protein to be present in the outer segments of the mouse. The authors suggest that the presence in the RPE would explain a role in maintaining the photoreceptor function.

This paper is the only one demonstrating any functional effect of this protein and gene. Our patients all had had photoreceptor dysfunction, which corroborates their findings.

However, the expansive phenotypes in our families suggest that there are further functions, which are as yet unknown.

Three patients from two families (AII:1,AII:2 and BII:1) had lenticular changes (early cataracts) whilst AII:2 also suffered from EL. The patient described by Aldahmesh and colleagues[1] also suffered EL. AII:2 and BII:1 also presumably suffered a vitreoretinopathy resulting in early onset RD. These two features are very similar to the phenotype of KNO. This may suggest that ADAMTS18 and COL18A1 may play collaborative roles in ophthalmic development.

However, there were other similarities in our patients. All the patients had anterior segment anomalies; particularly microcornea.

Microcornea is a manifestation of ocular dysgenesis with a prevalence of 0.001%[396]. It can occur alone, but is usually accompanied by other ocular dysgenesis such as anterior microophthalmos, coloboma and cataract[397] [398, 399]. Recently, heterozygous mutations in *PAX6* [400] and *BMP4* [401] have also been described as causative in microcornea. Of further interest, Couprey described two families with EP, microcornea (and other ocular features similar to Axenfeld Rieger anomaly) with diffuse periventricular leukoencephalopathy[402]. These patients all had mutations in *COL4A1*.

The exact mechanism of microcornea is unclear, but certainly mutations in genes involved in ocular development can result in microcornea. It is worth comparing the combination of phenotypes shared by AII:2 with the autosomal dominantly inherited condition microcornea, rod-cone dystrophy, cataract, and posterior Staphyloma (MRCS) (OMIM 193220)[403, 404]. Although some genetic heterogeneity is suggested, mutations in *VMD2* have been attributed to this and autosomal dominant vitreoretinochoroidopathy (ADVIRC)[161]. The region of this gene on 11q12.3 was not in any of the regions of homozygosity; reducing the likelihood of a recessive effect of this gene.

The phenotype of our patients and the two published patients with *ADAMTS18* mutations is in table 15.

	Aldahamesh [1] (KNO2)	Family 1	Family 2		Family 3	Peluso [22] (Retinal dystrophy)
		IV:1	AII:1	AII:2	BII:1	
Ectopia Lentis	✓			✓		
Fibrillar vitreous/ RD	✓			✓	✓	
Occipital Defect	✓					
Myopia	✓		✓		✓	
Hypermetropia				✓		✓
Cryptless smooth Iris	✓				✓	
Childhood Cataract	✓		✓	✓	✓	
Retinal Dystrophy	✓	✓	✓		✓	✓
Exotropia			✓			✓
Nystagmus			✓			✓
RP phenotype						✓
Ectopia pupillae		✓				
Micro-cornea		✓	✓	✓	✓	

Table 15: Phenotype of all patients published with homozygous mutations in *ADAMT18*.

KNO2: Knobloch Syndrome 2
✓: Present in this affected member
RD: Rhegmatogenous Retinal Detachment
RP phenotype: Retinitis Pigmentosa phenotype includes attenuated retinal vessels, posterior subcapsular cataract, cystoid macular

Three different mutations have been described in our patients with *ADAMTS18* mutations. One (c.2159G>C (p.C720S)) is in exon 14, which encodes a peptidase domain. Traditionally it is suggested that the structural role of the ADAMTS proteins, which has been assumed to influence the ocular phenotype caused by mutations in the *ADAMTS* genes, depends on their ancillary domains[16]. Our data may suggest a role for the protease domains in ocular development. The second mutation (c.1952G>A [p.R651Q]) does not encode a particular domain. The third mutation c.1067T>A [p.L356*] is a nonsense mutation, and is more than 55 nucleotides from the Exon-Exon boundary; it is likely to result in a mRNA transcript which undergoes NMD[268]. The phenotypes of those with the first two mutations (which are missense) are more similar to the patient with the nonsense mutation; which may suggest a genotype-phenotype relationship. This cannot be inferred reliably, as this number of patients is too small. As more patients are discovered, this speculation will be further clarified.

Of interest in family 2 (AII:1 and AII:2) was the neurological imaging findings which were consistent and shared. Dural ectasia is a feature of MFS. It was re-classified as a minor criterium in 2010; offering a systemic score of 2 if present[186]. It occurs in up to 70% of patients with MFS, most commonly affects the lumbo-sacral region and is usually asymptomatic[405]. Dural ectasia is a result of the defective fibrillin-1 in the connective tissue of the dura mater. Intracranial ectasia are rarely reported in MFS alone. AII:1 and AII:2 did not have symptoms from these. These findings may suggest a mild connective tissue disorder (MFS was excluded in this family by cardiological review) as a result of *ADAMTS18* mutations. Alternatively, it may suggest functional linkage of this protein with fibrillin-1, as has been suggested with other members of the ADAMTS family[279, 406]. However, this finding was not consistently found in the affected proband in family 3 and imaging from IV:1 was not available.

The manifestation of EL, early cataract and EP is particularly interesting in the context of the ADAMTS proteins. In this thesis, it has already been shown that recessive mutations in *ADAMTSL4* and *ADAMTS17* can result in these anterior segment phenotypes. ELetP has only been demonstrated to be inherited recessively, and to date only known to be caused by mutations in *ADAMTSL4*. IV:1 in this study was found to have EP. Although the aetiology and molecular genetics of ocular coloboma are extensively investigated [407], the aetiology of EP is less well understood[408]. Differentiating between them can be challenging, particularly with very displaced pupils

in EP; and as both EP and iris coloboma may be bilateral [407]. EP is likely to be a result of a dysfunction in ocular development.

3.5.3. FAMILY 5

No definitive diagnosis was made for this family, and neither was a causative mutation definitely found. We did discover some variants in the proband which are worth elaborating.

The mode of inheritance in this family may be X-linked recessive (with two affected boys), or autosomal recessive. In view of the small tribe both parents originate from, and probable subsequent endogamy in the pedigree and with only one generation being affected, autosomal recessive inheritance was more probable.

3.5.3.1. *FBN1* variant

The most common genetic cause of EL is thought to be in *FBN1*. Although this is usually inherited in a dominant fashion, homozygous recessive mutations in this gene have been described causing recessive MFS[409]. With the marfanoid habitus, *FBN1* was therefore screened. This variant found (c.8300A>G (p.N2767S) was heterozygous. One must consider, on discovering this mutation whether this was in fact a dominant condition caused by a de-novo *FBN1*1 mutation (because of the normal parents) in the affected proband. However, to have all four affected children manifest the same de-novo pathogenic change is unlikely[342].

Next we must consider the functional effects this variant might have. The variant we discovered in the proband was heterozygous c.8300A>G (p.N2767S). This variant lies within an N-glycosylation domain.

N-glycosylation is a post translational modification involving addition of complex carbohydrates by covalent bonding to the nitrogen atom of an amide group on an amino acid (most commonly asparagine)[410]. These sites occur where the sequence *Asn-X-Ser/Thr* occurs; with *X* representing any amino acid other than proline; as this is thought to interfere with the ability of the peptide to conform to the appropriate structure[411] . It is believed that these sugar side chains are important for the correct folding of proteins, and may be important in protein-protein interactions[412].

This modification is more common in transmembrane or extracellular proteins. The process usually commences in the endoplasmic reticulum, subsequently occurring in the Golgi apparatus[342]. The role of such modification is dependent on the protein in question. In humans, defects affecting glycosylation most commonly result in neurological and developmental disorders[410].

Within *FBN1*, there is precious little known regarding mutations affecting these domains. Lonnqvist and colleagues demonstrated a missense mutation in *FBN1* resulting in an extra N-glycosylation site[413]. They suggest that excessive n-glycosylation leads to impaired secretion of the protein. The reported case had neonatal MFS. Conversely, in vitro work by Whiteman and Handford [414] suggested that certain missense mutations might result in a lack of complex glycosylation which wild type fibrillin-1 undergoes, thus leading to an accumulation of this protein in the endoplasmic reticulum. The missense mutations both these groups investigated did not directly affect N-glycosylation domains; in fact affected cb-EGF domains. It is well established that mutations affecting these domains are very common in fibrillinopathies[187]. It is therefore unclear whether it is a disruption of the cb-EGF domain itself, or the resulting extra N-glycosylation domain in these descriptions which leads to disrupted fibrillin-1 molecules. The effect of N-glycosylation on disease is therefore controversial. Furthermore, there have been no reports in the literature, or the database of over 300 *FBN1* mutations at the Sonalee laboratory (St George's University of London) (personal communication), of mutations in these domains causing disease. In our patient, the sequence of amino acids creating the affected domain were *Asn-Ile-Ser*. In vitro work suggests that substitution of threonine with serine results in reduced glycosyl transfer[415], which may suggest reduced such activity at domains with serine in the sequence *in vivo*. Furthermore, there are suggestions that not all N-glycosylation sites on fibrillin-1 are normally utilised[416]. One can also consider online prediction algorithms (SIFT[244]PolyPhen[245]) which suggest this mutation to be non-pathogenic.

Considering all this together, there is compelling evidence that the variant we found in *FBN1* is not pathogenic. Of course further segregation analysis would help to confirm this.

3.5.3.2. *PAPILIN*

This gene is 25 exons and spans 37.1kb of genomic DNA. The encoded protein is papilin. It has been reported as an ECM protein found in basement membranes [417, 418]. It is thought to have high homology with the ADAMTS proteases and interact with them in the ECM. Interestingly, it is believed to play a role in the molecular pathways involving fibrillin-1 and ADAMTS10. This seemed therefore a good candidate gene to screen. Although it was not found to harbour a mutation, it is certainly worth considering as a candidate in the future if it lies in areas of interest in patients with disorders of ocular development.

3.5.3.3. *LTBP2*

One homozygous variant was discovered in *LTBP2*. This gene (OMIM 602091) was first characterised in 2009[227] and has been demonstrated to be expressed throughout the eye [419]. Unlike other members of its protein family, LTBP2 does not bind to latent transforming growth factor, and instead its C-terminus has high affinity for the N terminus of fibrillin-1. The many ocular manifestations of mutations in this gene, include primary congenital glaucoma[419], and EL with microspherophakia and meglocornea (OMIM 251750)[420, 421]. Mutations in this gene have also been recently described in Weill-Marchesani 3[422]. The function of this gene and its protein is unclear, but its role with fibrillin-1 and ocular disease made it a good candidate gene for analysis.

Only one potential homozygous missense single nucleotide variant ((c.785C>T (p.Pro262Leu) was discovered. This variant is a registered SNP (rs143106228). However, it is very rare. Out of the 4502 chromosomes sequenced by the Exome Sequencing Project[246], the T allele was only described in the heterozygous manner, in less than 1% of cases. The minor allele SNV was never described in the homozygous state. This was therefore interesting to consider as a pathogenic variant. However, *in silico* analysis of this mutation suggests that it is benign [244, 351] [245] We would like to perform segregation analysis on this family to investigate this mutation further.

In summary, we have not discovered the genetic source of the phenotype in this family. There are further candidates we could investigate in the regions of homozygosity. One must consider that this has strong phenotypic characteristics of KNO, and neurological

imaging would help to confirm this. Although *COL18A1* was not within any of the large regions of homozygosity, it must be considered that compound heterozygous mutations in this gene may be present. There are examples of allelic and locus heterogeneity in consanguineous families[423]. Though the proband CII:1 has multiple large regions of homozygosity , this family does not report obvious consanguinity. The possibilities of non-homozygous mutations therefore must be considered.

3.5.4. FAMILY 6

Family 6 presented with EL and a phenotype similar to WMS and WML. WMS was first described by Weill[424] and Marchesani[425] with over 200 cases being described since. Although no formal diagnostic criteria have been described, characteristic features include short stature, brachydactyly, joint stiffness and EL (commonly manifested as microspherophakia)[426]. Cardiac malformations have been reported to include prolonged QT interval and mitral valve prolapse[427] and pulmonary stenosis[426]. These occur very occasionally, with Faivre and colleagues suggesting this to occur in only 39% of autosomal recessive cases and 13% of autosomal dominant cases[428]. The clinical description of WML by Morales and colleagues[226] described cases in which brachydactyly and joint stiffness were excluded. The former seems to therefore be crucial in the differentiation of WMS and WML. WMS was defined in the classification of genetic skeletal disorders[429]. Although brachydactyly can be associated in isolation or with many syndromes[430] there is no definition of which type of brachydactyly is seen in WMS. In summary, a ratio of the middle phalanx to the length of the palm is most commonly used[430]. On discussion with a clinical geneticist (personal communication; Dr Sabha Mansour, St George's Hospital, London) it was believed that this family manifested brachydactyly. With regard to joint stiffness, this is a more subjective assessment. Although Beighton score analysis[136] can be undertaken for the opposite extreme for joint mobility, it has less utility for stiff joints. On discussion with the clinical geneticist regarding EIV:1, it was believed that joint stiffness was manifest. No cardiac anomaly was detected, although this is not a discriminating factor in WMS or WML. He was therefore diagnosed with WMS, and *ADAMTS10* was screened on this basis.

WMS is inherited in an autosomal dominant or recessive pattern[428]. The former (OMIM 608328) is thought to be caused by mutations in *FBN1* [431, 432], specifically mutations affecting heparin binding of the eight-cysteine domain (TB) number 5

(TB5)[433]. A genetic basis for autosomal recessive WMS (OMIM 277600) was first described by three mutations in *ADAMTS10* in three families[280], subsequently confirmed in 3 further families with two more mutations[226]. Interestingly, mutations in *LTBP2* have recently been demonstrated to cause WMS[422]. This latter report also described patients with what they termed "Weill-Marchesani Like syndrome" with mutations in *LTBP2*. However none of those patients had any ocular features, which were cardinal in the first description of WML [226].

ADAMTS17 was first described in the seminal paper which highlighted seven of the ADAMTS proteins and genes, including *ADAMTS18*[17]. It is found on 15q26.3 and its protein (Figure 3.34) has high homology, particularly the catalytic domains, with ADAMTS19. The gene has two isoforms of 22 exons (1095 amino acids) and 16 exons (502 amino acids).

Its role, as with all in this family of proteins is unclear. Morales et al [226] first described homozygous mutations in *ADAMTS17* in a consanguineous family causing EL and short stature. They coined this condition as "Weill-Marchesani-Like syndrome" (OMIM 613195) (WML). Distinguishing this from WMS is challenging.

The three mutations of *ADAMTS17* in three families with WML [226], with confirmation of a further mutation in the same gene by the same group in a further family[324] are the only convincing mutations causing WML.

Whether our patients had WMS or WML is unclear. EIV:1 was initially diagnosed, clinically, with WMS, and *ADAMTS10* screening was undertaken on this basis. His son, EV:1 did not fulfil the systemic features of this condition, and would therefore more likely be a candidate to have a *ADAMTS17* mutation. Our genetic analysis has not been conclusive. The causative mutation is likely to affect Exon 15 of *ADAMTS17*. We believed that exon 15 was screened and present in EIV:1. However, the presence of the heterozygous variant initially was confusing. This was however repeated and this variant was not found. On homozygosity mapping the largest region shared between father, son and cousin was a 4.9mb region covering chromosome 15q25-26. This indicated that a homozygous mutation in this region was most likely. The most likely candidate in this region was *ADAMTS17*.

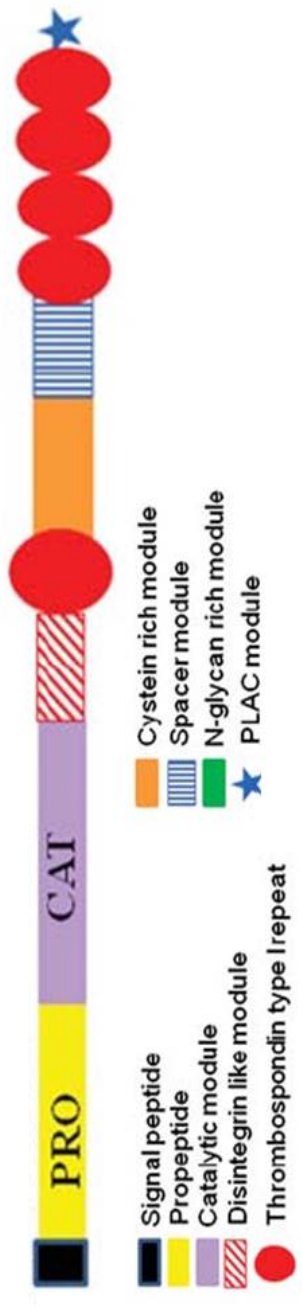

Figure 3.34: ADAMTS17. Schematic image of *ADAMTS17* demonstrating domains *Adapted from Le Goff et al[16]*

Assuming that no mutation was found in the coding regions of *ADAMTS17* we needed to consider other possibilities.

Having assumed that all the exons had been screened, it was considered that an alternative, deep intronic change within this gene may be responsible. There are numerous examples of such mutations causing ophthalmic disease[434, 435]. Most recently, mRNA analysis identified the creation of a pseudoexon in *USH2A* caused by a deep intronic change[355]. It was hoped that a similar explanation would fit in our family.

Although amplifying the region between exons 11-13 using primers described by Morales et al[226], doing so for the whole gene proved impossible. However, concurrently, exome sequencing had been undertaken.

The next generation exome sequencing experiment on EIV:1 and EV6 revealed that exon 15 on *ADAMTS17* was not amplified. This was confirmed by PCR amplification, and suggests that this exon deletion is the pathogenic cause of this phenotype.

Deletion of whole exons is not an unusual process and can be caused by numerous pathways. This includes splicing errors and genomic rearrangements. With no splicing errors discovered on direct sequencing, it was likely that genomic rearrangements would be causative.

3.5.4.1. GENOMIC REARRANGEMENT

Exonic deletions may be part of large deletions as a consequence of structural genomic rearrangements. Such a process occurs during recombination, where a crossover of chromatids from parental DNA occurs. This is characterised by allelic regions of homology sharing DNA. However, there are triggers which may result in this process not occurring accurately, including increased proximity of chromosomes, cellular stress, DNA sequence or structural features and inappropriate repair[436]. The former two are certainly important in cancer genetics. It is suggested that as replication and translation occur at the same template, any interruption at this junction can lead to “replication stress” thus increase the rate of structural abnormalities[437]. Furthermore, as double stranded breaks occur at regions of replication, this increases the risk of rearrangements at these sites. Certain DNA characteristics are more prone to such breaks. It is thought that regions which contain strings of CGG or AT repeats may be more prone to

breaks[438]. Also regions of DNA which do not conform to the characteristic “B-DNA helical shape” may be more susceptible[439]. Finally there are numerous avenues of inappropriate repair. The most common is when non-allelic homologous regions line up (Figure 3.35). Areas of repetitive DNA (“segmental duplications” or “low copy numbers”) are susceptible to this. These regions are also more likely to slow down the replication process, and thus make the segment more prone to structural abnormalities. In regions of non-allelic homology, the process of non-allelic homologous recombination (NAHR) may occur[342]. This can happen at the intrachromatidal, interchromosomal or intrachomosomal level. The former will only produce deletions whilst the latter can produce duplications or deletions[440]. This also depends on the orientation of the segmental duplications at which point alignments tend to occur[441]. For there to be homozygous regions downstream to such a structural rearrangement, as would be the case in our family, would suggest that the NAHR occurred between homologous chromosomes, rather than chromatids[442].

The deletion of exon 15 was demonstrated by exome sequencing of *ADAMTS17*. Sanger sequencing of this gene however was inaccurate. The saliva samples which were sent from Sri Lanka included a sample of an unaffected individual (EIV:2). These samples were likely to have been mislabelled. The presence of the heterozygous variant should have alerted us to this. However on repeat sequencing, this SNP was deemed to be homozygous. On reflection again of this chromatograph, it is not likely to be homozygous. No reverse sequence was available to confirm this.

This was an expensive error and led to many months of work attempting to amplify RNA from leucocytes in search of a deep intronic change causing a pseudo-exon. In fact, the causative skipped exon was in front of us.

This illustrates some of the difficulties of acquiring DNA from remote areas. Although delivering swabs/ samples for DNA extraction through the post has been demonstrated to be successful[443], small errors such as these are costly.

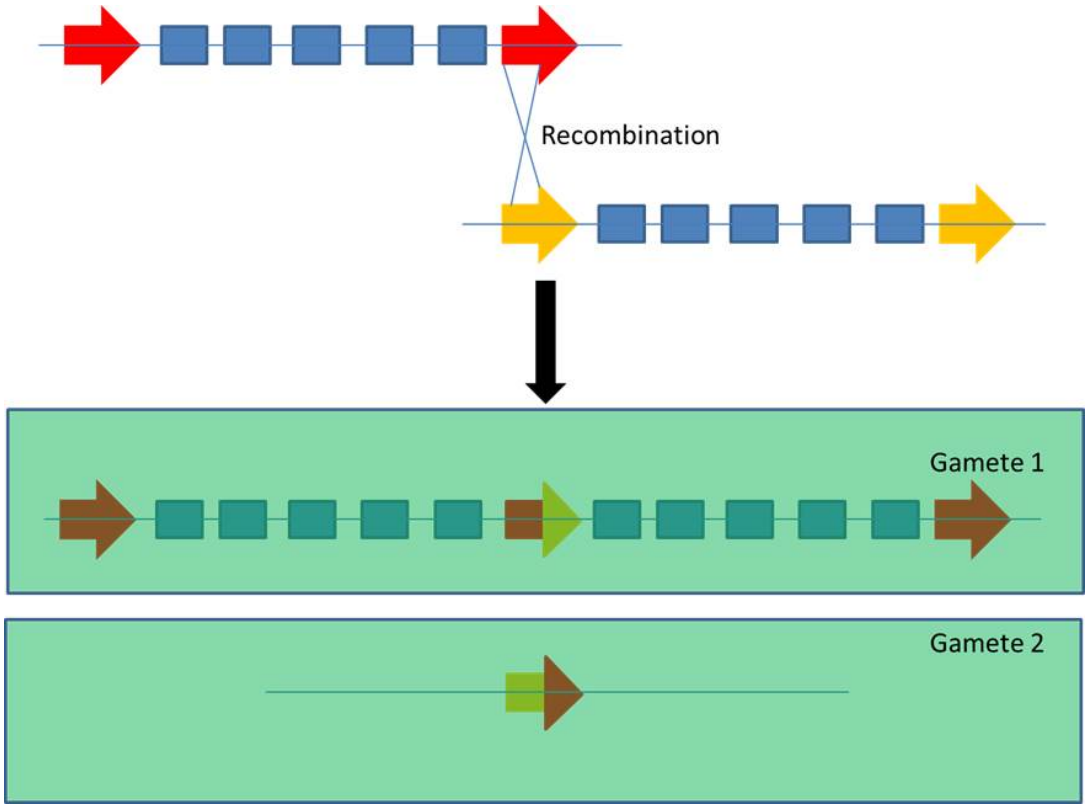

Figure 3.35: Non allelic homologous recombination. Arrows represent Low Copy numbers (repeat sequences prone to non-allelic pairing). Blue boxes represent genes. The result can be insertion or deletion, as evident in the gametes produced.

3.5.4.2. Mutations in *ADAMTS17*

There are four mutations in four consanguineous Saudi families. c.2458_2459insG, c.1721+1G > A, c.760 C > T[226] and c.652delG[324]. The latter two mutations are in Exon 4 and 2 and result in PTC. Interestingly, the first mutation was predicted to produce a truncated protein. The splice site mutation abolished the consensus donor sequence thus causing a deletion of exon 12. The authors of these papers suggest that the catalytic domains would be retained by this latter mutation, but the C terminus would be abolished. It is difficult to predict what an unknown mutation in our family would result in; however, exon 15 does encode a peptidase domain of ADAMTS17.

To confirm our finding further of a deletion of exon 15, we could consider techniques such as multiplex ligation dependent probe amplification[444] or Comparative Genomic Hybridization array technology[445] may be employed to allow characterisation of deletions of single and multiple exons.

In summary, work in this chapter has investigated EL and RD in six families. It has been successful in delineating a novel ocular phenotype consisting of microcornea and a cone predominant dystrophy, in association with congenital lenticular abnormalities (cataracts and EL) and early onset RD. Recessive mutations in *ADAMTS18* appear to be responsible for this phenotype.

This work has also provided novel features to Knobloch syndrome, and suggested a novel genomic rearrangement in *ADAMTS17* as causing WML. It has also made evident that the ADAMTS family of proteins have an important part to play in ocular development. There are considered to be at least 12 major genes involved in anterior segment disorders[446]. This work helps towards suggesting that the ADAMTS proteins will be recognised in this group. It is possible that the ADAMTS proteins may also be shown to influence photoreceptor development.

Finally, we have one further family to date with an as yet undiscovered genetic mutation causing EL and RD. Our group is continuing to work with this family to establish the genetic cause.

CHAPTER 4: THE GENETIC ASSOCIATIONS AND PHENOTYPE OF NON-MENDELIAN RHEGMATOGENOUS RETINAL DETACHMENT

Publications arising from work related to this chapter:

(i) Kirin M, **Chandra** A, Charteris DG, Hayward C, Campbell S, Celap I, Bencic G, Vatavuk Z, Kirac I, Richards AJ, Tenesa A, Snead MP, Fleck BW, Singh J, Harsum S, Maclaren RE, den Hollander AI, Dunlop MG, Hoyng CB, Wright AF, Campbell H, Vitart V, Mitry D.

Genome-wide association study identifies genetic risk underlying primary rhegmatogenous retinal detachment**.**

Hum Mol Genet 2013 Aug 1;22(15):3174-85

(ii) **Chandra** A., Mitry D., Webster AR., Wright A., Campbell H., Charteris DG.

Genome wide association studies: Applications and Insights gained in Ophthalmology

Under review at time of thesis submission: *Eye*

A proportion of the work presented in this chapter is a result of collaboration with the MRC Genetics Unit at the University of Edinburgh.

4.1. INTRODUCTION

4.1.1. COMPLEX DISEASE GENETICS

Tradition has dictated that genetic predisposition to disease be termed Mendelian or Non-Mendelian. The term Mendelian is reserved for those phenotypes which a single genetic locus attributes to its aetiology. This has been the basis of investigations so far in this thesis. Non-Mendelian traits are everything else. In reality, this represents a spectrum. However, the term "complex" is generally reserved for conditions which are influenced by multiple loci as well as the environment. Although DNA variants may be individually insufficient to cause complex phenotypes and have small effects; they are thought to influence the various factors which in combination contribute to disease susceptibility [447]. The genetic components may be dependent on each other's effects (polygenic inheritance), interact with each other (epistasis) or act independent (genetic heterogeneity)[448]. Furthermore the environment-gene interactions may influence the final phenotype[449].

Genetic investigations for multifactorial disease fall broadly into two groups: candidate gene studies and genome wide studies. Candidate studies involve prior understanding of genetic function and pathogenesis of the trait in question. These have traditionally been very expensive and laborious, with very few successes [450]. There have also been many un-replicated results[451].

Genome wide studies encompass linkage and genome wide association studies. Utilising the former can involve subsets of families who may display "near-Mendelian" inheritance. In studying these families, it may be possible to perform segregation analysis to establish a theoretical genetic model[452]. This model can then be used within traditional parametric linkage analysis. Non parametric linkage has been used widely with mixed results [453] with some notable successes, such as inflammatory bowel disease[454]; occasionally in conjunction with association studies [455] in complex diseases. However regions which are highlighted, may cover in excess of 10cM, thus requiring further candidate studies to narrow this down.

In 1996, Risch and Merikangas[456] demonstrated mathematically that the power of association analysis for complex conditions was greater than linkage studies. They suggested that the future of complex disease analysis lay in large scale association studies.

4.1.1.1. COMMON DISEASE –COMMON VARIANT

Theories about the genetic factors involved in complex genetic disorders include the "common disease – common variant" hypothesis (CD-CV) [457]. This considers that these factors are susceptibility loci, influencing but not determining overall disease risk. This hypothesis explains that genetic factors associated with these conditions are common (>1%) and many generations old.

The implications of this are that these factors must have a small impact on the final phenotype; otherwise the prevalence of the disease would be equal to that of the genetic variants. Secondly, if common factors have a small genetic effect, and common disorders show hereditability, then multiple such factors may influence disease phenotype. These loci individually have low effect, but in combination and with epigenetic effects (e.g. environment) have an additive contribution.

Investigating for such low impact factors is highly prohibitive with linkage studies. Association studies were first suggested as a means of detecting weak genetic factors in 1996 [456]. Association studies aim to statistically identify alleles associated with a certain phenotype.

Associations may be direct or indirect. Direct association studies are designed such that the variants investigated are thought to be causative. This is therefore very powerful, and utilises variants in likely candidate genes[458]. This method is however limited in that a priori hypotheses are required. Indirect association studies have been more successful, and are discussed in section 4.1.6.

4.1.2. SINGLE NUCLEORTIDE POLYMORPHISM (SNP)

Association studies are based on the most basic unit of genetic variation: the single nucleotide polymorphism (SNP). SNPs are single base pair changes in the DNA sequence; and are the most frequent form of genetic variation in the population[248]. Because of their abundance, they are the preferred markers for such large scale population studies. Indeed, they are also the preferred marker for any genome wide study; as demonstrated in Chapter 3. The definition of common SNPs has been suggested as having minor allele frequencies (MAF) of greater than 0.5% whilst rare are sometimes classified as <0.5%[459], though this fine definition is debateable[327].

4.1.3. INTERNATIONAL HapMap PROJECT

The understanding of SNPs increased rapidly with the development of the International HapMap project and of rapid massive parallel genotyping. The International HapMap Project is a large international collaboration that began in 2002 and sought to determine the common patterns of DNA sequence variation in the human genome. It has done this by characterising sequence variants, their frequencies and the correlations between them in 269 DNA samples from populations with ancestry from parts of Africa, Asia and Europe. It therefore provided detailed genotype data in over 1 million SNPs. It was a huge and successful collaboration that made all data freely available in the public domain [460]. This catalogue of genetic variation has provided a 'blueprint' of human genetic variation; and in particular SNP locations. Along with the Human Genome Project [353] and the SNP Consortium [461], over 10 million DNA variants have been identified. With the advent of NGS this has since been augmented by such endeavours as the 1000 genomes project[248] and the NHLBI GO Exome Sequencing Project[246].

4.1.4. HARDY WEINBERG EQUILIBRIUM

When investigating variants in population genetics, one of the most important principles is estimating genotype frequencies. Genotype frequencies are determined, partly, by mating pattern. If one assumes that mating is random, there are no overlapping generations, the allele frequency is equal between men and women, the allele frequencies do not alter between generations (i.e. no mutations, migration or natural selection) and that the population is large enough not to be affected by sampling error (ideally an infinite population; but realistically over 500) one can draw the following inferences in table 16.

			Male gametes	
		Allele	**A**	**a**
	Allele	Frequency	p	q
Female Gametes	**A**	p	**AA** p^2	**Aa** pq
	a	q	**aA** qp	**aa** q^2

Table 16: Punnett Square

In this table (known as a Punnett square[462]): **A** and **a** are the two alleles at a locus. p is the frequency of the allele A and q is the frequency of a in the zygotes of any generation.

From this box, one can see that the frequencies of the alleles in the population would be:

$$p^2 + 2pq + q^2 = 1$$

This equation was described independently, by G.H Hardy and W Weinberg in 1908[463] (Hardy-Weinberg Equilibrium; HWE).

Although the assumptions upon which this equation is based may seem incorrect, the HWE is used as a reference model for tracking allele frequencies. These frequencies are the same from generation to generation, and will be attained in just on generation (with the assumptions in place).

4.1.4.1. TESTING FOR HARDY WEINBERG EQUILIBRIUM

When investigating allele frequencies, it is important to deduce whether the observed frequencies are significantly deviated from expected (in accordance with HWE). This may be calculated with chi-square tests, taking into account the degrees of freedom. This would then help determine a threshold p-value (comparing observed to expected allele frequencies). This p value is the probability that chance could produce a deviation between the observed and expected values. A large value would suggest that chance alone could account for the differences seen. A small value would suggest that the observed values are not in HWE. The threshold is determined in advance. An example for the p value threshold is the Welcome Trust Case Control Consortium (WTCCC) GWAS[464] where this was to reject SNPs which had $p < 5.7 \times 10^{-7}$ when assessing for HWE. Within such GWAS, deviations from HWE are likely to indicate severe genotyping errors[465].

4.1.5. LINKAGE DISEQUILIBRIUM

Linkage Disequilibrium (LD) was first coined in 1960 [466]. It refers to the non-random association of alleles at two or more loci within populations. Alleles in LD share a common ancestor and travel together through generations; this relationship is not eroded by recombination. Confusingly, it does not require linkage; thus leading to some authors

terming it gametic phase disequilibrium[467]. Famously R. Lewontin (who first coined the phrase) “regretted using the term “linkage disequilibrium”.

LD is most influenced by the recombination rate between two loci and time; measured in generations. The frequency of recombination (“r”) between genes depends on whether they are present on the same chromosome and the physical distance between them. LD is therefore strongly influenced by physical distance[468] and recombination hotspots[469] (whereby nucleotides either side of a hotspot will share little or no LD because of recombination at that juncture). It reflects population history, breeding patterns, geographic structure, mutation and natural selection. Older populations tend to have shorter conserved segments, as the population would have experienced more recombination; leading to lower LD[470]. Finally, rare variants tend to have larger areas of LD[464]. These variants are likely to be evolutionarily younger; therefore be less likely to have undergone recombination.

LD can travel long chromosome distances. When tracked across the genome, these regions are termed haplotype blocks [471], and are separated by recombination hotspots. The characterisation of these haplotype blocks was undertaken by the International HapMap project (see Section 4.1.3)[460].

4.1.5.1. MEASURING LINKAGE DISQEQUILIBRIUM

The measurement of LD has three components. “D” is used to represent the linkage disequilibrium parameter. Simply put, this is the difference in allele frequency in chromosomes that underwent recombination, and those which did not. If D=0, this represents no recombination. This value, however, is dependent on the individual allele frequencies, and therefore is difficult to use across a region or genome. Therefore the magnitude of LD is usually demonstrated by a quantity known as D’.

D’ is a measure which is defined as D/D_{max}. This range is -1 to 1, and therefore allows comparisons between genomic regions, or populations or even species.

r^2 is often used as an alternative measure of LD. This is another confusing nomenclature, as r is used for the frequency of recombination between genes. This is directly related to the correlation coefficient in the allelic state between alleles in the same gamete. The maximum value of r^2 is 1, when there is perfect LD.

4.1.6. INDIRECT ASSOCIATION STUDIES and Tag SNPs

Direct association studies initially had very limited success. Indirect association studies take full advantage of the understanding of LD to distinguish associations between alleles and phenotypes. Critical to this is the utility of "Tag SNPs". These are SNPs which are selected because of the knowledge of their LD patterns. By genotyping these SNPs informs about their tagged SNPs (Figure 4.1). These Tag SNPs are usually chosen so that they may have r^2>0.8 with common SNPs[472]. Thus these Tag SNPs would be able to provide detail on true polymorphisms associated with disease or phenotype thus reducing the number of SNPs that need to be tested[473]. This is the principle of imputation. Imputation is particularly useful in meta-analysis, where different SNP chips may have been utilised in different studies.

Genome Wide Association Studies (GWAS) utilise this technique by genotyping large set of SNPs (>100,000) across the human genome to determine the most common genetic variations that have a role in disease or to identify heritable quantitative traits [20].

4.1.6.1. GENOTYPING CHIPS

The success of the International HapMap and the understanding that emanated motivated commercial companies to develop generic "chips" for GWAS analysis. The market is dominated by two such companies. Illumina, which uses fibreoptic technology, and Affymetrix, which uses DNA probe microarrays. The former chose tag SNPs based on reliability for genotyping, whilst the latter concentrate on an even spread

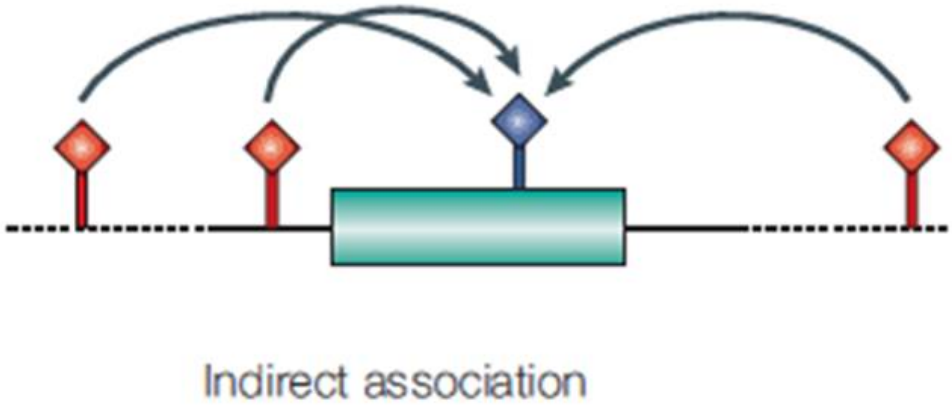

Figure 4.1: Indirect association: The tag-SNP (in blue) is genotyped, which provides information on those variants in LD with it (in red). *Adapted from* [20]

across the genome. Both companies provide comparable power[474]. The first wave of these chips (2005-7) had between 100,000 – 500,000 SNPs. Currently, chips may have 1,000,000 SNPs; approximately one per 3kb.

4.1.7. GWAS ISSUE AND STUDY DESIGN

The typical GWAS has four parts: a) selection of a large number of individuals with the disease or trait of interest and, in a binary condition, a suitable comparison group; b) DNA isolation, genotyping and quality control; c) statistical tests for associations between the SNPs that pass quality control thresholds and the disease/trait; d) replication of identified associations in independent population samples or experimental examination of functional implications. By far the most common design in published GWAS comprises a case-control study with a binary outcome. Other study designs include individuals with measured continuous phenotypic variables (e.g. refractive error) analysed as a quantitative trait and family based designs such as trios (proband and parents) or other pedigrees of related individuals. It is ideal to recruit case subjects and control subjects systematically from the same population of single ancestry as case-control differences in ancestry (population stratification; see Section 4.1.7.3) can confound association test results.

4.1.7.1. CASE AND CONTROL SELECTION

This is an important aspect of case-control GWAS. Most successful GWAS involve numerous centres, and strict case definition and ensuring the same population is a crucial part of successful GWAS[475]. Ideally, control samples should be collected at the same institution concurrently; then genotyped at the same time on the same chip; this may reduce the batch effect seen in large scale genotyping experiments[476]. However, it is more common place to use common control databases. This is useful in relatively rare conditions, as the proportion of cases in the control set will be negligible.

This method was used successfully in the Wellcome Trust Case Control Consortium[464].

4.1.7.2. SAMPLE SIZE

Experience has shown that large sample sizes (2,000) are needed to detect common genotypic variants likely to have a low relative risk (1.2-2) and to offset the large

number of independent SNP association testing [477]. Contemporary genotyping platforms have specific advantages and limitations, however most provide a high level of genomic coverage estimated to capture between 67-90% of common SNP variation in Caucasian ethnicity [478]. After genotyping, extensive data cleaning (quality control) is required to detect problems that can result in false negative or false positive findings, such as genotyping errors, duplicate samples, unexpected relatedness among subjects and strong deviations from HWE [479].

4.1.7.3. POPULATION STRATIFICATION

One of the most challenging issues to account for is population stratification. This is the presence of differences in allele frequencies between populations; particularly evident in those of different ancestry. It is caused by non-random mating followed by genetic drift[462]. Even small degree of population stratification can result in errors in GWAS[480]; because of the large samples sizes required. A famous example suggested a significant association with *LCT* (a gene which has undergone strong selection in certain European populations) for height; which was then markedly reduced once population ancestry was matched[481]. Careful selection of controls of same ancestry can minimise this. Nevertheless, Quality Control methods can be employed to assess for this. A common method used is to examine for genome wide identity by state (IBS) and identity by descent (IBD: Figure 3.2). IBS represents individuals who have an independent copy of a particular allele, whilst those who share IBD have the identical copy of the same ancestral allele. Using the genome-wide proportion of alleles shared IBS, individuals may be clustered based on their IBS compared to the sample average. Using these, a multivariate statistical method can be devised (primary component analysis (PCA)) to analyse for stratification. PCA is a method used to generate uncorrelated variables ("principal components") from data containing observations across correlated variables. In genotyping data, the observations are individuals and the variables are markers, or SNPs[480]. Using this method, it is therefore important to remove regions of high LD, to reduce the correlation of the SNPs (variables) as much as possible[482].

4.1.7.4. ANALYSIS

Analysing for association studies have used a standard χ^2 test for independence on 2 degrees of freedom (allowing for 3 genotypes at a SNP; two homozygous and a

heterozygous). If one was to presume an inheritance (dominant or recessive); this could result in a reduction of the number of genotypes included in the analysis; thus the degrees of freedom. If there is a presumption of this kind; a Cochran-Armitage Trend Test (CATT) may be used.

Alternatively logistic regression may be used in case/ control studies. This allows predictors to be included in analysis (such as age, gender etc.). This has further utilities in that interactions between loci, and environmental effects may be incorporated into the model.

4.1.7.5. MULTIPLE TESTING

This is an important consideration in GWAS analysis. With a p value set at 0.05, and multiple tests being undertaken (SNPs genotyped); a large number of false positives would be generated. The expected number of errors ("family wide error rate") when undertaking N tests would be αN (where α= significance level). Therefore a more stringent measure of significance is required. The most famous method of addressing this is the Bonferroni correction; named after the Italian mathematician, Carlo Emilio Bonferroni. This is equivalent to multiplying all p-values by N and applying a threshold of α. To achieve an α= 5% if conducting 100,000 independent tests the actual threshold for genome wide significance of association is $P<5X10^{-7}$. A suggested cut off has been suggested as $5x10^{-8}$ for modern GWAS[483].

Within GWAS this is however complicated by LD: as SNPs are correlated. The Bonferroni correction may therefore be overly conservative. Alternatively a permutation test may be used. In this method, the genotype data is fixed, and the phenotype data is shuffled randomly. This is then analysed again, and the minimum p value is compared with the original p value. Repeating this N times, the corrected p value is (R+1)(N+1), where R is the number of times that the permutation p value is less than the original p value. It is suggested that this method may be more powerful than Bonferroni, when SNPs are in LD[484].

There are challenges of separating the many false positives from the few true positive associations. Therefore, putative genetic variants that are identified and reach genome wide significance need to be replicated in additional case-control cohorts, preferably of larger size, as the best method to verify a true association[485]. Finding a true causal

variant however only represents the beginning; genetic association does not imply causality but offers a genetic hypothesis of an underlying biological pathway that warrants further exploration.

There are many examples of GWAS proving a success in elucidating the genetic architecture of ophthalmic traits and diseases. A few are illustrated below.

4.1.8. GENOME WIDE ASSOCIATION STUDIES IN OPHTHALMIC CONDITIONS

4.1.8.1. AGE RELATED MACULAR DEGENERATION

A genetic predisposition to age related macular degeneration (AMD) has been suggested for almost thirty years [486] with familial aggregation studies[487], twin [488] and linkage studies [489] providing most of the evidence.

Initial investigative techniques focussed on assessing candidate genes which primarily comprised those associated with macular dystrophies and similar phenotypes to AMD [490]. Over 45 such loci were investigated[491], with most failing to yield replicated associations. Linkage studies proved challenging because of the difficulty in recruiting large affected families and the late age of onset of the disease. Genome wide linkage studies have suggested numerous loci, but only two (on chromosome 10q26 and 1q32) have been replicated convincingly. The former of these contains over 70 genes, including peroxiredoxin 3 (*PRDX3*) gene, which encodes a protein with antioxidant function. Interestingly chromosome 1q contains the well characterised gene complement factor H (*CFH*).

The first GWAS success story was the discovery of the association *CFH* with AMD which was independently described in three cohorts [492-494]. A coding variant Y402H in exon 9 of *CFH* was significantly associated with AMD. This finding was replicated throughout the world in many ethnic groups. This mutation affects the binding properties of CFH, thus resulting in inappropriate complement activation [495]

The discovery led to investigations of other complement factors in AMD, and the understanding of the association with complement factor B and complement component C2 [496], further replicated across the world [497-499] adding to the understanding of this condition.

Previous linkage studies had long established 10q26 as a candidate locus for AMD [489]. Age related maculopathy 2 gene (*ARMS2* -previously known as *LOC387715*) was subsequently suggested as the candidate locus [500], in particular SNP rs10490924. However the pathogenesis of this gene was not clarified. A GWAS undertaken by DeWan [501] highlighted an alternative gene in the locus 10q26; high temperature requirement A1 (*HTRA1)*, in 96 Oriental patients with neovascular AMD (nAMD). The risk SNP rs11200638 (in complete linkage disequilibrium with rs10490924) was found to be highly associated with wet AMD. It encodes a heat shock serum protease expressed in human retina that is activated by cellular stress [502, 503]. Meta-analysis has suggested that both *ARMS2* and *HTRA1* may contribute towards AMD independently with an augmented combined affect [504]

Kopplin *et al.* [505] completed a GWAS on patients with late AMD in conjunction with a family based GWAS. They not only confirmed previously associated risk genes, but went further to suggest protective functions of genes *MYRIP* and *SKIV2L*. The former of these is involved in trafficking melanosomes in the RPE [506] and thus may prevent or delay declines in RPE function. *SKIV2l* is involved in breakdown of RNA, and may have a role in autophagy [507]. Variations in *SKIV2L* have additionally been associated with a protective role in polypoidal choroidal vasculopathy [508].

Risk factors associated with AMD have additionally been studied in relation to risk alleles. It has been shown that smoking and high body mass index (BMI) with at risk alleles significantly increase the risk of developing AMD, adding considerations as to possible interactions [509]. Further interactions of risk factors with *CFH* genotypes were explored by Seddon and colleagues [510]. They reported a risk profiling system which illustrated that established risk factors in combination with genotypes could predict progression to advanced AMD independent of demographic factors and ocular phenotype. Alternative predictive schemes have followed [511]. In addition, algorithms have been suggested for predicting treatment prognoses [512]. Predictions of treatment outcomes with modern anti-VEGF agents have been suggested based on genotype variations of *CFH* and *HTRA1*[513]. These steps toward a personalised risk profile, may provide for a more target approach to prevention and management of this condition.

The influence of the complement system in AMD has now even extended to novel treatments, aimed at modulation of this system[514]. The landmark GWAS in AMD

have paved the way for almost 50% of the hereditability of this condition now being explained. This genetic understanding is unrivalled by any other complex diseases.

4.1.8.2. GLAUCOMA

4.1.8.2.1. Primary open angle glaucoma

The first gene implicated in the pathogenesis of primary open angle glaucoma (POAG) was Myocilin (*MYOC*) [515] where mutations may result in a breakdown of the extracellular matrix structure in the trabecullar meshwork. Mutations in this gene are responsible for up to 4% of POAG cases [516]. Mutations in optineurin (*OPTN*)[517] and WD Repeat Domain 36 gene (*WDR36*)[518] have also been shown to be causative. However, mutations in these genes have however been shown to be infrequent and can explain only a small proportion of the genetic architecture of POAG [519].

Nakano [520] et al published the first GWAS in POAG in a Japanese population, with meta-analysis revealing 3 associated loci with moderate but not genome wide significance. Six polymorphisms were identified: near *ZP4* gene, and *PLXDC2* gene. The functionality of these associated genes and the markers were not discussed or replicated and were absent in an independent Indian population [521].

Thorleifsson et al [522] conducted a large multiethnic GWAS. They found two SNPs (rs 4236601, rs1052990) which were in the same linkage disequilibrium block as genes *CAV1* and *CAV2*, which encode caveolin 1 and 2. Both these proteins are expressed throughout ocular tissue [523]. Caveolin 1 is thought to play a regulatory role in the function of endothelial nitric oxide synthase and TGFβ signalling, mechanisms that have been implicated in the pathogenesis of POAG [524, 525]. The most statistically significant variant (rs4236601) however did not have an effect on IOP or central corneal thickness.

Thorleifsson *et al* found differences in rs4236601 within ethnicities. When compared to European populations, this variant was absent in a Japanese cohort but posed a greater risk with lower frequency in a Chinese population[526]. Osman and colleagues[527] also showed significant association with *CAV1* and *CAV2*, amongst other genes, in a GWAS on an Asian cohort. However, these findings were not replicated in a North American cohort [523].

Burdon and colleagues analysed 590 patients with advanced open angle glaucoma [528]. They found two regions of significance, near the *TMCO1* gene and the *CDKN2B-AS1* gene both of which were shown to be expressed throughout ocular tissue.*CDKN2B* was shown to be upregulated in response to raised IOP. These genes have been suggested to play a role in apoptosis[529], with the link thus with glaucoma. Of further interest, *CDKN2B* was shown previously to be related to optic disc cupping [530](section 4.1.9). The particular SNP in that study had a P value = $3.9x10^{-7}$, further implicating an association of this region with OAG. *TMCO1* has subsequently been associated with intraocular pressure (section 4.1.9.5), providing further evidence to its role in disease aetiology.

This paper raised further interesting issues. Firstly, they validated the efficacy of using extreme phenotypes in GWAS; the variants found in their discovery cohort of severe OAG were replicated in cases with less severe disease. Secondly, many of the cases in this study were used as a replication in Thorleifsson's GWAS[522]. Interestingly, although in that paper the analysis confirmed a role for *CAV1* & *CAV2*, this was not found to be so in this full GWAS with the same cases. This is not a novel situation, and highlights some of the challenges of interpreting GWAS and replication data. Conversely, this adds further credibility to those associations which are replicated in full hypothesis free GWAS.

More recent GWAS [527, 531] and targeted genotyping [532] have provided further evidence for the association with *CDKN2B*, in numerous ethnicities. This gene has now been shown to be significant in multiple independent GWAS in both normal tension glaucoma (section 4.1.8.2.2) and POAG. Some have suggested its role is therefore on optic nerve susceptibility[520], perhaps via effects on the TGF-beta pathway[531]. Certainly its role in glaucoma is now established, and further understanding of its role and effect on phenotype is now warranted.

4.1.8.2.2. Normal tension glaucoma

Normal tension glaucoma (NTG) is an important subset of primary open angle glaucoma, with a high prevalence in Japanese populations [533]. Studies have implicated several genes , including optic atrophy 1 [534-536], optineurin [537], p53 [538] and apolipoprotein E [539, 540]. The mechanism of these genes may involve

abnormal regulation of apoptosis [541], but this remains controversial and represent a small proportion of NTG patients.

The first GWAS investigating NTG compared 305 Japanese NTG patients to 355 controls [114] under the age of 60. The most significant SNP (rs3213787) along with the 7 next SNPs they found lay in the gene for S1 RNA Binding Protein 1 (*SRBD1*). This group established expression of this gene in brain, bone marrow and retinal ganglion cells (RGC) of neonatal mice and demonstrated that the at risk allele resulted in enhanced *SRBD1* expression. Although the function of this gene is unknown, they suggest that over expression may result in apoptosis and inhibition of cell growth; leading to retinal ganglion cell and optic nerve axon loss. Also rs735860, a SNP of genome wide significance, lies within the elongation of long-chain fatty acids family member 5 (*ELOVL5*) gene. This is one of a family of enzymes expressed in mammalian retina that involved in long chain polyunsaturated fatty acid synthesis (LCPUFA). Alteration in LCPUFA expression implies potential mechanism towards RGC apoptosis.

The same investigators have since replicated the significant SNPs in a separate population of NTG and high tension open angle glaucoma (HTG) patients, with a wider age range than the original cohort [542]. Although *SRBD1* and *ELOVL5* are thought to be non-IOP related genetic factors, both SNPs (rs3213787 & rs735860) were found to be associated with NTG and HTG. There was no difference in the maximum IOP between the HTG patients with the at risk alleles, leading to the suggestion that these SNPs act independent of IOP. Their findings also implied that these genes are associated in late onset open angle glaucoma. Further replication of these results have yet to be done.

More recently, large independent GWAS and meta-analysis on GWAS cohorts[543, 544] investigating over 1500 NTG patients have suggested the role of *CDKN2B* in the aetiology of Japanese NTG. This gene is highly relevant to high pressure open angle glaucoma (see Section 4.1.8.2.1). The importance of this gene on glaucomatous optic neuropathy[545] suggests its role is likely to be IOP independent[546].

4.1.8.2.3. Pseudoexfoliation

Genetic factors contributing towards the development of pseudoexfoliation (PXF) and pseudoexfoliation glaucoma (PXG) are established, with a demonstrated increased risk to relatives [547]. Multiple modes of inheritance have been postulated [548]. Pseudoexfoliation has been associated with an increased production of microfibrillar material, such as fibrillin-1, latent transforming growth factor β binding proteins (LTBP) and transforming growth factor (TGFβ). It has also been associated with a decreased level of clusterin; which may increase abnormal aggregation of microfibrillar material. Of these candidates, only polymorphisms encoding for clusterin (*CLU*) had been associated with PXF and PXG [549].

Thorleifsson et al [550] performed a GWAS initially on 195 patients with glaucoma. They found moderate significance of SNP rs2165241 in this group. However, significance was very high in the subgroup of 75 patients with PXG (OR=3.4). This SNP was sequenced in additional Swedish and Icelandic cohorts and confirmed to be associated with PXG. It is found in an intron of the lysyl oxidase–like protein 1 (*LOXL1*) gene. Although no mutations in the *LOXL1* gene itself were determined to cause PXF, certain sequence variations were found more frequently in cases; suggesting an association with this gene. The association of *LOXL1* with pseudoexfoliation has been replicated numerous times [551-558]. The LOXL1 protein is part of a family of enzymes which catalyses deamination of tropoelastin resulting in formation of elastin fibres and is essential in homeostasis of elastic and connective tissue [559]. Furthermore, it is suggested that PXF material consists of elastin microfibrillar components [560]. Functional studies have demonstrated reduced expression of *LOXL1* in ocular tissue of PXF and PXG [561] and specifically in lens capsule of patients with PXG [562]. Functional studies have demonstrated reduced cross linking domains in elastin and decreased expression of *LOXL2* , an enzyme from the same family and with similar activity as LOXL1, in a black American population compared to a white population, perhaps increasing susceptibility to glaucomatous optic nerve damage [563].

Krumbiegel and colleagues [564] performed a GWAS with DNA pooling and confirmed the association of the *LOXL1* locus. Additionally they highlighted a locus within the *CNTNAP2* gene on chromosome 7, which did not reach genome wide statistical significance. *CNTNAP2* encodes contactin-associated protein-like 2 (CNTNAP2) a neuronal membrane protein[565]. Its function is not yet clear, though it

may be involved in potassium channel trafficking [566]. Krumbiegel et al [564] demonstrated widespread expression of *CNTNAP2* mRNA and protein throughout ocular tissue, including retinal ganglion cells and trabecullar endothelial cells, although no difference was demonstrable between pseudoexfoliation and control tissue.

4.1.8.2.4. Primary angle closure glaucoma

Primary angle closure glaucoma (PACG) is a separate condition aetiologically and genetically from the more common POAG[567]. Few studies have investigated a genetic predisposition to PACG[568]. Vithana and colleagues[569] performed the only GWAS to date on 1854 cases from across Asia, replicated in 1917 cases from Asia and UK. They suggested two novel genes to be associated with PACG. Firstly, *PLEKHA7* on 11p15.1 was demonstrated as significant. *PLEKHA7* has a role in paracellular permeability. It is distributed widely in the eye, and the authors suggest it may be involved in fluidic aspects related to PACG.

They also suggest an association with *COL11A1*, a gene which causes the monogenic conditions of Marshall (OMIM 154780), and Sticklers type 2 (STL2: OMIM 604841). They note the paradox that PACG is normally co-existent with hypermetropia, whilst Marshall and STL2 are normally associated with progressive axial myopia. The existence of COL11A1 protein in the trabecular meshwork suggests to the authors that alterations in this gene may influence numerous sites in eyes with PACG.

Finally a third locus on 8q was suggested, although no definitive gene could be identified.

It is probable that these associations will help future investigations into PACG, and perhaps ocular structural development.

4.1.8.3. CORNEA

4.1.8.3.1. Fuchs endothelial dystrophy

Fuchs corneal endothelial dystrophy (FCED) is thought to occur in 38% of first degree relatives of probands [570]. Linkage studies first revealed a missense mutation in *COL8A2* in a multigenerational affected pedigree [571]. However some controversy exists over the reported findings. Additionally, rare autosomal dominant mutations in *SLC4A11*[572] *ZEB1* [573]& *KCNJ13* [155] have been reported.

The first GWAS in FCED was published in 2010[574]. Baratz K.H. et al found numerous SNPs within the Transcription Factor 4 (*TCF4*) locus independently associated with FCED. The most strongly associated haplotypes spanned one exon, with the impact of the most significant variants increasing with disease severity. The authors however were unable to define a variation within the coding region, and suggested that a non-coding regulatory region around the encoded protein is important.

The protein encoded by *TCF4* is called E2-2. It is a member of the class I basic helix–loop–helix (bHLH) transcription factors that are involved in cellular growth and differentiation [575]. E2-2 itself, found within the corneal endothelium, may influence FCED formation by altering the expression of *ZEB1*. If variants reduce the expression of E2-2, deficient proliferation or migration of endothelial cells may be causative. Alternatively enhanced ECM deposition may be causative if variants result in increased expression of E2-2.

This original GWAS was replicated by Li *et al* [576] in 450 cases with genome wide linkage on 64 families with 215 affected members. They confirmed the significance of the SNP rs613872 with their former analysis ($p=9.33x10^{-35}$). Linkage revealed the significant region was on chromosome 18 – only 1.5mb from *TCF4*. Further evidence in other ethnicities has followed, with Thalamuthu et al [577] confirming the association of TCF4 with FECD in a Chinese population.

4.1.8.3.2. Keratoconus

A genetic contribution towards the aetiology of keratoconus (KC) has been established for over a decade[578]. All modes of Mendelian inheritance has been suggested [579], with various loci suggested. The lack of consensus loci, suggests that the inheritance is likely to be complex[580]. Two large GWAS to date have investigated keratoconus. Li and colleagues[581] completed a GWAS on 222 Caucasians with keratoconus replicating in a further 611 cases, and suggested an association with *RAB3GAP1* on 2q21.3. This association was most significant, after meta-analysis,and has since been replicated[582].This gene is involved in neurotransmitter exocytosis[583], and defects in this gene are known to cause Warburg Micro Syndrome[584] (which includes microcornea in the ocular phenotype). Simultaneously, this group performed a meta-analysis with a GWAS performed by Australian colleagues, suggesting the promoter region of *HGF* to be significantly associated with keratoconus[585]. *HGF* had

previously been shown to be associated with myopia[586]. It has also been associated with narrow angle closure [568], suggesting that this gene may well play a role in structural development of the anterior segment. The encoded protein is also found in the cornea, particularly the stroma[587], and the authors suggest that this gene may play a role in keratoconus pathogenesis via an inflammatory pathway.

The different genes suggested in these papers based on data from the same cohort may seem conflicting, however, they offer novel pathways in KC. Replication will be crucial for validation.

4.1.8.4. DIABETIC RETINOPATHY

Diabetic retinopathy (DR) is the leading cause of visual loss in the working ages of the developed world[588] There is growing evidence that the genetic contribution towards DR is significant[589], with suggestions of the heritability of severe retinopathy being between 25-50%.[590]

Prior to the advent of GWAS, genome wide linkage studies highlighted regions on chromosomes 1, 3, 9 and 12. Numerous candidate genes were also investigated (for review see Patel *et al*. [591]). However, the era of GWAS further illuminated our understanding.

The two largest GWAS of DR in Type 1[592] and Type 2[593] diabetes mellitus (DM) investigated 973 and 749 cases respectively. Grassi and colleagues performed GWAS on 2 different platforms on 2 separate cohorts with proliferative diabetic retinopathy (PDR) and macular oedema, imputing results to combine the data. They found a significant SNP between two genes (*AKT3* and *ZNF238*) on chromosome 1. The former of these is known to be activated by insulin-like growth factor and platelet-derived growth factor – both of which are activated in PDR[594]. They also analysed 281 patients with DR without nephropathy, and demonstrated association with an intergenic SNP on chromosome 6. Furthermore, they also investigated SNPs tagging Copy Number Variants (CNV); and showed an association with CNVR6685.1 on chromosome 16. A number of genes involved in transcriptional regulation (*CCDC101*), post-translational protein modification (*SULT1A1* & *SULT1A2*) and apoptosis (*NUPR1*) are in within or in linkage disequilibrium to this region. However, this same group were unable to later replicate these findings in another cohort[595].

Huang and colleagues [593] published in the same year on a cohort of 749 Taiwanese patients with type 2 diabetes with proliferative and non-proliferative retinopathy. They demonstrated regions of interest on chromosomes 1, 5, 10, and 13, mapping to 4 known genes. 2 of these genes (*ARHGAP22* and *PLXDC2*) are involved in endothelial cell angiogenesis. They also confirmed the results of a previous genome wide linkage study associating 1q32 with DR[596], re-iterating the importance of this region. It is particularly interesting that neither GWAS investigating the retinopathy in type 1 and 2 DM found overlapping regions.

Publications of GWAS into diabetic retinopathy are novel, and more will be on the horizon. They are undoubtedly providing insights into the genetic architecture of these conditions, and separating them from the genetics of diabetes. It is worth noting, that the cohorts in both GWAS had had diabetes for significantly longer than controls. It would be prudent to control for this in future studies to ensure findings are related to DR, and not age of onset of disease.

4.1.9. GENOME WIDE ASSOCIATION STUDIES IN OPHTHALMIC QUANTITATIVE TRAITS

Quantitative traits refer to continuous phenotype data (e.g. blood pressure, blood glucose, height). When investigating complex diseases, there are many factors which may have influential roles (e.g. total cholesterol, total low density lipoproteins, total triglycerides and the risk of cardiovascular disease). One way of further understanding the complexities of these conditions, is to study these quantitative risk traits (sometimes termed “endophenotypes”).

4.1.9.1. REFRACTIVE ERROR

Much of the current information on human myopia molecular genetics can be drawn from familial studies of high myopia. To date there are at least 16 loci listed on the OMIM database (http:// www.ncbi.nlm.nih.gov/omim) (MYP2–MYP17) for non-syndromic high myopia, common myopia or ocular refraction that are distributed among 13 chromosomes. At least seven loci for refractive phenotypes (MYP1, MYP3, MYP6, MYP11, MYP12, MYP14 and MYP17) have been successfully replicated in independent linkage datasets and identified as being associated with myopia.

Most of the biological information derived from these studies has implicated connective tissue growth and extra cellular matrix reorganization in the pathogenesis of myopia. This group includes genes that encode matrix metalloproteinases (*MMP1*, *MMP2*, *MMP3*, and *MMP9*), growth factors and growth factor receptors (*HGF*,*TGFB1*, *TGFB2*, and *MET*), collagens (*COL1A1*and *COL2A1*), and proteoglycans (*LUM*). (see Wojciechowski R[597] for summary)

GWAS and linkage disequilibrium mapping have for the first time implicated mitochondrial and apoptotic pathways in the pathogenesis of myopia[598]. Andrew *et al*. demonstrated an association of refractive error with *MFN1, PSARL* and *SOX2OT*, while Nakashiki et al. identified a polymorphism (rs577948) at 11q24.1(near BLID) that was associated with an elevated risk of pathological myopia (OR = 1.37). *MFN1*, *PSARL* and *BLID* are expressed in mitochondria and are involved in mitochondrial-led cellular apoptosis[598]. In addition, a further GWAS identified a polymorphism (rs9318086) at 13q12.12 significantly associated with an increased risk of high myopia in a Han Chinese population (OR=1.64)[599]. This region contains the genes *MIPEP* and *C1QTNF9B-AS1*. The former is expressed in the retina and is involved in oxidative phosphorylation and processing in the inner mitochondrial matrix. Given that the retina is the most energy consuming tissue in the eye, these discoveries have led to increasing interest in role of the mitochondrial pathway in refractive error [599].

In a large twin based GWAS of refractive error in a European population, several polymorphisms at 15q25 near the *RASGRF1* gene were found to be associated with ocular refraction[130]. *RASGRF1* was shown to be highly expressed in human retina and its expression is regulated by muscarinic receptors[600]. This provides another intriguing biological mechanism as anti-muscarinic agents can prevent ocular elongation in animal myopia models[601] and have been employed to reduce myopia progression in human trials [602]. In a companion paper, Solouki et al reported another European GWAS with a polymorphism (rs634990) at 15q14 significantly associated with refractive error [131]. This polymorphism was found in a putative regulatory region near the genes *GJD2* and *ACTC1*, both of which are expressed in the retina. *GJD2* encodes a neuron-specific protein (connexin36) that is present in photoreceptors, amacrine and bipolar cells, and is thought to play an important role in the transmission process of the retinal circuitry by enabling intercellular transport of small molecules and ions[131]. This novel finding suggests for the first time that modulators of retinal visual

signals may have a role in susceptibility to refractive error. More recent reports have replicated loci at 15q14 that underscore a risk for high myopia, in particular an association with axial length[132] and a further GWAS for high myopia in a French population have refined a risk locus at MYP10 implicating a role for microRNA variation in predisposition to high myopia[133].

There have now been eight GWAS investigating myopia or related endophenotypes. Most recently, two very large GWAS have been published which have greatly furthered our understanding. The largest GWAS of refractive error (n=45,771) was published in early 2013[603]. This group discovered 20 novel loci in a European cohort associated with myopia. These included the strongest association with a SNP in the intron of *LAMA2*. Laminins are structural proteins which are integral to the ECM. They also found an association 17kb upstream from *ANTXR2*; which binds type IV collagen; thus further implicating ECM remodelling. Further pathways highlighted were by association with *RDH5* and *KCNQ5*. Both play a significant role in the visual cycle. They also implicated genes involved in eye growth (*PRSS56*, *BMP4*, *BMP3, ZBTB38*, and *DLX1*). Associations with *ZIC2* and *ZMAT4* suggested a role retinal ganglion outgrowth in development. Finally, the authors suggested a role of genes involved in neuronal development, which were not involved in the vision cycle (*KCNMA1*, *RBFOX1*, *LRRC4C*, *DLG2*, *TfP2*). Of further interest in this study was the method of recruitment. All of the cohort were paid members of 23andMe Inc, and self-reported their myopia. This may have resulted in misclassification. However, many of their findings were confirmed by the Consortium for Refractive Error and Myopia (CREAM) who conducted a meta-analysis on well-defined and phenotyped cohort. They co-discovered[604] 16 of the 20 novel findings from Kiefer and 23andI cohort. Of the 22 novel loci discovered by CREAM, 14 were replicated by Kiefer. CREAM not only confirmed previous locus [605], but also confirmed roles in ECM remodelling, ion channel transportation and eye development[604]. Both these studies illustrate the importance in very large sample size in successful GWAS; and Kiefer and colleagues even demonstrate the possible dismissal of expensive phenotyping in conditions with early onset; such as myopia. It is likely that a combination of both will be required to demonstrate further success. Finally, further studies are likely to require incorporating measures of environmental exposure into the statistical analysis of GWAS.

4.1.9.2. OPTIC DISC PARAMETERS

Optic disc area and vertical cup: disc (VCDR) are important parameters in the development of numerous ophthalmic conditions, including anterior ischaemic optic neuropathy, Leber's hereditary optic neuropathy, and open angle glaucoma. The hereditability of optic disc area and VCDR are estimated as 52-58% and 48-80%. However, few studies prior to the advent of GWAS in quantitative traits attempted to analyse optic disc parameters in the normal population.

Ramdas *et al.* [530] investigated 7360 Caucasians (of whom 188 had POAG) from Rotterdam. They found three genetic loci associated with optic disc area, and six associated with VCDR which persisted when the 188 patients with POAG and the 115 with myopia were excluded. Their findings were replicated in 4455 Dutch and British Caucasians. Three SNPs within one locus (10q21.3-q22.1) were found to be significant in both traits, accounting for 2.7% of the variation within optic disc area and 2.2% of the VCDR variation. The most significant common related gene to these loci was atonal homolog 7 (*ATOH7*), more so in VCDR. Several genes were found to be associated with VCDR and included: *CDKN2B* (chromosome 9p21); which encodes a cyclin dependant kinase, thought to play a role in cell growth regulation [606], *SIX1* (chromosome 14q22-23); which is involved in eye development and linked to anophthalmia[607], *SCYL1* (chromosome 11q13); which is associated with optic atrophy in mice [608], *CHEK2* (chromosome 22q12.1); which has no previous association with ocular conditions, *DCLK1* (chromosome 13q13) and *BCAS3* (chromosome 17q23). Additionally, for optic disc area *TGFBR3* on chromosome 1p22 was shown to interact with *ATOH7* influencing VCDR parameters.

Macgregor and colleagues subsequently performed a GWAS on two Australian twin cohorts [609] and confirmed the association with *ATOH7*. This was further replicated in a UK cohort [609].

Optic disc parameters are known to vary between races [610]. Khor [611] however confirmed the association of *ATOH7* and *TGFBR3* through a further GWAS on 2132 Indians and 2313 Malays in Singapore. Additionally, they found most significance associated with a novel gene *CARD10*, on Chromosome 22q13.1, which encodes Caspase recruitment domain containing protein 10. This protein plays a role in

apoptosis via a transcription factor called NfkappaB [612]. This pathway has been implicated in other neurodegenerative disorders, such a Alzheimer's disease [613].

The most common condition related to optic disc parameters is of course glaucoma. Ramdas[614] performed a meta-analysis, investigating SNPs found to be related to optic disc parameters in populations of POAG upon whom GWAS have been completed. Of particular interest, they confirmed 3 loci associated with optic disc parameters also having an association with POAG. These included *ATOH7*.

Burdon and colleagues [528] discovered an association between *CDKN2B-AS1* gene and primary open angle glaucoma providing further evidence to the role of this locus 9p21 in OAG and optic disc morphology.

4.1.9.3. CENTRAL CORNEAL THICKNESS

Central corneal thickness (CCT) is a normally distributed quantitative trait known to be associated with ocular hypertension and primary open angle glaucoma [615]. Family and twin studies have suggested the hereditability of CCT range between 0.6-0.95 [616] however, candidate gene analysis provided limited results. Previous studies have focussed on genetic mutations associated with collagen disorders and complex conditions: *FBN-1* [194], collagen V (Ehlers-Danlos)[617], and *PAX-6* (Aniridia)[618] .

Lu *et al* published a multi-staged GWAS in CCT [619]. They initially performed GWAS on two population groups that individually provided weak associations. Meta-analysis revealed 4 associated SNPs – on chromosomes 16, 13 and 10. They performed replication GWAS on further population cohorts, and two SNPs were most significant. These were closest to the gene *ZNF469* on chromosome 16q24 and *FOXO1* on chromosome 13q14.1.

The authors calculate that *FOXO1* may account for 1.2% of the variability of CCT. The exact role of *FOXO1* is unclear. Within the eye, *FOXC1* is a transcription factor involved in the development of the anterior segment and involved in anterior segment dysgenesis. *FOXC1* seems to regulate the expression of *FOXO1* [620], thus perhaps suggesting a role for the latter in anterior segment formation.

Mutations in *ZNF469* had already been described in a Brittle Cornea Syndrome [621]. However, the mutations in this condition are very rare, compared to the SNPs found in

the GWAS with a minor allele frequency of 0.44. It has been suggested that Linkage Disequilibrium is unlikely between these two variants in this gene. This further suggests that although there may be similarity between the roles of these variants, there may also be significant differences.

A further GWAS on a Scottish and three Croatian populations further confirmed the association of *ZNF469* [622]. Meta-analysis with the previously published GWAS confirmed the association of *FOXC1*. Additionally, three further SNPs reached genome-wide significance. The first was on chromosome 13q12.11 near the transcription factor gene *AVGR8* (Autogenous Vein Graft Remodelling associated protein 8). The next SNP is on chromosome 15q25.3, the linkage block of which extends into the gene *AKAP13*. The encoded protein is thought to link cell surface receptors and transcription factors which may regulate collagen production in the ECM in the gastrointestinal tract via FOXF2 [623]; a similar role may be postulated within the cornea. The third SNP on 9q34.3 is near *COL5A1*. This is of interest particularly, as it initially appeared significant in the first GWAS. Functionally, this is an attractive candidate gene. Not only are collagen V present within the cornea [624, 625], but mouse models have shown that heterozygote *COL5A1* null mouse cornea is 25% thinner with fewer collagen fibrils than wild type mice [626].

More recently, a large GWAS on Caucasians from throughout Europe confirmed the association of *ZNF469* and *COL5A1* [627]. These genes therefore particularly, appear to genuinely play a role in corneal thickness.

4.1.9.4. CORNEAL CURVATURE

Hereditary influence for corneal curvature have been estimated between 60-92%. Previous investigations focussing on candidate genes [628] and monogenic disorders affecting corneal morphology [629]provided limited insight into the complex trait.

Han and colleagues have recently published the first GWAS into this trait[630]. They found significant loci associated with FK506 binding protein rapamycin complex-associated protein 1 (*FRAP1*) gene and platelet-derived growth factor receptoralpha (*PDGFRA*) gene. These associations were corroborated in a cohort of Indian adults and Chinese children. Both these genes encode enzymes with kinase properties. The former has effects on cell growth and proliferation [631], whilst the latter induces intracellular

kinase activity via enzymes such as MAP kinase, which are known to influence collagen fibres [631]. Indeed the role of *PDGFRA* in cell growth [632] has implicated it in fibrotic diseases of the eye such as proliferative vitreoretinopathy [633]. The replication of the data within a young population reassures of the role these genes may have in corneal development. The ethnic variety within this cohort suggests that the role of these genes may be conserved throughout these populations.

Mishra *et al* [525]performed meta-analysis on two GWAS Caucasian cohorts, and suggest a further gene, *TRIM29*. This is shown to be expressed in patients with keratoconus[634] and to be associated with CC variation. More relevantly, they confirmed the association of *PDGFRA* in corneal curvature variation[525]. This gene has also been demonstrated to be significantly associated with corneal astigmatism in a GWAS of over 8000 Asian individuals[635]. This gene in particular has become a very likely candidate for the heritability of corneal curvature.

4.1.9.5. INTRAOCULAR PRESSURE

The greatest controllable determinant towards the aetiology of glaucoma (IOP) is thought to have a hereditability of up to 0.62[636]. Van Koolwijk and colleagues[637] performed a GWAS, including 11972 affected Caucasians from 4 cohorts, replicated in 7482 further patients. They found significant association with *GAS7* and *TMCO1*. The former of these is thought to play a role in the outflow of the trabecular meshwork and has previously been shown through linkage studies to be associated with POAG[638]. *TMCO1,* as mentioned previously, has been suggested to be associated with POAG[528]. Van Koolwijk and colleagues also investigated the effect of the minor alleles of these genes on POAG. The minor allele of *GAS7*, which decreased IOP by 0.19mmHg, reduced the glaucoma risk (OR = 0.88, 95%CI = 0.78–0.98). That of *TMCO1*, which increased IOP by 0.28mmHg, increased the risk of POAG (OR= 1.31 (95%CI = 1.12–1.53). The evidence of the importance of these genes in the aetiology of IOP and POAG is therefore growing. The major success of GWAS in all disease and traits is demonstrated in Figure 4.2.

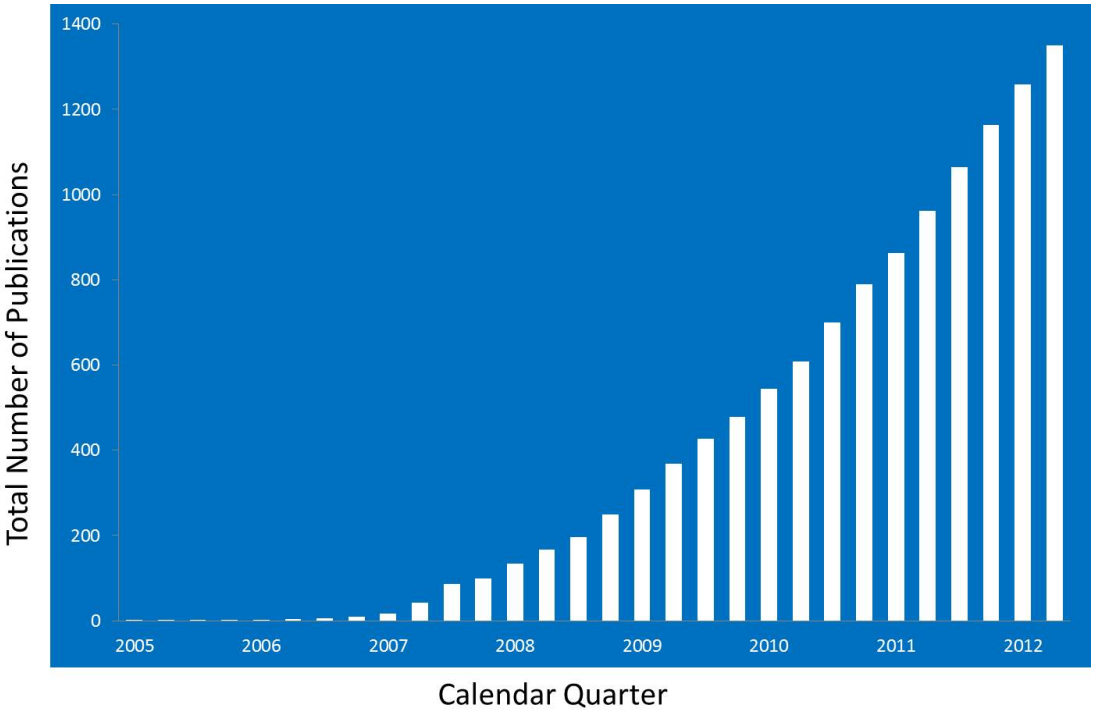

Figure 4.2: Published GWAS Reports (2005 – 6/2012)
Adapted from http://www.genome.gov/gwastudies/

4.1.10. MISSING HERITABILITY

In spite of the over 12000 loci for over 160 complex disorders and traits being discovered, it is estimated that the proportion of the heritability of these is minimal; as low as 1.5% in fasting glucose[639], to as high as at least 50% in AMD. Therefore the term "missing heritability" has been used for this large majority of the genetic architecture which is not understood for many complex diseases. The theories behind this are varied. Firstly, this may be secondarily to a simply inflated estimate of heritability[640]. Further considerations are to the fact that most GWAS to date have been performed on European Caucasian populations[641]. There is ample evidence that allele frequencies [642] and LD patterns[643] differ between different populations. With greater genetic variation in those of African descent[478], it is perhaps unsurprising that a large proportion is unknown. With a growing number of GWAS being undertaken in different populations, this may be addressed in time.

Secondly, there is growing consensus that structural variants play a role in the genetic aetiology of complex conditions. The role that copy number variants, copy number polymorphisms, insertions, deletions, and complex rearrangements have in Mendelian inheritance has been studied at length; however this remains largely unknown for complex conditions[644], though in recent years is growing in prominence[645], including eye disease[646].

There has also been debate as to whether our understanding of LD is complete[647]. Furthermore, incomplete tagging by current genotyping SNPs may result in missing causal variants[459].

4.1.10.1. RARE VARIANT

The largest proportion of the missing heritability is thought to lie in an alternative concept to the CD-CV theory. The "rare variant" theory suggests that complex diseases are the result of a summation of high penetrance, low frequency variants[648]. Low frequency alleles are defined as having a minor allele frequency (MAF) between 0.5%-5%, whilst rare are sometimes classified as <0.5% [459]. The recent exponential human population growth, particularly over the last 400 generations, has distorted the principle of population genetics, resulting in an abundance of these rare alleles[649]. These variants may have significant effect sizes (even three fold increases) without conferring

a Mendelian segregation[475]. It is thought that rare variants may well be the missing link, and may contribute greater to the inheritance of multifactorial conditions than common variants[648]. They are more likely to be directly affecting amino acids. It is suggested that they may act in a mildly dominant or dominant-negative affect[648].

This concept has been discussed for over a decade, with the role of rare variants in High-density lipoprotein (HDL) phenotype being one of the earliest discussions on this topic[650]. The most telling examples of these rare variants having a significant role came from the findings of rare missense variants in the *APC* gene contributing significantly to the aetiology of non-familial colorectal cancer[651], which accounts for 30-40% of this condition.

There are numerous other arguments supporting the role of multiple rare variants. It is thought that the relatively recent expansion in population may result in numerous functionally important rare variants which may influence phenotype[652]. Secondly, the role of numerous rare variants to monogenic diseases[653], suggests that such a process is possible for complex diseases. Thirdly, the identity of multiple functional variants associated with quantitative phenotypes[654], suggests that this may well be relevant for other clinical phenotypes.

The effect of and search for rare and common variants in complex diseases is illustrated in Figure 4.3.

The exact role that rare variants have may be acting synergistically with common variants to influence a phenotype. Alternatively, they may be acting independently or as a subset of rare variants in certain locations influencing the phenotype together. A very compelling argument is that a given susceptibility gene may contain numerous individual rare variants which have differing effect sizes. These may combine and in aggregate contribute a significant population attributable risk[655].

Rare variants are likely to be “younger” (perhaps 10-20 generations old), more population specific and may have higher greater effect sizes than common variants[648].

A major challenge is where and how to search for these rare variants. An obvious start is, as with the HDL and colorectal cancer examples above, to sequence candidate genes. This harks back to the days before association studies, which had yielded limited

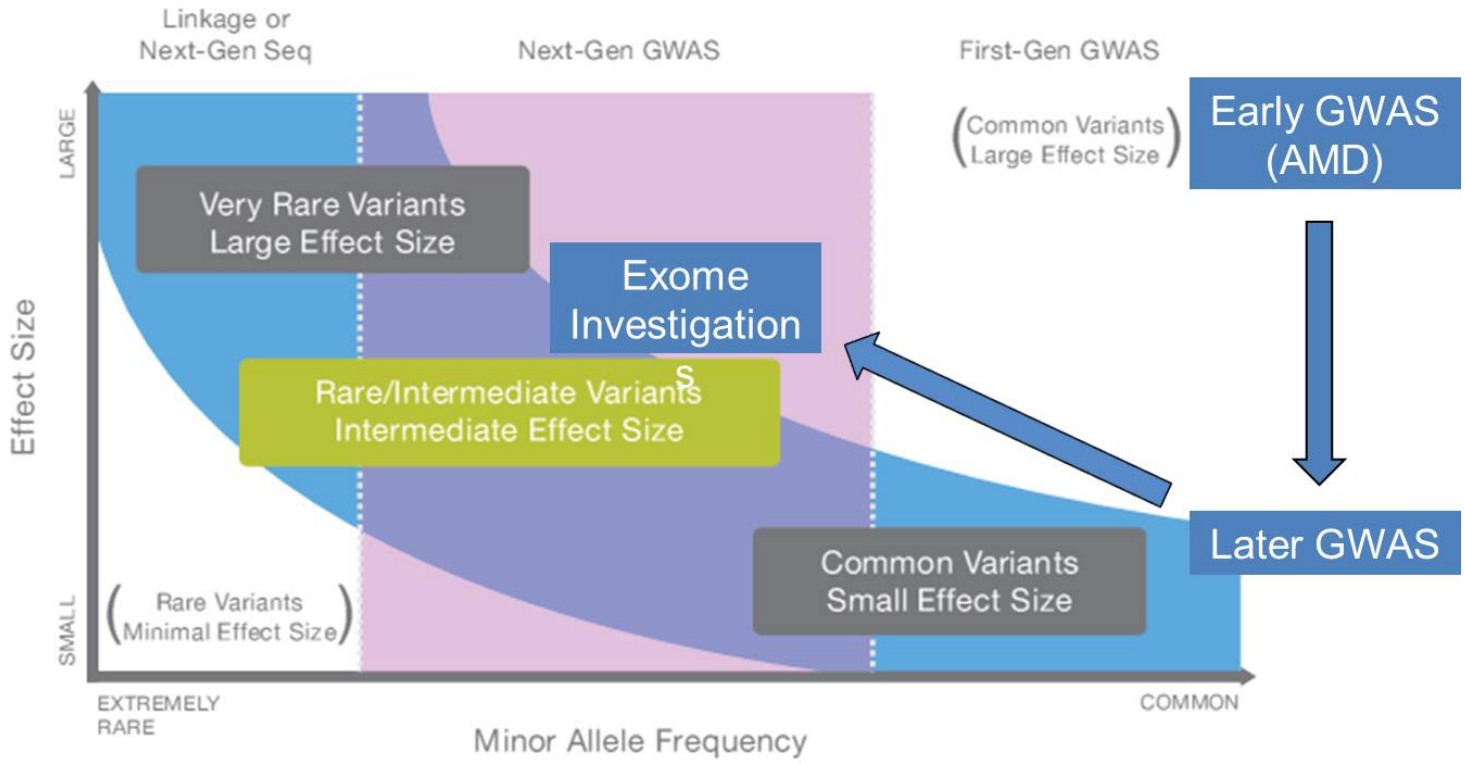

Figure 4.3: The move in search for variants in GWAS. From early GWAS (e.g. AMD) search for relatively high impact variants to the findings of subsequent GWAS and now towards the hunt for rare variants; particularly in the Exome

results. The major advantage of having a hypothesis free approach is the novel inroads made with such approaches. Nevertheless, genotyping chips have been designed to search for variants based in genes which are thought to play an important role in specific conditions with some success[656, 657].

The logical target therefore for a hypothesis free approach would be to investigate the exome. It is estimated that there are 180,000 exons in the human genome, encompassing 23000 genes; approximately 1% of the human genome[658]. It is suggested that 85% of mutations with an effect on human disease are in the exome[659]. Taking this further to complex conditions specifically, Lehne and colleagues found a significant concentration of association signals in exons and genes for diseases genotyped as part of the Wellcome Trust Case Control Consortium[660]. This was analysing data of common genome wide SNPs, and one might therefore envisage this association may be greater if the variants were specifically targeted at exonic variants.

Investigating for rare exome variants has over the last 3 years undergone an exponential growth, with the combination of exome capture and NGS. For Mendelian traits and conditions, as mentioned in chapter 3, it has proven very successful[18], including in ophthalmic traits[661]. It is undoubtedly true that this method has unrivalled power to discover rare exome variants. However, the power gains may be small compared to genotyping arrays[662], and the cost are still prohibitive for large scale analysis. Although there is much debate as to the utilisation of NGS in complex conditions, and probably the future of association studies[663], the design and analysis are challenging[664]. A summary is presented in table 17.

Microarray genotyping may be utilised as an alternative to exome capture NGS. By selecting variants from the large scale whole genome and whole exome (such as [246, 248]) studies, and focussing on those which are predicted to affect protein structure, it is possible to select a significant proportion to be included on a genotyping array, which are most likely to have a functional effect on almost every gene in the genome.

Towards investigating the exome on a large scale, in 2011, the two genotyping companies released genotyping arrays specifically towards this. These include the Illumina HumanExome BeadChip and the Affymetrix Axiom ® Exome genotyping array.

Rare variant genotyping	**Exome Sequencing**	**Array**
Coverage of exomic variants	+++	+
Throughput	+	+++
Cost per sample	+++	++
Ease of analysis	+	+++
Scalability to large studies	+	+++

Table 17: Exome sequencing and array based analysis.

4.2. AIMS

The aims of this chapter are three fold. Firstly, it describes and discusses the ocular phenotype of 1302 consecutively collected unrelated patients with non-Mendelian RD presenting to Moorfields Eye Hospital. Secondly, the cases collected contributed towards the first GWAS into RD. This work was based at the MRC Human Genetics Unit, University of Edinburgh. This GWAS is presented here. Following on from this GWAS, further work is being undertaken to investigate the role of rare exome variants in non-Mendelian RD. This chapter describes the initial quality control of data of genotyping 2000 samples on the Illumina HumanExome BeadChip.

4.3. METHODS

Consecutive patients presenting with a primary RD to the vitreoretinal department at Moorfields Eye Hospital were phenotyped and had blood extraction. For the analysis, two racial groups were focussed on; White Caucasians (defined as persons whose both parents were are of European descent) and patients who were South Asian (defined as persons whose parents were ethnically from India, Pakistan, Bangladesh or Sri Lanka). These races were chosen as it is believed that the numbers of patients from these racial groups represent the greatest number of RD cases presenting to Moorfields Eye Hospital. Other units in the UK have similar experiences[665]. The intention was to provide comparative data, and provide a biobank of DNA for investigations in different racial groups. Patients who have had previous retinal surgery or penetrating injury were excluded, as were patients who had had complicated cataract surgery (associated with vitreous loss) or any cataract surgery within the previous two years. The blood was stored in a freezer in the vitreoretinal emergency (VRE) clinic. When appropriate (approximately every month), the samples were transferred to the UCL Institute of Ophthalmology (IoO) department of Genetics. However, on the 18th February 2011, I was informed that the freezer at the IoO in which 236 samples had been stored had had a power failure, which was not noticed for at least 48 hours. The samples had all defrosted. On this realisation, all the samples were transferred to KBiosciences (now LGC Genomics (Herts, UK)) for permanent storage and DNA extraction. We were fortunate that the 48 hours of defrosting had not adversely affected the DNA concentrations. Samples were subsequently transferred directly from the VRE freezer to LGC Genomics (Herts, UK) for DNA extraction.

4.3.1. DATA COLLECTED

Each patient was examined and phenotyped. Patient demographics were collected.

Demographic data included: age, sex, ethnicity, parental ancestry, Occupation, History of ocular trauma and type of trauma and Family history of eye disease.

4.3.2. PHENOTYPE DATA

Refractive error and axial length (prior to cataract or retinal surgery) was collected. This was achieved (if phakic) by autorefraction (NIDEK) or focimetry through participants' glasses.:

Axial length was assessed using the IOL master (Carl Zeiss Meditex, Jena, Germany), if the fovea was attached) or Bscan. Previous ophthalmic history, including date of any previous ophthalmic surgery or laser treatment.

Family history of RD: A positive family history was regarded as any first or second degree relative affected by RD.

Snellen Chart visual acuity: This was assessed at 6 meters using a standard Snellen chart. Best corrected visual acuity (BCVA) was assessed for individual eyes.

The anterior segment was assessed and pupils were pharmacologically dilated (G. Phenylephrine 2.5% and G. Tropicamide 1%). Fundus examination was performed on both eyes, and indirect ophthalmoscopy with indentation was performed. Detailed retinal phenotype was assessed.

4.3.2.1. OCULAR FEATURES

A myopic refractive error was defined as spherical equivalence (SE) of -1DS or greater, and hypermetropic refractive error as greater than +1DS.

Rhegmatogenous Retinal Detachment was regarded as a full thickness break in the neuroretina accompanied by two disc diameters or greater of sub retinal fluid.

Posterior vitreous detachment (PVD) is regarded as separation of the vitreous from the inner limiting membrane of the retina. Although diagnosis can be challenging, the presence of a Weiss ring is regarded as indicating a complete PVD[666].

Trauma was regarded as direct or indirect trauma to the eye resulting in an ophthalmic review.

Proliferative vitreoretinopathy (PVR): this abnormal scarring of the retina was graded according to the Retina Society Committee[667].

Details collected regarded the phenotype of the RD at presentation: quadrants involved (1-4), macular involvement, PVR presence and grade, type of break (atrophic holes, tractional tears, dialysis, giant tear) – documented by standardised retinal drawing. Characteristics of the vitreous were documented: – attached or detached. If both eyes were affected, this data

was collected from both eyes. If unilateral presentation, phenotype of the vitreous and retina were collected regarding the contralateral eye – documented by retinal drawing.

DNA samples were collected and used as part of two genotyping experiments. The first was part of the "Scottish Retinal Detachment Genome Wide Association Study". Secondly, 1000 samples were used as part of a novel genotyping analysis investigating the Exome; using the Illumina HumanExome BeadChip.

4.3.3. GENOME WIDE ASSOCIATION STUDY ON RHEGMATOGENOUS RETINAL DETACHMENT

Most of this work was undertaken by my colleagues Dr Veronique Vitart and Mirna Kirin, at the MRC Human Genetics unit at the University of Edinburgh. I attended where possible, and undertook some analysis, under supervision. In particular, I undertook association analysis of significant SNPs between the cases recruited from Moorfields Eye Hospital and controls.

The GWAS was designed in 2-stages. Satagopan and Elston[668] demonstrated that this method was a cost effective approach to discovery stage of GWAS. In this method, all markers are genotyped in a subset of cases and controls. The most promising markers are subsequently genotyped in the remaining individuals. They are then analysed in all individuals in stage 2. They illustrate that this method can be very effective compared with one step method; and significantly reduce the costs of genotyping.

The first stage involved genotyping DNA from 912 Scottish RD study which recruited all primary RD cases from the six vitreoretinal surgical centres in Scotland during October 2007- November 2009[669]. These samples were genotyped using the Illumina CNV370v3 Quad genotyping array comparing the genotypic counts with 1,986 ethnicity matched Scottish controls that were previously genotyped using the Illumina Hap 300 and Hap240S in the Scottish Colorectal Cancer Study[670]. This cohort was collected between 1996-2009, as part of the population-based study of colorectal cancer in Scotland. Although there was an age difference between the RD cases and the SOCCS controls (RD mean age(Standard Deviation))=58.9(13.8); SOCCS controls mean age(SD)= 50.16(6.1); $p<0.001$)), and a gender imbalance ((RD(N) cases: Male(513):Female(355) = 1.44:1 and SOCCS cases and controls(N): Male(1,003):Female(965)= 1.04:1 ; $\chi 2$ difference –15.92;$p<0.0001$)), this group was

still deemed a suitable control group; particularly as there was no difference in geographical origin between the two groups. Furthermore, the chip used by the controls (Illumina Hap300 and Hap240S) which together cover 95% of the SNPs on the Illumina CNV370v3, used in the cases.

After quality control, 299737 SNPs were genotyped on 867 cases and 1953 controls. An association analysis was performed on these. The P value was corrected with a Bonferroni correction based on 197628 independent SNPs; being $1.27x10^{-7}$. This was the first discovery stage.

In the second discovery stage, 4347 SNPs were taken forward to be genotyped on 748 cases from the UK (457 of which were recruited at Moorfields Eye Hospital), 252 cases from the Radboud University Nijmegan Medical Centre, Netherlands, and 2912 controls (2592 from the 1958 birth cohort and 320 from the control candidates of a Dutch schizophrenia study). These SNPs consisted of, initially, 4706 SNPs from the first stage which reached a significance of $p<10^{-3}$ and 1275 SNPs tagging ($r^2>0.8$) 18 candidate genes (Table 18). These candidate genes had been chosen as potentially biologically relevant in RD.

Quality control resulted in the 4347 SNPs being analysed. Association testing was done for each cohort separately, and then re-run in a meta-analysis. The p-value was set at the same $1.27x10^{-7}$.

The seven most significant SNPs from this discovery cohort were taken forward for replication. These were genotyped on 846 samples collected from Moorfields Eye Hospital, 2737 controls from the National Blood Service[464], 120 cases collected from the University Clinical Hospital, Zagreb, Croatia and 269 controls which had been collected for a colorectal study based on Croatia. The analysis of the Moorfields Eye Hospital samples in this stage was undertaken by myself directly under supervision by Dr Veronique Vitart and Mirna Kirin in Edinburgh. This was undertaken in PLINK[671] by creating PED and MAP files.

Candidate gene	*Number of selected tagging SNPs per gene (Number successfully tested)*	*Candidate gene*	*Number of selected tagging SNPs per gene (Number successfully tested)*
COL11A1	34 (14)	*LAMA1*	161 (67)
COL18A1	58 (29)	*LAMB1*	54 (24)
COL2A1	54 (21)	*LAMC1*	41 (13)
COL4A4	62 (42)	*OPTC*	33 (7)
COL6A1	39 (16)	*VERSICAN*	116 (42)
COL9A1	89 (45)	*FBN1*	56 (20)
HAS1	95 (50)	*FN1*	46 (12)
KCNJ13	16 (4)	*FZD4*	62 (24)
HAPLN	28 (13)	*COL11A2*	48 (15)

Table 18: Genes believed to be biologically relevant to RD, for which tagging SNPs were chosen to take forward to stage 2 of the discovery stage.

Association was performed, and subsequently, results from both the discovery stages and replication stages were combined in a meta-analysis. For this overall meta-analysis, the p value was set at the conventional[483] $5x10^{-8}$, corrected for the use of two genetic models to $2.5x10^{-8}$. A summary of the methodology is in Figure 4.4

4.3.3.1. PATHWAY ANALYSIS

A challenge upon highlighting important regions (for example haplotype blocks tagged by SNPs) is to identify key genes from within these regions which may be related and thus be involved in common pathways. Beyond LD, there are likely to be other related genes which contribute to the phenotype. The most used method to highlight these has involved using protein function to prioritise genes in regions[672, 673]. Identifying shared function can involve using established molecular networks[673] or starting with sets of genes with known common functions[672]. Alternatively, functions thought to be relevant to the disease or phenotype may be used to identify genes [674]. Raychaudhuri and colleagues devised an approach which relied on two key methods: a novel statistical strategy which assessed the significance of gene relatedness; and a similarity measure based on text in PubMed abstracts to score relatedness of two genes. This system was called "Gene Relationships Among Implicated Loci (GRAIL)[675]. The system has variable statistical thresholds to consider relatedness; with narrow regions having lower thresholds, and large regions higher. In this manner, large regions with many genes are prevented from dominating the analysis. They have demonstrated that their system was able to link genes which had not till then had established common pathways defined, and compared favourably to other established methods. Other groups have since successfully utilised GRAIL[676, 677].

The first six top ranking SNPs displaying the same direction of effect from the meta-analysis (thus with low heterogeneity) were selected to be further analysed using GRAIL.

The genes highlighted through GRAIL were then investigated for pathway analyses using Ingenuity® Systems (www.ingenuity.com). This software uses regularly updated internal databases to identify networks between related genes. These networks are thought to represent important biological functions. The molecules which are entered are then added to molecules from the ingenuity database (with a maximum total of 35 molecules) to create networks.

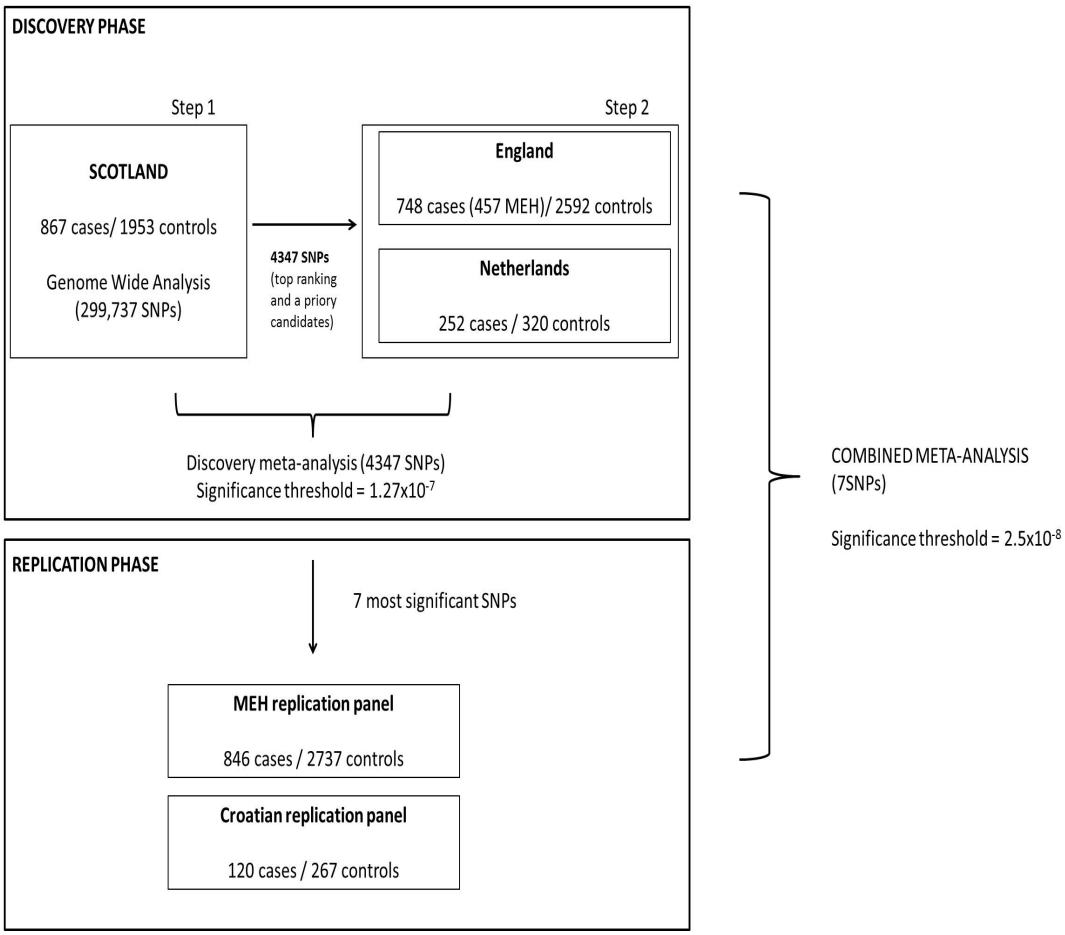

Figure 4.4. Schematic diagram illustrating methodology for GWAS in RD

These are then scored based on the number of molecules in the network and the size of the network. This score is converted into a statistical p-value; which represents the likelihood of the molecules interacting together randomly. This system has been used successfully to uncover pathways from GWAS findings[678, 679] and is comparable to other pathway analytic systems[680].

The parameters used for this analysis were; only direct relationships were used, high confidence reliability (experimentally observed) and pathways involved in all diseases, biofluids and all possible mutations were included.

4.3.4. EXOME WIDE ASSOCIATION STUDY ON RHEGMATOGENOUS RETINAL DETACHMENT

Subsequent to the GWAS performed, it was decided to further investigate for the missing hereditability of RD. As mentioned, it is believed that rare variants may play a significant role in this. Exome rare variants are likely to be particularly significant. Although NGS would undoubtedly offer the deepest coverage to investigate for these, the limitations both financial and bioinformatic are not insignificant. We therefore decided to consider an alternative approach.

As mentioned in the introduction to this chapter, Illumina and Affymetrix in 2011 had released novel genotyping arrays aimed at investigating for variants based within the exome. These seemed the perfect tools to enable our investigations.

4.3.4.1. POWER CALCULATIONS

Power calculations for GWAS are challenging[681]. Furthermore, calculations for rare variants are not well defined. Certain assumptions, upon which most power calculators are based, may not be valid in rare variant analysis. For example if utilising collapsing methods for allele analysis (see Section 4.6.1.2), the correction for multiple testing used in GWAS may be conservative. Nevertheless, no specific calculators are available for Exome Wide Association Studies.

Using the Genetic Power Calculator (http://pngu.mgh.harvard.edu/~purcell/gpc/) we explored the number of cases required to provide 80% power at a genome wide type I error rate of $1x10^{-7}$. Most GWAS have demonstrated a genotypic relative risk (GRR) of 1.1-1.7 [682]. Assuming for GRR of 1.5, in perfect LD with typed marker (r^2=1),

MAF=0.1 (rare), disease prevalence of 0.0001 and a multiplicative inheritance model, we estimated that 1483 cases would be sufficient to provide 80% power for an type I error rate of $1x10^{-7}$ (Table 19).

On this basis we were successfully awarded two grants; The Major Project Grant from the Royal College of Surgeons of Edinburgh (2012); and Research Grant from the Special Trustees of Moorfields Eye Hospital (2012). I then approached various institutions regarding genotyping our cohort of 1996 Caucasians collected from Moorfields Eye Hospital (n=999) and as part of the Scottish Retinal Detachment study (n=997) with RD on one of the above Exome centred arrays. The Institute of Psychiatry at King's College London offered the most cost effective and timely service for genotyping the samples on the Illumina HumanExome BeadChip 12 v1.1. This laboratory was also able to provide PLINK files from 5963 samples collected as part of the British 1958 birth cohort which would be genotyped on the same array. This cohort would be valuable to be used as control data. In addition, our collaborators in Edinburgh are part of the team analysing genotype data of samples from the Biobank Generation Scotland (http://www.generationscotland.org/). This biobank has over 30000 DNA samples to be used as controls in the investigation of complex diseases. Over 10,000 of these samples have been genotyped with the Illumina HumanExome BeadChip. Access to this dataset would prove a further valuable resource for control data, and would be used to match the Scottish cases in the analysis and control for population stratification.

4.3.4.2. ILLUMINA HUMANEXOME BEADCHIP

This array was designed and released in December 2011. It is based on exome and whole genome sequencing of over 12000 individuals, from a wide range of ethnicities (Table 20-21).

This chip is designed to therefore provide a cost effective method of investigating variants which are thought to be functional and which may be causative in complex phenotypes and diseases. Its utility has recently been demonstrated in analysis of the role of rare variants in cardiovascular disease[683] and type 2 diabetes[684].

Alpha	**Power**	**N cases for 80% power**
0.1	1	276
0.05	1	344
0.01	1	497
0.001	0.9999	704
1e-07	0.9694	1483

Table 19: Power calculation for various type 1 errors for GWAS on above parameters: (From http://pngu.mgh.harvard.edu/~purcell/cgi-bin/cc2.html) Highlighted is the power calculation described

.

Contributor	Enrichment	Major Ethnicity	N
NHLBI Exome Sequencing Project (5 tranches)	Cardiovascular Traits, Lung Traits, Obesity	European, African American	4260
Autism (2 tranches)	Autism	European	1778
GO T2D (2 tranches)	Type 2 diabetes	European	1618
1000 Genomes Project (2 tranches)	Random Sample	Diverse	1128
Sweden Schizophrenia Study	Schizophrenia	European	525
SardiNIA	Random Sample	European	508
Sanger / CoLaus	Overweight, Diabetes, Fasting Glucose	European	456
Cancer Genome Atlas	Cancer	European	422
T2D Genes	Type 2 diabetes	Hispanic	362
Cancer Cohort Study	Cancer	Chinese	327
Pfizer – MGH – Broad	Type 2 diabetes extremes of risk	European	182
Lipid Extremes	Lipid Extremes	European	131
Int'l HIV Controllers Study	HIV Controllers	European	121
SAEC DILI (merged w/Autism tranches)	Augmentin DILI	European	117
I2B2 - Major Depression	Major Depression, Major Depressive Disorder	European	50
BMI Extremes	BMI Extremes	European	46

Table 20: Illumina HumanExome BeadChip genetic data source. *Adapted from* http://genome.sph.umich.edu/wiki/Exome_Chip_Design

Illumina Assay Design Summary	
SNP Set	Number of Successful Designs
Coding Content	243,094
GWAS Tag SNPs	5,325
Grid of Common Variants	5,286
Randomly Selected Synonymous SNPs	4,651
AIM - African Ancestry	3,241
AIM - Native American Ancestry	998
HLA Tags	2,459
ESP Requests	843
Fingerprint SNPs	259
MicroRNA Target Sites	270
Mitochondrial Variants	246
Chromosome Y	128
Indels	181

Table 21: Content of Illumina HumanExome BeadChip. *Adapted from* http://genome.sph.umich.edu/wiki/Exome_Chip_Design

4.4. OCULAR PHENOTYPE OF 1309 CONSECUTIVELY RECRUITED PATIENTS

4.4.1. RESULTS

Between April 2010 and August 2010, 457 blood samples from white Caucasian patients who had suffered a RD were sent to Edinburgh to be analysed in the Scottish GWAS into RD.

Between August 2010 and December 2012, 1309 patients with primary RD were collected and phenotyped. It is not possible to accurately assess what proportion of primary RD of those seen at Moorfields Eye Hospital that this represents. It is estimated that the hospital sees 1000 patients a year with the diagnosis of RD. Our total would represent approximately 65.6% of the patients seen with this diagnosis over this period. However, the figure of 1000 per year is only a rough estimate, and does not differentiate between primary or re detachments. This denominator does not take into account the criteria we set for inclusion and exclusion. We therefore reasonably assume that the eligible number of patients over this period was significantly less than can be estimated. Our proportion is therefore likely to be greater than 65%.

These included 136 non Caucasians; of which 96 were regarded as from the Indian Subcontinent (herein termed “South Asians”), and the rest (n=40) were regarded as “Other”. These other races included “Chinese”, “Black”, and “unknown”. For the purpose of analysis, racial differences were analysed between Caucasian and South Asians; as the numbers in other groups were too small and heterogeneous. A summary of the phenotype demographic and phenotype data is in table 22.

4.4.1.1. AGE

The mean age was 57.72 years (SD: 13.26years) (Figure 4.5). Racial differences were seen. The Caucasian population had a mean age of 58.27 years (SD: 13.09). The South Asian population had a mean age of 54.49 (SD: 13.9) and were significantly younger than the Caucasian patients (P=0.006).

		TOTAL	CAUCASIAN	ASIAN	OTHER
Sex	Male	851	756	71	24
	Female	458	417	25	16
Age Groups (Years)	0-9	0	0	0	0
	10-19	4	4	0	0
	20-29	45	33	9	3
	30-39	82	67	7	8
	40-49	186	170	11	5
	50-59	363	318	31	14
	60-69	399	365	31	3
	70-79	156	147	7	2
	80+	50	49	1	0
Affected Eye	Right	617	556	49	12
	Left	620	555	46	19
	Both	14	12	0	2
Lens Status	Phakic	892	814	52	26
	Pseudophakic	310	267	37	6
	Aphakic	7	4	2	1

Table 22: Demographic and lens status of patients recruited for RD Study.

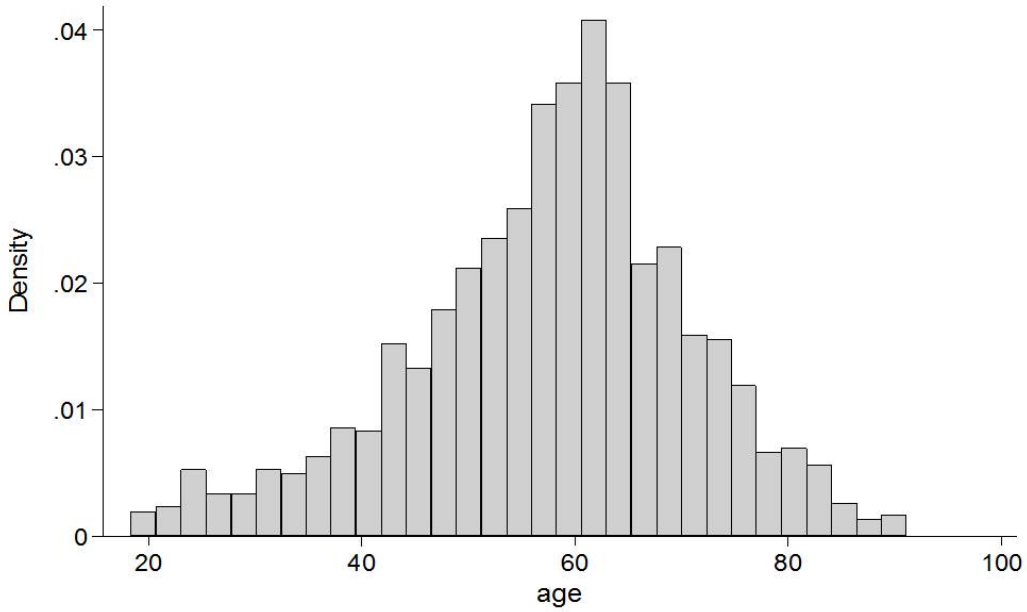

Figure 4.5: Age distribution (years) of patients recruited

4.4.1.2. LATERALITY

There were an equal proportion of left and right eyes affected (621 and 617 respectively). There were 14 (1.1%) of eyes which were affected bilaterally. There was no significant difference regarding this laterality. Neither was there a difference between the races.

4.4.1.3. GENDER

There were 442 females and 827 males (1:2.84) affected in the two main ethnic groups. This suggests prevalence for men to be affected. Additionally, the proportion of men was greater in South Asians (74.0%) than in Caucasians (64.5%) and suggested a significant trend (P=0.06).

4.4.1.4. LENS STATUS

14 aphakic patients were recruited. Their blood was however not forwarded for DNA extraction. 75.3% of Caucasians were phakic, whilst 58.4% of Asians were phakic. This was a statistically significant difference (P<0.001). Asian patients were more likely to be pseudophakic (or aphakic) than Caucasians.

4.4.1.5. BREAK TYPE

The break type was reported in 1247 of affected eyes. The most common type of NSR break was a horseshoe tear, followed by a round hole. Other types of NSR breaks are documented in the table 23. There was no significant difference between these groups.

	Study Eye		
	TOTAL	CAUCASIAN	SOUTH ASIANS
HST	977	868	75
Round	214	182	17
GRT	31	23	2
Dialysis	25	20	0

Table 23: Types of neurosensory retina breaks found in the RD cohort.
HST: Horseshoe Tear. GRT: Giant Retinal Tear

4.4.1.6. FAMILY HISTORY

A positive family history (first or second degree relative) was demonstrated in 171 cases (13.2%). This was reported in 149 (12.8%) Caucasian cases, and 19 (19.4%) South Asians. There was no significant difference in the rate of family history between the ethnic groups.

4.4.1.7. LATTICE DEGENERATION

Lattice degeneration was present in 218 patients. This was present in 149 (12.8%) of the Caucasian patients, and 19 (19.4%) of the South Asian patients.

This difference was significant (P=0.003). South Asian patients with RD were more likely to have lattice degeneration in the affected eye.

4.4.1.8. REFRACTIVE ERROR & AXIAL LENGTH

The mean spherical equivalence for phakic affected right eyes was -4.48DS (SD 4.07). The mean axial length in this eye was 25.08mm (SD 1.9).

The mean spherical equivalence for phakic affected left eye was -4.18DS (SD 3.92). The mean axial length in this eye was 25.07 (SD 1.78). There were no significant differences with between the eyes.

Comparisons between races, revealed that South Asians were significantly more myopic (mean -6.1DS) compared to Caucasians (-4.2DS) (P=0.032). Mean axial lengths was 25.06mm (SD 1.82) in Caucasians and 25.65mm (SD 2.30) in Asians (P=0.014). This significance was maintained in phakics (25.03mm (SD 1.80) in Caucasians, 25.85mm (SD 2.47) in South Asians: P=0.01)).

Correlating axial length with spherical equivalence revealed a good correlation; increasing axial length being associated with decreasing spherical equivalence (Figure 4.6).

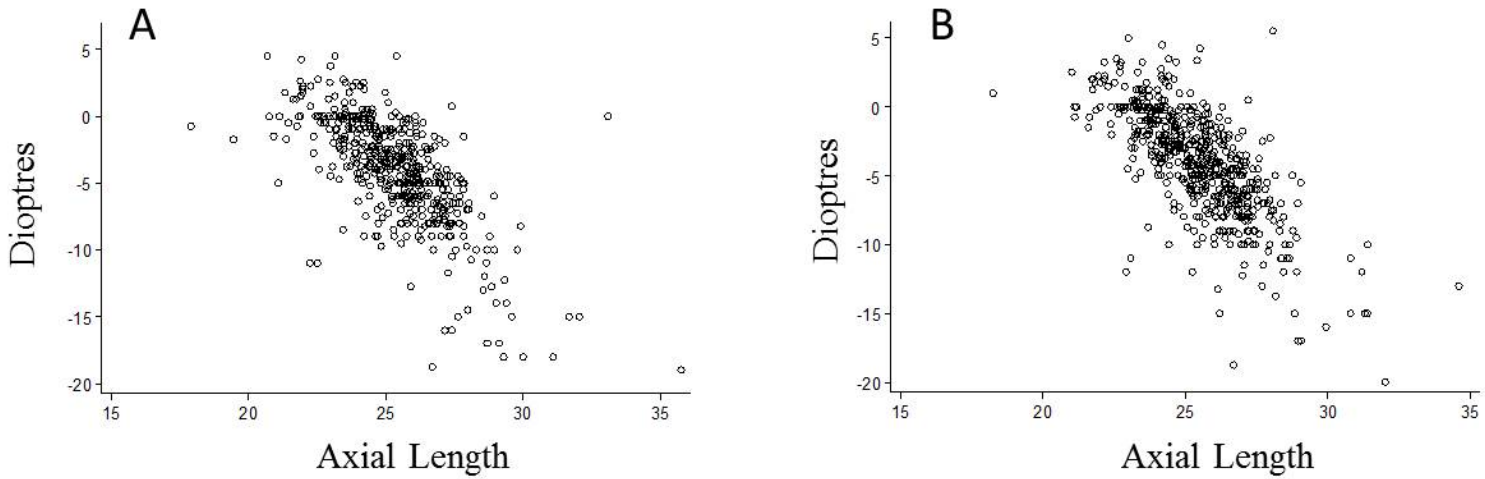

Figure 4.6: Correlation between axial length and spherical equivalence (DS)
A: Right eyes. B: Left eyes

4.4.1.9. MACULA STATUS

Macular status was recorded for 1016 (86.4%) of Caucasians and 91 (92.9%) of Asians. The proportion of patients with macula on or bisecting was 50.51% (Caucasians) and 44.9% (South Asians). This was not significant.

4.4.1.10. LOGISTIC REGERESSION

A logistic regression model was performed to analyse the predictors which would determine the different types of NSR breaks.

For the purpose of these analyses, age was determined as a continuous variable, per year. Sex was comparing males vs. females. Axial length was analysed as a continuous variable, per mm. Ethnicity was analysed for Caucasians compared to South Asians.

The interpretation for these is that age is the strongest determinant for the type of break seen. Younger patients are more likely to experience a round hole, whilst older patients a HST. Furthermore, it appears that ethnicity was also important in the development of a HST; with Asians more likely to suffer a HST RD.

The relationship between race and age is further demonstrated in Figure 4.7. It suggests a steeper relationship with age and risk of developing a HST RD for Asians.

Round Holes:

Round Holes:	Odds ratio	Stand Error	P Value	95% CI
Age	0.93	0.008	<0.0001	0.92 - 0.95
Gender	1.33	0.28	0.18	0.88-2.02
Axial length	1.01	0.055	0.84	0.91- 1.12
Family History	0.85	0.25	0.59	0.48-1.51
Ethnicity	0.75	0.29	0.46	0.35- 1.61

Horseshoe tear:

HST	Odds ratio	Stand Error	P Value	95% CI
Age	1.06	0.007	<0.0001	1.04- 1.07
Gender	0.88	0.16	0.45	0.62-1.24
Axial length	1.04	0.049	0.37	0.95- 1.14
Family History	1.13	0.28	0.61	0.70-1.83
Ethnicity	2.14	0.77	0.035	1.05-4.34

Table 24: Results of logistic regression model using different types of NSR breaks as outcome. Highlighted are the statistically significant variables.

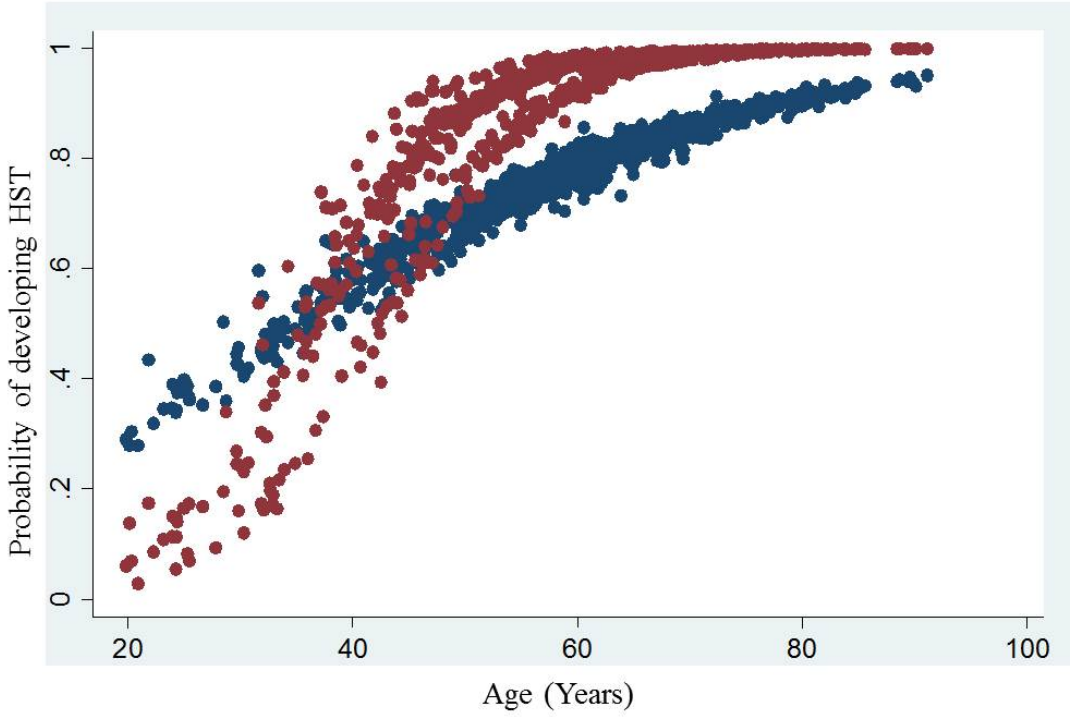

Figure 4.7: Relationship between race, age and development of a horseshoe tear RD

- Asians
- Caucasian

4.4.2. DISCUSSIONS

The ocular phenotype of 1309 consecutive patients with primary RD was acquired over 28 months from the vitreoretinal department of Moorfields Eye Hospital. The majority of the patients were Caucasian (89.6%), with 7.3% being Asian and 3.05% being other.

Differences in phenotype were analysed between the two largest racial groups in this cohort; Caucasians and those ethnically South Asian.

4.4.2.1. AGE

The peak age for RD is between 60-69[96, 685-687]. The incidence in this age bracket has been reported as high as 70 per 100,000 in one 20 year epidemiological study[688]. Our data agrees with this (Table 22), across both racial groups. This peak age bracket has not been explained adequately. Although the rate of PVD (the invariable pre-cursor for most horseshoe tear (HST) RD) is known to increase with age[689] it has been suggested to be present in 11% of 60-69 year old, and 46% of 80-89 year old[690]. One could infer from this that the incidence of RD should continue to increase. Furthermore, the pathological event of RD is likely to occur more frequently in an "incomplete PVD"[81]. In a prospective study using modern imaging techniques to diagnose incomplete PVD, Shao and colleagues[691] suggest that the prevalence of an incomplete PVD is higher in younger age Chinese; with a minimal prevalence occurring between 75-80 years. The reason why the peak age for RD is between 60-69 years is therefore uncertain. This may suggest that PVD occurring in younger patients (60-69 years) may present with an abnormal PVD more frequently than those at a later age. Alternatively, there may be simply other health factors influencing the number of more elderly patients presenting with RD. Indeed, the life expectancy in England in 2010 was 78.2 years for men and 82.3 years for women[692]. This may influence the rate.

It has been suggested that there is a bimodal incidence pattern; with a smaller peak between 20-29[105, 685, 693, 694]. However, the largest UK epidemiological study into this condition did not replicate such a bimodal distribution[687]. Our age spread was in keeping with this latter epidemiological study. This suggests that the main determinant of RD is likely to be vitreous liquefaction, which increases with age.

The racial differences in age are novel. This data suggests that South Asians patients with RD were younger than Caucasians, particularly in the development of HST.

Rosman and colleagues[695] analysed 916 RD cases in Singapore over a 4 year period. The mean age for RD (for three Racial groups in the study; Chinese, Malay and Indian) was 46.1 years; and this group were the first to postulate that RD may occur at a younger age in Asians (their terminology included the three races in their study). 68.1% of the 22 Indians in their cohort were aged under 60 years old.

Few other robust studies have documented a racial difference in RD. Mowatt and colleagues[665] investigated the rate in the Midlands in the UK. They demonstrated that Indians had a rate of 2-4.6 per 100,000, whilst the incidence in Caucasians ranged from 6.3-13.0 per 100,000 in two different towns eight miles apart. The age differences in between Indians, Caucasians and Black patients were not described in this study. Wong and colleagues[105]also describe a lower incidence amongst Indians (3.9 per 100,000) compared with Chinese (11.6 per 100,000). A small study from India described the mean age of those with unilateral RD as 38.8 years[696]. No explanation has been given to the differences between races.

4.4.2.2. GENDER

There were a higher number of men affected by RD (1.85:1). This trend was more marked in South Asians (2.84:1) compared to Caucasians (1.81:1), which although did not reach statistical significance (P=0.06), does suggest a trend. The reason behind men being more prone to RD has often been suggested as trauma[90]. However our cohort did not include traumatic RD. The difference is maintained, when excluding for trauma[686, 687, 694]. It is possible that the higher rate of myopia seen in men, or the earlier extension of the vitreous base seen in men[77, 101] may be significant contributing factors. These differences may be more pronounced in Asians.

4.4.2.3. LENS STATUS

25.80% of the cohort was pseudophakic. This is in agreement with the largest UK epidemiological study; which demonstrated a rate of 21.6%[687]. Other large cohorts suggest this rate to range between 10-30%[693, 697]. The rates have decreased since the advent of extracapsular and phacoemulsification cataract surgery. There are however reports that the proportion of pseudophakia is increasing, in line with the increase in cataract extraction over the last two decades[698, 699].

It has been suggested that phenomenon may be secondary to higher rates of PVD and vitreous collapse after uncomplicated cataract extraction[82, 700]. What is particularly interesting is the higher rate of pseudophakia in Asians (P<0.001) which has not been previously demonstrated. It is suggested that the age of onset of cataract is younger in British Asians compared to Caucasians[701], thus the rate of cataract surgery may be greater. However, as a proportion; lens extraction is a more important feature in Asians than Caucasians. This may be due to vitreous differences in Asians; making this group more susceptible to changes after cataract surgery. This would need further investigation to offer any further speculation.

4.4.2.4. LATTICE DEGENERATION

Lattice degeneration was present in 16.7% of the cases. This is lower than previous historic reports[69]. However, European reports range from 7%- 29%[108, 702]. The largest UK study suggested lattice degeneration to be present in 18.7%[97]. Our data is therefore consistent with this range.

The statistically significantly increased rate seen in South Asian patients poses interesting results. Rosman *et al.*[695] suggest that lattice was present in 31.8% of Indians with RD (a small cohort of 22 patients). This higher prevalence of lattice degeneration may explain the younger age of Asians with RD. It is likely that this data has confirmed the suggestion that lattice degeneration is more common in patients with RD from this racial group.

4.4.2.5. REFRACTIVE ERROR AND AXIAL LENGTH

The myopic error found in phakic patients was not markedly different to previous reports[97]. This may be secondary to the urbanised catchment area of Moorfields Eye Hospital; urbanisation has been shown to be associated with higher rates of myopia[703]. Moreover, it is of interest that Asians appeared to be more myopic than Caucasians. Rosman and colleagues[695] did not provide mean refractive error for their cohort, but 7 out of 22 (31.8%) were reported as having myopia > -5DS.

The correlation between axial length and refractive error agrees with epidemiological studies investigating this in a similar population[704].

Certain features of the cohort did not demonstrate significant differences between the two racial groups.

4.4.2.6. LATERALITY

It has been suggested that RD occurs more frequently in right eyes [108, 687, 688]. The current data did not confirm this, and was consistent between two races.

4.4.2.7. BREAK TYPE

The most common type of break was a HST; which is in keeping with previous studies[687]. This is due to the combination of traction on the retina; at the tip of the horseshoe, increasing the likelihood of liquefied vitreous tracking underneath[34]. The only determinants in the logistic regression models were age; round holes appearing in younger patients and HST in older. This relationship is well established.

4.4.2.8. MACULA STATUS

The proportion of patients presenting with a macula involving RD was similar to UK epidemiological studies[97]; suggesting a good access to health care for these patients.

4.4.2.9. FAMILY HISTORY

The proportion of patients who admitted a first or second degree relative with RD is greater than previous reports, which report rates between 1% - 8.2%[96, 97, 170]. This may reflect population differences between the various studies. Alternatively, the direct questioning in this dataset may have revealed a true higher rate. There was no difference between the races; and is consistent with other complex inherited ocular conditions.

In summary, much of the data from this cohort agrees with findings from large epidemiological studies. Furthermore, differences in the phenotype of the two main ethnicities investigated here is novel. It appears that patients from the Indian subcontinent, although are suggested to suffer from RD at a lower rate to Caucasians, seem to have more severe phenotype if affected. This includes having more severe myopia if phakic, greater axial lengths, a greater proportion of lattice degeneration and have a younger age of onset for disease.

4.5. GENOME WIDE ASSOCIATION STUDY ON RHEGMATOGENOUS RETINAL DETACHMENT

4.5.1. RESULTS

In total after quality control measures, the case-control analysis included 299,869 SNP in 870 cases of RD and 1,968 controls. Case control analysis was performed by the group based in Edinburgh using both PLINK and the GENABEL software in R. After logistic regression analysis, with the stringent significance rates applied, one SNP reached genome wide significance ($1.88x10^{-9}$); rs10510663 on 3p22.3 (Figure 4.8). This SNP was not significantly associated in the second discovery stage in either the Moorfields Eye Hospital (p=0.86) or Dutch (p=0.24) samples. After meta-analysis the top ranked SNPs and their genes are in table 25.

This highest ranked SNP was rs12960119, located on 18q11.2 in an intron of *SS18*. The direction of effect was consistent across the three populations. This was true for most SNPs with $p<10^{-4}$.

Using GRAIL for the six most significant SNPs with the same direction of effect revealed gene relatedness shown in table 26.

4.5.1.1. INGENUITY NETWORK ANALYSIS

When analysed using IPA (www.ingenuity.com) revealed on highly significant ($p=10^{-62}$) network (Figure 4.9). This network showed enrichment for molecules involved in DNA replication and cell death. The most significant systems involved were the development of the haematological system.

4.5.1.2. REPLICATION PHASE

The six most significant SNPs and one further with low heterogeneity across studies were taken forward for replication. These SNPs are listed in table 26. These were typed in 846 samples from our cohort at Moorfields Eye Hospital, and 120 cases from Croatia. This was done by myself in conjunction with colleagues in Edinburgh.

This is undertaken using PLINK[671]. PED and MAP files were created. Subsequently, SNPs of interest were extracted from control database acquired from the 1958 birth cohort (provided as BED and BIM files).

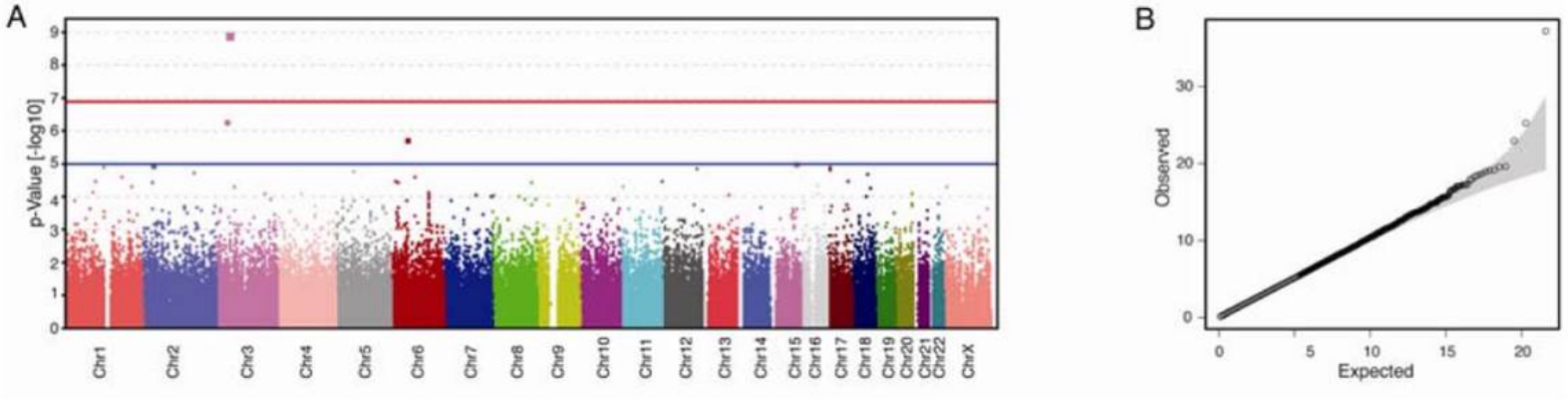

Figure 4.8: Manhattan plot (A) and Quantile-quantile (B) plot for the discovery stage1 genome wide scan results. Statistics from a logistic regression adjusting for age sex and co-ancestry, performed on 867 Scottish RD cases and 1953controls (SOCCS participants) using 299,737 genotyped SNPs which passed quality control, are displayed. In the Manhattan plot (A) -log10 (P-value) is plotted on the x axis, and chromosomal location on the y axis. In the QQ-plot (B), distributions of observed and expected chi-square values are compared.

SNP	Minor allele	CHR	CEU MAF	OR (95%CI)	Association p -value	Direction	GRAIL input genes	Genes in LD block r^2>0.8 with index SNP
rs12960119	G	18	0.075	1.46 (1.26-1.67)	1.58E-07	+++	*PSMA8, TAF4B, SS18*	*SS18, PSAM8*
rs267738	C	1	0.275	0.79 (0.71-0.87)	6.7E-06	---	*GOLPH3L, CTSK, FAM63A, SETBD1, CTSS, MCL1, CERS2, ANXA9, PRUNE, ARNT, HORMAD1, ADAMTSL4, ENSA*	*CERS2*
rs955943	A	4	0.067	1.54 (1.27-1.87)	9.9E-06	+++	*LDB2*	*LDB2*
rs7097067	A	10	0.075	1.65 (1.32-2.07)	1.28E-05	-++	*PPA1, NPFFR1,TYSND1,AIMF2, SAR1A*	*PPA1,NPFFR1*
rs1074463	A	5	0.092	1.31 (1.16-1.48)	1.28E-05	+++	*CDH12*	*CDH12*
rs2045084	G	8	0.425	1.21 (1.11-1.31)	1.54E-05	+++	*TSTA3*	*TSTA3*
rs8132771	A	21	0.075	1.43 (1.21-1.69)	1.96E-05	+++	*TIAM1, SOD1, SCAF4*	*SOD1, SCAF4*
rs11259960	A	15	0.200	1.35 (1.17-1.54)	2.36E-05	+-+	*HOMER2*	*HOMER2*
rs2368106	A	2	0.125	1.35 (1.17-1.54)	2.58E-05	-++	*CW22*	*CW22,UB 2E3*
rs7234959	A	18	0.083	1.34 (1.17-1.53)	2.68E-05	+++	*TAF4B,PSMA8, SS18*	*SS18, PSMA8*
rs6070015	A	20	0.067	1.67 (1.31-2.13)	2.91E-05	+++	*RAE1, SPO11, BMP7, RBM38*	*BMP7*
rs913444	A	9	0.250	1.22 (1.11-1.34)	3.00E-05	+++	*TRKB*	*TRKB,AGTPBP1*
rs4893905	A	2	0.100	1.33 (1.16-1.52)	3.32E-05	+++	*CW22*	*CW22,UB 2E3*
rs1477441	A	5	0.124	1.31 (1.15-1.49)	4.03E-05	+++	*CDH12*	*CDH12*
rs12193473	G	6	0.375	1.20 (1.10-1.31)	4.25E-05	+++	*C6orf170*	*MAN1A,C6orf170*
rs218843	A	6	0.375	1.20 (1.10-1.31)	4.40E-05	+++	*C6orf170*	*MAN1A,C6orf170*
rs4715056	G	6	0.275	0.81 (0.73-0.90)	4.94E-05	+--	*GPR115, OPN5,CD2AP, GPR111*	*C6orf38*
rs2817896	G	1	0.242	1.24 (1.12-1.37)	5.35E-05	-++	*EPHB2*	*EPHB2*
rs10515162	C	5	0.050	0.72 (0.61-0.85)	6.48E-05	---	*RGNEF*	*RGNEF*
rs11181447	A	12	0.150	1.28 (1.13-1.45)	6.68E-05	+++	*GLT8D3, YAF2, ZCRB1, PPHLN1, PRICKLE1*	*ZCRB1, PPHLN1, PRICKLE1*
rs12202993	A	6	0.375	1.20 (1.10-1.31)	7.48E-05	+++	*C6orf170*	*MAN1A,C6orf170*
rs564351	A	6	0.208	0.79 (0.70-0.89)	7.49E-05	+--	*GPR115, OPN5,CD2AP, GPR111*	*OPN5, PTCHD4*
rs6035211	C	20	0.117	1.30 (1.14-1.47)	8.66E-05	+++	*SLC24A3*	*C20orf79 SLC24A 3*

Table 25. Highest ranking RD association signals in the meta-analysis of the 3 discovery studies. Odds ratios with 95% confidence intervals are given with respect to the minor allele for an additive model of allelic effect, association p-values, direction of the minor allele effect in Netherlands, England, Scotland study (+increasing, - decreasing). Genes potentially underlying each SNP signal as identified by GRAIL and genes falling within the higher LD block tagged by the top associated SNP (defined as markers in high LD: r^2>0.8)

SNP	Chromosome	Genes	Gene in LD block r^2>0.8 with index SNP
rs12960119	18	*TAF4B, PSMA8, SS18*	*SS18, PSAM8*
rs267738	1	*GOLPH3L, CTSK, FAM63A, SETDB1 CTSS, MCL1, ANXA9, PRUNE, ARNT, HORMAD1, ADAMTSL4, ENSA*	*CERS2*
rs955943	4	*LDB2*	*LDB2*
rs1074463	5	*CDH12*	*CDH12*
rs8132771	21	*TIAM1, SOD1, SFRS15*	*SOD1, SCAF4*
rs2045084	8	*TSTA3*	TSTA3

Table 26: GRAIL input of most significant SNPs with same direction of effect for minor allele

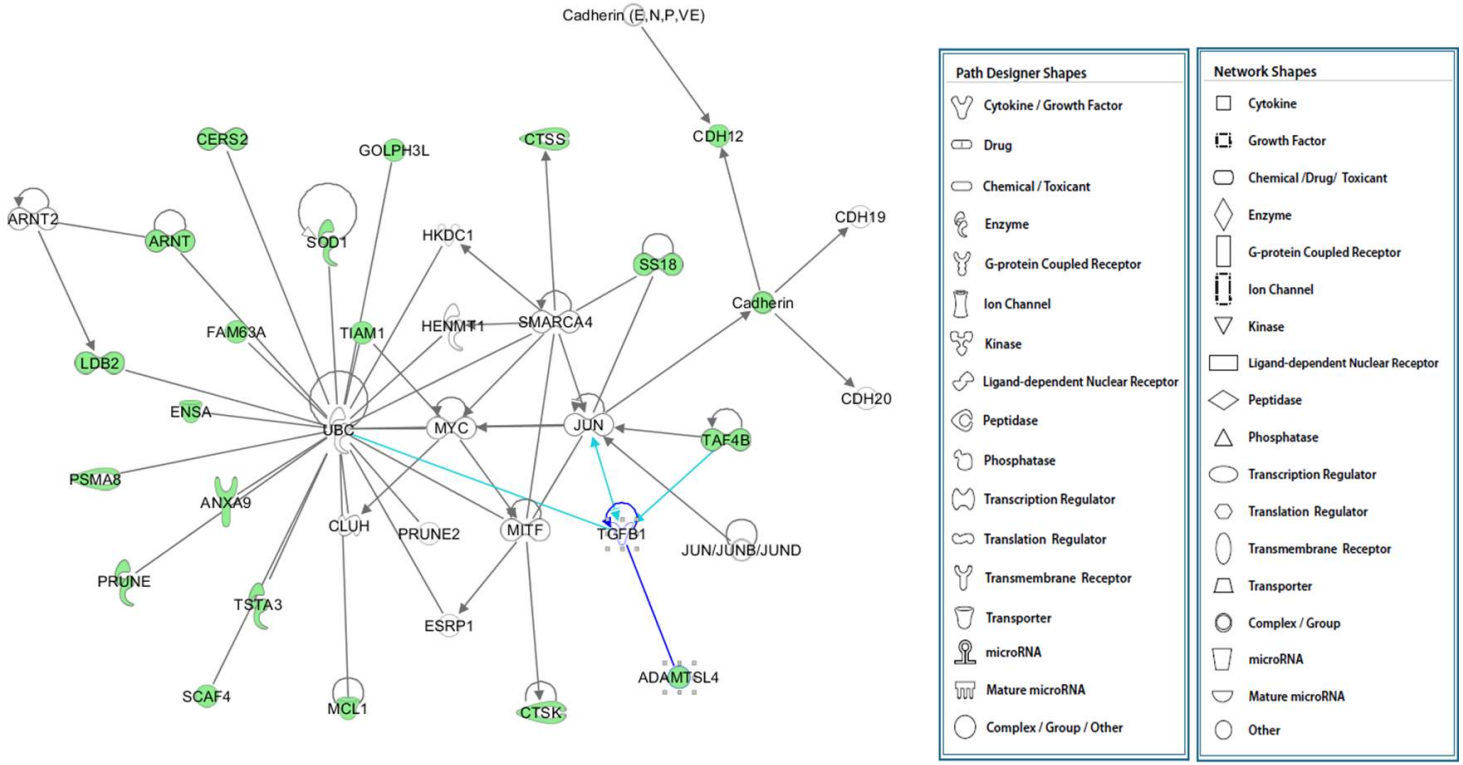

Figure 4.9: Pathway analysis.
Most significant network inferred by the Ingenuity IPA system based on the genes highlighted as significant by GRAIL from the most significant SNPs suggested on discovery and meta-analysis of GWAS. Those genes in green are directly related to SNPs of significance. Pathway highlighted in blue is the potential role of *ADAMTSL4* in this network.

All but rs1074463 demonstrated the same direction of effect in the replication analysis compared with those in the discovery analysis. The most significant SNPs were rs2045084 with $p=9x10^{-4}$, OR 1.32 (dominant model) an rs267738 with $p=7.1x10^{-3}$, OR=0.83. Of interest, rs12960119 did not replicate in the Moorfields Eye Hospital samples. The minor allele (G) effect was in the same direction , however, the frequency of the allele in the WTCCC National Blood service (used for the replication) was greater (MAF:0.087) compared to the WTCCC 1958BC (MAF: 0.075) (used in the discovery cohort).

4.5.1.3. META-ANALYSIS

An overall meta-analysis of the seven SNPs analysed on both the discovery and replication steps revealed one variant (rs267738) reaching genome-wide significance (table 27).

The significant SNP is in an exon of *CERS2* (*Ceramide Synthase 2*). The minor allele C is thought to have an odds ratio of 0.81 (additive model) and 0.78 (dominant model): thus it is thought to be protective.

The effect was consistent amongst all populations; with an excess of the major allele homozygous AA. Another SNP (rs267733) demonstrated suggestive significance in the discovery meta-analysis ($p=5.3x10^{-5}$); this is 5' of *CERS2*.

.

	Additive model				Dominant model			
SNP	OR	95%CI	p-value	Direction	OR	95%CI	p-value	Direction
rs267738	0.81	0.75-0.88	$1.43x10^{-7}$	-- --	0.78	0.71-0.85	$2x10^{-8}$	--- -
rs2045084	1.16	1.09-1.24	$2.85x10^{-6}$	++++	1.25	1.15-1.36	$2.59x10^{-7}$	++++
rs12960119	1.26	1.14-1.39	$2.49x10^{-6}$	+++++	1.27	1.15-1.41	$2.04x10^{-6}$	+++++
rs955943	1.41	1.21-1.64	$5.45x10^{-6}$	++++	1.42	1.21-1.66	$1.51x10^{-5}$	+++
rs81327771	1.31	1.16-1.46	$1.65x10^{-5}$	++++	1.31	1.16-1.49	$1.64x10^{-5}$	++++
rs913444	1.17	1.09-1.26	$2.09x10^{-5}$	++++	1.17	1.08-1.29	$3.38x10^{-4}$	++++
rs1076663	1.15	1.05-1.26	$2.59x10^{-3}$	+++-	1.21	1.09-1.35	$2.9x10^{-4}$	+++-

Table 27: Meta-analysis of combined discovery and replication phases. Highlighted in red are those SNPs which had been inputed into GRAIL

4.5.2. DISCUSSIONS

This study was undertaken to investigate the genetic predisposition to non-Mendelian RD, the majority of the cases of which were contributed from our collections. The most significant SNP (rs267738) was highlighted after meta-analysis of the most significant 7 SNPs found after the initial two step discovery stage. It is a missense variation (c.344A>C [p.Glu115Ala]) in exon 4 of *CERS2*. The encoded protein is part of the ceramide synthetase family. Ceramides are lipid signalling molecules which are an intermediate in sphingolipid biosynthesis[705]. Sphingolipids are a class of lipids which are involved in signalling pathways[705]. Ceramide itself is thought to play an important role in cell proliferation and survival[706]. *CERS2* is the most abundant and most widely distributed of this family, and has high specificity for fatty acyl-CoA[707]. Its precise role is unclear, but it has been suggested that the ceramides have an important role to play in most cells, perhaps as a housekeeping gene[707].

Ceramides have been demonstrated to play a role in apoptosis of RPE cell lines[708, 709] and mammalian photoreceptors[710]. A precise role in the pathogenesis of RD is therefore unclear. Gene identification based on the most significant SNPs highlighted 21 genes with high relatedness[675]. It is noteworthy that one of these SS18 (the protein encoded by *SS18*; the gene tagged by the most significant SNP in the discovery phase; rs12960119) interact with cytoplasmic actin filaments and play a role in the ability of cells to bind and react to extracellular matrices[711]. Ablation of it from cultured human cells has been demonstrated to result in compromised adhesion to ECM substrates (collagen I, IV and fibronectin)[711]. This is thought to be via modulation of integrins[712], which are transmembrane glycoproteins involved in this process. A further significant gene *TSTA3* encodes the enzyme GDP-L-Fucose-synthetase. Many adhesion molecules are fucosylated by TSTA3, such as cadherins[713] and integrins[714]. Such a cell adhesion role is attractive in RD.

Of particular interest was the identification of *ADAMTSL4* by GRAIL. The methods used by GRAIL suggested that it was significantly related to the most significant SNP after meta-analysis (rs267738). It must be considered that the relatedness to each SNP is very directed by proximity to the marker in question. All the genes highlighted by GRAIL as being related to rs267738 are within 500kb from the SNP within *CERS2* (Figure 4.10). It has been suggested that most LD blocks are <500kb and the most gene enhancers and repressors are also <500kb[672]. However, many genes within this

distance are not included in the list of related genes (Figure 4.10), and the methodology of GRAIL has been validated compared to other such gene identifying methods[675].

The interactions of these proteins was annotated with IPA (www.ingenuity.com), demonstrating a pathway with high reliability ($p=10^{-62}$). The most significant known pathway involving the relationships in this network was the haematological system. However, there are also parts of this network known to be involved in cell-cell adhesion and connective tissue development (Figure 4.11). This is an attractive pathway for RD.

When analysing the role of ADAMTS-Like 4, the connection within the network is based its action on TGFβ1. This association has been suggested for numerous members of the ADAMTS family, particularly those in which mutations may result in EL (*ADAMTS10, 17, 18* and *ADAMTSL4*[16]. TGFβ1 is a member of the TGFβ family of multifunctional cytokines which regulate adhesion, differentiation, migration and proliferation. Once secreted, it is cleaved into a latency –associated peptide, and latent TGFβ1-binding protein http://www.ncbi.nlm.nih.gov/gene/7040). Almost all cells have receptors for it and dysregulation of its activity may lead to apoptosis. Of particular interest is its potential role in connective tissue regulation. This has been demonstrated by work on MFS. It has been suggested that TGFβ interacts with ECM in the presence of *FBN1* mutation[715]. Furthermore there is an excess of TGFβ activity in humans with and mouse models of MFS[716, 717]. It is also been demonstrated that ADAMTS-Like 6 (of the same protein clad as ADAMTS-Like 4) attenuates the excessive release of TGFβ signals it's associated downstream signal in the mouse model of MFS[718].

As previously discussed in this thesis, authors have suggested that *ADAMTSL4* has a role in cell adhesion[719]. This is most likely an assumption based on the TSR domain common to the ADAMTS family; which has an important role in ECM anchoring, as will be discussed in chapter 5. This role of cell adhesion may therefore be critical to the involvement of this pathway in RD. Furthermore, as will be discussed further in chapter 5, the TSR domains regulate MMP2[720]; which is found in the vitreous[721] and modulates, amongst other substrates collagen XI, VII, V IV and fibronectin. Such MMPs have been demonstrated to play a role in RD[722]. It is therefore possible that ADAMTS-Like 4 has a similar role via its TSR. Furthermore, it is important to note that the ADAMTS proteins themselves are members of the MMP family. In addition to their role described above, MMPs have a role to play in the development of ocular structures; particularly sclera, lens, cornea and trabecular meshwork[723].

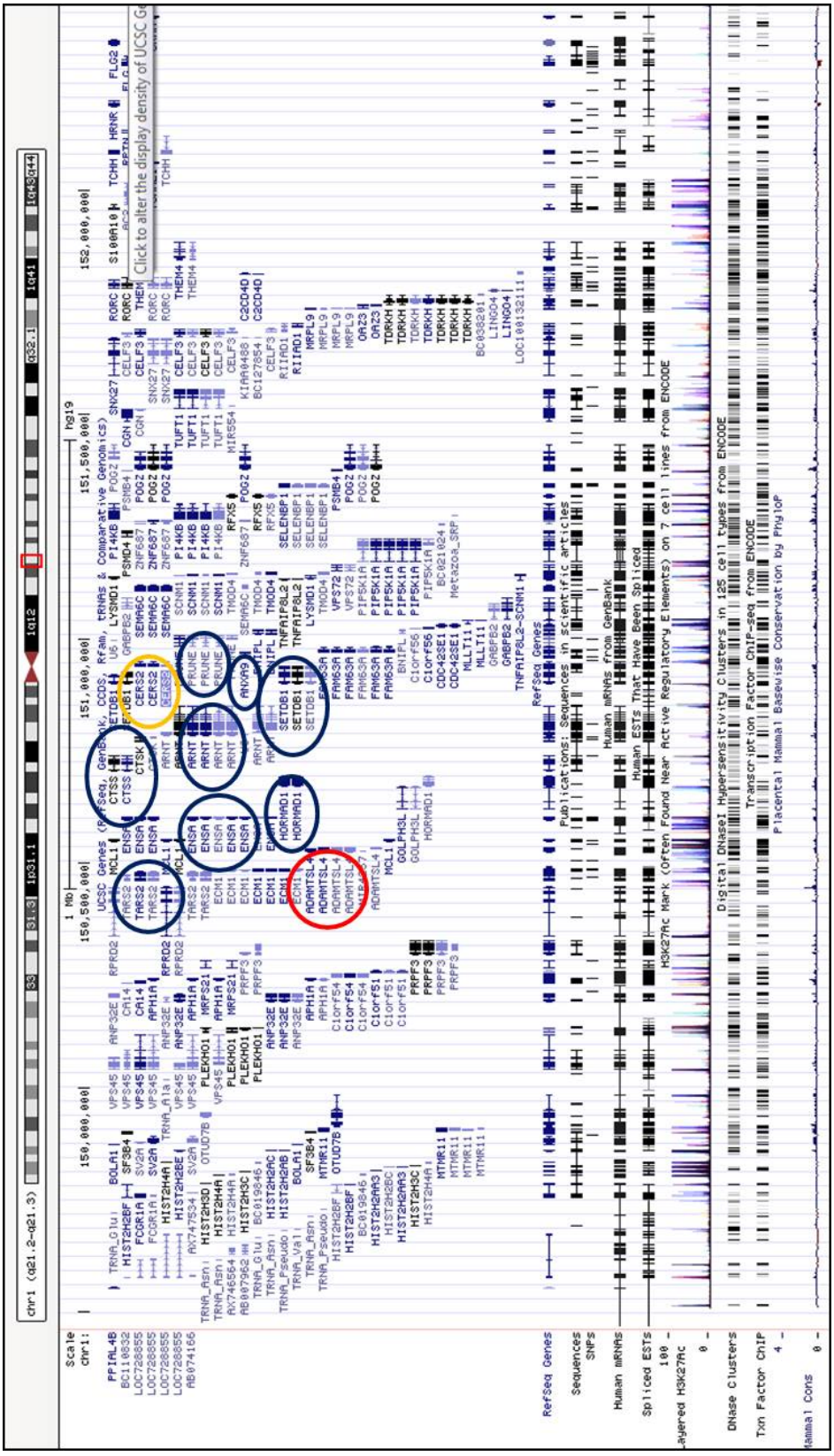

Figure 4.10: Location of *CERS2* and related genes as suggested by GRAIL. In Yellow is *CERS2*. In Blue are the related genes. Red is *ADAMTSL4*. *Image adapted from* http://genome.ucsc.edu/.

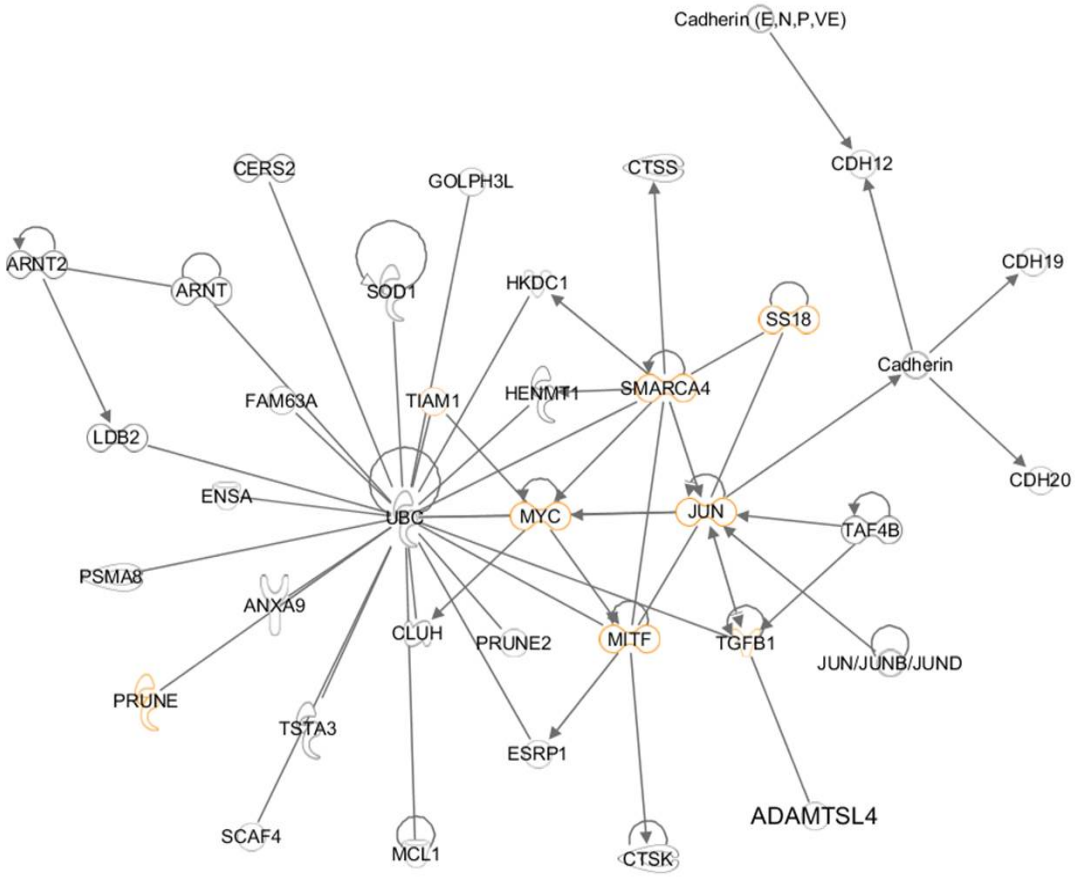

Figure 4.11: Molecules (orange) which are involved in cell-cell contact and connective tissue pathways.

One may speculate that any disruption of these proteins may affect this development and result in myopia; thus increasing the risk of RD. As discussed in section 2.5.2, *ADAMTSL4* may play a role in the development of myopia; either as a consequence of early onset EL or as a result of a direct role in ocular development.

Additionally, Stupka and colleagues[724] demonstrated that the ADAMTS proteins (particularly ADAMTS5) played a role in breakdown and modelling of precellular versican. As has been discussed earlier, versican is an important component of the vitreous, with the monogenic condition of Wagner's vitreoretinopathy (characterised by RD) caused by mutations in *Versican*. There may be a role for the ADAMTS proteins in RD by disrupting the versican of the vitreous in a similar way to the ECM[724]; thereby the vitreoretinal adhesions and thus playing a role in RD. Whether this speculation would be true for the non-enzymatic *ADAMTSL4* is further debatable; but the pathway analysis based on the results of this GWAS suggest that this may be an avenue for future investigations.

These findings must be taken with some caution. It must be remembered that *ADAMTSL4* was one of 13 genes highlighted by GRAIL. Only one gene was in a LD block r^2 >0.8 (*CERS2*); not *ADAMTSL4*. The pathway analysis involves genes not directly highlighted by the GWAS or GRAIL (such as *UBC*); so may only be theoretical. Furthermore, no direct relationships were highlighted between the molecules inputed from GRAIL. Additionally, the common link in the centre of the network is *UBC* (OMIM 191340). The protein (UBC) is widely expressed and has a large range of activities in cell processes, and therefore it may not be surprising that the genes from the GRAIL search are connected to it. Therefore, although statistically significant, this pathway is a suggestion, and would certainly need more investigations to clarify it.

This study nevertheless was the first to determine a genetic predisposition towards complex RD. Although no replicated variant was determined, it does provide a platform to further investigate the genetic aetiology to this condition. It will be of interest to attempt to replicate the findings in future cohorts. In the first instance, it would be valuable to ascertain whether these findings are replicated in the cohort of South Asians we have already collected. Our future work would involve larger cohorts, perhaps a cohort enriched for disease severity.

4.6. EXOME WIDE ASSOCIATION ANALYSIS OF RHEGMATOGENOUS RETINAL DETACHMENT

4.6.1. RESULTS

The work described below was undertaken by Dr Valentina Cipriani and myself at the UCL Institute of Ophthalmology and the UCL Genetics Institute.

1996 samples were genotyped on the Illumina HumanExome BeadChip at the KCL Institute of Psychiatry. The laboratory performed the genotyping on the Illumina HumanExome BeadChip 12 v1.1 on our samples, and genotype calling. Genotype calling can be challenging on arrays with rare variants. The type 1 error rate may be greater with calling rare SNVs; particularly if the common homozygote is called as the heterozygote[725].

Genotype calling for the Illumina HumanExome BeadChip was done using z-call [726], a variant caller to be used within GenCall in GenomeStudio (http://www.illumina.com/software/genomestudio_software.ilmn), specifically designed for rare SNVs. Briefly, this novel genotype calling software determines a threshold for common allele homozygosity based on GenCall (or other standard calling software). Rare homozygous allele threshold are then estimated though linear regression to determine mean and standard deviation of the call intensities of successfully genotyped common (MAF >=5%) SNVs. This is then used to determine a z score for the whole cohort thus allowing genotype calls to make for even rare alleles.

Thus they provided two sets of genotype files; with data for 1,996 cases and ,5963 controls.

The data was generated using Genome Studio to create a .bsc file. This was converted into PLINK files, upon which we undertook quality control.

Initial inspection of the dataset demonstrated that 12 samples in the PLINK file provided on cases data had been duplicated. 12 cases were therefore dropped, leaving genotype data on 1984 cases. We also excluded controls which were not labelled as the same ethnicity as the cases (White Caucasian). This removed 40 controls, leaving 5923 controls.

Quality control of data must be performed per-individual and per-marker. It is generally advisable to perform the former first, as removal of any marker is potentially a lost disease association. The impact of this is thought to be greater than the loss of a single individual[482]. All analysis was done using PLINK (http://pngu.mgh.harvard.edu/purcell/plink/) [671].

The first step checked for gender discordance between labelled gender on the sample manifest and genotyped results. This would therefore highlight potential sample mix-up or plating errors. Genetic gender verification is done by analysing the homozygosity rate of markers on the X chromosome. Males have only one X chromosome, and therefore cannot be heterozygous for markers on the X chromosome. For males the X chromosome homozygosity rate is therefore 1.0. Conversely, females, are expected to have a rate <0.2. Thus male samples which are labelled as female would have a higher than expected homozygosity rate, and vice versa. The methodology for assessing X chromosome homozygosity is therefore to calculate the average rate for all markers on this chromosome for an individual, and comparing it to the expected value (>0.8 for males, <0.2 for females). This process is particularly important if gender will be used as a co-variate, but also to ensure sample mix up has not occurred.

For cases, there were 25 gender mismatches. The records of these patients were re-checked, leaving 10 individuals with persistent imbalances. They were removed from the dataset. This resulted in 1974 cases (M=1234, F=740). The same was done for control data and three individuals were removed. This left 5290 control individuals (M=3318, F=2602).

Subsequent steps were aimed at assessing DNA sample quality, as these may have considerable impact on genotype accuracy. Genotype failure rate and heterozygosity are measures of DNA sample quality.

We evaluated those individuals in which >2.5% of genotyped SNVs were missing, and excluded them (Table 28 and Figure 4.12). This is a conservative figure compared to some large GWAS[464]. This threshold is determined by analysis of the distribution of missing genotypes across the whole samples set; and is indicative of the good quality of DNA in our cohort. Subsequently, heterozygosity was examined across the whole set. This involves assessing the rate of heterozygosity of the variants typed in the individuals. This differs amongst populations and genotyping arrays, and therefore is

	MAF	HETEROZYGOSITY Outside 3 Standard Deviations from mean	MISSING RATE: >2.5%
CASES	>1%	9	2
	<1%	0	
CONTROLS	>1%	63	0
	<1%	54	

Table 28: Number of individuals failing heterozygosity and missing genotype quality control assessment on Illumina HumanExome BeadChip.

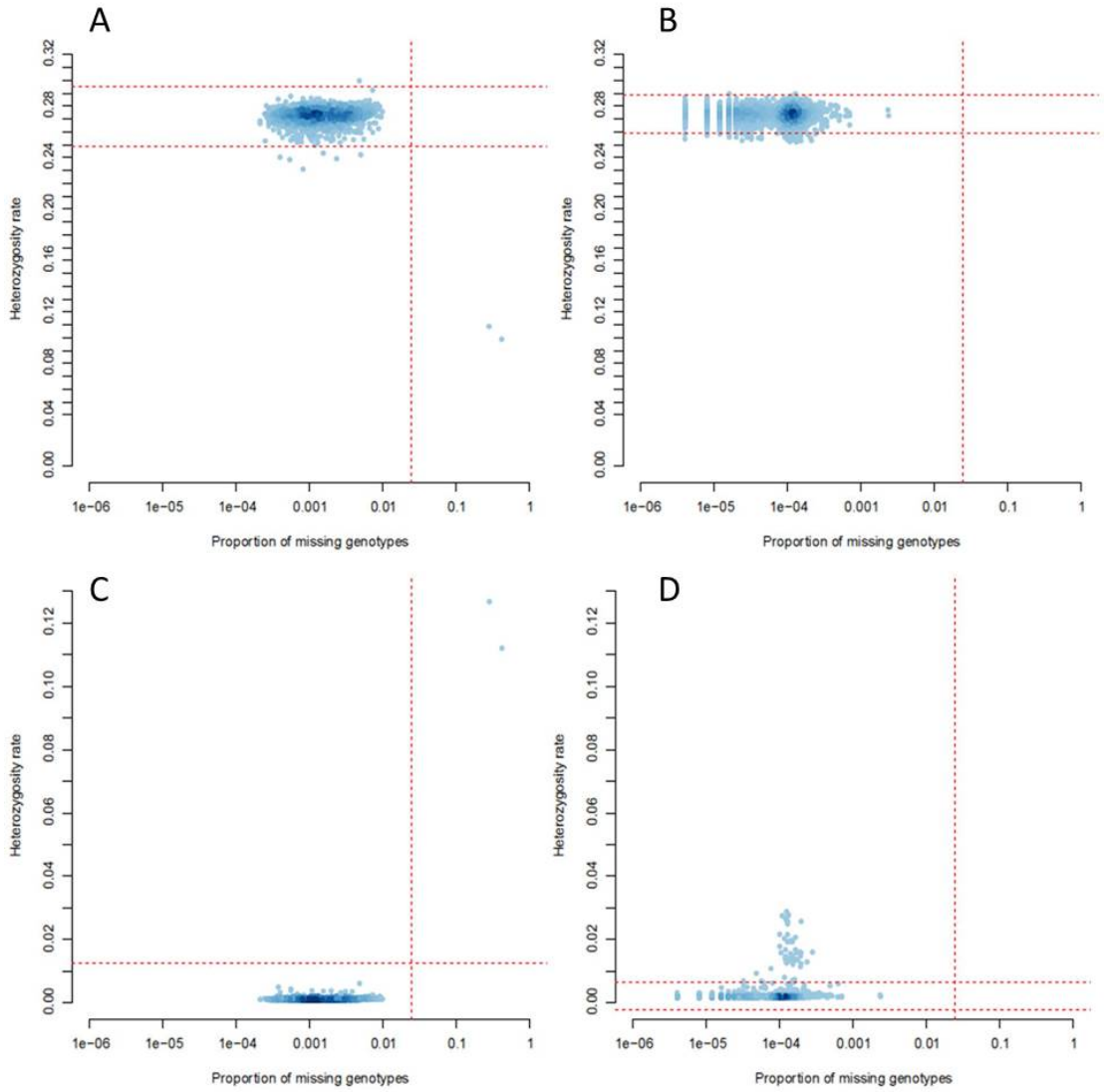

Figure 4.12: HETEROZYGOSITY vs PER-SAMPLE CALL RATE for VARIANTS CALLED ON ILLUMINA HUMANEXOME BEADCHIP

A & B: Common Variants (MAF>1%) for cases (A) and controls (B)
C & D: Rare Variants (MAF<1%) for cases (C) and controls (D).
Tramlines on y-axis represent 3 standard deviations from the mean heterozygosity
Tramline on x axis represents 2.5% missing genotype data
Individuals outside the 3 SD markers and to the right of the 2.5% heterozygosity line were excluded

unique to each study. Mean heterozygosity across the autosomal SNVs was then determined, and the subsequent cluster examined. Heterozygosity is calculated with the equation

$$(N-O)/N$$

N= number of non-missing genotypes, O= Observed number of homozygous genotypes for a given individual.

This rate would vary for common and rare alleles, being greater in the former. This was therefore analysed separately for common (MAF>1%) and rare SNVs (MAF</=1%). Furthermore, it was done separately on 1984 cases and 5293 controls (Figure 4.12).

Any individual with heterozygosity values +/- 3 standard deviations from the mean were excluded. Excessive heterozygosity may represent contamination, whilst decreased heterozygosity; inbreeding.

There were thus 9 cases (the two cases with high missing rates were also part of those which failed heterozygosity control) which were due to be excluded. Two of these were already dropped from the gender analysis. Therefore seven cases were excluded. 116 controls (one case failed both in rare and common variants) were also excluded.

At this stage of quality control there were therefore 1967 cases (M=1229, F=738) and 5804 controls (M=3272, F=2532). Further steps in per-individual quality control involve assessing for unknown relatedness. Identity by State (IBS) is calculated between each pair; based on the mean proportion of alleles shared in common at SNVs genotyped. Variants across the genome are used, excluding the HLA regions and SNPs with r^2>0.2[482]. Duplicates or monozygotic twins would then be denoted as those with IBS=1. It is generally regarded therefore that IBD indicates relatedness in a population cohort as ours. IBD can then be determined by the genome-wide IBS. It would be estimated that IBD shared between first degree relatives would be 0.5, between second degree relatives 0.25 and between third degree relatives 0.125. One of a pair with IBD>0.1875 is generally removed[482]. Using rare markers on this chip for this analysis is challenging. The Scottish samples had had this analysis already done as part of the GWAS (section 4.3.3). This stage of the quality control on the samples collected from Moorfields Eye Hospital will be completed in due course. It is expected that this will be low in the cohort, as patients were all asked about family histories of patients

with RD, and there were no patients recruited who knew of relatives who had taken part in the study

Finally, analysis for population stratification (ancestral differences) is undertaken. Rare variants are likely to be more population specific[648], and thus the issue of population stratification must be closely considered. This is undertaken by utilising primary component analysis (PCA; as described in section 4.1.7.3). Generally, it is required that variants across the genome are used, which may then be compared to HapMap genotype data [727] from the different continental origins included in this, to detect large scale ancestral differences. For such analysis, it is therefore challenging to use SNVs from the Illumina HumanExome BeadChip, which are not genome-wide, are rare and focussed in and around the exome. There are no published examples yet available of completing this. Ancestral analysis has already been completed for the samples from Scotland as part of the GWAS. PCA analysis for stratification will be attempted in the Scottish cohort using SNVs from the Illumina HumanExome BeadChip. This may be done for SNVs of differing MAF. Outliers will then be estimated. This will be compared to the outliers defined using the GWAS chip in this cohort. Such a comparison would then offer an indication as to the utility of the Illumina HumanExome BeadChip SNVs in population stratification analysis. It would then be used on the Moorfields Eye Hospital samples and samples from the 1958 birth cohort controls. This analysis is underway by Dr Vitart in the MRC Human Genetics Unit (Edinburgh).

Subsequently per-marker quality control is undertaken. This was done although the final per-sample QC had not been completed. It is expected that the effect of stratification and relatedness control will be negligible and that the final figures after the per-marker is completed will not be altered significantly.

4.6.1.1. VARIANT DIFFERENCES BETWEEN CASES AND CONTROLS

On assessing the SNVs between cases and controls, it became apparent that there was discordance between the SNVs in cases and the controls. 14 SNVs were present in cases alone and 4969 in controls alone, leaving 242,901 SNVs in common.

We contacted the laboratory at KCL Institute of Psychiatry; who informed us that this was due to the fact that the cases and controls were in fact genotyped on different

versions of the Illumina HumanExome BeadChip. The controls were genotyped on Version 1.0, whilst our cases on the newer version 1.1. There are 4969 SNVs on the version 1.0 which are not on the newer version 1.1. A further 21 SNVs failed genotyping on controls (14 of which were successfully genotyped on cases). There were therefore 242,887 SNVs genotyped in common.

We had not been aware that different versions of the Illumina HumanExome BeadChip were being used in the cases and controls. We therefore were not aware that this discordance of SNVs existed, or that it would affect our analysis.

For assessing SNV quality, it is best practice to complete this in cases and controls individually[482]. Therefore, 247849 SNVs underwent quality control in the 5804 control individuals, and 232901 SNVs underwent this in the 1967 cases.

Firstly, it is then important to remove SNVs which deviate significantly from HWE. However, if there is an association between an SNV and RD, there may be a deviation from HWE in cases; and removing these would be undesirable. Therefore it is general practice to remove those with HWE deviation in the control cohort; particularly population control cohorts such as ours. The threshold for exclusion varies between studies, ranging between $p=0.001$ and $5.7x10^{-7}$. For this study we have chosen $p=10^{-6}$. Using this threshold, 662 SNVs were excluded.

Subsequently, SNVs with high missing rates (unsuccessfully called in a high number of individuals) were removed. This is crucial as they may result in false positives, however must be balanced with the potential exclusion of disease associated variants. Markers with <95% call rate are removed from some studies[728], though this does vary between studies. For this study, we elected to remove common and rare SNVs with a call rate <97.5% in cases and controls (Figure 4.13). This resulted in 2510 SNVs being removed from cases. The total genotyping rate in the remaining case individuals was 0.9981. 46 SNVs were excluded from controls. The genotyping rate in the remaining control individuals was 0.999.

Further to this, it is important to know the minor allele frequencies of the markers genotyped. In GWAS, it is generally suggested that a threshold MAF of 1-2% is used[482] for exclusion. This is because of the difficulties in genotyping these SNVs, and the challenges of interpreting association analysis demonstrated by these SNVs.

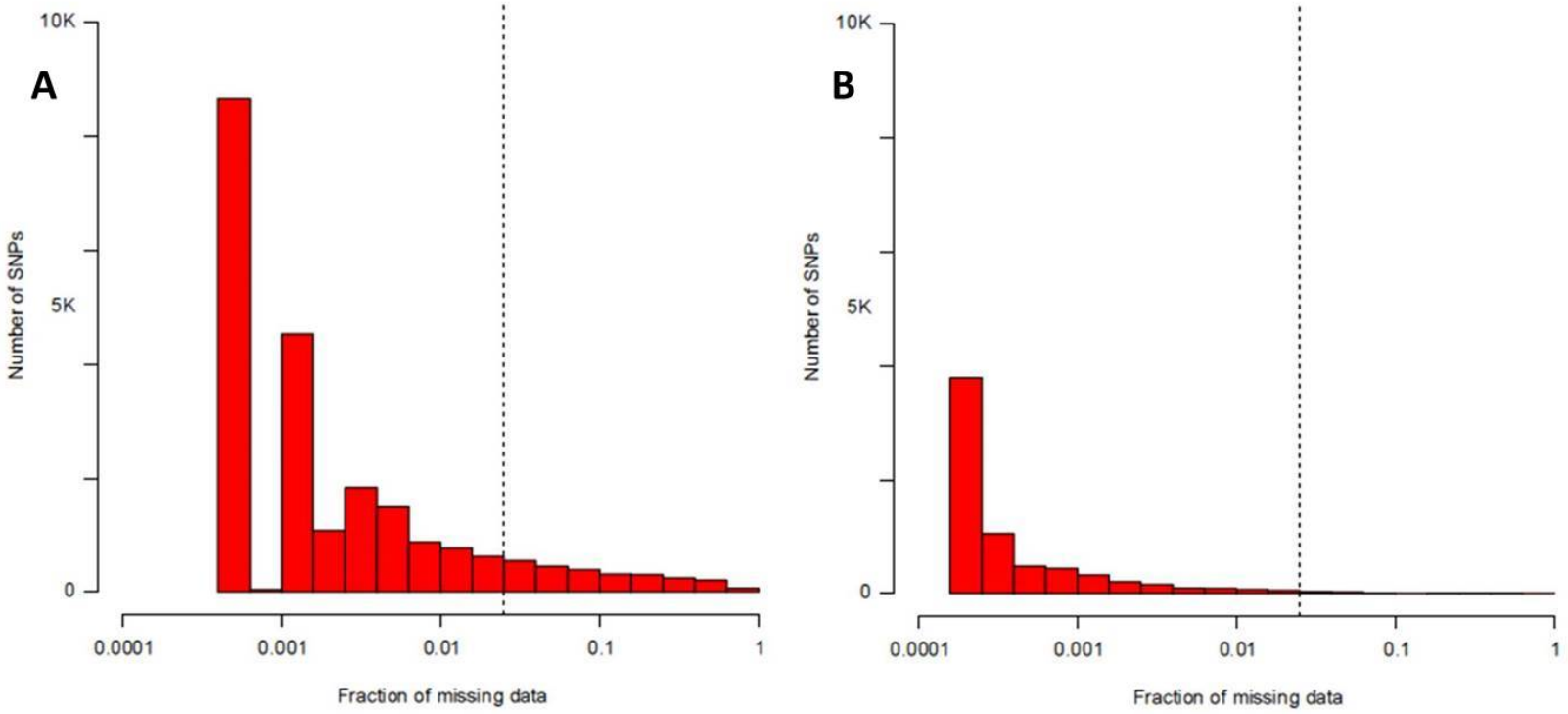

Figure 4.13: Variant missing data:
QC of missing call rate for variants in cases (A) and controls (B).
Those variants with a missing rate of >2.5% (Dashed line) or greater are excluded.

However for this study, excluding these SNVs would be unwanted, considering the makeup of the Illumina HumanExome BeadChip. Thus this step will not be undertaken; rather a description of the variant MAF was done. There were 204188 and 209935 rare variants (MAF<1%) genotyped in cases and controls respectively. There were 36203 and 37206 common variants (MAF>1%) typed on cases and controls respectively.

After these stages of quality control there remained 1967 cases, 5804 controls, which had successful genotype data on 240,391 and 247,141 SNVs respectively. A summary of this process is in Figure 4.14.

Prior to association analysis between cases and controls, it is necessary to merge the data files of cases and controls. When successful, association analysis may be undertaken.

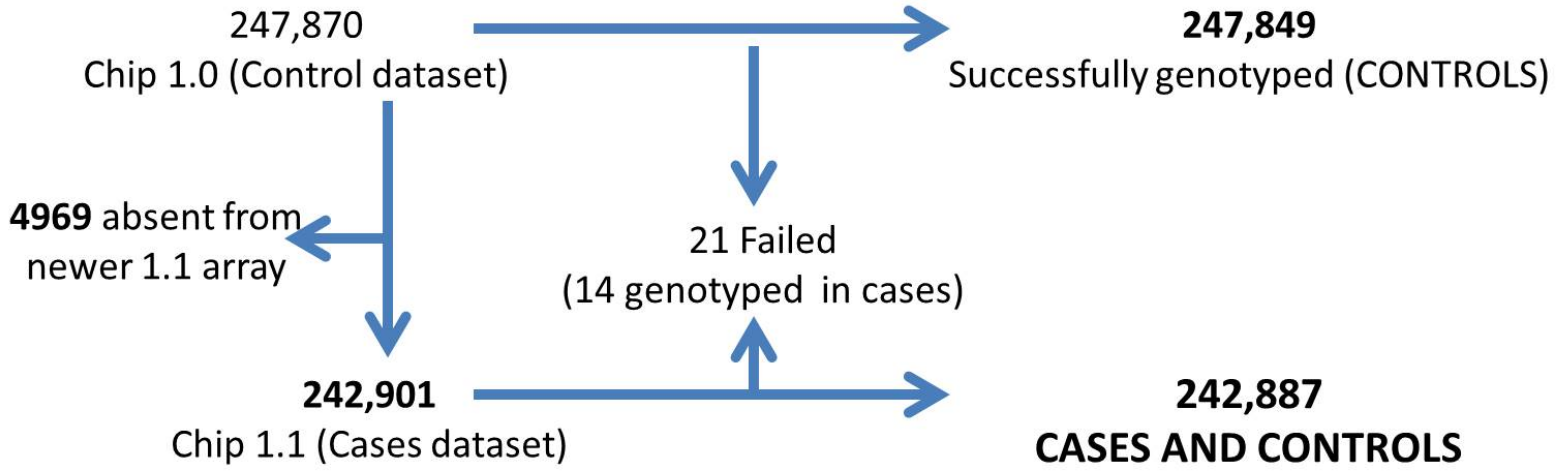

Figure 4.14: Summary of Quality control of variants typed on in cases and controls (Illumina HumanExome BeadChip)

4.6.1.2. EXOME CHIP QC and ASSOCIATION

Further to Quality Control, association analysis will be undertaken over the next two years by our team; led by Dr Veronique Vitart (University of Edinburgh) and Dr Valentina Cipriani (UCL Institute of Ophthalmology).

However there are significant challenges to analysing variants, in which a majority are rare SNVs.

Firstly one must consider the power of studies. The power to detect an association with rare SNVs is low[729]. There is a possibility therefore that this study will be under powered to elucidate putative variants.

To combat the issue of power, some authors recommend initially performing individual locus analysis on rare variants (however they are acquired); initially to act as an additional quality control stage[663]. Subsequently, the most common method of increasing the power is to "collapse" variants into a single group, and test their collective frequency differences against controls[730] ("burden" of many variants). These variants may be collapsed based on numerous criteria, including function, location and biological pathways of the genes in which the SNV are found.

Specific methods of analysing these collapsed variants are numerous. This can be based on summary statistics of variant frequencies between cases and controls. An example of this is the cohort allelic sums test (CAST)[730]; whereby the frequency of individuals carrying one of a group of variants is compared. Alternatively, the combined multivariate and collapsing method (CMC)[731] collapses the variants and uses them all as one statistic. This method is thought to control type 1 error, and can be used in a regression model.

Collapsing can also be done based on similarities of DNA sequences. This is based on the consideration that the nucleotide background of a rare variant can influence the phenotype; thus analysing in this manner may assume some form of interaction amongst variants[729].

With regard to using data acquisition focussed on the exome (sequencing or genotyping), Price and colleagues first suggested a method based on the CAST methods, incorporating predicted functional impact of each SNV[732]. Han and

colleagues have subsequently devised methods incorporating the direction of the effect of the SNV[733]. Numerous methods have since been devised (for review see[729]).

In summary, analysing exome data specifically; two methods are employed. This may employ counting the number of rare variants across a gene, and then comparing between cases and controls[731]. Variants can be weighted (for the purpose of tabulations and subsequent analysis) such that a greater score is given to SNV which would be thought to have greater functional consequences[663]. Alternatively, methods may be devised to assess whether the number of variants which have an effect exceeds the expectation[734, 735]. Variants in exome analysis can furthermore be grouped according to their likelihood of damage; with splice site, frameshift and nonsense mutations being the most pathogenic SNVs.

A final consideration of analysing rare, coding variants is the replication of findings from these experiments. If an association is detected as a result of a burden of numerous SNV, it may be necessary to undertake targeted sequencing of the relevant genes highlighted from the initial analysis. We have now developed collaborations with units across numerous units and countries. These include Guy's and St Thomas' Hospitals (King's College London, UK), Addenbrookes Hospital (University of Cambridge, UK), Calgary Retina Consultants (University of Calgary, Alberta, Canada) and the Department of Ophthalmology at Royal Victoria Eye and Ear Hospital (University of Melbourne, Victoria, Australia). Over the next few years, it is hoped that a significant cohort will be in place to replicate and extend findings from this work.

CHAPTER 5: HUMAN OCULAR EXPRESSION AND PROTEIN MODELLING OF ADAMTSL4

Publications arising from work related to this chapter:

(i) **Chandra** A., Jones M., Cottrill P., Eastlake K., Limb GA., Charteris DG.

The gene expression and protein distribution of ADAMTSL-4 in human iris, choroid and retina.

British Journal of Ophthalmology 2013 Sep;97(9):1208-12

(ii) **Chandra** A , D'Cruz L, Aragon-Martin JA, Charteris DG, Limb GA, Child AH, Arno G.

Focus on molecules: ADAMTSL4.

Experimental Eye Research. 2012 Nov;104:95-6

5.1. INTRODUCTION

The role of the ADAMTS family of proteins and encoding genes has been discussed at length in this thesis. In particular, the role of *ADAMTSL4* has been highlighted as important in EL and RD. However, the definitive presence of this gene and protein in ocular tissue has not been well defined.

ADAMTSL4 being part of the *ADAMTS* family of genes is therefore a part of the TSR superfamily of genes. This superfamily is characterised by the Thrombospondin Repeat domain.

5.1.1. THROMBOSPONDIN REPEAT DOMAIN

The TSR domain is an ancient extracellular domain found throughout vertebrate and invertebrate proteins[736]. The structure of these domains includes three strands, an irregular A strand and 2 regular (B and C) strands with a β structure[737] (Figure 5.1).

The TSRs are in secreted proteins or in the ECM part of transmembrane proteins. Almost 100 proteins contain this extracellular domain, with a wide range of functions[738]. The role they play in proteins varies from neuronal axonal outgrowth, angiogenesis, tumour progression, activation of TGFβ, wound healing and ECM remodelling[26, 737]. The most relevant in the ADAMTS proteins is the role in ECM anchoring. A major component of the ECM includes glycosaminoglycans (GAGs). It is believed that positive charges across the front face of a TSR domain is crucial for the high-affinity binding to GAGs[737].

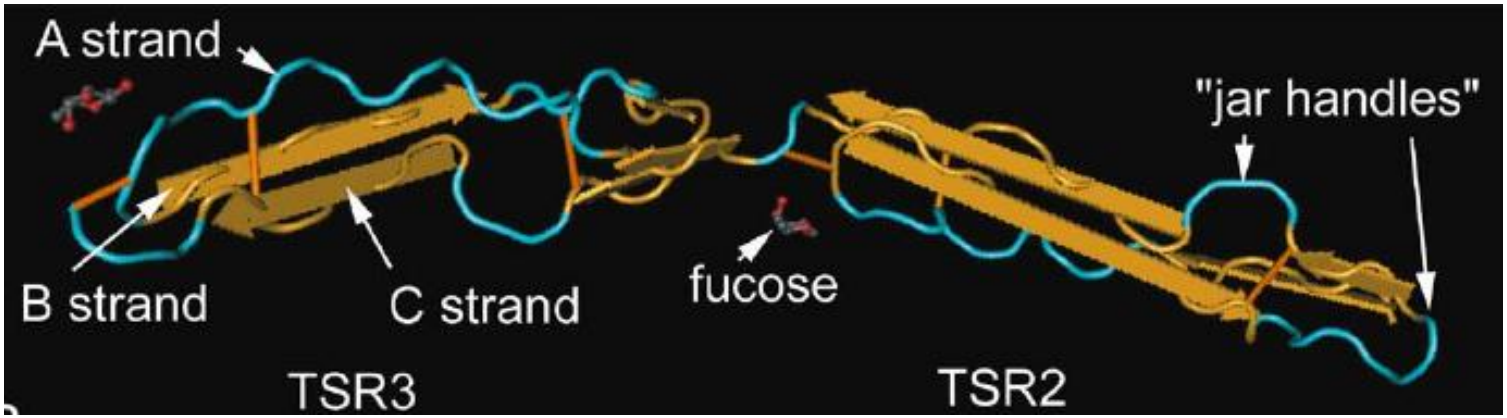

Figure 5.1: The Thrombospondin repeat domain. *Adapted from* [26]
One end of the "jar handles" between the B and C strands form a hydrogen bond with the first tryptophan in the A strand. The other polar end is exposed to ligands, and may therefore play a role in the adhesion role of the TSR domains.

5.1.2. ADAMTS PROTEINS

The ADAMTS proteins are a family of enzymes. Beyond the TSR domains, they frequently contain four other domains; prodomain, metalloprotease domain, disintegrin domain and cysteine-rich domains[739]. The former three of these constitute the catalytic domain at the N terminus. The latter, along with the TSR domains in conjunction with protein specific domains constitute the ancillary domain at their C terminus. The ancillary domain is crucial in determining substrate specificity (Figure 5.2). Excision of the propeptide is an important step post translation. Of interest, some ADAMTS proteins ancillary C terminus domains may have independent roles after excision. As mentioned in chapter 3 (section 3.5.1) this is the case with a fragment of ADAMTS18[361].

These proteins play a role in a wide range of biological processes, including cell migration, coagulation, angiogenesis and ECM regulation[21]. They have a particular role in maturation of procollagen (ADAMTS2, ADAMTS3, ADAMTS14) and von Willebrand factor (ADAMTS13). It is suggested that these proteins may cooperate with each other to maintain enzymatic function[21].

5.1.3. ADAMTS-LIKE PROTEINS

The ADAMTS-Like proteins are products of distinct genes, and are closely related in structure to the ADAMTS ancillary proteases, including at least one TSR domain. They however lack the catalytic domain, thus do not have enzymatic activity[16]. ADAMTS-Like 4 and ADAMTS-Like 6 form part of one clade, differing from ADAMTS-Like 1, ADAMTS-Like 3 and ADAMTS-Like 7 by lacking immunoglobulin repeat regions.

The function of these proteins is unclear. Mutations in *ADAMTSL2* result in a condition known as geleophysic dysplasia[740]. This condition is characterised by high levels of TGFβ activity, and has systemic phenotypes similar to WMS[740]. The protein ADAMTS-Like 2 binds to latent TGFβ-1 (a fibrillin-1 ligand) and fibrillin-1. EL is a common phenotype of mutations in these genes. It has been suggested that some of the genes which cause EL may also be involved in the TGFβ pathway[16]. Alternatively, ADAMTS-Like proteins may have independent functions in the ECM, but these are not yet clear.

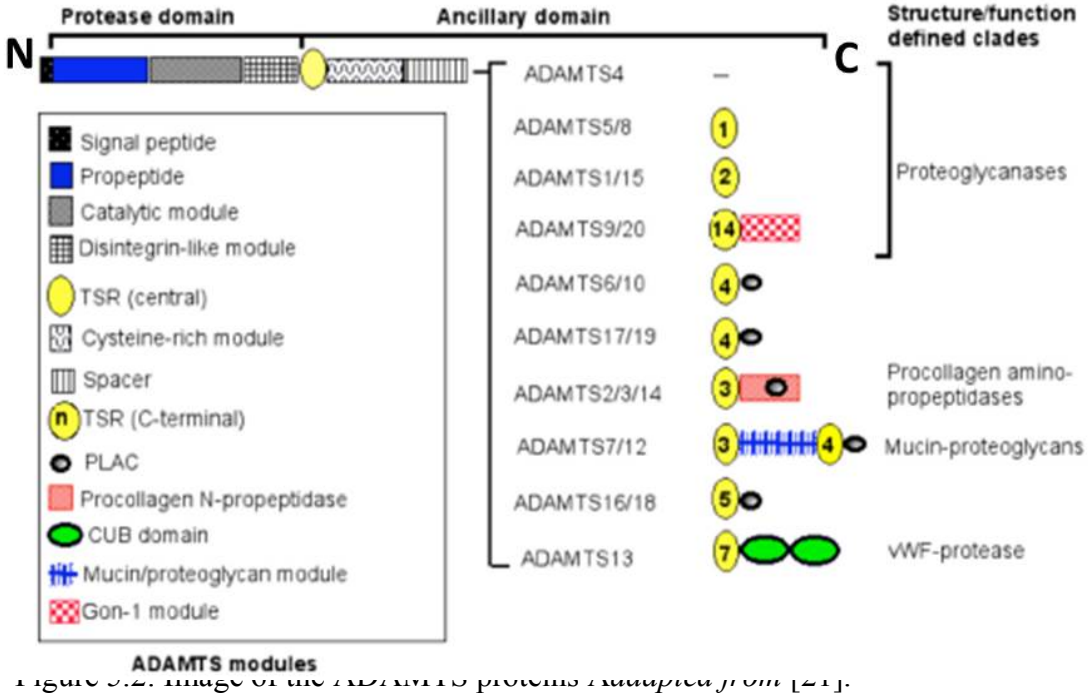

Figure 3.2: Image of the ADAMTS proteins *Adapted from* [21].
The common stem of each ADAMTS protein is at the top. The specific ancillary C-terminus domain of each ADAMTS protein is shown on the right.

5.1.3.1. ADAMTSL4

ADAMTSL4 (A Disintegrin And Metalloproteinase and Thrombospondin Motifs Like 4) is one of seven of the *ADAMTSL* genes and has been discussed at length in this thesis. First described in 2003, it was initially termed *TSRC1* (Thrombospondin Repeat Containing Gene 1)[239]. Buchner [239]suggested that a chromosomal inversion involving an ancient *ADAMTS* gene may have generated two separate genes, *ADAMTSL4* and *ADAM15*, a protein containing four of the ADAMTS domains, but lacking the TSR domains. This would have to have occurred prior to the separation of the mouse and human lineage, as they are closely related in both.

It has 79% nucleotide sequence identity and 76% amino acid homology with mouse *TSRC1* and encodes a 1074 amino acid protein; ADAMTS-Like 4. This differs from the mouse protein by 38 amino acids; most of which are encoded within the large divergent Exon 6.

ADAMTS-Like 4 contains seven Thrombospondin type 1 repeat domains, six of which are clustered towards the C Terminus. Other domains present in the full length protein are an ADAMTS spacer 1 domain, a ADAMTS cysteine rich module and a PLAC (Protease and Lacunin) domain[279] (Figure 5.3). Like other ADAMTS-Like proteins it lacks enzymatic activity, and thus further suggests that it may play a role only in maintenance or anchoring the ECM; indeed this proposed function has been discussed at length in this thesis.

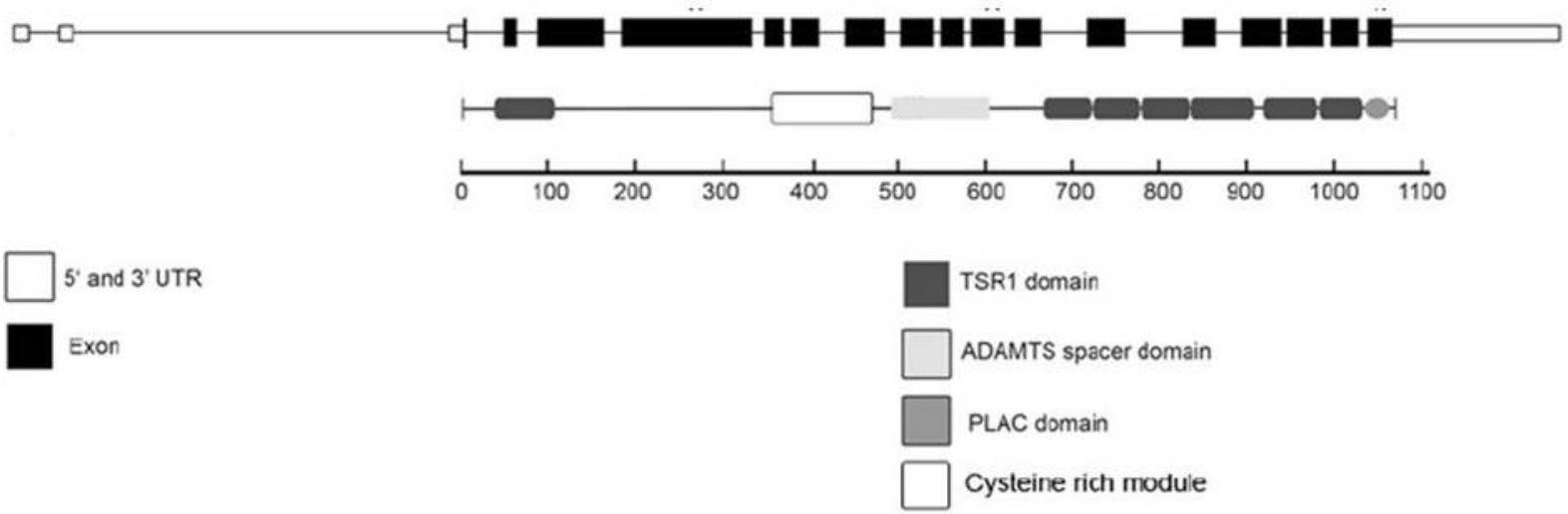

Figure 5.3: Schematic diagram of *ADAMTSL4* and its protein, demonstrating different protein domains.

5.2. AIMS OF THIS CHAPTER

The aims of this chapter are to further understand the *ADAMTSL4* gene and protein.

Firstly, already in this thesis it has been demonstrated that *ADAMTSL4* has an important role to play in EL, and potentially in RD. Although the encoded protein, ADAMTS-Like 4 is known to be extracellular [741], and is distributed widely throughout the body[2], its distribution within ocular tissue is not clear. It is not yet known to be causative or associated with any extraocular phenotype, yet papers describing the expression of the gene and protein, either did not investigate [2] or provide no evidence for [239] ocular expression and distribution. We therefore aimed to investigate the mRNA expression and protein distribution patterns of *ADAMTSL4* in human ocular tissue.

For this project, I was privileged to work in the laboratory of Professor Astrid Limb (ORBIT, UCL Institute of Ophthalmology), and supported by her team.

Secondly, although the primary structure of ADAMTS-Like 4 is established ,the further secondary and tertiary structures are unknown. Protein structure is best defined by formal protein crystallography[742]. The crystalline structures of ADAMTS-1[743], ADAMTS-4, ADAMTS-5[744] and part of the non-catalytic region (residues 287-685) of ADAMTS13[745] have been described. However, none of the crystalline structures of the other ADAMTS or any of the ADAMTS-Like proteins have been deposited onto the Protein Data Bank (PDB: http://www.rcsb.org/pdb/home/home.do)[746]. An alternative to crystallography is comparative or homology modelling. This has been proven to be very accurate method of protein structure prediction[747]. We therefore planned to model the protein structure of ADAMTS-Like 4 using this methodology.

For this endeavour, I was fortunate to work with Dr Leon D'Cruz (St George's University of London), who was instrumental in this process.

5.3. METHODS

5.3.1. EXPRESSION OF ADAMTSL4 IN OCULAR TISSUE

Acquisition of human tissue adhered to the tenets of the declaration of Helsinki. Following approval of the local research ethics committee, eyes with consent for research were obtained from Moorfields Hospital Eye Bank.

5.3.1.1. PREPARATION OF OCULAR TISSUE

Ocular tissue was acquired within 24-48 hours post-mortem. Three eyes underwent preparation for immunostaining. Tissues from five eyes were isolated to provide RNA and protein for experimental studies.

Instruments were sterilised with sodium hypochlorite (diluted 1 in 10) followed by several washes with sterile phosphate buffered saline (PBS). Gentle dissection was required to allow isolation of lens, retina, choroid and iris, from the eye cup. The eye was dissected (Figure 5.4) and iris was isolated from the anterior chamber. The vitreous was then removed. Retina was dissected off with sterile PBS. Choroid was then isolated.

The three different ocular tissues were then subjected to various biochemical treatments to either extract RNA or protein from the disrupted cells as described below.

5.3.1.2. RNA EXTRACTION

Tissue was disrupted and the lysate homogenised in Buffer RLT Plus (Qiagen, UK). This lysate was then centrifuged for 3 minutes at maximum speed. The supernatant was then removed by pipetting. This was then transferred to a gDNA Eliminator spin column placed in a 2ml collection tube and centrifuged for 30s (at ≥8000 x *g* (≥10,000 rpm). The flow through was saved and 350µl of 70% ethanol was added, and mixed well by pipetting. Up to 700µl of the sample, including any precipitate, was transferred to an RNeasy spin column placed in a 2ml collection tube, which was centrifuged for 15 s at ≥8000 x *g*. The flow-through was then discarded. 700µl of Buffer RW1 was added to the RNeasy Mini spin column (in a 2 ml collection tube) and centrifuged for 15 s at ≥8000 x *g*. The flow-through was again discarded. This was repeated with 500µl Buffer RPE with the same centrifuge settings and the flow-through discarded. 500µl Buffer

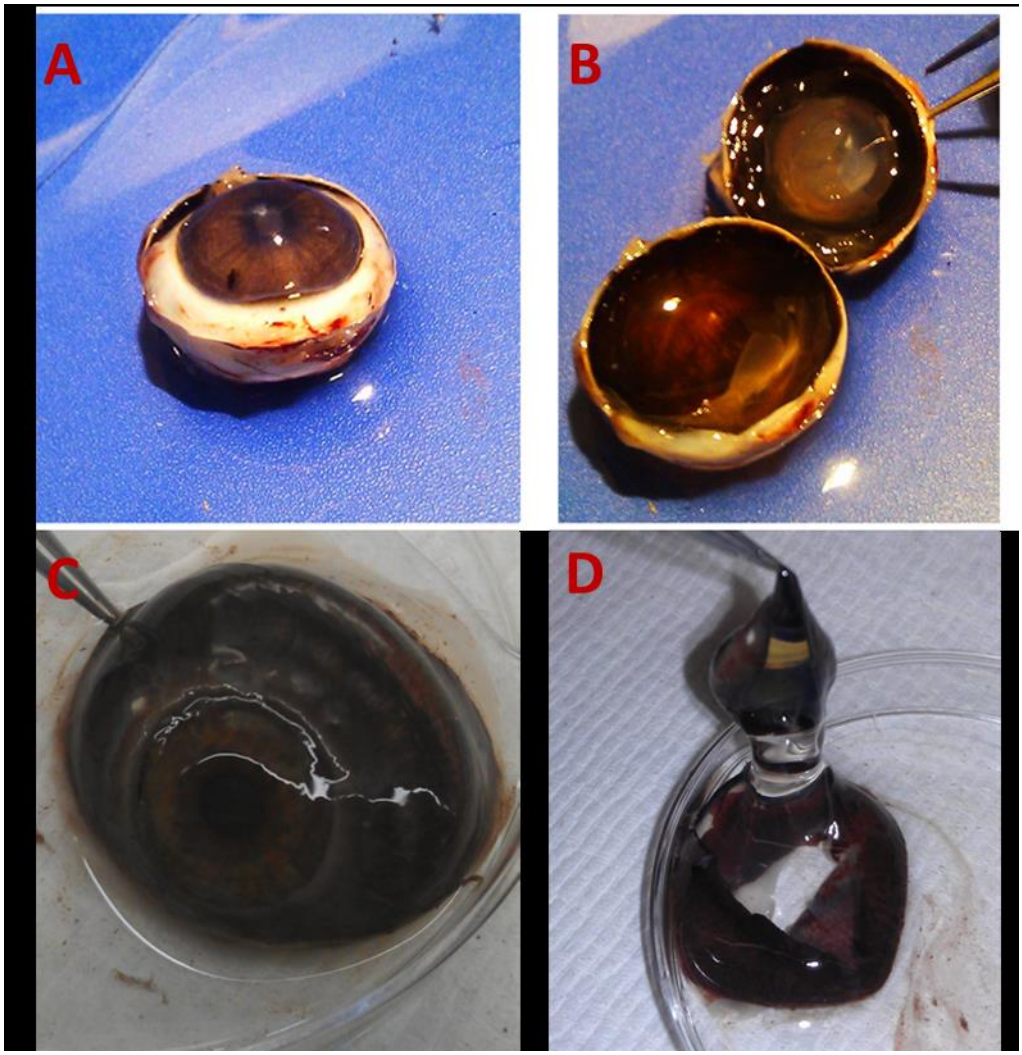

Figure 5.4: Preparation and isolation of ocular tissue post-mortem.
A and B: Dissection of human eye. C: Isolation of choroid and iris.
D: Removal of vitreous

RPE was added to the RNeasy spin column and a further centrifuge for 2 min at ≥8000 x *g* (≥10,000 rpm) was undertaken. The membrane of the RNeasy spin column was then dried by one further centrifuge for 1min. 30–50µl of RNase-free water was added directly to the spin column membrane and a final centrifuge for 1 min at ≥8000 x *g* was undertaken to elute the RNA. DNase (RNase-Free DNase Set, Qiagen, 79254) treatment was applied during RNA isolation to eliminate any genomic DNA contamination of the RNA isolated. This involved 8µl RNA being treated with 1µl of DNAse and 1µl of DNAse buffer at 37^0C for 30 minutes. This reaction was stopped with 1µL stop solution and incubated for 10 minutes at 65^0C.

The concentration of RNA was determined using a spectrophotometer (Nanodrop-1000, Thermoscientific) (see section 2.3.4). RNA was then stored at -80 degrees and thawed on ice before use for RT- PCR.

5.3.1.3. RT-PCR

RNA (1µg) was transcribed into cDNA using AMV Reverse Transcriptase (Roche). The reaction was performed in a final volume of 20 µl consisting of 5 mM $MgCl_2$, 1 mM dNTP, 1 U/µl RNase inhibitor, 0.8 U/µl AMV reverse transcriptase and 80 ng/µl oligo dT-15 primers. The mixture was incubated for 10 min at 25^0C, 60 min at 42^0C, 5 min at 99^0C and 5 min at 4^0C in a thermal cycler (Eppendorf, http://www.eppendorf.co.uk). The cDNA was then either used immediately for PCR reactions or stored at -20^0C.

The cDNA (5 µl) was used for PCR reactions to amplify *ADAMTSL4* using the High Fidelity PCR kit (Roche). The amplification was performed in a final reaction volume of 25µl consisting of 1.5 mM MgCl 2 , 0.2 mM dNTP, 2.5 U Expand HiFi Taq DNA polymerase, 0.4 mM primers in 50 mM KCL (Primers: GCGGCAACAGGTGGCTGTGT and GCCTGGGGCCCTGTGAGAGA), 10 mM Tris/HCl, pH 8.0. The primers were predicted to produce a product of 470base pair (Figure 5.5). The mixture was incubated at 94^0C for 2 min followed by 30 cycles under the following conditions: 94^0C for 30 s, 57^0C for 30 s, 72^0C for 30s and 1 cycle of 72^0C for 5 min. Products were run on 1% agarose gel containing 1 in 15,000 dilution of GelRed (Biotium). GAPDH primers (CCAGTGCAAAGAGCCCAAAC and GCACGGACACTCACAATGTTC) were used as an internal control.

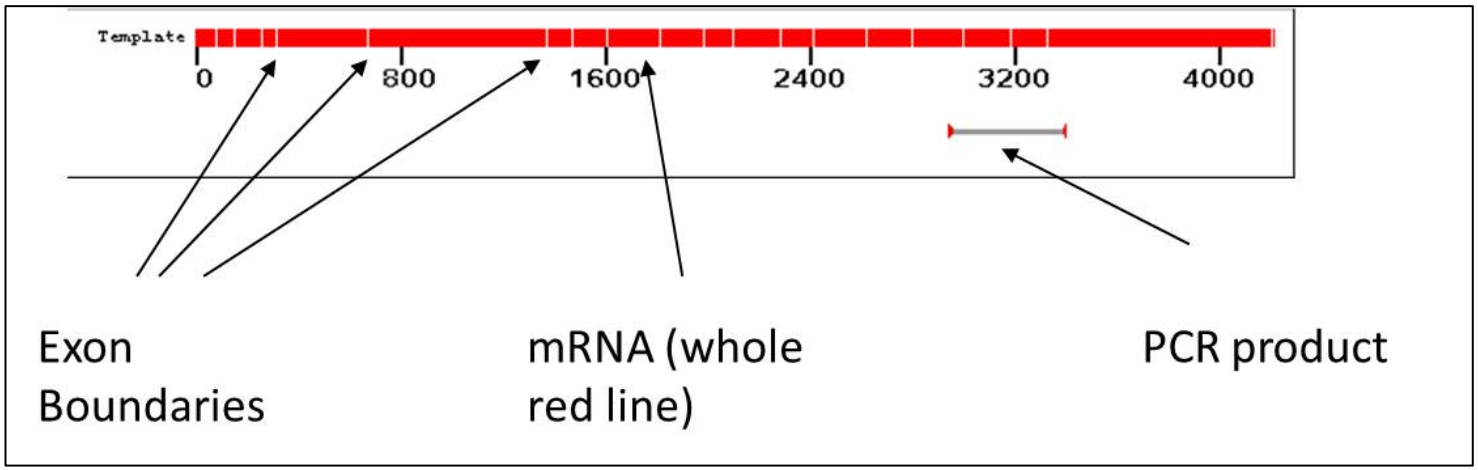

Figure 5.5: *ADAMTSL4* mRNA and product of rtPCR. (http://www.ncbi.nlm.nih.gov/tools/primer-blast/)

5.3.1.4. PROTEIN EXTRACTION

Eye tissues (iris, retina and choroid) were cut with a scalpel on slide in PBS. The tissue was resuspended in 100 µl of ice cold Radio Immuno Precipitation Assay (RIPA) buffer containing protease inhibitors as indicated below. This buffer was used to isolate both nuclear and cytoplasmic proteins. A homogenous suspension was ensured by vigourous pippeting and vortexing. The mixture was placed on ice for 5 minutes to allow the cells to swell and lyse. After then centrifuging for 5 minutes at 8-10,000 rpm to pellet any debris, the supernatant was extracted. This contains proteins of interest and can be collected and stored at -20^0C. In this manner protein was extracted from 3 choroidal tissues, 2 iris tissues and 3 retinal tissues.

5.3.1.4.1. Preparation of RIPA buffer with protease inhibitors

RIPA lysis buffer was prepared just before use. The following were added:

- Protease Inhibitor Cocktail (Sigma) P-8340 (stored at -20^0C). A concentration of 10µl / ml of buffer was used.
- 0.5M DTT (dithiothreitol) (1 µl/ml of buffer (1/1000)) to a final concentration of 0.5mM.
- 0.5M PMSF (Phenyl Methyl Sulfonyl Fluoride) was added (2 µl/ml of buffer (1/500) to a final concentration of 1mM was added.
- 0.6 M Sodium Orthovanadate- $Na_3\ VO_4$ (Phosphatase inhibitor, stored at -20) : 5 µl/ ml (1/200) to a final concentration of 3mM

This was kept on ice till tissues were prepared as above.

5.3.1.5. PROTEIN CONCENTRATION ESTIMATION

Using the Biorad DC Protein Assay Protocol (Bio-Rad, Hemel Hempstead, U.K. www.biorad.com), based on the Bradford assay, protein concentrations were determined The Bradford Assay is based on the dye Coomassie-blue G-250. This is a hydrophobic dye which binds to hydrophobic protein molecules. It exists in two forms, red and blue. When the red form binds to the arginine residues in proteins it absorbs maximally at 595nm, and the blue form of the dye becomes more stable. The absorbance at 595nm is proportional to the protein concentration, which can therefore be quantified.

The method involved the following steps:

First a standard curve was made by preparing 3-5 dilutions of a protein standard containing from 0.2 mg/ml to about 1.5 mg/ml protein. Samples were diluted (1/10 and 1/20). 5 µl of standards and samples were pipetted into a clean, dry microtiter plate. 25 µl of reagent A was placed into each well, followed by 200 µl of reagent B. The plate was mixed for 5 seconds. The samples were incubated at room temperature for 5-15 minutes.

The entire sample and standard were placed into cuvettes. A control level was measured using control samples, and the samples were then measured using a spectrophotometer.

5.3.1.6. WESTERN BLOT ANALYSIS

Western blot analysis was performed using the NuPAGE electrophoresis gel system (Invitrogen, UK). Running buffers were prepared initially. MES SDS running buffer were diluted to 1X (commercially available as 20X). 500 µl of antioxidant was added to 200ml of running buffer. The loading buffer was warmed so as to dissolve the salts. Finally a reducing agent (containing Dithiothreitol) was prepared (used to break disulphide bonds and resolve proteins secondary and tertiary structures).

Proteins samples were prepared such that the volume was 19.5µl at the same concentrations. Thus the lowest concentration in a batch of samples was used as a reference.

The 30µl loading samples consisted of 3µL of reducing agent, 7.5µL of loading buffer and 19.5µl protein sample.

Loading sample was warmed for 10 minutes at 70^0C to denature the proteins further and ensure only the primary structures were present. After centrifuging for 10seconds, the samples were loaded into premade NuPAGE electrophoresis gel (Life Technologies, Paisley, Scotland,http://www.invitrogen.com) for Western blot analysis. A 10%Bis-Tris Gel was used in conjunction with MOPS SDS running buffer (NP0001, Invitrogen, UK). This was used as the protein size we expected was 140kDa. Protein samples were loaded into 15 well gels. These were then fitted into the XCell *Sure*Lock™ Mini-Cell mini vertical electrophoresis system (Invitrogen, UK). After closure of the chamber, running buffer with antioxidant was added, and the gel was run at 200V for 50 minutes.

Whilst the gel ran, transfer buffer was prepared (400mL of 1 in 20 dilution with 60mL of 15% methanol). Transfer membranes (Polyvinylidene Fluoride (PVDF) – Hybond-P # RPN303F, Amersham, Little Chalfont, U.K. http://www.gelifesciences.com) were soaked in methanol for 2 minutes, proceeded by washing in distilled water before being transferred to the transfer buffer. The transfer was then carried out at 35V for 90 minutes.

Membranes were blocked in Tris Buffered Saline with 0.1% Tween-20, 5% skimmed milk and 3% FBS at 37^0C for 1 h. Primary antibodies Anti-ADAMTSL4 (HPA006279; Rabbit; 1 in 100, Sigma Life Sciences, USA. http://www.sigma-aldrich.com) and β-actin (1:5000; monoclonal; Sigma)) were diluted in blocking buffer**.** Membranes were incubated overnight at 4^0C with the primary antibodies, before incubation with a secondary antibody conjugated with Horseradish peroxidase (1:10,000, Jackson Laboratories http://www.jacksonimmuno.com) for 1 h at room temperature. On removal of the secondary antibody, the membrane was washed again over an hour with TBS with 0.1% Tween 20, and Blots were visualised by chemiluminescence using ECL advanced detection reagent (GE Healthcare http://www.gelifesciences.com).

5.3.1.7. IMMUNOFLUORESCENCE STAINING OF TISSUE

Whole eyes were fixed in 4% Paraformaldehyde for 10 min and cryoprotected with 30% sucrose. After imbedding tissue in Optimum Cutting Temperature compound (OCT; TissueTek MSDS), cryostat sections were prepared (Figure 5.6). Sections were prepared of approximately 15μm thick, and placed on Superfrost Plus Slides. Blocking agent was prepared in advance (0.5% in PBS, microwaved for 10s and shaken further till uniform cloudy appearance was present). Slides were blocked for 1 hour in this Blocking Solution. Primary antibodies were diluted in the blocking reagent and incubated with the cells overnight at 4^0C in a humidified chamber. The primary antibody used was Anti-ADAMTSL4 (HPA006279; Rabbit; 1 in 100, Sigma Life Sciences, USA. http://www.sigma-aldrich.com). In parallel, an incubation with only secondary antibody was included to control for background staining of this antibody. Specific binding of primary antibodies was detected using secondary antibody; donkey anti-IgG labelled with Alexa Fluor 448 or 668 (Molecular Probes, Invitrogen) reacting with Rabbit; (the species in which the primary antibody was raised) for 1 hour at room temperature in the dark.

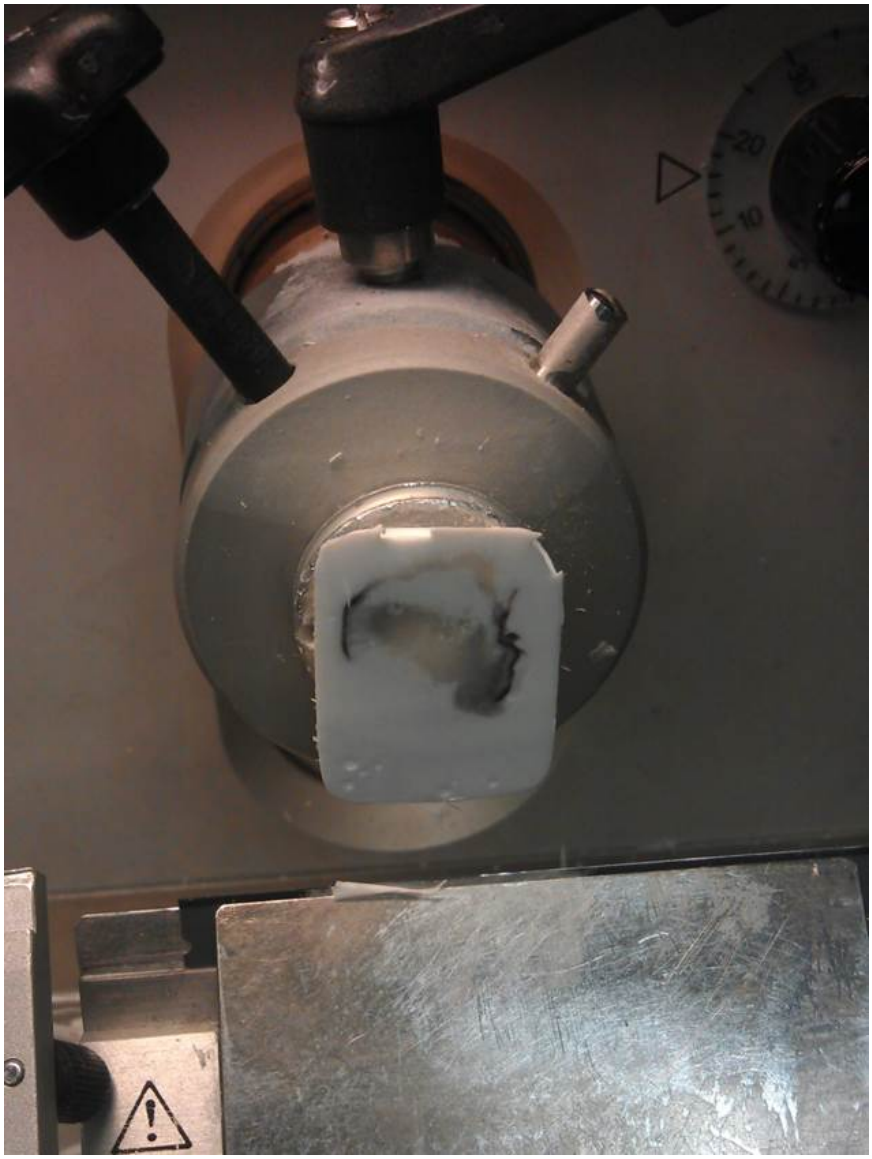

Figure 5.6: Cryostat preparation of eye fixed in Optimum Cutting Temperature compound. Anterior segment structures (lens) visible

Slides were then washed with Tris Buffered Saline (TBS), before incubating with DAPI (Sigma) to visualise cell nuclei and mounted using Vectashield (Vector Laboratories, U.S.A. http://www.vectorlabs.com). Fluorescent images were recorded using confocal microscopy (Leica TCS SP2 AOBS, Leica, Germany http://www.leica-microsystems.com) using a 40x oil objective. Images were analysed using the Leica Confocal software.

Corresponding sections to those fluorescently labelled were also stained with haematoxylin and eosin to further illustrate morphology, using the following protocol:

The slides were immersed in isoparaffinic hydrocarbon (Safeclear) for 10 minutes, 5 minutes and 1 minute. They were then immersed in alcohol at 100% for 1 minute then alcohol 70% for a further 1 minute. This was followed by washing in running water to remove any residual alcohol They were stained in Gill's 3 haematoxylin for 5 minutes, washed in running tap water for 2 minutes, differentiated in acid alcohol for 8 seconds, placed in lithium carbonate 1% for 1 minute, then washed in running tap water for 1 minute. Following this they were counterstained in eosin (1%, made up in tap water) for 3 minutes then washed in running tap water for 30 seconds. The slides were then immersed in 90% alcohol for 30 seconds, then 4 changes of absolute alcohol for 2 minutes each, then immersed in isoparaffinic hydrocarbon for 5 minutes, 2 minutes and 1 minute. The slides were drained briefly on a tissue, then the sections were mounted in Safeclear mountant and covered with a coverslip.

5.3.2. PROTEIN MODELLING

The most definite methods of understanding the structure of a protein is crystallography, mostly via X-ray, Nuclear magnetic resonance (NMR) spectroscopy or 3 dimensional electron microscopy. There are over 70,000 proteins and peptides with such structures now deposited on the PDB[748]. However, this is laborious and expensive. Although ab initio protein modelling is undertaken, the prediction of many proteins by comparative modelling is considered more accurate[747]. It involves predicting the structure of an unknown protein (target) based on homology to known structures (template).

Successful protein model building requires four basic steps. Firstly, a template must be identified. This template should have an experimentally determined 3D structure. For it to act as a template, it should show significant amino acid sequence similarity

(homology) with the candidate protein sequence. Homology refers to both sequence identity and residue properties (such as hydrophobicity). The predictive modelling is then grounded on the assumption that residues will conform to a similar structure in two different proteins or domains based on a similar linear amino acid sequence. The three dimensional structure of proteins in a same family can be more conserved than their linear sequence[749]. Therefore, if there is sequence similarity, some structural similarity may be assumed[747]. Specifically, it is generally accepted within the structural community that within a stretch of at least 80 amino acids, 30% sequence homology is the minimum needed prior to modelling an unknown protein sequence by comparative modelling[19]. Choosing the template can be based on amino acid sequence-sequence homology[750]. Alternatively, the selection can be more iterative, and involve not only amino acid sequence, but also evolutionary history, residue characteristics, and domain and protein family function[751]. Other factors such as the function of the template and the target, and the quality of the templates crystallography structure should be considered. Frequently, proteins are divided into domains which may have homology or evolutionary relationships with domains on templates. We used Protein BLAST (blast.ncbi.nlm.nih.gov/Blast.cgi?PAGE=Proteins) and CLUSTAL[752] to generate templates.

Subsequently, the target and template sequence are aligned. In doing so, statistical analysis can be undertaken to evaluate the homology. There are various methods of model building which are equally accurate if used optimally. We used MODELLER[6], which is based on restraining the predicted structure based on distances and angles of residues in the template protein. Further constraints based on molecular mechanics of bonds are also superimposed. A major advantage of this method is that constraints or restraints from numerous sources may complement those of the homology driven restraints. This may add accuracy to and improve the quality of the model, particularly in more challenging modelling cases.

Models then need to be evaluated, and there are a variety of programs which may do this. They assess if the model has the correct fold. This is primarily reliant on sequence homology, as the greater the homology (particularly over 30%), the greater the chance of structural similarity. Evaluation also assesses the environment of predicted domains. For example calcium binding domains may undergo conformational structural changes when bound to calcium. If modelled on similar domains without calcium bound, the

model is likely to be inaccurate. Finally, bond stereochemistry (e.g. bond length, torsional bond angle, side chain torsion angles) are evaluated in the model. These were done with a programme called PROCHECK[753]. This compares every bond structure, particularly angle and distance, to a database of all bonds (Ramachandran plot[754]). To assess the feasibility of the model based on amino acid charges and ionic repulsions, the software CHARMM (Chemistry at HARvard Macromolecular Mechanics)[755] was used. Adjustments to the model structure in conjunction via both programs, before the final structure is created.

5.4. RESULTS

5.4.1. GENE EXPRESSION AND PROTEIN DISTRIBUTION

5.4.1.1. GENE EXPRESSION OF *ADAMTSL4* IN OCULAR TISSUE

Amplification of cDNA derived from iris, choroid and retina, using primers targeted at *ADAMTSL4,* gave a product of 470bp (consistent with that expected from the designed primers). The product was observed in both choroidal and iris tissue, but was absent from retinal tissue (Figure 5.7A). Band quantification using ImageJ software [756], revealed a significant difference ($P<0.01$) in product band intensity between choroidal and retina tissue (Figure 5.7B). These findings suggest that mRNA expression of *ADAMTSL4* is abundant within the choroid but absent within the retina.

5.4.1.2. PROTEIN EXPRESSION OF ADAMTS-LIKE 4 IN OCULAR TISSUE

Western blot analysis of choroidal, retinal and iris extracts using ADAMTS-Like 4 antibody, revealed a product of 140kDa from choroid and iris tissue, which was absent from retina (Figure 5.8A). This product has previously been suggested to be the major species of this protein within ocular tissue [406]. Quantification of band intensity showed the greatest abundance in the choroid but absent from the retina (Figure 5.8B). Although not a significant difference ($P=0.06$), this trend was consistent with the RNA expression work.

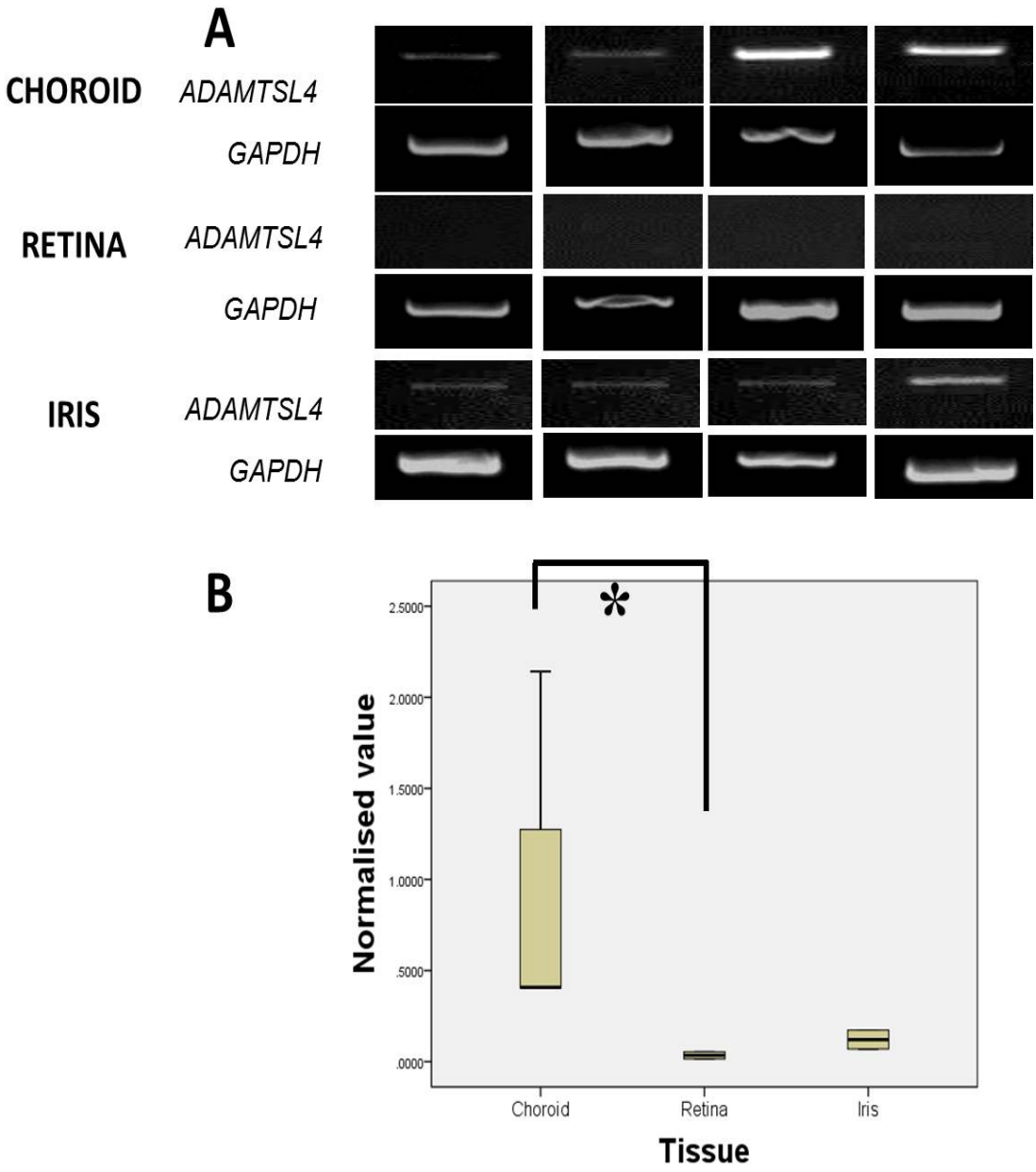

Figure 5.7: GENE EXPRESSION OF *ADAMTSL4* IN OCULAR TISSUE

Figure 5.7A: Expression of *ADAMTSL4* and *GAPDH* (control) mRNA from ocular tissue of four donors. A product of 600bp for *GAPDH* was obtained from all samples, but the 470bp product for *ADAMTSL4* was obtained only in iris and choroid and is absent from neural retina.

Figure 5.7B: Quantification of *ADAMTSL4* expression in choroid, retina and iris. The above bands were analysed by Image J and showed a statistically significant ($P<0.01$) [indicated by *] difference between the choroid and retina.

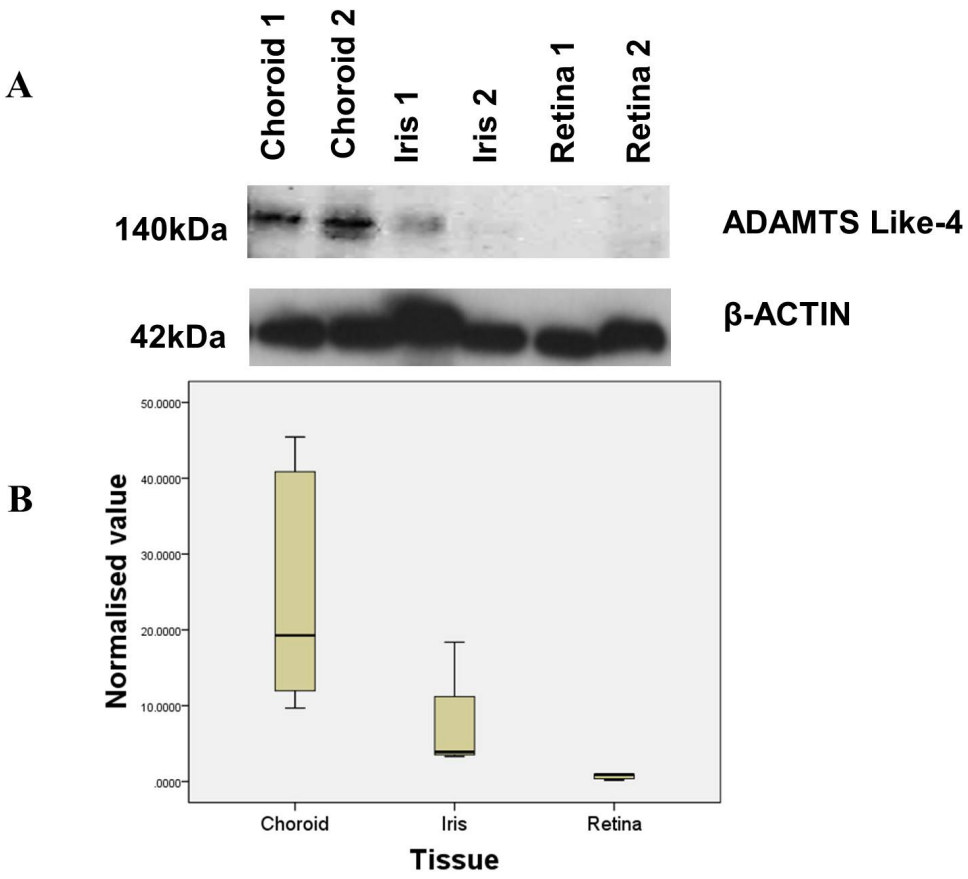

Figure 5.8: ADAMTS-LIKE 4 PROTEIN EXPRESSION IN OCULAR TISSUE

Figure 5.8a: Western blot illustrating a product of 140kDa within choroid and iris. This is thought to be the size of the major species of ADAMTS-Like 4.
A product of 42kDa, consistent with β-Actin, was seen in all three tissues (choroid, iris and retina).

Figure 5.8b: Quantification of western blot band intensity from choroid, iris and retina. This suggests ADAMTS-Like 4 expression to be greatest in choroid, intermediate in iris, and least within retina.

5.4.1.3. LOCALIZATION OF ADAMTS-LIKE 4 PROTEIN IN OCULAR TISSUE

Immunofluorescence (IF) staining demonstrated that ADAMTS-Like 4 is widespread within the eye. It is clearly evident within the ocular anterior segment, particularly in the ciliary body and processes (Figure 5.9a). Ocular posterior segment investigations suggest that ADAMTS-Like 4 localises within the choroid, RPE and the retinal outer segments (Figure 5.9b). Control ocular tissue without primary antibody did not stain (Figure 5.9c). These results corroborate the findings from the protein and mRNA expression work.

5.4.2. PROTEIN MODELLING

To fit with the required 30% sequence homology, two different templates were used. Firstly, the structure of the Exosite-Containing Fragment Of Human ADAMTS13 (Protein Database ID = 3GHM), showed between 29-60% homology to the specific regions of the ADAMTS-Like 4 molecule.

Subsequently, the Thrombospondin homologous region was aligned to another template; the Thrombospondin-1 TSR Domains 2 And 3 (Protein Data Base ID : 3R6B)[757]. This template showed approximately 33%-57% sequence homology to specific areas of the ADAMTS-Like 4.

The regions of strong homology are therefore non-contiguous. Figure 5.10 shows the regions where amino acid sequence homology to known structures in the PDB databank is found. The best homologies are to the protein 3GHM, which is the Crystal Structure Of The Exosite-Containing Fragment Of Human ADAMTS13[745]. However, sequence homologies to other structures are also found in other parts of the protein as described in the legend.

Although sequence homologies are found to the above proteins (Figure 5.10), they bear no relationship to the family of proteins to which ADAMTS-Like 4 belongs.

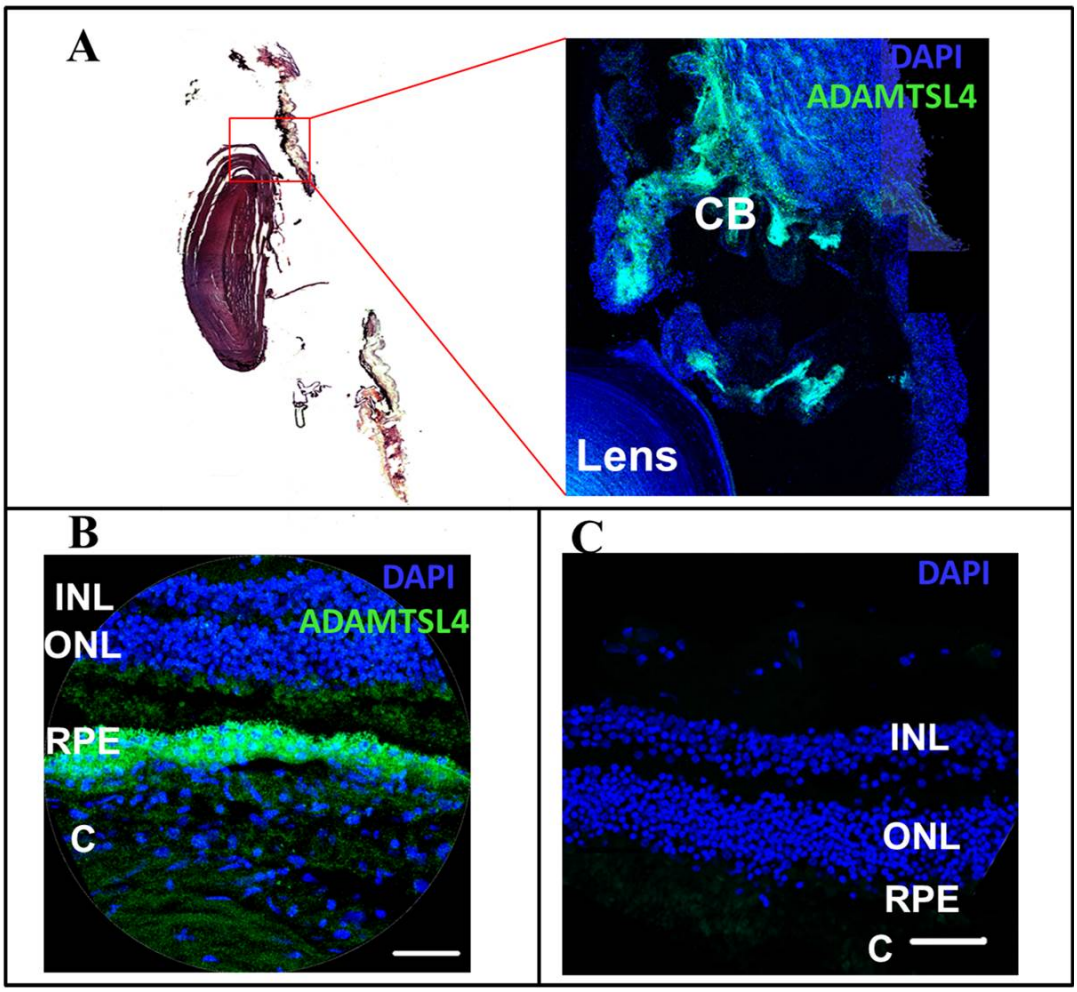

Figure 5.9: LOCALISATION OF ADAMTS-LIKE 4 PROTEIN IN OCULAR TISSUES

Figure 5.9a: Immunofluorescence of anterior segment tissues illustrating expression within ciliary body and processes. CB: Ciliary Body.

Figure 5.9b: Immunofluorescence of ADAMTS-Like 4 within ocular posterior segment illustrating presence within choroid and retinal pigment epithelium.

Figure 5.9c: Immunohistochemistry of control ocular tissue (without primary antibody). Bar: 50µm

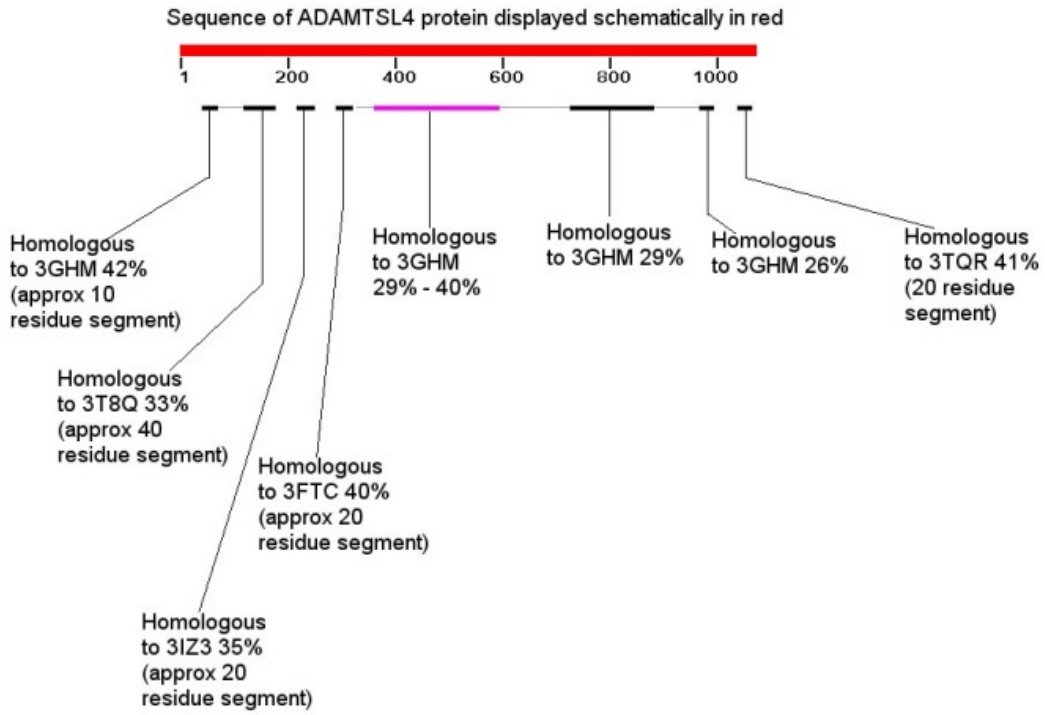

Figure 5.10: Schematic diagram demonstrating sequence homology to other known structure. 3GHM: Protein database ID (PDID) for ADAMTS13 (http://www.rcsb.org/pdb/explore/explore.do?structureId=3GHM).
3T8Q: PDID Crystal Structure Of Mandelate racemase muconate lactonizing enzyme Family Protein From Hoeflea Phototrophica (a marine aerobic alphaproteobacterium[12].
3IZ3: CryoEm Structure Of Cytoplasmic Polyhedrosis Virus[13].
3FTC: Structural Model For The Large Subunit Of The Mammalian Mitochondrial Ribosome[15]).
3TQR: Structure of the Phosphoribosylglycinamide Formyltransferase (Purn) In Complex with CHES from Coxiella Burnetii (http://www.rcsb.org/pdb/explore/explore.do?structureId=3TQR))

Thus, modelling such areas based on these proteins as a template is technically possible; however the interpretation of the results subsequently would be open to debate. Whilst sequence normally determines the nature of the protein fold, one should also take into account the family of proteins that it is being compared with. Large areas of the protein encompassing the mutation prone areas[2, 7, 10, 27, 30], such as the mutations described in chapter 2, have no sequence homology to any proteins in the database; these are represented by the broken line areas. Furthermore, there would be no empirical evidence to show that those areas would fold or adopt structures as the purely mathematical/theoretical methods predict. These areas in principle could be also assigned structural coordinates using ab initio theoretical modelling procedures

The areas modelled are illustrated in Figure 5.11.

5.5. DISCUSSION

5.5.1. GENE EXPRESSION AND PROTEIN DISTRIBUTION

Whilst completing this project investigating the distribution and expression of ADAMTSL4, a publication emerged investigating a similar expression profile and relationship with fibrillin-1[406]. It was of great interest, and provided valuable comparisons.

The described work in this chapter has shown, by both western blot and IF analysis, that ADAMTS-Like 4 is expressed in choroid and iris, but is absent from retina. This finding is in slight contrast to the protein expression pattern suggested by Gabriel and colleagues, whose immunohistochemical (IHC) staining showed a broad distribution of ADAMTS-Like 4 in many ocular tissues including the ciliary body, sclera, cornea, and retina, and associated with both cells and fibrillar ECM [406]. This difference, where retinal localisation was not found by IF, is most probably due to either the use of different antibody in this study, or to the method (IF) possibly being more specific than IHC (used by Gabriel *et al*[758]), leading to a limited protein distribution being detected. Confocal microscopy with high resolution imaging does provide better image qualities than is possible from chromatic immunohistochemistry. The major disadvantage of IF is the stability of the images is shorter, therefore providing no long term record, as it is available through IHC. The findings of a lack of protein expression in the retina are also supported by a lack of mRNA expression in the retina, which was not undertaken by Gabriel and colleagues[758].

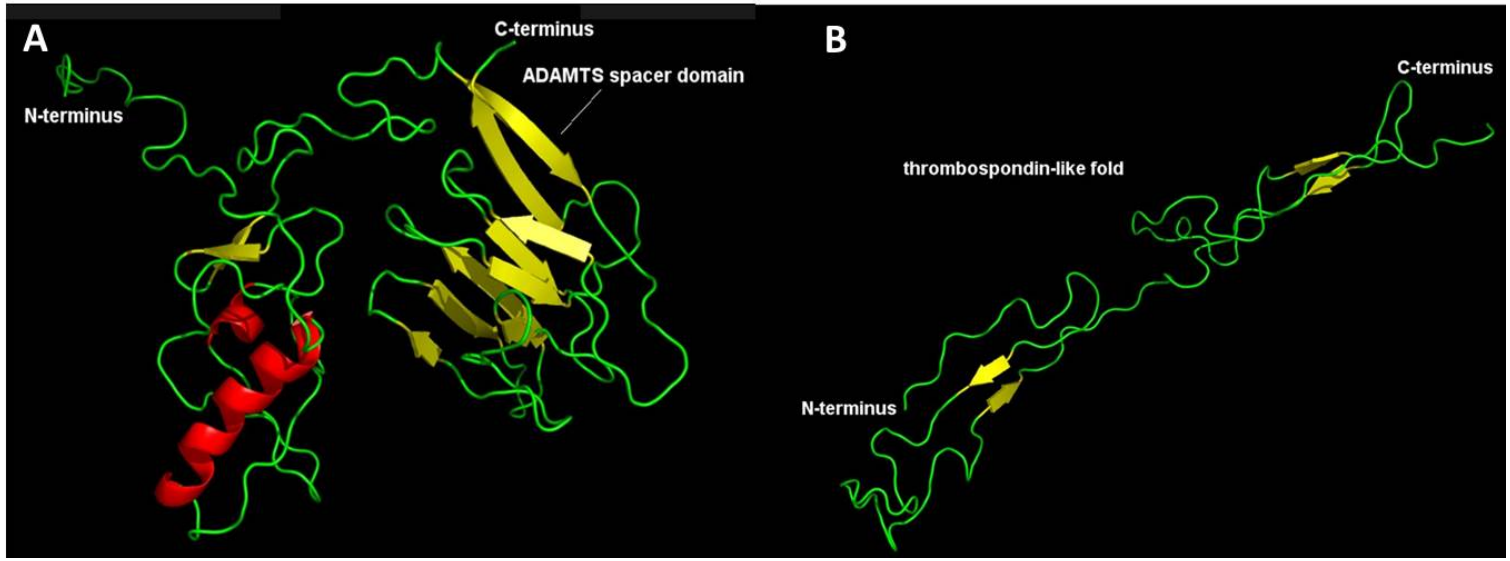

Figure 5.11: Model of ADAMTS-Like 4

A) Homology representative model of the ADAMTS-Like 4 protein between residues 353-602. Modelling was carried out using MODELLER v.6[6], using 3GHN as a template. This requires at least 30% sequence homology to known proteins[19] Here, the region known to be homologous to the "ADAMTS spacer domain" is represented as a series of beta-pleated folds (in yellow).

B) The thrombospondin-like fold within the ADAMTS-Like 4 protein.

This does provide further evidence, as it is recognised that mRNA levels are correlated with protein expression levels[759].

We could not demonstrate ADAMTS-Like 4 presence in the retina by western blot as was achieved by Gabriel *et al*., however, although their pure retina sample did demonstrate clear bands, another sample of mixed vitreous and retinal tissue did not, possibly suggesting sample variation. It is therefore arguable that, contrary to the previous findings, this gene is not expressed in the retina. The work in this chapter did not attempt to quantify values, and the PCR bands cannot therefore reflect the intensity of IF.

Considering the shared phenotype caused by mutations in *ADAMTSL4* and *FBN1*, it is a reasonable hypothesis that an interaction exists between fibrillin-1 and certain ADAMTS proteins in which mutations cause EL. The identification of a very similar ocular phenotype within WMS with *FBN1* and *ADAMTS10* and *ADAMTS17* (OMIM 607511) mutations [225] first suggested an interaction between the proteins. It has been postulated that ADAMTS10 not only co-localises with fibrillin-1, but also participates in microfibril biosynthesis [281]. Certain domains of fibrillin-1 were thought to interact specifically with certain ADAMTS-Like proteins [432]. Furthermore, ADAMTS-Like 6 was first shown to promote fibrillin-1 matrix assembly [760] and one isoform (ADAMTS-Like 6β) even improves fibrillin-1 microfibril assembly in a mouse model of MFS [718]. ADAMTS-Like 4 and ADAMTS-Like 6 being closely homologous, it is therefore possible that a similar interaction between ADAMTS-Like 4 and fibrillin-1 exists. In support of this, Gabriel and colleagues have demonstrated co-localisation of ADAMTS-Like 4 and fibrillin-1 in cultured fibroblasts [406]. They also suggest that ADAMTS-Like 4 may play a role in formation or maintenance of fibrillin-1.

This chapter demonstrated expression of *ADAMTSL4* and its protein within human iris and choroidal tissue but not in retinal tissue. Although fibrillin-1 has been demonstrated throughout various ocular tissues [193, 761, 762], the retina has not convincingly been shown to be a fibrillin-1 containing structure. In view of suggested co-localisation of fibrillin-1 and ADAMTS-Like 4 [406], this would be in line with the present finding of an absence of the latter in the retina. In contrast, fibrillin-1 has been shown to be present in the iris and choroid [193], and these results suggest that ADAMTS-Like 4 is also present within these tissues. Although it was not possible to isolate ciliary body and zonules for western blot analysis, our IF results do confirm the presence of ADAMTS-

Like 4 within the ciliary body. It is however of interest to consider Cain and colleagues' work [763]. They dissected microfibrils from various tissues, including human zonules, and used mass spectrometry to investigate the protein constituents beyond fibrillin-1. They discovered, in addition to fibrillin-1 and MAGP-1, that there were collagens II and IV, α- and β-crystallins, annexin V, TIMP-3 and histones. They however did not determine ADAMT-Like 4. This work was published before the identification of the role of *ADAMTSL4* mutations in EL[2]. It would be of interest if this were repeated, in light of our current understanding.

The relative abundance in the choroid is of great interest. It is well documented that fibrillin microfibrils are constituents of arterial walls[764], and although the same level of evidence is limited for ocular vasculature[193], it is probable that a similarly high expression is found in choroidal vasculature. The highly vascular component of the choroid may thus also be the host to ADAMTS-Like 4. It would be interesting to know if this choroidal expression is affected in view of the axial myopia demonstrated in those with *ADAMTSL4* mutations in chapter 2 of this thesis. Certainly, choroidal thickness is inversely related to axial length and may contribute towards myopic degeneration [765].

Finally, the present IF results suggest ADAMTS-Like 4 expression within human RPE, which has also been shown to express fibrillin-1[193]. It has been suggested that ablation of the RPE leads to arrested ocular development[766]. Mutations in genes expressed in the RPE, such as *VMD2*[161][767], and *MFRP* [768], have been shown to affect eye development and axial length. The mechanism behind this phenomenon is unclear. A similar role may be played with regard to ADAMTS-Like 4, its RPE localization, and increased axial length in patients with mutations in its gene. This would need to be confirmed.

It is probable that ADAMTS-Like 4 has additional roles to its suggested effects on the structure and function of ciliary zonules. Indeed, the possible pleiotropy of ADAMTS-Like 4 has been suggested by the GWAS pathway (section 4.5.2) and the patient described in section 2.4.5[301]. Furthermore, there have been reports investigating the expression of this protein in ocular tissue, beyond the work on cDNA libraries done by initial investigators[2]. Schwenk and colleagues[769] investigated plasma and serum protein profiles of patients with Metabolic Syndrome using an antibody array based approach. They demonstrated higher levels in both serum and plasma of ADAMTS-

Like 4 in patients with high HDL cholesterol and low triacylglycerol and suggested that it may be utilized as a clinical biomarker. Juric and colleagues demonstrated differential expression of *ADAMTSL4* in different subgroups of Acute lymphoblastic leukaemia patients[719]. They suggested that the cell adhesion modulation role of ADAMTS-Like 4 may lead it, amongst others, to be a candidate gene likely to play a role in certain leukemogenesis. The implications of these two papers need yet to be understood fully.

As previously described, the other *ADAMTS* genes associated with similar ocular phenotypes (*ADAMTS10*[225], *ADAMTS17* [226] and *ADAMTS18* [1]) (Table 9) all contain Thrombospondin repeat (TSR) regions and a protease and lacunin (PLAC) domain[21]. The role of the TSR domain in cell adhesion has been discussed. Additionally, mutations in *ADAMTSL4* affecting the PLAC domain have been reported by our group in IEL [7], which may suggest that it too may have a role to play in this function. .

In summary, the present observations have confirmed the gene and protein expression of ADAMTS-Like 4 in the human iris and choroid, but could not demonstrate expression in the retina. Taking these findings together with published expression patterns of fibrillin-1; it may be possible to suggest that ADAMTS-Like 4 and fibrillin-1 be closely related functionally. Closer inspection of other ocular and non-ocular tissue known to manifest fibrillin-1 may further elucidate the relationship between these two proteins in pathological conditions associated with mutations in these genes.

5.5.2. PROTEIN STRUCTURE

Comparative or homology modelling is a highly accurate method of structure prediction[747]. We undertook this using known structures available on PDB, and then used MODELLER[6] to undertake homology modelling. The model was then evaluated using PROCHECK[753] and CHARMM[755].

The protein modelling was limited by incomplete sequence homology. The closest protein with crystalline structures was ADAMTS13. This protein's structure itself has not been completely described[745]. We were however able to model the TSR domain. In our modelling, this was based on high sequence homology with Thrombospondin 1, TSR domains 2 and 3[757]. As described previously, this domain may play an important role in adhesion of the ECM.

When considering the TSR domains, it is of interest, to discuss the role of *B3GALTL* in Peter's Plus anomaly, an autosomal recessive condition characterised by developmental defects of the brain, skeletal system and the anterior segment of the eye (OMIM 261540)[770]. The cause of Peter's Plus anomaly has been suggested to be secondary to mutations in *B3GALTL*[770]. The encoded protein beta1,3-glucosyltransferase (B3GALTL) is thought to act to join a glucose (Glc) moiety to O-linked fucose (Fuc) forming a glucose-β1,3-fucose disaccharide [771]. This has been shown to specifically occur in Thrombospondin Type 1 Repeats (TSR1)[25]. The list of proteins with this domain includes, amongst others, Thrombospondin 1, ADAMTS-Like 1 and ADAMTS13. The region of this interaction is shown in the Figure 5.12.

Although this particular motif is not found in the ADAMTS-Like 4 protein sequence, there is high homology within the domains encoding the TSR domains (Figure 5.13) between ADAMTS-Like 4 and the template protein 3R6B.

However, no complete homology was found for these motifs. It is possible therefore that 3 dimensional structure of the TSR region of ADAMTS-Like 4 is different to those TSR regions which are crucial to the function of B3GALTL. It is unlikely that the same interaction is involved in ADAMTS-Like 4, and the mechanism of disease development different. However, the role of TSR domain in developmental disorders of the anterior segment of the eye bears considering, in view of the disease manifestation of mutations in *ADAMTSL4* and *B3GALTL*.

Other suggested roles of the TSR domain include regulating matrix metalloproteinase 2 (MMP2)[720]. The substrates of MMP2 include Gelatin, collagen IV, V, VII, XI and fibronectin. This and other MMPs have been demonstrated in the vitreous[721] and subretinal fluid[772], and may play a role in the development of RD[722]. To understand the role of TSR proteins, including ADAMTS-Like 4, in the development of RD, it would be important to identify the presence of this protein and the expression of the gene in the vitreous of eyes affected by this condition. Our model of the TSR in ADAMTS-Like 4 may help the understanding of this domain in the future.

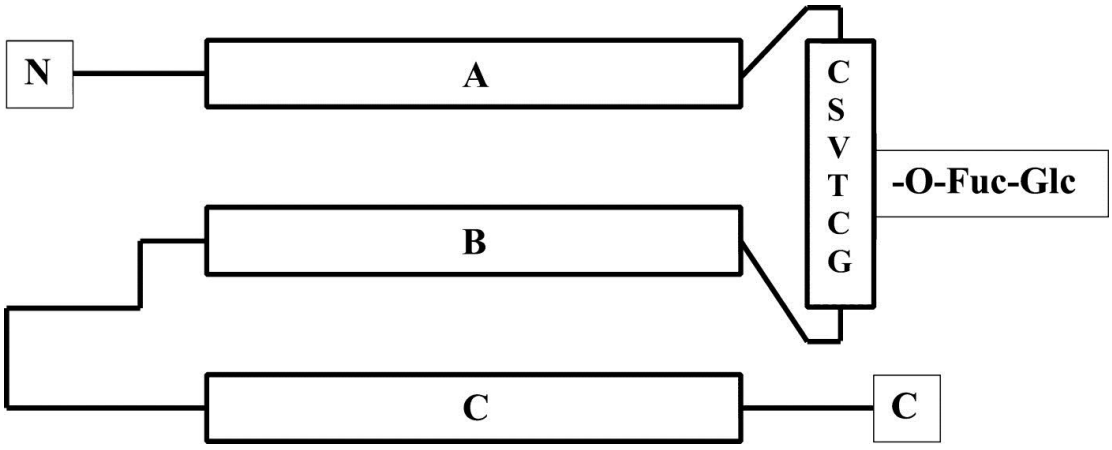

Figure 5.12: The thrombospondin type 1 repeat (TSR). *(Adapted from Heinonen et al [25]).* This demonstrates the secondary structural elements, showing the three antiparallel strands as horizontal rectangles (A, B, and C). The loop between strands A and B contains the sequence motif, indicated by the amino acids inside the vertical rectangle, to which the Glc-Fuc disaccharide is attached. Glc=glucose; Fuc=fucose.

Figure 15.13 The TSR residue of ADAMTS-Like 4 and 3R6B.
Between the two sequences is the highlighted homology (17/36: 47.2%)

We modelled the ADAMTS-spacer domain. This domain, which is adjacent to a cysteine rich domain (CRD), is part of the “ancillary domain” of all ADAMTS proteins[21]. Within the ADAMTS proteases, this CRD-spacer domain is an ECM binding domain[773]. This may have a crucially similar role within ADAMTS-Like 4.

Although the limitations of comparison modelling are noted[774], there are numerous examples of applications of results from predictive modelling. These have included designing mutants to examine hypothesis of the function of a protein[775], modelling substrate specificity[776] and protein-protein interactions[777]. Although we were unable to model domains affected by mutations in the gene, we have been able to provide some information on crucial structures of the protein. These would provide avenues for future understandings of the function and interactions of ADAMTS-Like 4.

CHAPTER 6: GENERAL DISCUSSIONS & FUTURE WORK

This work aimed at understanding further the genetic predispositions towards Rhegmatogenous Retinal Detachments (RD) and Ectopia Lentis (EL). They have been known to be associated conditions for many years, but rarely studied in parallel. There have been significant challenges faced in this process, collaborations forged and much learned and added to the understanding of these conditions.

6.1. CHALLENGES

As with any study, there were administrative and logistic challenges. Gaining ethical approval for the multiple stages of the research was a novel undertaking, and the experiences will continue to help in my research career. Ethical approval was acquired for four separate projects.

The daily commitment of recruiting patients from the vitreoretinal clinics and emergency service and advertising the project proved successful eventually. Choosing the DNA extracting facility and arranging the administration between the research unit and KBioscience took many months to establish. It was forced by the inadvertent failure of a freezer in the UCL Institute of Ophthalmology; where 236 blood samples had defrosted. Fortunately, this had not impacted the DNA quality. Samples from then were transferred directly from the vitreoretinal service at Moorfields Eye Hospital to KBiosciences.

During the PhD, I was fortunate to be working in five different units on these projects. These were at Moorfields Eye Hospital vitreoretinal research unit; MRC Human Genetics Unit, University of Edinburgh; Sonalee Laboratory, St George's University of London; Department of Genetics (Professor Andrew Webster's laboratory) and the Division of Ocular Biology and Therapeutics (ORBIT; Professor Astrid Limb's laboratory), both of UCL Institute of Ophthalmology. The challenges of combining these five units, both geographically and logistically were not insignificant. However, as a consequence, I was privileged to work with different scientists, technicians, statisticians and supervisors. I also learned many different techniques.

Writing grant applications is an important skill in academic medicine. I practiced the art of this during my PhD. I was fortunate to be a co-investigator on a successful grant (Fight For Sight; Grant Number 1982) and ultimately a principle investigator on a further successful grant from the Royal College of Surgeons of Edinburgh (Major

Project grant) to fund the Illumina HumanExome BeadChip genotyping. These skills will continue to improve, and I hope to grow to be more successful in such ventures in my career.

Successful research also depends on successful collaborations. With regard to the genetic predispositions of complex conditions large such networks are crucial. I have personally forged such collaborations with the MRC Human Genetics Unit (University of Edinburgh, UK), Department of Ophthalmology at Guy's and St Thomas' Hospitals (King's College London, UK), Department of Ophthalmology at Addenbrookes Hospital (University of Cambridge, UK), Calgary Retina Consultants (University of Calgary, Alberta, Canada) and the Department of Ophthalmology at Royal Victoria Eye and Ear Hospital (University of Melbourne, Victoria, Australia). With regard to the Mendelian work in this thesis, collaborations have been established with Department of Ophthalmology, Ninewells Hospital Dundee; Department of Clinical Genetics, Guy's and St Thomas' Hospital London; Department of Clinical Genetics, St George's Hospital London; Dept. of Ophthalmology, Justus-Liebig-University, Giessen, Germany; and the Department of Genetics, Alfaisal University Riyadh, Saudi Arabia. Developing these relationships has been of great professional satisfaction, and I hope that these collaborations will continue to foster successful research.

6.2. SUCCESSES

The understanding of the *ADAMTS* proteins has been extended by this work. *ADAMTSL4* was first described ten years ago; in 2003. In 2009, the role of this protein in EL was first described, and since then the importance of this gene has been greatly expanded by this work. We have suggested that some of the ocular phenotypes, particularly corneal features, caused by mutations in this gene are very similar to those with *FBN1* mutations. It has been suggested[758] that ADAMTS-Like 4 co-localises with fibrillin-1 and thus is likely to act to augment the role of this protein. To some extent, the gene expression and protein distribution work in this thesis has provided further evidence for such a co-localisation. However, it must be considered that it is possible that co-localisation does not necessarily equate to co-function. Further work in this thesis does suggest that there may be independent roles for ADAMTS-Like 4; in view of the younger age of onset, and subsequent higher myopia compared to those with *FBN1* mutations. These two features may be related to each other. On the other hand these may be manifestations of the fact that this gene plays an important role in ocular

development. We demonstrated its expression within the RPE, and other proteins present in this tissue are known to affect ocular development and axial length. It would be valid to establish whether a disruption of the ERG or EOG is evident in patients with *ADAMTSL4* mutations. This is work that our group is considering undertaking in the future.

The potential pleiotropic effect of this gene has not been discussed prior to this thesis. We first demonstrate a potential role for mutations in this gene causing defects in the cranial sutures. Whether this is secondary to a role in microfibril development or an independent role remains to be proved. The genome wide association study undertaken as part of this work has been the first to suggest that proteins involved in cell adhesion may play a role in the molecular pathway leading to RD. Among these genes was *ADAMTSL4*. This is a fascinating connection between EL and RD and would need further confirmation. When the data from the Illumina HumanExome BeadChip is ready for analysis, it will be useful to investigate if variants, both common and rare in this gene are significant. If it is replicated; it would be of interest to establish whether the role of this protein in these two separate phenotypes is common. The axial myopia seen in those with *ADAMTSL4* mutations must be remembered and considered when discussing RD.

Alternatively, it is more likely that ADAMTS-Like 4 may have an important function in cell adhesion; particularly involving the ECM. This may play a role in the ciliary zonules for EL, and at the vitreoretinal junction for RD. With regard to such a role, further expression and protein localisation work of *ADAMTSL4* in these structures would be invaluable. Although this work demonstrated no ADAMTS-Like 4 in the inner retina; it would still be worth investigating the vitreoretinal junction; particularly the internal limiting membrane. The cell adhesive function is as yet undefined, but if true, is likely to involve the TSR domain of the protein. The modelling work of this domain done as part of this thesis may thus prove useful in further understanding this function.

It would be important to understand extra-ocular effects of ADAMTS-Like 4. As work in this thesis has demonstrated, the majority of probands labelled as “isolated ectopia lentis” caused by *FBN1* mutations would have their diagnosis altered to Marfan syndrome with the new Ghent criteria. With the suggested co-localisation of ADAMTS-Like 4 with fibrillin-1 and cooperative role in extracellular microfibril

deposition, it would be pertinent to understand if ADAMTS-Like 4 has a role to play in other tissues which are affected by abnormal microfibrils. It is as yet unknown whether patients with *ADAMTSL4* mutations have abnormal cardiovascular and skeletal features, as those with *FBN1* mutations often do. Although it is assumed that this is not the case; confirming this is crucial for these patients, and our understanding of the protein. Our group is currently investigating cardiovascular parameters in our cohort. Beyond this; examining gene and protein expression in cardiac and skeletal tissue would also be enlightening.

The role of other ADAMTS proteins has been additionally extended in this work. Mutations in *ADAMTS17* have been demonstrated in four WML families to date. We have demonstrated a novel exon deletion lesion; which may have interesting implications. The challenges in the investigations of this gene have provided lessons. The expense of mislabelling and possible contamination cannot be overstated, as with the work invested in this family. More work is yet to be done to further evaluate this gene and confirm its role in other families.

Furthermore, we have delineated a novel ocular phenotype; characterised by micro-cornea, cone dystrophy, and a propensity for RD, early onset cataracts and EL. The phenotype has been demonstrated in this thesis to be caused by recessive mutations in *ADAMTS18*. The exact role of the protein in ocular development is unknown, but the wide range of disruptions caused does suggest that this protein has an effect on global ocular development. Further understanding this will take many formats. Establishing localisation and expression of this gene, as was done for *ADAMTSL4* would be useful; as would comparing it to other genes which manifest similar phenotypes. This would include members of the *ADAMTS* family, but also *COL18A1*, which shares many phenotypic features with our cohort. In particular, it would be valuable to understand the role ADAMTS18 may play in the zonules, lens, photoreceptors, RPE and at the vitreoretinal interface. COL18 is known to localise at the ILM, and comparing this with ADAMTS18 would help demonstrate if a relationship exists. The features of RD and EL may indicate a structural role of ADAMTS18; as with other proteins which tend to cause these phenotypes. The phenotypic heterogeneity of those with mutations in *ADAMTS18* does suggest that other epigenetic and environmental factors may be at play.

Traditional theories of the ADAMTS proteins suggest an enzymatic role; however it is possible that certain members have a predominantly structural function. This can be more easily envisaged for the ADAMTS-Like family; which lack the enzymatic domain. The work in this thesis has started to suggest that the function of certain members of these proteins is very different to these traditional beliefs. As with ADAMTS-Like 4, the role of the TSR domain in other members of this family would be particularly interesting. It would be valuable to evaluate the role that variants within these genes may have in complex non-Mendelian RD.

There are common phenotypic features of those with mutations in the *ADAMTS* genes investigated in this thesis. Firstly anterior segment pathology was common; micro-cornea and lenticular abnormalities. Reis and colleagues[446] postulated that there are 12 major genes which cause anterior segment dysgenesis (ASD). It is thought that there is inter- and intra- familial heterogeneity in the phenotypes caused; similar to our families. Furthermore, many of the causative genes are considered to share common downstream pathways. It will be useful to add the ADAMTS family to this list, and investigate for relationships with the established ASD genes. Understanding the role in ocular development could involve investigations in foetal ocular tissue; firstly for gene expression. Comparisons to genes involved in global ocular development (e.g. *OTX2, SOX2, STRA6, HCCS, BMP4, SMOC1, GDF6, VSX2, RAX, SHH, SIX6* and *PAX6)* would also provide interesting insight.

Axial myopia is a further phenotype shared. There are over 20 loci allocated to non-syndromic myopia to date. The aetiologies behind these may be secondary to the early lenticular abnormalities; or direct impact on axial length development. No studies investigating complex myopia have highlighted any of the *ADAMTS* genes.

Further genes are still to be discovered in familial RD and EL. With regard to EL, we have at least one family with isolated EL and three affected brothers in whom no causative gene has been found. The work in this thesis also suggest a recessive mutation causing RD and EL is yet to be found. This family shares phenotype features with Knobloch syndrome (though missing the crucial occipital defect), and with our families with *ADAMTS18* mutations. Having excluded numerous candidate genes, and having suggestive regions of autozygosity, our group is continuing to investigate this family. The first step in this process will involve acquiring samples from other family members; affected and unaffected, to clarify the variants found.

The GWAS on RD has illuminated a potential associated gene. The biological impact of *CERS2* is yet to be fully understood, but does provide avenues of further research. It is a widely expressed gene, and understanding the role at the vitreoretinal junction is challenging. Replication in further cohorts is crucial, and our group is continuing to recruit patients from our own institution, and the numerous institutions with whom collaborations have been made. Prior to this, it will be useful to understand the impact of rare exonic variants when the results of the genotyping using the Illumina HumanExome BeadChip are fully analysed. The quality control of SNVs demonstrated numerous challenges. The realities of using cohorts collected at different times in different centres and comparing with controls separately collected and genotyped are common to all working in GWAS. Successful GWAS have mastered these challenges. The work done will lay a platform for analysis of the common SNVs from the Illumina HumanExome BeadChip. Further steps in quality control are required, prior to association analysis over the next year. It is likely that many positive findings will be highlighted from this first stage of analysis and the large replication cohort will be critical. Our team is continuing to expand the work in this field.

Further work will need to be done to try and delineate if there is any interplay in the genetic aetiology of myopia and RD. Although the genetics of complex myopia has progressed rapidly in the last 5 years, there is still much to be understood. Meta-analyses of the large GWAS into myopia to date, are now underway. These studies have been made possible by multinational collaborations, and comprehending the genetics of RD will also involve such groups; which we have now instigated. Alternate approaches may involve “un-phenotyped” cohorts who self-report a history of RD. This perhaps surprising methodology has proved successful for myopia[603] and may provide a rapid, cheaper method of increasing the power required. Comparing cohorts of myopia and RD may eventually help delineate different pathological mechanisms involved in these two related conditions.

Carefully phenotyping patients in our cohorts will however continue to hold value. Determinants such as axial length will prove useful as a covariate in future analysis to help with the question of myopia. Furthermore, although the genetic aetiology of lattice degeneration[114] and proliferative vitreoretinopathy [778, 779] is under debate, our cohorts will be able to contribute significantly towards the understanding of these conditions.

Finally, the genetic determinants of RD and EL in Mendelian and non-Mendelian inheritance must be taken in the context of the racial origin of those studied. There are many examples of Mendelian mutations aggregating in certain ethnic groups. In complex conditions, the issue of population stratification is critical and has been made previously. Work in this thesis has demonstrated that there are phenotypic differences between Caucasians and South Asians with multifactorial RD. This further underlines the value of phenotyping large cohorts. Not only are the phenotypic features novel, but they also suggest that different genetic determinants and interactions may be involved in alternate ethnicities. Confirming findings such as *CERS2* in our cohort from South Asia will be the first step in this process. Furthermore, those from South Asia may prove to be a valuable cohort to investigate some of the features shown to be more common; such as lattice degeneration.

CHAPTER 7: CONCLUSIONS

The work in this thesis has investigated the genetic predisposition of two closely related ocular phenotypes; rhegmatogenous retinal detachment and ectopia lentis. Using numerous techniques, much has been demonstrated in this field. Although genetic investigations still are divided into “Mendelian and non-Mendelian“, and the techniques used in this thesis are further testament to this division, there is a natural convergence, with the common currency being genetic variation. Unifying groups and methodologies to investigate such conditions with similar and related phenotypes will provide an exciting future in genetics. With the advent of next generation technologies, this future may not be so distant. Although costs are reducing, currently this and the bio-informatic support systems still offer some challenges. As John Hardy, professor of neuroscience at UCL Institute of Neurology, said in 2010 at a round table debate “I am reminded of the great Warren Zevon song ‘Lawyers, Guns and Money’. (We need) Samples, Kit and money”.

As with any scientific endeavour, it seems that in answering some questions, this thesis has created many more. These fields are uniquely placed in their relative novelty, and being part of the groups investigating them will provide great interest for my academic career ahead.

CHAPTER 8: REFERENCES

1. **Aldahmesh, M.A., et al., *Identification of ADAMTS18 as a gene mutated in Knobloch syndrome.* Journal of medical genetics, 2011. 48(9): p. 597-601.**

2. **Ahram, D., et al., *A homozygous mutation in ADAMTSL4 causes autosomal-recessive isolated ectopia lentis.* American journal of human genetics, 2009. 84(2): p. 274-8.**

3. **Jin, M., et al., *Regulation of RPE intercellular junction integrity and function by hepatocyte growth factor.* Investigative ophthalmology & visual science, 2002. 43(8): p. 2782-90.**

4. **O'Sullivan, J., et al., *A paradigm shift in the delivery of services for diagnosis of inherited retinal disease.* Journal of medical genetics, 2012. 49(5): p. 322-6.**

5. **Le Goff, M.M. and P.N. Bishop, *Adult vitreous structure and postnatal changes.* Eye, 2008. 22(10): p. 1214-22.**

6. **Sali, A. and T.L. Blundell, *Comparative protein modelling by satisfaction of spatial restraints.* Journal of molecular biology, 1993. 234(3): p. 779-815.**

7. **Aragon-Martin, J.A., et al., *Role of ADAMTSL4 mutations in FBN1 mutation-negative ectopia lentis patients.* Human mutation, 2010. 31(8): p. E1622-31.**

8. **Christensen, A.E., et al., *A novel ADAMTSL4 mutation in autosomal recessive ectopia lentis et pupillae.* Investigative ophthalmology & visual science, 2010. 51(12): p. 6369-73.**

9. **Neuhann, T.M., et al., *A Homozygous Microdeletion within ADAMTSL4 in Patients with Isolated Ectopia Lentis: Evidence of a Founder Mutation.* Investigative ophthalmology & visual science, 2011. 52(2): p. 695-700.**

10. **Greene, V.B., et al., *Confirmation of ADAMTSL4 mutations for autosomal recessive isolated bilateral ectopia lentis.* Ophthalmic genetics, 2010. 31(1): p. 47-51.**

11. **Handford, P.A., *Fibrillin-1, a calcium binding protein of extracellular matrix.* Biochimica et biophysica acta, 2000. 1498(2-3): p. 84-90.**

12. **Biebl, H., et al., *Hoeflea phototrophica sp. nov., a novel marine aerobic alphaproteobacterium that forms bacteriochlorophyll a.* International journal of systematic and evolutionary microbiology, 2006. 56(Pt 4): p. 821-6.**

13. Cheng, L., et al., *Atomic model of a cypovirus built from cryo-EM structure provides insight into the mechanism of mRNA capping.* Proceedings of the National Academy of Sciences of the United States of America, 2011. 108(4): p. 1373-8.

14. Bourge, J.L., et al., *Zonular fibers, multimolecular composition as related to function (elasticity) and pathology.* Pathologie-biologie, 2007. 55(7): p. 347-59.

15. Tu, C., et al., *Structural basis for binding of RNA and cofactor by a KsgA methyltransferase.* Structure, 2009. 17(3): p. 374-85.

16. Le Goff, C. and V. Cormier-Daire, *The ADAMTS(L) family and human genetic disorders.* Human molecular genetics, 2011. 20(R2): p. R163-7.

17. Cal, S., et al., *Cloning, expression analysis, and structural characterization of seven novel human ADAMTSs, a family of metalloproteinases with disintegrin and thrombospondin-1 domains.* Gene, 2002. 283(1-2): p. 49-62.

18. Goh, G. and M. Choi, *Application of whole exome sequencing to identify disease-causing variants in inherited human diseases.* Genomics & informatics, 2012. 10(4): p. 214-9.

19. Chothia, C. and A.M. Lesk, *The relation between the divergence of sequence and structure in proteins.* The EMBO journal, 1986. 5(4): p. 823-6.

20. Hirschhorn, J.N. and M.J. Daly, *Genome-wide association studies for common diseases and complex traits.* Nature reviews. Genetics, 2005. 6(2): p. 95-108.

21. Apte, S.S., *A disintegrin-like and metalloprotease (reprolysin-type) with thrombospondin type 1 motif (ADAMTS) superfamily: functions and mechanisms.* The Journal of biological chemistry, 2009. 284(46): p. 31493-7.

22. Peluso, I., et al., *The ADAMTS18 gene is responsible for autosomal recessive early onset severe retinal dystrophy.* Orphanet journal of rare diseases, 2013. 8(1): p. 16.

23. Davis, E.C., et al., *Ultrastructural properties of ciliary zonule microfibrils.* Journal of Structural Biology, 2002. 139(2): p. 65-75.

24. Seppinen, L. and T. Pihlajaniemi, *The multiple functions of collagen XVIII in development and disease.* Matrix biology : journal of the International Society for Matrix Biology, 2011. 30(2): p. 83-92.

25. **Heinonen, T.Y. and M. Maki, *Peters'-plus syndrome is a congenital disorder of glycosylation caused by a defect in the beta1,3-glucosyltransferase that modifies thrombospondin type 1 repeats.* Annals of medicine, 2009. 41(1): p. 2-10.**

26. **Tucker, R.P., *The thrombospondin type 1 repeat superfamily.* The international journal of biochemistry & cell biology, 2004. 36(6): p. 969-74.**

27. **Chandra, A., et al., *A Genotype-Phenotype Comparison of ADAMTSL4 and FBN1 in Isolated Ectopia Lentis.* Investigative ophthalmology & visual science, 2012. 53(8): p. 4889-96.**

28. **Richards, A.J., J.D. Scott, and M.P. Snead, *Molecular genetics of rhegmatogenous retinal detachment.* Eye, 2002. 16(4): p. 388-92.**

29. **Metzker, M.L., *Sequencing technologies - the next generation.* Nature reviews. Genetics, 2010. 11(1): p. 31-46.**

30. **Sharifi, Y., et al., *Ectopia lentis et pupillae in four generations caused by novel mutations in the ADAMTSL4 gene.* Br J Ophthalmol, 2013.**

31. **Ware, J.S., *Chirurgical observations relative to the eye: with an appendix on the introduction of the male catheter and the treatment of hæmorrhoids. The second edition, with ... additions. (Observations on the Cataract and Gutta Serena; including a translation of Wenzel's on the Cataract, etc.)*1805, London: J. Mawman.**

32. **Helmholtz, H.v., *Beschreibung eines Augenspiegels zur Untersuchung der Netzhaut in Lebenden Auge*1851, Berlin: A Forstner'sche Verlagsbuchhandlung.**

33. **Gonin, J., *La pathologenie du decollement spontane de la retine.* Ann d'Oculist (Paris), 1904. 132: p. 30.**

34. **Ryan, S.J. and C.P. Wilkinson, *Retina*. 3rd ed. ed2001, St. Louis ; London: Mosby.**

35. ***Karl Stellwag von Carion.* BMJ, 1904. 2(2293): p. 1615-6.**

36. **Williams, E., *Rare cases, with practical remarks.* Trans Am Ophthalmol Soc, 1875. 2: p. 291-301.**

37. Forrester, J.V., *The eye : basic sciences in practice*. 3rd ed. ed2008, Edinburgh: W. B. Saunders.

38. Mieziewska, K., *The interphotoreceptor matrix, a space in sight.* Microscopy Research and Technique, 1996. 35(6): p. 463-71.

39. Fatt, I. and K. Shantinath, *Flow conductivity of retina and its role in retinal adhesion.* Experimental eye research, 1971. 12(2): p. 218-26.

40. Gingell, D. and J.A. Fornes, *Demonstration of intermolecular forces in cell adhesion using a new electrochemical technique.* Nature, 1975. 256(5514): p. 210-1.

41. Marmor, M.F. and X.Y. Yao, *The metabolic dependency of retinal adhesion in rabbit and primate.* Archives of ophthalmology, 1995. 113(2): p. 232-8.

42. Foos, R.Y., *Vitreoretinal juncture--simple epiretinal membranes.* Albrecht von Graefes Archiv fur klinische und experimentelle Ophthalmologie. Albrecht von Graefe's archive for clinical and experimental ophthalmology, 1974. 189(4): p. 231-50.

43. Yamada, E., *Some structural features of the fovea centralis in the human retina.* Archives of ophthalmology, 1969. 82(2): p. 151-9.

44. Matsumoto, B., J.C. Blanks, and S.J. Ryan, *Topographic variations in the rabbit and primate internal limiting membrane.* Investigative ophthalmology & visual science, 1984. 25(1): p. 71-82.

45. Ponsioen, T.L., et al., *Collagen distribution in the human vitreoretinal interface.* Investigative ophthalmology & visual science, 2008. 49(9): p. 4089-95.

46. Hindson, V.J., et al., *Opticin binds to heparan and chondroitin sulfate proteoglycans.* Investigative ophthalmology & visual science, 2005. 46(12): p. 4417-23.

47. Fukai, N., et al., *Lack of collagen XVIII/endostatin results in eye abnormalities.* The EMBO journal, 2002. 21(7): p. 1535-44.

48. Bishop, P.N., et al., *Identification of alternatively spliced variants of type II procollagen in vitreous.* Biochemical and biophysical research communications, 1994. 203(1): p. 289-95.

49. Bishop, P.N., et al., *Extraction and characterization of the tissue forms of collagen types II and IX from bovine vitreous.* The Biochemical journal, 1994. 299 (Pt 2): p. 497-505.

50. Snead, M.P. and J.R. Yates, *Clinical and Molecular genetics of Stickler syndrome.* Journal of medical genetics, 1999. 36(5): p. 353-9.

51. Le Goff, M.M., et al., *Characterization of opticin and evidence of stable dimerization in solution.* The Journal of biological chemistry, 2003. 278(46): p. 45280-7.

52. EA. Balazs, J.D., *Ageing changes in the vitreous*, in *Ageing and human visual function*, K. Dismukes, Editor 1982, Alan R Liss, Inc: New York. p. 45-47.

53. Theocharis, D.A., et al., *Hyaluronan and chondroitin sulfate proteoglycans in the supramolecular organization of the mammalian vitreous body.* Connective Tissue Research, 2008. 49(3): p. 124-8.

54. Miyamoto, T., et al., *Identification of a novel splice site mutation of the CSPG2 gene in a Japanese family with Wagner syndrome.* Investigative ophthalmology & visual science, 2005. 46(8): p. 2726-35.

55. Lund-Andersen, H., et al., *Quantitative vitreous fluorophotometry applying a mathematical model of the eye.* Investigative ophthalmology & visual science, 1985. 26(5): p. 698-710.

56. Kaufman, P.L. and A. Alm, *Adlers physiology of the eye*. 10th ed. / edited by Paul L. Kaufman, Albert Alm. ed2003, St. Louis, Mo. ; London: Mosby.

57. Fatt, I., *Flow and diffusion in the vitreous body of the eye.* Bulletin of Mathematical Biology, 1975. 37(1): p. 85-90.

58. Hogan, M.J., *The Vitreous, Its Structure, and Relation to the Ciliary Body and Retina. Proctor Award Lecture.* Investigative Ophthalmology, 1963. 2: p. 418-45.

59. Spencer, L.M., R.Y. Foos, and B.R. Straatsma, *Enclosed bays of the ora serrata. Relationship to retina tears.* Archives of ophthalmology, 1970. 83(4): p. 421-5.

60. Rutnin, U. and C.L. Schepens, *Fundus appearance in normal eyes. II. The standard peripheral fundus and developmental variations.* American journal of ophthalmology, 1967. 64(5): p. 840-52.

61. **Foos, R.Y. and R.A. Allen, *Retinal tears and lesser lesions of the peripheral retina in autopsy eyes.* American journal of ophthalmology, 1967. 64(3): p. Suppl:643-55.**

62. **Schepens, C.L., *Retinal detachment; diagnostic and prognostic factors as found preoperative examination.* Transactions - American Academy of Ophthalmology and Otolaryngology. American Academy of Ophthalmology and Otolaryngology, 1952. 56(3): p. 398-412.**

63. **Freeman, H.M., *Fellow eyes of giant retinal breaks.* Transactions of the American Ophthalmological Society, 1978. 76: p. 343-82.**

64. **Byer, N., *The peripheral retina in profile: a stereoscopic atlas*1982, Torrence: Criterion Press.**

65. **J., G., *Pathogenie et anatomie pathologique des decollemends retiniens.* . Bull Mem Soc Ophtalmol, 1920(33): p. 1.**

66. **Byer, N.E., *Lattice degeneration of the retina.* Survey of ophthalmology, 1979. 23(4): p. 213-48.**

67. **Straatsma, B.R., et al., *Lattice degeneration of the retina. XXX Edward Jackson Memorial Lecture.* American journal of ophthalmology, 1974. 77(5): p. 619-49.**

68. **Byer, N.E., *Changes in and prognosis of lattice degeneration of the retina.* Transactions - American Academy of Ophthalmology and Otolaryngology. American Academy of Ophthalmology and Otolaryngology, 1974. 78(2): p. OP114-25.**

69. **Dumas, J. and C.L. Schepens, *Chorioretinal lesions predisposing to retinal breaks.* American journal of ophthalmology, 1966. 61(4): p. 620-30.**

70. **Lewis, H., *Peripheral retinal degenerations and the risk of retinal detachment.* American journal of ophthalmology, 2003. 136(1): p. 155-60.**

71. **Hogan, M.J., J.A. Alvarado, and J.E. Weddell, *Histology of the human eye : an atlas and textbook*1971, Philadelphia, London: Saunders.**

72. **Wolter, J.R., *Pores in the Internal Limiting Membrane of the Human Retina.* Acta ophthalmologica, 1964. 42: p. 971-4.**

73. **Bishop, P.N., *Structural macromolecules and supramolecular organisation of the vitreous gel.* Progress in retinal and eye research, 2000. 19(3): p. 323-44.**

74. **Bishop, P.N., et al., *Age-related changes on the surface of vitreous collagen fibrils.* Investigative ophthalmology & visual science, 2004. 45(4): p. 1041-6.**

75. **Bos, K.J., et al., *Collagen fibril organisation in mammalian vitreous by freeze etch/rotary shadowing electron microscopy.* Micron, 2001. 32(3): p. 301-6.**

76. **Ueno, N., et al., *Effects of visible-light irradiation on vitreous structure in the presence of a photosensitizer.* Experimental eye research, 1987. 44(6): p. 863-70.**

77. **Wang, J., et al., *Age-dependent changes in the basal retinovitreous adhesion.* Investigative ophthalmology & visual science, 2003. 44(5): p. 1793-800.**

78. **Foos, R.Y. and N.C. Wheeler, *Vitreoretinal juncture. Synchysis senilis and posterior vitreous detachment.* Ophthalmology, 1982. 89(12): p. 1502-12.**

79. **Morita, H., M. Funata, and T. Tokoro, *A clinical study of the development of posterior vitreous detachment in high myopia.* Retina, 1995. 15(2): p. 117-24.**

80. **Akiba, J., *Prevalence of posterior vitreous detachment in high myopia.* Ophthalmology, 1993. 100(9): p. 1384-8.**

81. **Sebag, J., *Anomalous posterior vitreous detachment: a unifying concept in vitreo-retinal disease.* Graefe's archive for clinical and experimental ophthalmology = Albrecht von Graefes Archiv fur klinische und experimentelle Ophthalmologie, 2004. 242(8): p. 690-8.**

82. **Ghazi, N.G. and W.R. Green, *Pathology and pathogenesis of retinal detachment.* Eye, 2002. 16(4): p. 411-21.**

83. **Karaman, K., et al., *[The incidence of retinal tears in patients with posterior vitreous detachment].* Acta medica Croatica : casopis Hravatske akademije medicinskih znanosti, 2006. 60(2): p. 129-32.**

84. **Foos, R.Y., *Letter: Retinal tears.* Archives of ophthalmology, 1974. 91(6): p. 519-20.**

85. **Foos, R.Y., K.B. Simons, and N.C. Wheeler, *Comparison of lesions predisposing to rhegmatogenous retinal detachment by race of subjects.* American journal of ophthalmology, 1983. 96(5): p. 644-9.**

86. **Ross, W.H., *Retinal dialysis: lack of evidence for a genetic cause.* Canadian journal of ophthalmology. Journal canadien d'ophtalmologie, 1991. 26(6): p. 309-12.**

87. **Verdaguer, T.J., B. Rojas, and M. Lechuga, *Genetical studies in nontraumatic retinal dialysis.* Modern problems in ophthalmology, 1975. 15: p. 34-9.**

88. **Michels, R.G., C.P. Wilkinson, and T.A. Rice, *Retinal Detachment*1990: Mosby.**

89. **Ang, G.S., J. Townend, and N. Lois, *Interventions for prevention of giant retinal tear in the fellow eye.* Cochrane database of systematic reviews, 2012. 2: p. CD006909.**

90. **Mitry, D., et al., *The epidemiology of rhegmatogenous retinal detachment: geographical variation and clinical associations.* Br J Ophthalmol, 2010. 94(6): p. 678-84.**

91. ***Hospital Episode Statistics*. Available from: http://www.hscic.gov.uk/hes.**

92. **Vitale, S., R.D. Sperduto, and F.L. Ferris, 3rd, *Increased prevalence of myopia in the United States between 1971-1972 and 1999-2004.* Archives of ophthalmology, 2009. 127(12): p. 1632-9.**

93. **Burton, T.C., *The influence of refractive error and lattice degeneration on the incidence of retinal detachment.* Transactions of the American Ophthalmological Society, 1989. 87: p. 143-55; discussion 155-7.**

94. ***Risk factors for idiopathic rhegmatogenous retinal detachment. The Eye Disease Case-Control Study Group.* American journal of epidemiology, 1993. 137(7): p. 749-57.**

95. **McBrien, N.A., *Regulation of scleral metabolism in myopia and the role of transforming growth factor-beta.* Experimental eye research, 2013. 114:128-40**

96. **Zou, H., et al., *Epidemiology survey of rhegmatogenous retinal detachment in Beixinjing District, Shanghai, China.* Retina, 2002. 22(3): p. 294-9.**

97. **Mitry, D., et al., *The Predisposing Pathology and Clinical Characteristics in the Scottish Retinal Detachment Study.* Ophthalmology, 2011. 118(7):1429-34**

98. Hilford, D., et al., *Posterior vitreous detachment following cataract surgery.* Eye, 2009. 23(6): p. 1388-92.

99. Clark, A., et al., *Risk for retinal detachment after phacoemulsification: a whole-population study of cataract surgery outcomes.* Archives of ophthalmology, 2012. 130(7): p. 882-8.

100. Saidkasimova, S., et al., *Retinal detachment in Scotland is associated with affluence.* Br J Ophthalmol, 2009. 93(12): p. 1591-4.

101. Mitry, D., et al., *Laterality and gender imbalances in retinal detachment.* Graefe's archive for clinical and experimental ophthalmology = Albrecht von Graefes Archiv fur klinische und experimentelle Ophthalmologie, 2010.

102. Peters, A.L., *Retinal detachment in black South Africans.* South African medical journal = Suid-Afrikaanse tydskrif vir geneeskunde, 1995. 85(3): p. 158-9.

103. Brown, P.R. and R.P. Thomas, *The Low Incidence of Primary Retinal Detachment in the Negro.* American journal of ophthalmology, 1965. 60: p. 109-10.

104. Yorston, D. and S. Jalali, *Retinal detachment in developing countries.* Eye, 2002. 16(4): p. 353-8.

105. Wong, T.Y., J.M. Tielsch, and O.D. Schein, *Racial difference in the incidence of retinal detachment in Singapore.* Archives of ophthalmology, 1999. 117(3): p. 379-83.

106. Byer, N.E., *Clinical study of lattice degeneration of the retina.* Transactions - American Academy of Ophthalmology and Otolaryngology. American Academy of Ophthalmology and Otolaryngology, 1965. 69(6): p. 1065-81.

107. Tornquist, R., S. Stenkula, and P. Tornquist, *Retinal detachment. A study of a population-based patient material in Sweden 1971-1981. I. Epidemiology.* Acta ophthalmologica, 1987. 65(2): p. 213-22.

108. Laatikainen, L., E.M. Tolppanen, and H. Harju, *Epidemiology of rhegmatogenous retinal detachment in a Finnish population.* Acta ophthalmologica, 1985. 63(1): p. 59-64.

109. Morse, P.H. and H.G. Scheie, *Prophylactic cryoretinopexy of retinal breaks.* Archives of ophthalmology, 1974. 92(3): p. 204-7.

110. Everett, W.G., *Study of a family with lattice degeneration and retinal detachment.* American journal of ophthalmology, 1968. 65(2): p. 229-32.

111. Delaney, W.V., Jr., W. Podedworny, and W.H. Havener, *Inherited retinal detachment.* Archives of ophthalmology, 1963. 69: p. 44-50.

112. Lewkonia, I., M.S. Davies, and J.D. Salmon, *Lattice degeneration in a family: with retinal detachment and cataract.* Br J Ophthalmol, 1973. 57(8): p. 566-71.

113. Murakami, F. and N. Ohba, *Genetics of lattice degeneration of the retina.* Ophthalmologica. Journal international d'ophtalmologie. International journal of ophthalmology. Zeitschrift fur Augenheilkunde, 1982. 185(3): p. 136-40.

114. Meguro, A., et al., *Common variants in the COL4A$ gene confer susceptibility to lattice degeneration of the retina.* PLoS One. 2012, 7(6): e39300

115. Ross, W.H., *Traumatic retinal dialyses.* Archives of ophthalmology, 1981. 99(8): p. 1371-4.

116. Hagler, W.S., *Retinal dialysis: a statistical and genetic study to determine pathogenic factors.* Transactions of the American Ophthalmological Society, 1980. 78: p. 686-733.

117. Snead, M.P., et al., *Stickler syndrome, ocular-only variants and a key diagnostic role for the ophthalmologist.* Eye, 2011. 25(11): p. 1389-400.

118. Chaudhry, N.A., H.W. Flynn, Jr., and H. Tabandeh, *Idiopathic giant retinal tears in identical twins.* American journal of ophthalmology, 1999. 127(1): p. 96-9.

119. Vaiser, A. and B.F. Jost, *Bilateral inferotemporal dialysis in identical twins.* Annals of Ophthalmology, 1992. 24(10): p. 378-80.

120. Tang, W.C., M.K. Yap, and S.P. Yip, *A review of current approaches to identifying human genes involved in myopia.* Clin.Exp.Optom., 2008. 91(1): p. 4-22.

121. Kempen, J.H., et al., *The prevalence of refractive errors among adults in the United States, Western Europe, and Australia.* Arch.Ophthalmol, 2004. 122(4): p. 495-505.

122. Klein, A.P., et al., *Heritability analysis of spherical equivalent, axial length, corneal curvature, and anterior chamber depth in the Beaver Dam Eye Study.* Archives of ophthalmology, 2009. 127(5): p. 649-655.

123. Guggenheim, J.A., et al., *Coordinated genetic scaling of the human eye: shared determination of axial eye length and corneal curvature.* Investigative ophthalmology & visual science, 2013. 54(3): p. 1715-21.

124. Hui, J., L. Peck, and H.C. Howland, *Correlations between familial refractive error and children's non-cycloplegic refractions.* Vision research, 1995. 35(9): p. 1353-8.

125. Yap, M., et al., *Role of heredity in the genesis of myopia.* Ophthalmic Physiol Opt., 1993. 13(3): p. 316-319.

126. Hammond, C.J., et al., *Genes and environment in refractive error: the twin eye study.* Invest Ophthalmol Vis.Sci., 2001. 42(6): p. 1232-1236.

127. Farbrother, J.E., et al., *Family aggregation of high myopia: estimation of the sibling recurrence risk ratio.* Invest Ophthalmol Vis.Sci., 2004. 45(9): p. 2873-2878.

128. Guggenheim, J.A., G. Kirov, and S.A. Hodson, *The heritability of high myopia: a reanalysis of Goldschmidt's data.* J Med.Genet, 2000. 37(3): p. 227-231.

129. Wojciechowski, R., et al., *Heritability of refractive error and familial aggregation of myopia in an elderly American population.* Investigative ophthalmology & visual science, 2005. 46(5): p. 1588-92.

130. Hysi, P.G., et al., *A genome-wide association study for myopia and refractive error identifies a susceptibility locus at 15q25.* Nature genetics, 2010. 42(10): p. 902-5.

131. Solouki, A.M., et al., *A genome-wide association study identifies a susceptibility locus for refractive errors and myopia at 15q14.* Nat.Genet., 2010. 42(10): p. 897-901.

132. Schache, M., et al., *Genetic Association of Refractive Error and Axial Length with 15q14 but Not 15q25 in the Blue Mountains Eye Study Cohort.* Ophthalmology, 2012.

133. Meng, W., et al., *A Genome-Wide Association Study Provides Evidence for Association of Chromosome 8p23 (MYP10) and 10q21.1 (MYP15) with High Myopia in the French Population.* Investigative ophthalmology & visual science, 2012. 53(13): p. 7983-8.

134. Stickler, G.B., et al., *Hereditary Progressive Arthro-Ophthalmopathy.* Mayo Clinic proceedings. Mayo Clinic, 1965. 40: p. 433-55.

135. Pachydaki, S.I. and L.H. Young, *Genetics of hereditary vitreoretinal degenerations.* Seminars in ophthalmology, 2007. 22(4): p. 219-27.

136. Beighton, P., L. Solomon, and C.L. Soskolne, *Articular mobility in an African population.* Annals of the rheumatic diseases, 1973. 32(5): p. 413-8.

137. Richards, A.J., et al., *Stickler syndrome and the vitreous phenotype: mutations in COL2A1 and COL11A1.* Human mutation, 2010. 31(6): p. E1461-71.

138. Richards, A.J., et al., *COL2A1 exon 2 mutations: relevance to the Stickler and Wagner syndromes.* Br J Ophthalmol, 2000. 84(4): p. 364-71.

139. Richards, A.J., et al., *A family with Stickler syndrome type 2 has a mutation in the COL11A1 gene resulting in the substitution of glycine 97 by valine in alpha 1 (XI) collagen.* Human molecular genetics, 1996. 5(9): p. 1339-43.

140. Parentin, F., et al., *Stickler syndrome and vitreoretinal degeneration: correlation between locus mutation and vitreous phenotype. Apropos of a case.* Graefe's archive for clinical and experimental ophthalmology = Albrecht von Graefes Archiv fur klinische und experimentelle Ophthalmologie, 2001. 239(4): p. 316-9.

141. McLeod, D., G.C. Black, and P.N. Bishop, *Vitreous phenotype: genotype correlation in Stickler syndrome.* Graefe's archive for clinical and experimental ophthalmology = Albrecht von Graefes Archiv fur klinische und experimentelle Ophthalmologie, 2002. 240(1): p. 63-5; author reply 66.

142. Van Camp, G., et al., *A new autosomal recessive form of Stickler syndrome is caused by a mutation in the COL9A1 gene.* American journal of human genetics, 2006. 79(3): p. 449-57.

143. Baker, S., et al., *A loss of function mutation in the COL9A2 gene causes autosomal recessive Stickler syndrome.* American journal of medical genetics. Part A, 2011. 155A(7): p. 1668-72.

144. Griffith, A.J., et al., *Marshall syndrome associated with a splicing defect at the COL11A1 locus.* American journal of human genetics, 1998. 62(4): p. 816-23.

145. Annunen, S., et al., *Splicing mutations of 54-bp exons in the COL11A1 gene cause Marshall syndrome, but other mutations cause overlapping Marshall/Stickler phenotypes.* American journal of human genetics, 1999. 65(4): p. 974-83.

146. Maumenee, I.H., H.U. Stoll, and M.B. Mets, *The Wagner syndrome versus hereditary arthroophthalmopathy.* Transactions of the American Ophthalmological Society, 1982. 80: p. 349-65.

147. Graemiger, R.A., et al., *Wagner vitreoretinal degeneration. Follow-up of the original pedigree.* Ophthalmology, 1995. 102(12): p. 1830-9.

148. Hirose, T., K.Y. Lee, and C.L. Schepens, *Wagner's hereditary vitreoretinal degeneration and retinal detachment.* Archives of ophthalmology, 1973. 89(3): p. 176-85.

149. Mukhopadhyay, A., et al., *Erosive vitreoretinopathy and wagner disease are caused by intronic mutations in CSPG2/Versican that result in an imbalance of splice variants.* Investigative ophthalmology & visual science, 2006. 47(8): p. 3565-72.

150. Brown, D.M., et al., *Erosive vitreoretinopathy. A new clinical entity.* Ophthalmology, 1994. 101(4): p. 694-704.

151. Brown, D.M., et al., *Genetic linkage of Wagner disease and erosive vitreoretinopathy to chromosome 5q13-14.* Archives of ophthalmology, 1995. 113(5): p. 671-5.

152. Hirose, T., K.Y. Lee, and C.L. Schepens, *Snowflake degeneration in hereditary vitreoretinal degeneration.* American journal of ophthalmology, 1974. 77(2): p. 143-53.

153. Hirose, T., E. Wolf, and C.L. Schepens, *Retinal functions in snowflake degeneration.* Annals of Ophthalmology, 1980. 12(10): p. 1135-46.

154. Lee, M.M., et al., *Snowflake vitreoretinal degeneration: follow-up of the original family.* Ophthalmology, 2003. 110(12): p. 2418-26.

155. Hejtmancik, J.F., et al., *Mutations in KCNJ13 cause autosomal-dominant snowflake vitreoretinal degeneration.* American journal of human genetics, 2008. 82(1): p. 174-80.

156. Zhang, W., et al., *Characterization of the R162W Kir7.1 mutation associated with snowflake vitreoretinopathy.* American journal of physiology. Cell physiology, 2013. 304(5): p. C440-9.

157. Kusaka, S., et al., *Functional Kir7.1 channels localized at the root of apical processes in rat retinal pigment epithelium.* The Journal of physiology, 2001. 531(Pt 1): p. 27-36.

158. Sergouniotis, P.I., et al., *Recessive mutations in KCNJ13, encoding an inwardly rectifying potassium channel subunit, cause leber congenital amaurosis.* American journal of human genetics, 2011. 89(1): p. 183-90.

159. Chavala, S.H., et al., *An Arg311Gln NR2E3 mutation in a family with classic Goldmann-Favre syndrome.* Br J Ophthalmol, 2005. 89(8): p. 1065-6.

160. Edwards, A.O., *Clinical features of the congenital vitreoretinopathies.* Eye, 2008. 22(10): p. 1233-42.

161. Yardley, J., et al., *Mutations of VMD2 splicing regulators cause nanophthalmos and autosomal dominant vitreoretinochoroidopathy (ADVIRC).* Investigative ophthalmology & visual science, 2004. 45(10): p. 3683-9.

162. Kaufman, S.J., et al., *Autosomal dominant vitreoretinochoroidopathy.* Archives of ophthalmology, 1982. 100(2): p. 272-8.

163. Traboulsi, E.I. and J.W. Payne, *Autosomal dominant vitreoretinochoroidopathy. Report of the third family.* Archives of ophthalmology, 1993. 111(2): p. 194-6.

164. Kondo, H., et al., *Delineation of the critical interval for the familial exudative vitreoretinopathy gene by linkage and haplotype analysis.* Human genetics, 2001. 108(5): p. 368-75.

165. Chen, Z.Y., et al., *A mutation in the Norrie disease gene (NDP) associated with X-linked familial exudative vitreoretinopathy.* Nature genetics, 1993. 5(2): p. 180-3.

166. Poulter, J.A., et al., *Recessive mutations in TSPAN12 cause retinal dysplasia and severe familial exudative vitreoretinopathy (FEVR).* Investigative ophthalmology & visual science, 2012. 53(6): p. 2873-9.

167. Yang, H., et al., *Identification of FZD4 and LRP5 mutations in 11 of 49 families with familial exudative vitreoretinopathy.* Molecular vision, 2012. 18: p. 2438-46.

168. Knobloch W. H., L.J.M., *Retinal Detachment and ecephalocele.* J. Pediat. Ophthal., 1971. 8: p. 181-4.

169. Francois, J., *The role of heredity in retinal detachment.* International ophthalmology clinics, 1968. 8(4): p. 965-98.

170. Wilkes, S.R., et al., *The incidence of retinal detachment in Rochester, Minnesota, 1970-1978.* American journal of ophthalmology, 1982. 94(5): p. 670-3.

171. Go, S.L., et al., *Autosomal dominant rhegmatogenous retinal detachment associated with an Arg453Ter mutation in the COL2A1 gene.* Investigative ophthalmology & visual science, 2003. 44(9): p. 4035-43.

172. Edwards, T.L., et al., *Familial retinal detachment associated with COL2A1 exon 2 and FZD4 mutations.* Clinical & experimental ophthalmology, 2012. 40(5): p. 476-83.

173. Go, S.L., C.B. Hoyng, and C.C. Klaver, *Genetic risk of rhegmatogenous retinal detachment: a familial aggregation study.* Archives of ophthalmology, 2005. 123(9): p. 1237-41.

174. Mitry, D., et al., *Population based estimate of the sibling recurrence risk ratio for rhegmatogenous retinal detachment.* Investigative ophthalmology & visual science, 2011.

175. Streeten, B.W., *The zonular insertion: a scanning electron microscopic study.* Investigative ophthalmology & visual science, 1977. 16(4): p. 364-75.

176. Traboulsi, E.I., et al., *Microfibril abnormalities of the lens capsule in patients with Marfan syndrome and ectopia lentis.* Ophthalmic genetics, 2000. 21(1): p. 9-15.

177. Robert, B., et al., *Studies on the nature of the "microfibrillar" component of elastic fibers.* European journal of biochemistry / FEBS, 1971. 21(4): p. 507-16.

178. Biery, N.J., et al., *Revised genomic organization of FBN1 and significance for regulated gene expression.* Genomics, 1999. 56(1): p. 70-7.

179. Robinson, P.N. and M. Godfrey, *Marfan syndrome : a primer for clinicians and scientists*2004, Georgetown, TX: Landes Bioscience/Eurekah.com.

180. Yuan, X., et al., *Solution structure of the transforming growth factor beta-binding protein-like module, a domain associated with matrix fibrils.* The EMBO journal, 1997. 16(22): p. 6659-66.

181. Gleizes, P.E., et al., *Identification and characterization of an eight-cysteine repeat of the latent transforming growth factor-beta binding protein-1 that mediates bonding to the latent transforming growth factor-beta1.* The Journal of biological chemistry, 1996. 271(47): p. 29891-6.

182. Zhang, H., W. Hu, and F. Ramirez, *Developmental expression of fibrillin genes suggests heterogeneity of extracellular microfibrils.* The Journal of cell biology, 1995. 129(4): p. 1165-76.

183. Werneck, C.C., et al., *Identification of a major microfibril-associated glycoprotein-1-binding domain in fibrillin-2.* The Journal of biological chemistry, 2004. 279(22): p. 23045-51.

184. Eldadah, Z.A., et al., *Expression of a mutant human fibrillin allele upon a normal human or murine genetic background recapitulates a Marfan cellular phenotype.* The Journal of clinical investigation, 1995. 95(2): p. 874-80.

185. Maumenee, I.H., *The eye in the Marfan syndrome.* Transactions of the American Ophthalmological Society, 1981. 79: p. 684-733.

186. Loeys, B.L., et al., *The revised Ghent nosology for the Marfan syndrome.* Journal of medical genetics, 2010. 47(7): p. 476-85.

187. Faivre, L., et al., *Effect of mutation type and location on clinical outcome in 1,013 probands with Marfan syndrome or related phenotypes and FBN1 mutations: an international study.* American journal of human genetics, 2007. 81(3): p. 454-66.

188. Faivre, L., et al., *Pathogenic FBN1 mutations in 146 adults not meeting clinical diagnostic criteria for Marfan syndrome: further delineation of type 1 fibrillinopathies and focus on patients with an isolated major criterion.* American journal of medical genetics. Part A, 2009. 149A(5): p. 854-60.

189. Trask, T.M., et al., *N-terminal domains of fibrillin 1 and fibrillin 2 direct the formation of homodimers: a possible first step in microfibril assembly.* The Biochemical journal, 1999. 340 (Pt 3): p. 693-701.

190. Mir, S., et al., *A comparative histologic study of the fibrillin microfibrillar system in the lens capsule of normal subjects and subjects with Marfan syndrome.* Investigative ophthalmology & visual science, 1998. 39(1): p. 84-93.

191. Ganesh, A., et al., *Immunohistochemical evaluation of conjunctival fibrillin-1 in Marfan syndrome.* Archives of ophthalmology, 2006. 124(2): p. 205-9.

192. Kielty, C.M., et al., *Marfan syndrome: fibrillin expression and microfibrillar abnormalities in a family with predominant ocular defects.* Journal of medical genetics, 1995. 32(1): p. 1-6.

193. Wheatley, H.M., et al., *Immunohistochemical localization of fibrillin in human ocular tissues. Relevance to the Marfan syndrome.* Archives of ophthalmology, 1995. 113(1): p. 103-9.

194. Sultan, G., et al., *Cornea in Marfan disease: Orbscan and in vivo confocal microscopy analysis.* Investigative ophthalmology & visual science, 2002. 43(6): p. 1757-64.

195. Iordanidou, V., et al., *In vivo corneal confocal microscopy in marfan syndrome.* Cornea, 2007. 26(7): p. 787-92.

196. Konradsen, T.R., et al., *Corneal curvature, pachymetry, and endothelial cell density in Marfan syndrome.* Acta ophthalmologica, 2012. 90(4): p. 375-9.

197. Kara, N., et al., *Corneal biomechanical properties and intraocular pressure measurement in Marfan patients.* Journal of cataract and refractive surgery, 2012. 38(2): p. 309-14.

198. Heur, M., et al., *The value of keratometry and central corneal thickness measurements in the clinical diagnosis of Marfan syndrome.* American journal of ophthalmology, 2008. 145(6): p. 997-1001.

199. Burian, H.M. and L. Allen, *Histologic study of the chamber angel of patients with Marfan's syndrome. A discussion of the cases of Theobald, Reeh and Lehman, and Sadi de Buen and Velazquez.* Archives of ophthalmology, 1961. 65: p. 323-33.

200. Izquierdo, N.J., et al., *Glaucoma in the Marfan syndrome.* Transactions of the American Ophthalmological Society, 1992. 90: p. 111-7; discussion 118-22.

201. Leibowitz, H.M., et al., *The Framingham Eye Study monograph: An ophthalmological and epidemiological study of cataract, glaucoma, diabetic retinopathy, macular degeneration, and visual acuity in a general population of 2631 adults, 1973-1975.* Survey of ophthalmology, 1980. 24(Suppl): p. 335-610.

202. Sigal, I.A., et al., *The optic nerve head as a robust biomechanical system.* Investigative ophthalmology & visual science, 2012. 53(6): p. 2658-67.

203. Strouthidis, N.G. and M.J. Girard, *Altering the way the optic nerve head responds to intraocular pressure-a potential approach to glaucoma therapy.* Current opinion in pharmacology, 2013. 13(1): p. 83-9.

204. Braunsmann, C., et al., *Evaluation of lamina cribrosa and peripapillary sclera stiffness in pseudoexfoliation and normal eyes by atomic force microscopy.* Investigative ophthalmology & visual science, 2012. 53(6): p. 2960-7.

205. Harrison, D.A., et al., *Management of ophthalmic complications of homocystinuria.* Ophthalmology, 1998. 105(10): p. 1886-90.

206. Konradsen, T.R. and C. Zetterstrom, *A descriptive study of ocular characteristics in Marfan syndrome.* Acta ophthalmologica, 2013.

207. Nemet, A.Y., et al., *Current concepts of ocular manifestations in Marfan syndrome.* Survey of ophthalmology, 2006. 51(6): p. 561-75.

208. Rahi, J.S. and C. Edelsten, *The British Ophthalmological Surveillance Unit: the study of uncommon ophthalmic disorders made easier.* Eye, 1997. 11 (Pt 6): p. 766-7.

209. Hubbard, A.D., D.G. Charteris, and R.J. Cooling, *Vitreolensectomy in Marfan's syndrome.* Eye, 1998. 12 (Pt 3a): p. 412-6.

210. Celorio, J.M. and R.C. Pruett, *Prevalence of lattice degeneration and its relation to axial length in severe myopia.* American journal of ophthalmology, 1991. 111(1): p. 20-3.

211. Wallace, R.N., B.W. Streeten, and R.B. Hanna, *Rotary shadowing of elastic system microfibrils in the ocular zonule, vitreous, and ligamentum nuchae.* Current Eye Research, 1991. 10(1): p. 99-109.

212. Ohno-Jinno, A., et al., *Versican and fibrillin-1 form a major hyaluronan-binding complex in the ciliary body.* Investigative ophthalmology & visual science, 2008. 49(7): p. 2870-7.

213. Tolentino, F.I., C.L. Schepens, and H.M. Freeman, *Vitreoretinal disorders : diagnosis and management*1976, Philadelphia ; London: Saunders.

214. Abboud, E.B., *Retinal detachment surgery in Marfan's syndrome.* Retina, 1998. 18(5): p. 405-9.

215. Sharma, T., et al., *Retinal detachment in Marfan syndrome: clinical characteristics and surgical outcome.* Retina, 2002. 22(4): p. 423-8.

216. Remulla, J.F. and F.I. Tolentino, *Retinal detachment in Marfan's syndrome.* International ophthalmology clinics, 2001. 41(4): p. 235-40.

217. Vail, D., *The zonule of Zinn and ligament of Wieger; their importance in the mechanics of the intracapsular extraction of cataract.* Transactions. Ophthalmological Society of the United Kingdom, 1957. 77: p. 441-99.

218. Eisner, G., *Clinical examination of the vitreous.* Transactions of the ophthalmological societies of the United Kingdom, 1975. 95(3): p. 360-3.

219. Slezak, H. and E. Arocker-Mettinger, *[Topographic relation of dislocated lenses to the ciliary body and vitreous base].* Klinische Monatsblatter fur Augenheilkunde, 1988. 193(6): p. 635-6.

220. Foos, R., *Zonular traction tufts o the peripheral retina in cadaver eyes.* Archives of ophthalmology, 1969. 82(5): p. 620-32.

221. Carson, N.A. and D.W. Neill, *Metabolic abnormalities detected in a survey of mentally backward individuals in Northern Ireland.* Arch Dis Child, 1962. 37: p. 505-13.

222. Burke, J.P., et al., *Ocular complications in homocystinuria--early and late treated.* Br J Ophthalmol, 1989. 73(6): p. 427-31.

223. Passos-Bueno, M.R., et al., *Knobloch syndrome in a large Brazilian consanguineous family: confirmation of autosomal recessive inheritance.* American journal of medical genetics, 1994. 52(2): p. 170-3.

224. Khan, A.O., et al., *The distinct ophthalmic phenotype of Knobloch syndrome in children.* Br J Ophthalmol, 2012. 96(6): p. 890-5.

225. Faivre, L., et al., *Homozygosity mapping of a Weill-Marchesani syndrome locus to chromosome 19p13.3-p13.2.* Human genetics, 2002. 110(4): p. 366-70.

226. Morales, J., et al., *Homozygous mutations in ADAMTS10 and ADAMTS17 cause lenticular myopia, ectopia lentis, glaucoma, spherophakia, and short stature.* American journal of human genetics, 2009. 85(5): p. 558-68.

227. Ali, M., et al., *Null mutations in LTBP2 cause primary congenital glaucoma.* American journal of human genetics, 2009. 84(5): p. 664-71.

228. Comeglio, P., et al., *Identification of FBN1 gene mutations in patients with ectopia lentis and marfanoid habitus.* Br J Ophthalmol, 2002. 86(12): p. 1359-62.

229. Vanita, V., et al., *A recurrent FBN1 mutation in an autosomal dominant ectopia lentis family of Indian origin.* Molecular vision, 2007. 13: p. 2035-40.

230. Zhao, J.H., et al., *Ophthalmic findings in a family with early-onset isolated ectopia lentis and the p.Arg62Cys mutation of the fibrillin-1 gene (FBN1).* Ophthalmic genetics, 2012.

231. Ades, L.C., et al., *Ectopia lentis phenotypes and the FBN1 gene.* American journal of medical genetics. Part A, 2004. 126A(3): p. 284-9.

232. Edwards, M.J., et al., *Clinical and linkage study of a large family with simple ectopia lentis linked to FBN1.* American journal of medical genetics, 1994. 53(1): p. 65-71.

233. Loeys, B., et al., *Genotype and phenotype analysis of 171 patients referred for molecular study of the fibrillin-1 gene FBN1 because of suspected Marfan syndrome.* Archives of Internal Medicine, 2001. 161(20): p. 2447-54.

234. Pepe, G., et al., *Is ectopia lentis in some cases a mild phenotypic expression of Marfan syndrome? Need for a long-term follow-up.* Molecular vision, 2007. 13: p. 2242-7.

235. **Zadeh, N., et al., *Ectopia lentis as the presenting and primary feature in Marfan syndrome.* American journal of medical genetics. Part A, 2011. 155A(11): p. 2661-8.**

236. **Falls, H.F., Cotterman, C. W., *Genetic studies on ectopia lentis: a pedigree of simple ectopia of the lens.* Archives in Ophthalmology, 1943. 30: p. 610-20.**

237. **Ruiz, C., et al., *Familial simple ectopia lentis. A probable autosomal recessive form.* Ophthalmic paediatrics and genetics, 1986. 7(2): p. 81-4.**

238. **al-Salem, M., *Autosomal recessive ectopia lentis in two Arab family pedigrees.* Ophthalmic paediatrics and genetics, 1990. 11(2): p. 123-7.**

239. **Buchner, D.A. and M.H. Meisler, *TSRC1, a widely expressed gene containing seven thrombospondin type I repeats.* Gene, 2003. 307: p. 23-30.**

240. **Lang, R.M., et al., *Recommendations for chamber quantification.* Eur J Echocardiogr, 2006. 7(2): p. 79-108.**

241. **Sahn, D.J., et al., *Recommendations regarding quantitation in M-mode echocardiography: results of a survey of echocardiographic measurements.* Circulation, 1978. 58(6): p. 1072-83.**

242. **Steve Rosen, H.J.S., *Primer3 on the WWW for general users and for biologist programmers*, in *Bioinformatics Methods and Protocols. Methods in Molecular Biology*, M.S. Krawetz S., Editor 2000, Humana Press: Totowa, NJ. p. 365-386.**

243. **Mullis, K.B., *The unusual origin of the polymerase chain reaction.* Scientific American, 1990. 262(4): p. 56-61, 64-5.**

244. **Kumar, P., S. Henikoff, and P.C. Ng, *Predicting the effects of coding non-synonymous variants on protein function using the SIFT algorithm.* Nature protocols, 2009. 4(7): p. 1073-81.**

245. **Adzhubei, I.A., et al., *A method and server for predicting damaging missense mutations.* Nature methods, 2010. 7(4): p. 248-9.**

246. ***Exome Variant Server, NHLBI GO Exome Sequencing Project (ESP).* [cited 2012; Available from: http://evs.gs.washington.edu/EVS.**

247. ***Database of Single Nucleotide Polymorphisms (dbSNP).* [cited 2012; Available from: http://www.ncbi.nlm.nih.gov/SNP/.**

248. ***A map of human genome variation from population-scale sequencing.*** **Nature, 2010. 467(7319): p. 1061-73.**

249. **Seddon, J.M., S. Sharma, and R.A. Adelman,** ***Evaluation of the clinical age-related maculopathy staging system.*** **Ophthalmology, 2006. 113(2): p. 260-6.**

250. **Turner, C.L., et al.,** ***Detection of 53 FBN1 mutations (41 novel and 12 recurrent) and genotype-phenotype correlations in 113 unrelated probands referred with Marfan syndrome, or a related fibrillinopathy.*** **American journal of medical genetics. Part A, 2009. 149A(2): p. 161-70.**

251. **Reese, M.G., et al.,** ***Improved splice site detection in Genie.*** **Journal of computational biology : a journal of computational molecular cell biology, 1997. 4(3): p. 311-23.**

252. **Beroud, C., et al.,** ***UMD (Universal mutation database): a generic software to build and analyze locus-specific databases.*** **Human mutation, 2000. 15(1): p. 86-94.**

253. **Wright, K.W.P.o., et al.,** ***Pediatric ophthalmology and strabismus*****. 2nd ed. / editors, Kenneth W. Wright, Peter H. Spiegel, illustrators, Timothy C. Hengst, Susan Gilbert, Faith Cogswell. ed2003, New York ; London: Springer.**

254. **Jensen, S.A., et al.,** ***Structure and interdomain interactions of a hybrid domain: a disulphide-rich module of the fibrillin/LTBP superfamily of matrix proteins.*** **Structure, 2009. 17(5): p. 759-68.**

255. **Mellody, K.T., et al.,** ***Marfan syndrome-causing mutations in fibrillin-1 result in gross morphological alterations and highlight the structural importance of the second hybrid domain.*** **The Journal of biological chemistry, 2006. 281(42): p. 31854-62.**

256. **Whiteman, P., et al.,** ***Cellular and molecular studies of Marfan syndrome mutations identify co-operative protein folding in the cbEGF12-13 region of fibrillin-1.*** **Human molecular genetics, 2007. 16(8): p. 907-18.**

257. **Dietz, H.C., et al.,** ***Clustering of fibrillin (FBN1) missense mutations in Marfan syndrome patients at cysteine residues in EGF-like domains.*** **Human mutation, 1992. 1(5): p. 366-74.**

258. **Comeglio, P., et al.,** ***Detection of six novel FBN1 mutations in British patients affected by Marfan syndrome.*** **Human mutation, 2001. 18(3): p. 251.**

259. Faivre, L., et al., *The new Ghent criteria for Marfan syndrome: what do they change?* Clinical genetics, 2012. 81(5): p. 433-42.

260. Collod-Beroud, G., et al., *Update of the UMD-FBN1 mutation database and creation of an FBN1 polymorphism database.* Human mutation, 2003. 22(3): p. 199-208.

261. Stenson, P.D., et al., *The Human Gene Mutation Database: 2008 update.* Genome medicine, 2009. 1(1): p. 13.

262. Yang, G., et al., *A novel FBN1 mutation in a Chinese family with isolated ectopia lentis.* Molecular vision, 2012. 18: p. 945-50.

263. Li, H., et al., *Identification and study of a FBN1 gene mutation in a Chinese family with ectopia lentis.* Molecular vision, 2012. 18: p. 504-11.

264. Micheal, S., et al., *Identification of a novel FBN1 gene mutation in a large Pakistani family with Marfan syndrome.* Molecular vision, 2012. 18: p. 1918-26.

265. Ball, E.V., et al., *Microdeletions and microinsertions causing human genetic disease: common mechanisms of mutagenesis and the role of local DNA sequence complexity.* Human mutation, 2005. 26(3): p. 205-13.

266. Viguera, E., D. Canceill, and S.D. Ehrlich, *Replication slippage involves DNA polymerase pausing and dissociation.* The EMBO journal, 2001. 20(10): p. 2587-95.

267. Kondrashov, A.S. and I.B. Rogozin, *Context of deletions and insertions in human coding sequences.* Human mutation, 2004. 23(2): p. 177-85.

268. Maquat, L.E., *Nonsense-mediated mRNA decay: splicing, translation and mRNP dynamics.* Nature reviews. Molecular cell biology, 2004. 5(2): p. 89-99.

269. Chandra, A., et al., *Focus on Molecules: ADAMTSL4.* Experimental eye research, 2012. Nov(104): p. 95-6.

270. M.R. Speicher, S.E.A., A.G. Motulsky, *Human Genetics*. 4 ed2009: Springer.

271. Hassell, J.R. and D.E. Birk, *The molecular basis of corneal transparency.* Experimental eye research, 2010. 91(3): p. 326-35.

272. Dimasi, D.P., et al., *Candidate gene study to investigate the genetic determinants of normal variation in central corneal thickness.* Molecular vision, 2010. 16: p. 562-9.

273. Setala, K., P. Ruusuvaara, and K. Karjalainen, *Corneal endothelium in Marfan syndrome. A clinical and specular microscopic study.* Acta ophthalmologica, 1988. 66(3): p. 334-40.

274. Azar-Arevalo, O. and J.F. Arevalo, *Corneal topography changes after vitreoretinal surgery.* Ophthalmic surgery and lasers, 2001. 32(2): p. 168-72.

275. Randleman, J.B., S.M. Hewitt, and R.D. Stulting, *Refractive changes after posterior segment surgery.* Ophthalmology clinics of North America, 2004. 17(4): p. 521-6, v-vi.

276. Wirbelauer, C., et al., *Corneal shape changes after pars plana vitrectomy.* Graefe's archive for clinical and experimental ophthalmology = Albrecht von Graefes Archiv fur klinische und experimentelle Ophthalmologie, 1998. 236(11): p. 822-8.

277. Citirik, M., et al., *Keratometric alterations following the 25-gauge transconjunctival sutureless pars plana vitrectomy versus the conventional pars plana vitrectomy.* Clinical & experimental optometry : journal of the Australian Optometrical Association, 2009. 92(5): p. 416-20.

278. De Paepe, A., et al., *Revised diagnostic criteria for the Marfan syndrome.* American journal of medical genetics, 1996. 62(4): p. 417-26.

279. Hubmacher, D. and S.S. Apte, *Genetic and functional linkage between ADAMTS superfamily proteins and fibrillin-1: a novel mechanism influencing microfibril assembly and function.* Cell Mol Life Sci, 2011. 68(19): p. 3137-48.

280. Dagoneau, N., et al., *ADAMTS10 mutations in autosomal recessive Weill-Marchesani syndrome.* American journal of human genetics, 2004. 75(5): p. 801-6.

281. Kutz, W.E., et al., *Functional analysis of an ADAMTS10 signal peptide mutation in Weill-Marchesani syndrome demonstrates a long-range effect on secretion of the full-length enzyme.* Human mutation, 2008. 29(12): p. 1425-34.

282. Wong, H.B., et al., *Ocular component growth curves among Singaporean children with different refractive error status.* Investigative ophthalmology & visual science, 2010. 51(3): p. 1341-7.

283. Brown, N.P., J.F. Koretz, and A.J. Bron, *The development and maintenance of emmetropia.* Eye, 1999. 13 (Pt 1): p. 83-92.

284. Meng, W., et al., *Axial length of myopia: a review of current research.* Ophthalmologica. Journal international d'ophtalmologie. International journal of ophthalmology. Zeitschrift fur Augenheilkunde, 2011. 225(3): p. 127-34.

285. Park, S.C., et al., *Axial growth and binocular function following bilateral lensectomy and scleral fixation of an intraocular lens in nontraumatic ectopia lentis.* Jpn J Ophthalmol, 2010. 54(3): p. 232-8.

286. Nickla, D.L. and K. Totonelly, *Dopamine antagonists and brief vision distinguish lens-induced- and form-deprivation-induced myopia.* Experimental eye research, 2011. 93(5): p. 782-5.

287. Wiesel, T.N. and E. Raviola, *Increase in axial length of the macaque monkey eye after corneal opacification.* Investigative ophthalmology & visual science, 1979. 18(12): p. 1232-6.

288. Rymer, J. and C.F. Wildsoet, *The role of the retinal pigment epithelium in eye growth regulation and myopia: a review.* Visual Neuroscience, 2005. 22(3): p. 251-61.

289. Wallman, J., *Retinal influences on sclera underlie visual deprivation myopia.* Ciba Foundation Symposium, 1990. 155: p. 126-34; discussion 135-41.

290. Morgan, I.G., *The biological basis of myopic refractive error.* Clinical & experimental optometry : journal of the Australian Optometrical Association, 2003. 86(5): p. 276-88.

291. Huo, L., et al., *A retrospective study: form-deprivation myopia in unilateral congenital ptosis.* Clinical & experimental optometry : journal of the Australian Optometrical Association, 2012. 95(4): p. 404-9.

292. Wallman, J., et al., *Local retinal regions control local eye growth and myopia.* Science, 1987. 237(4810): p. 73-7.

293. Nickla, D.L. and F. Schroedl, *Parasympathetic influences on emmetropization in chicks: evidence for different mechanisms in form deprivation vs negative lens-induced myopia.* Experimental eye research, 2012. 102: p. 93-103.

294. Wildsoet, C. and J. Wallman, *Choroidal and scleral mechanisms of compensation for spectacle lenses in chicks.* Vision research, 1995. 35(9): p. 1175-94.

295. Goldberg, M.F., *Clinical manifestations of ectopia lentis et pupillae in 16 patients.* Ophthalmology, 1988. 95(8): p. 1080-7.

296. Bernardes, C.S., L.V. Leite, and F.A. Castro, *[Ectopia lentis et pupillae: case report].* Arquivos Brasileiros de Oftalmologia, 2005. 68(6): p. 841-4.

297. Schmidt, D., et al., *Congenital ocular malformations (lens subluxation, pupillary displacement, cataract, myopia) and classic galactosaemia associated with Q188R and /or G1391A mutations.* Acta ophthalmologica, 2011. 89(5): p. 489-94.

298. Smith, E.L., 3rd, et al., *Effects of foveal ablation on emmetropization and form-deprivation myopia.* Investigative ophthalmology & visual science, 2007. 48(9): p. 3914-22.

299. Anstice, N.S. and J.R. Phillips, *Effect of dual-focus soft contact lens wear on axial myopia progression in children.* Ophthalmology, 2011. 118(6): p. 1152-61.

300. Ren, Y., et al., *Spontaneous high myopia in one eye will affect the development of form deprivation myopia in the fellow eye.* Current Eye Research, 2011. 36(6): p. 513-21.

301. Chandra, A., et al., *Craniosynostosis with Ectopia Lentis and a Homozygous 20-base Deletion in ADAMTSL4.* Ophthalmic genetics, 2012.

302. Melville, H., et al., *Genetic basis of potential therapeutic strategies for craniosynostosis.* American journal of medical genetics. Part A, 2010. 152A(12): p. 3007-15.

303. Lajeunie, E., et al., *Genetic study of nonsyndromic coronal craniosynostosis.* American journal of medical genetics, 1995. 55(4): p. 500-4.

304. Wilkie, A.O., et al., *Clinical dividends from the molecular genetic diagnosis of craniosynostosis.* American journal of medical genetics. Part A, 2007. 143A(16): p. 1941-9.

305. Howard, T.D., et al., *Mutations in TWIST, a basic helix-loop-helix transcription factor, in Saethre-Chotzen syndrome.* Nature genetics, 1997. 15(1): p. 36-41.

306. Marie, P.J., J.D. Coffin, and M.M. Hurley, *FGF and FGFR signaling in chondrodysplasias and craniosynostosis.* J Cell Biochem, 2005. 96(5): p. 888-96.

307. Sood, S., et al., *Mutation in fibrillin-1 and the Marfanoid-craniosynostosis (Shprintzen-Goldberg) syndrome.* Nature genetics, 1996. 12(2): p. 209-11.

308. Ades, L.C., et al., *FBN1, TGFBR1, and the Marfan-craniosynostosis/mental retardation disorders revisited.* American journal of medical genetics. Part A, 2006. 140(10): p. 1047-58.

309. Hiraki, Y., et al., *Craniosynostosis in a patient with a de novo 15q15-q22 deletion.* American journal of medical genetics. Part A, 2008. 146A(11): p. 1462-5.

310. Mizuguchi, T., et al., *Heterozygous TGFBR2 mutations in Marfan syndrome.* Nature genetics, 2004. 36(8): p. 855-60.

311. Pesme, Verger, and Montoux, *[Craniofacial dysostosis with displacement of the crystalline lens].* Arch Fr Pediatr, 1950. 7(4): p. 348-53.

312. Reichel, E., et al., *Oxycephaly, bilateral ectopia lentis, and retinal detachment.* Ann Ophthalmol, 1992. 24(3): p. 97-8.

313. Cruysberg, J.R., et al., *Craniosynostosis associated with ectopia lentis in monozygotic twin sisters.* American journal of medical genetics, 1999. 82(3): p. 201-5.

314. Quercia, N.L. and A.S. Teebi, *Craniosynostosis, ectopia lentis, and congenital heart defects: further delineation of an autosomal dominant syndrome with incomplete penetrance.* American journal of medical genetics, 2002. 107(1): p. 38-42.

315. Guven, D., et al., *Craniosynostosis and ectopia lentis in a propositus whose parents are cousins.* American journal of medical genetics. Part A, 2005. 134A(2): p. 231.

316. Reefhuis, J., et al., *Fertility treatments and craniosynostosis: California, Georgia, and Iowa, 1993-1997.* Pediatrics, 2003. 111(5 Part 2): p. 1163-6.

317. Kallen, B. and E. Robert-Gnansia, *Maternal drug use, fertility problems, and infant craniostenosis.* The Cleft palate-craniofacial journal : official publication of the American Cleft Palate-Craniofacial Association, 2005. 42(6): p. 589-93.

318. Fleiss, J.L., B.A. Levin, and M.C. Paik, *Statistical methods for rates and proportions*. 3rd ed. / Joseph L. Fleiss, Bruce Levin, Myunghee Cho Paik. ed2003, Hoboken, N.J. ; [Chichester]: Wiley-Interscience.

319. Gwet, K.L., *Handbook of inter-rater reliability : the definitive guide to measuring the extent of agreement among raters*2010, Gaithersburg, MD: Advanced Analytics, LLC.

320. Xu, H., et al., *A clinical grading system for retinal inflammation in the chronic model of experimental autoimmune uveoretinitis using digital fundus images.* Experimental eye research, 2008. 87(4): p. 319-26.

321. Rahman, R., A. Berry-Brincat, and V.T. Thaller, *A new grading system for assessing orbicularis muscle function.* Eye, 2003. 17(5): p. 610-2.

322. Traboulsi, E.I., *Genetic diseases of the eye*. 2nd ed. ed2012, Oxford: Oxford University Press.

323. Waiswol M., K.N., *Lens subluxation grading system:*

***predictive value for ectopia lentis surgical outcomes.* einstein, 2009. 7(1): p. 81-7.**

324. Khan, A.O., et al., *Familial spherophakia with short stature caused by a novel homozygous ADAMTS17 mutation.* Ophthalmic genetics, 2012. 33(4): p. 235-9.

325. Hutton, M., et al., *Association of missense and 5'-splice-site mutations in tau with the inherited dementia FTDP-17.* Nature, 1998. 393(6686): p. 702-5.

326. Harold, D., et al., *Genome-wide association study identifies variants at CLU and PICALM associated with Alzheimer's disease.* Nature genetics, 2009. 41(10): p. 1088-1093.

327. Antonarakis, S.E., et al., *Mendelian disorders and multifactorial traits: the big divide or one for all?* Nature reviews. Genetics, 2010. 11(5): p. 380-4.

328. Badano, J.L. and N. Katsanis, *Beyond Mendel: an evolving view of human genetic disease transmission.* Nature reviews. Genetics, 2002. 3(10): p. 779-89.

329. Sanger, F., S. Nicklen, and A.R. Coulson, *DNA sequencing with chain-terminating inhibitors.* Proceedings of the National Academy of Sciences of the United States of America, 1977. 74(12): p. 5463-7.

330. McKusick, V.A., *Mendelian Inheritance in Man and its online version, OMIM.* American journal of human genetics, 2007. 80(4): p. 588-604.

331. Ng, S.B., et al., *Targeted capture and massively parallel sequencing of 12 human exomes.* Nature, 2009. 461(7261): p. 272-6.

332. Ng, S.B., et al., *Exome sequencing identifies the cause of a mendelian disorder.* Nature genetics, 2010. 42(1): p. 30-5.

333. Bamshad, M.J., et al., *Exome sequencing as a tool for Mendelian disease gene discovery.* Nature reviews. Genetics, 2011. 12(11): p. 745-55.

334. Woods, C.G., et al., *A new method for autozygosity mapping using single nucleotide polymorphisms (SNPs) and EXCLUDEAR.* Journal of medical genetics, 2004. 41(8): p. e101.

335. Raghavan, M., et al., *Genome-wide single nucleotide polymorphism analysis reveals frequent partial uniparental disomy due to somatic recombination in acute myeloid leukemias.* Cancer Research, 2005. 65(2): p. 375-8.

336. Botstein, D. and N. Risch, *Discovering genotypes underlying human phenotypes: past successes for mendelian disease, future approaches for complex disease.* Nature genetics, 2003. 33 Suppl: p. 228-37.

337. Clark, A.G., *The size distribution of homozygous segments in the human genome.* American journal of human genetics, 1999. 65(6): p. 1489-92.

338. McQuillan, R., et al., *Runs of homozygosity in European populations.* American journal of human genetics, 2008. 83(3): p. 359-72.

339. Bruno, D.L., et al., *Pathogenic aberrations revealed exclusively by single nucleotide polymorphism (SNP) genotyping data in 5000 samples tested by molecular karyotyping.* Journal of medical genetics, 2011. 48(12): p. 831-9.

340. **Alkuraya, F.S., *Autozygome decoded.* Genetics in medicine : official journal of the American College of Medical Genetics, 2010. 12(12): p. 765-71.**

341. **Hamamy, H., et al., *Consanguineous marriages, pearls and perils: Geneva International Consanguinity Workshop Report.* Genetics in medicine : official journal of the American College of Medical Genetics, 2011. 13(9): p. 841-7.**

342. **Strachan, T. and A.P. Read, *Human molecular genetics*. 4th ed. ed2010, New York: Garland Science. xxv, 781 p.**

343. **Dryja, T.P., et al., *Chromosome 13 restriction fragment length polymorphisms.* Human genetics, 1984. 65(4): p. 320-4.**

344. **Nussbaum, R.L., et al., *Choroideremia is linked to the restriction fragment length polymorphism DXYS1 at XQ13-21.* American journal of human genetics, 1985. 37(3): p. 473-81.**

345. **Schmutz, J., et al., *Quality assessment of the human genome sequence.* Nature, 2004. 429(6990): p. 365-8.**

346. **Lopez-Bigas, N., et al., *Are splicing mutations the most frequent cause of hereditary disease?* FEBS letters, 2005. 579(9): p. 1900-3.**

347. **Desmet, F.O. and C. Beroud, *Bioinformatics and mutations leading to exon skipping.* Methods in Molecular Biology, 2012. 867: p. 17-35.**

348. **Marmor, M.F., et al., *ISCEV Standard for full-field clinical electroretinography (2008 update).* Documenta ophthalmologica. Advances in ophthalmology, 2009. 118(1): p. 69-77.**

349. ***UK10K*. Available from: http://www.uk10k.org/.**

350. ***Affymetrix Genome-Wide Human SNP Array 6.0*. Available from: http://www.affymetrix.com/estore/browse/products.jsp?productId=131533&categoryId=35642#1_1.**

351. **Schwarz, J.M., et al., *MutationTaster evaluates disease-causing potential of sequence alterations.* Nature methods, 2010. 7(8): p. 575-6.**

352. **Pagani, F. and F.E. Baralle, *Genomic variants in exons and introns: identifying the splicing spoilers.* Nature reviews. Genetics, 2004. 5(5): p. 389-96.**

353. Lander, E.S., et al., *Initial sequencing and analysis of the human genome.* Nature, 2001. 409(6822): p. 860-921.

354. Christie, P.T., et al., *X-linked hypophosphatemia attributable to pseudoexons of the PHEX gene.* The Journal of clinical endocrinology and metabolism, 2001. 86(8): p. 3840-4.

355. Vache, C., et al., *Usher syndrome type 2 caused by activation of an USH2A pseudoexon: implications for diagnosis and therapy.* Human mutation, 2012. 33(1): p. 104-8.

356. Jin, H., et al., *Epigenetic identification of ADAMTS18 as a novel 16q23.1 tumor suppressor frequently silenced in esophageal, nasopharyngeal and multiple other carcinomas.* Oncogene, 2007. 26(53): p. 7490-8.

357. Li, Z., et al., *High-resolution melting analysis of ADAMTS18 methylation levels in gastric, colorectal and pancreatic cancers.* Medical Oncology, 2010. 27(3): p. 998-1004.

358. Wei, X., et al., *Mutational and functional analysis reveals ADAMTS18 metalloproteinase as a novel driver in melanoma.* Molecular cancer research : MCR, 2010. 8(11): p. 1513-25.

359. van Hinsbergh, V.W., *Endothelium--role in regulation of coagulation and inflammation.* Seminars in immunopathology, 2012. 34(1): p. 93-106.

360. Dang, S., et al., *Optimized refolding and characterization of active C-terminal ADAMTS-18 fragment from inclusion bodies of Escherichia coli.* Protein Expression and Purification, 2012. 82(1): p. 32-6.

361. Li, Z., et al., *C-terminal ADAMTS-18 fragment induces oxidative platelet fragmentation, dissolves platelet aggregates, and protects against carotid artery occlusion and cerebral stroke.* Blood, 2009. 113(24): p. 6051-60.

362. Koller, D.L., et al., *Genome-wide association study of bone mineral density in premenopausal European-American women and replication in African-American women.* The Journal of clinical endocrinology and metabolism, 2010. 95(4): p. 1802-9.

363. Xiong, D.H., et al., *Genome-wide association and follow-up replication studies identified ADAMTS18 and TGFBR3 as bone mass candidate genes in different ethnic groups.* American journal of human genetics, 2009. 84(3): p. 388-98.

364. Lopez, L.M., et al., *A genome-wide search for genetic influences and biological pathways related to the brain's white matter integrity.* Neurobiology of Aging, 2012. 33(8): p. 1847 e1-14.

365. Wilson, C., et al., *Report of two sibs with Knobloch syndrome (encephalocoele and viteroretinal degeneration) and other anomalies.* American journal of medical genetics, 1998. 78(3): p. 286-90.

366. Czeizel, A.E., et al., *The second report of Knobloch syndrome.* American journal of medical genetics, 1992. 42(6): p. 777-9.

367. Keren, B., et al., *CNS malformations in Knobloch syndrome with splice mutation in COL18A1 gene.* American journal of medical genetics. Part A, 2007. 143A(13): p. 1514-8.

368. Paisan-Ruiz, C., et al., *Homozygosity mapping through whole genome analysis identifies a COL18A1 mutation in an Indian family presenting with an autosomal recessive neurological disorder.* American journal of medical genetics. Part B, Neuropsychiatric genetics : the official publication of the International Society of Psychiatric Genetics, 2009. 150B(7): p. 993-7.

369. Williams, T.A., et al., *A phenotypic variant of Knobloch syndrome.* Ophthalmic genetics, 2008. 29(2): p. 85-6.

370. Mahajan, V.B., et al., *Collagen XVIII mutation in Knobloch syndrome with acute lymphoblastic leukemia.* American journal of medical genetics. Part A, 2010. 152A(11): p. 2875-9.

371. Suzuki, O.T., et al., *Molecular analysis of collagen XVIII reveals novel mutations, presence of a third isoform, and possible genetic heterogeneity in Knobloch syndrome.* American journal of human genetics, 2002. 71(6): p. 1320-9.

372. Khaliq, S., et al., *Mapping of a novel type III variant of Knobloch syndrome (KNO3) to chromosome 17q11.2.* American journal of medical genetics. Part A, 2007. 143A(23): p. 2768-74.

373. Park, S.H. and S.Y. Shin, *Walker-Warburg Syndrome Manifesting as Leopard Spot Retinopathy, Retinal Detachment, and Microphthalmia.* Journal of pediatric ophthalmology and strabismus, 2009.

374. Sarra, G.M., et al., *Clinical description and exclusion of candidate genes in a novel autosomal recessively inherited vitreoretinal dystrophy.* Archives of ophthalmology, 2003. 121(8): p. 1109-16.

375. Weigell-Weber, M., et al., *Genomewide homozygosity mapping and molecular analysis of a candidate gene located on 22q13 (fibulin-1) in a previously undescribed vitreoretinal dystrophy.* Archives of ophthalmology, 2003. 121(8): p. 1184-8.

376. Simonelli, F., et al., *Retinal degeneration associated with ectopia lentis.* Ophthalmic genetics, 1999. 20(2): p. 121-6.

377. Noble, K.G., S. Bass, and J. Sherman, *Ectopia lentis, chorioretinal dystrophy and myopia. A new autosomal recessive syndrome.* Documenta ophthalmologica. Advances in ophthalmology, 1993. 83(2): p. 97-102.

378. Sertie, A.L., et al., *Collagen XVIII, containing an endogenous inhibitor of angiogenesis and tumor growth, plays a critical role in the maintenance of retinal structure and in neural tube closure (Knobloch syndrome).* Human molecular genetics, 2000. 9(13): p. 2051-8.

379. Menzel, O., et al., *Knobloch syndrome: novel mutations in COL18A1, evidence for genetic heterogeneity, and a functionally impaired polymorphism in endostatin.* Human mutation, 2004. 23(1): p. 77-84.

380. Najmabadi, H., et al., *Deep sequencing reveals 50 novel genes for recessive cognitive disorders.* Nature, 2011. 478(7367): p. 57-63.

381. Suzuki, O., et al., *Novel pathogenic mutations and skin biopsy analysis in Knobloch syndrome.* Molecular vision, 2009. 15: p. 801-9.

382. Saarela, J., et al., *The short and long forms of type XVIII collagen show clear tissue specificities in their expression and location in basement membrane zones in humans.* The American journal of pathology, 1998. 153(2): p. 611-26.

383. Ferreras, M., et al., *Generation and degradation of human endostatin proteins by various proteinases.* FEBS letters, 2000. 486(3): p. 247-51.

384. Elamaa, H., et al., *Endostatin overexpression specifically in the lens and skin leads to cataract and ultrastructural alterations in basement membranes.* The American journal of pathology, 2005. 166(1): p. 221-9.

385. O'Reilly, M.S., et al., *Endostatin: an endogenous inhibitor of angiogenesis and tumor growth.* Cell, 1997. 88(2): p. 277-85.

386. Quelard, D., et al., *A cryptic frizzled module in cell surface collagen 18 inhibits Wnt/beta-catenin signaling.* PloS one, 2008. 3(4): p. e1878.

387. Folkman, J., *Antiangiogenesis in cancer therapy--endostatin and its mechanisms of action.* Experimental Cell Research, 2006. 312(5): p. 594-607.

388. Maatta, M., et al., *Collagen XVIII/endostatin shows a ubiquitous distribution in human ocular tissues and endostatin-containing fragments accumulate in ocular fluid samples.* Graefe's archive for clinical and experimental ophthalmology = Albrecht von Graefes Archiv fur klinische und experimentelle Ophthalmologie, 2007. 245(1): p. 74-81.

389. Kliemann, S.E., et al., *Evidence of neuronal migration disorders in Knobloch syndrome: clinical and molecular analysis of two novel families.* American journal of medical genetics. Part A, 2003. 119A(1): p. 15-9.

390. Duh, E.J., et al., *Persistence of fetal vasculature in a patient with Knobloch syndrome: potential role for endostatin in fetal vascular remodeling of the eye.* Ophthalmology, 2004. 111(10): p. 1885-8.

391. Ackley, B.D., et al., *The NC1/endostatin domain of Caenorhabditis elegans type XVIII collagen affects cell migration and axon guidance.* The Journal of cell biology, 2001. 152(6): p. 1219-32.

392. Yu, L., et al., *Epidemiology, genetics and treatments for myopia.* International journal of ophthalmology, 2011. 4(6): p. 658-69.

393. Mutti, D.O., et al., *Candidate gene and locus analysis of myopia.* Molecular vision, 2007. 13: p. 1012-9.

394. Yip, S.P., et al., *A DNA pooling-based case-control study of myopia candidate genes COL11A1, COL18A1, FBN1, and PLOD1 in a Chinese population.* Molecular vision, 2011. 17: p. 810-21.

395. Joyce, S., et al., *Locus heterogeneity and Knobloch syndrome.* American journal of medical genetics. Part A, 2010. 152A(11): p. 2880-1.

396. Nirmalan, P.K., et al., *Consanguinity and eye diseases with a potential genetic etiology. Data from a prevalence study in Andhra Pradesh, India.* Ophthalmic Epidemiology, 2006. 13(1): p. 7-13.

397. Salmon, J.F., C.E. Wallis, and A.D. Murray, *Variable expressivity of autosomal dominant microcornea with cataract.* Archives of ophthalmology, 1988. 106(4): p. 505-10.

398. Khan, K., et al., *Genetic heterogeneity for recessively inherited congenital cataract microcornea with corneal opacity.* Investigative ophthalmology & visual science, 2011. 52(7): p. 4294-9.

399. Wang, K.J., et al., *A novel mutation in CRYBB1 associated with congenital cataract-microcornea syndrome: the p.Ser129Arg mutation destabilizes the betaB1/betaA3-crystallin heteromer but not the betaB1-crystallin homomer.* Human mutation, 2011. 32(3): p. E2050-60.

400. Wang, P., et al., *PAX6 mutations identified in 4 of 35 families with microcornea.* Investigative ophthalmology & visual science, 2012. 53(10): p. 6338-42.

401. Reis, L.M., et al., *BMP4 loss-of-function mutations in developmental eye disorders including SHORT syndrome.* Human genetics, 2011. 130(4): p. 495-504.

402. Coupry, I., et al., *Ophthalmological features associated with COL4A1 mutations.* Archives of ophthalmology, 2010. 128(4): p. 483-9.

403. Reddy, M.A., et al., *A clinical and molecular genetic study of a rare dominantly inherited syndrome (MRCS) comprising of microcornea, rod-cone dystrophy, cataract, and posterior staphyloma.* Br J Ophthalmol, 2003. 87(2): p. 197-202.

404. Michaelides, M., et al., *Evidence of genetic heterogeneity in MRCS (microcornea, rod-cone dystrophy, cataract, and posterior staphyloma) syndrome.* American journal of ophthalmology, 2006. 141(2): p. 418-20.

405. Ha, H.I., et al., *Imaging of Marfan syndrome: multisystemic manifestations.* Radiographics : a review publication of the Radiological Society of North America, Inc, 2007. 27(4): p. 989-1004.

406. Gabriel, L.A., et al., *ADAMTSL4, a secreted glycoprotein widely distributed in the eye, binds fibrillin-1 microfibrils and accelerates microfibril biogenesis.* Investigative ophthalmology & visual science, 2012. 53(1): p. 461-9.

407. Gregory-Evans, C.Y., et al., *Ocular coloboma: a reassessment in the age of molecular neuroscience.* Journal of medical genetics, 2004. 41(12): p. 881-91.

408. Kawasaki, A., *Disorders of Pupillary Function, Accommodation, and Lacrimation*, in *Clinical Neuro Ophthalmology*2005, Lippincott Williams & Wilkins: Philadelphia. p. 729-809.

409. de Vries, B.B., et al., *Homozygosity for a FBN1 missense mutation: clinical and molecular evidence for recessive Marfan syndrome.* European journal of human genetics : EJHG, 2007. 15(9): p. 930-5.

410. Spiro, R.G., *Protein glycosylation: nature, distribution, enzymatic formation, and disease implications of glycopeptide bonds.* Glycobiology, 2002. 12(4): p. 43R-56R.

411. Bause, E., *Structural requirements of N-glycosylation of proteins. Studies with proline peptides as conformational probes.* The Biochemical journal, 1983. 209(2): p. 331-6.

412. Hart, G.W., *Glycosylation.* Current Opinion in Cell Biology, 1992. 4(6): p. 1017-23.

413. Lonnqvist, L., et al., *A point mutation creating an extra N-glycosylation site in fibrillin-1 results in neonatal Marfan syndrome.* Genomics, 1996. 36(3): p. 468-75.

414. Whiteman, P. and P.A. Handford, *Defective secretion of recombinant fragments of fibrillin-1: implications of protein misfolding for the pathogenesis of Marfan syndrome and related disorders.* Human molecular genetics, 2003. 12(7): p. 727-37.

415. Bause, E. and G. Legler, *The role of the hydroxy amino acid in the triplet sequence Asn-Xaa-Thr(Ser) for the N-glycosylation step during glycoprotein biosynthesis.* The Biochemical journal, 1981. 195(3): p. 639-44.

416. Raghunath, M., C.M. Kielty, and B. Steinmann, *Truncated profibrillin of a Marfan patient is of apparent similar size as fibrillin: intracellular retention leads to over-N-glycosylation.* Journal of molecular biology, 1995. 248(5): p. 901-9.

417. Kramerova, I.A., et al., *Papilin in development; a pericellular protein with a homology to the ADAMTS metalloproteinases.* Development, 2000. 127(24): p. 5475-85.

418. Fessler, J.H., et al., *Papilin, a novel component of basement membranes, in relation to ADAMTS metalloproteases and ECM development.* The international journal of biochemistry & cell biology, 2004. 36(6): p. 1079-84.

419. Narooie-Nejad, M., et al., *Loss of function mutations in the gene encoding latent transforming growth factor beta binding protein 2, LTBP2, cause primary congenital glaucoma.* Human molecular genetics, 2009. 18(20): p. 3969-77.

420. Desir, J., et al., *LTBP2 null mutations in an autosomal recessive ocular syndrome with megalocornea, spherophakia, and secondary glaucoma.* European journal of human genetics : EJHG, 2010. 18(7): p. 761-7.

421. Khan, A.O., M.A. Aldahmesh, and F.S. Alkuraya, *Congenital megalocornea with zonular weakness and childhood lens-related secondary glaucoma - a distinct phenotype caused by recessive LTBP2 mutations.* Molecular vision, 2011. 17: p. 2570-9.

422. Haji-Seyed-Javadi, R., et al., *LTBP2 mutations cause Weill-Marchesani and Weill-Marchesani-like syndrome and affect disruptions in the extracellular matrix.* Human mutation, 2012. 33(8): p. 1182-7.

423. Benayoun, L., et al., *Genetic heterogeneity in two consanguineous families segregating early onset retinal degeneration: the pitfalls of homozygosity mapping.* American journal of medical genetics. Part A, 2009. 149A(4): p. 650-6.

424. G., W., *Ectopie du cristillins et malformations generales.* Ann. Oculist, 1932. 169: p. 21-44.

425. Marchesani, O., *Brachydaktylie und angeborene Kugellinse als Systemerkrankung.* Klin. Monatsbl. Aungenheilkd., 1939. 103: p. 392-406.

426. Tsilou, E. and I.M. MacDonald, *Weill-Marchesani Syndrome*, in *GeneReviews*, R.A. Pagon, et al., Editors. 1993: Seattle (WA).

427. Kojuri, J., M.R. Razeghinejad, and A. Aslani, *Cardiac findings in Weill-Marchesani syndrome.* American journal of medical genetics. Part A, 2007. 143A(17): p. 2062-4.

428. Faivre, L., et al., *Clinical homogeneity and genetic heterogeneity in Weill-Marchesani syndrome.* American journal of medical genetics. Part A, 2003. 123A(2): p. 204-7.

429. Superti-Furga, A. and S. Unger, *Nosology and classification of genetic skeletal disorders: 2006 revision.* American journal of medical genetics. Part A, 2007. 143(1): p. 1-18.

430. Temtamy, S.A. and M.S. Aglan, *Brachydactyly.* Orphanet journal of rare diseases, 2008. 3: p. 15.

431. Faivre, L., et al., *In frame fibrillin-1 gene deletion in autosomal dominant Weill-Marchesani syndrome.* Journal of medical genetics, 2003. 40(1): p. 34-6.

432. Sengle, G., et al., *Microenvironmental regulation by fibrillin-1.* PLoS genetics, 2012. 8(1): p. e1002425.

433. Cain, S.A., et al., *Fibrillin-1 mutations causing Weill-Marchesani syndrome and acromicric and geleophysic dysplasias disrupt heparan sulfate interactions.* PloS one, 2012. 7(11): p. e48634.

434. Dehainault, C., et al., *A deep intronic mutation in the RB1 gene leads to intronic sequence exonisation.* European journal of human genetics : EJHG, 2007. 15(4): p. 473-7.

435. Webb, T.R., et al., *Deep intronic mutation in OFD1, identified by targeted genomic next-generation sequencing, causes a severe form of X-linked retinitis pigmentosa (RP23).* Human molecular genetics, 2012. 21(16): p. 3647-54.

436. Mani, R.S. and A.M. Chinnaiyan, *Triggers for genomic rearrangements: insights into genomic, cellular and environmental influences.* Nature reviews. Genetics, 2010. 11(12): p. 819-29.

437. Aguilera, A., *The connection between transcription and genomic instability.* The EMBO journal, 2002. 21(3): p. 195-201.

438. Durkin, S.G. and T.W. Glover, *Chromosome fragile sites.* Annual Review of Genetics, 2007. 41: p. 169-92.

439. Wells, R.D., *Non-B DNA conformations, mutagenesis and disease.* Trends in Biochemical Sciences, 2007. 32(6): p. 271-8.

440. Stankiewicz, P. and J.R. Lupski, *Genome architecture, rearrangements and genomic disorders.* Trends in genetics : TIG, 2002. 18(2): p. 74-82.

441. Bailey, J.A., et al., *Recent segmental duplications in the human genome.* Science, 2002. 297(5583): p. 1003-7.

442. Hastings, P.J., et al., *Mechanisms of change in gene copy number.* Nature reviews. Genetics, 2009. 10(8): p. 551-64.

443. Kozlowski, L.T., et al., *Using a telephone survey to acquire genetic and behavioral data related to cigarette smoking in "made-anonymous" and "registry" samples.* American journal of epidemiology, 2002. 156(1): p. 68-77.

444. Zeng, F., et al., *Array-MLPA: comprehensive detection of deletions and duplications and its application to DMD patients.* Human mutation, 2008. 29(1): p. 190-7.

445. Barrett, M.T., et al., *Comparative genomic hybridization using oligonucleotide microarrays and total genomic DNA.* Proceedings of the National Academy of Sciences of the United States of America, 2004. 101(51): p. 17765-70.

446. Reis, L.M. and E.V. Semina, *Genetics of anterior segment dysgenesis disorders.* Current Opinion in Ophthalmology, 2011. 22(5): p. 314-24.

447. Marian, A.J., *Molecular genetic studies of complex phenotypes.* Translational research : the journal of laboratory and clinical medicine, 2012. 159(2): p. 64-79.

448. Cordell, H.J., *Detecting gene-gene interactions that underlie human diseases.* Nature reviews. Genetics, 2009. 10(6): p. 392-404.

449. Cordell, H.J., *Estimation and testing of gene-environment interactions in family-based association studies.* Genomics, 2009. 93(1): p. 5-9.

450. Vaisse, C., et al., *Melanocortin-4 receptor mutations are a frequent and heterogeneous cause of morbid obesity.* The Journal of clinical investigation, 2000. 106(2): p. 253-62.

451. Georges, M., *Mapping, fine mapping, and molecular dissection of quantitative trait Loci in domestic animals.* Annual review of genomics and human genetics, 2007. 8: p. 131-62.

452. Badner, J.A., et al., *A genetic study of Hirschsprung disease.* American journal of human genetics, 1990. 46(3): p. 568-80.

453. Altmuller, J., et al., *Genomewide scans of complex human diseases: true linkage is hard to find.* American journal of human genetics, 2001. 69(5): p. 936-50.

454. **Ogura, Y., et al., *A frameshift mutation in NOD2 associated with susceptibility to Crohn's disease.* Nature, 2001. 411(6837): p. 603-6.**

455. **Klein, A.P., et al., *Linkage analysis of Quantitative Refraction and Refractive Errors in the Beaver Dam Eye Study.* Investigative ophthalmology & visual science, 2011.**

456. **Risch, N. and K. Merikangas, *The future of genetic studies of complex human diseases.* Science, 1996. 273(5281): p. 1516-7.**

457. **Becker, K.G., *The common variants/multiple disease hypothesis of common complex genetic disorders.* Medical hypotheses, 2004. 62(2): p. 309-17.**

458. **Cordell, H.J. and D.G. Clayton, *Genetic association studies.* Lancet, 2005. 366(9491): p. 1121-31.**

459. **Manolio, T.A., et al., *Finding the missing heritability of complex diseases.* Nature, 2009. 461(7265): p. 747-53.**

460. ***A haplotype map of the human genome.* Nature, 2005. 437(7063): p. 1299-320.**

461. **Sachidanandam, R., et al., *A map of human genome sequence variation containing 1.42 million single nucleotide polymorphisms.* Nature, 2001. 409(6822): p. 928-33.**

462. **Hartl, D.L. and A.G. Clark, *Principles of population genetics*. 4th ed. ed2007, New York: W. H. Freeman ; Basingstoke : Palgrave [distributor].**

463. **Edwards, A.W., *G. H. Hardy (1908) and Hardy-Weinberg equilibrium.* Genetics, 2008. 179(3): p. 1143-50.**

464. ***Genome-wide association study of 14,000 cases of seven common diseases and 3,000 shared controls.* Nature, 2007. 447(7145): p. 661-78.**

465. **Teo, Y.Y., et al., *On the usage of HWE for identifying genotyping errors.* Annals of human genetics, 2007. 71(Pt 5): p. 701-3; author reply 704.**

466. **K., L.R.C.K., *The evolutionary dynamics of complex polymorphisms. .* Evolution, 1960. 14: p. 458-472.**

467. Wang, X., R.C. Elston, and X. Zhu, *The meaning of interaction.* Human Heredity, 2010. 70(4): p. 269-77.

468. Reich, D.E., et al., *Linkage disequilibrium in the human genome.* Nature, 2001. 411(6834): p. 199-204.

469. Jeffreys, A.J., L. Kauppi, and R. Neumann, *Intensely punctate meiotic recombination in the class II region of the major histocompatibility complex.* Nature genetics, 2001. 29(2): p. 217-22.

470. Jorde, L.B., *Linkage disequilibrium and the search for complex disease genes.* Genome research, 2000. 10(10): p. 1435-44.

471. Slatkin, M., *Linkage disequilibrium--understanding the evolutionary past and mapping the medical future.* Nature reviews. Genetics, 2008. 9(6): p. 477-85.

472. Orr, N. and S. Chanock, *Common genetic variation and human disease.* Advances in Genetics, 2008. 62: p. 1-32.

473. Carlson, C.S., et al., *Selecting a maximally informative set of single-nucleotide polymorphisms for association analyses using linkage disequilibrium.* American journal of human genetics, 2004. 74(1): p. 106-20.

474. Spencer, C.C., et al., *Designing genome-wide association studies: sample size, power, imputation, and the choice of genotyping chip.* PLoS genetics, 2009. 5(5): p. e1000477.

475. McCarthy, M.I., et al., *Genome-wide association studies for complex traits: consensus, uncertainty and challenges.* Nature reviews. Genetics, 2008. 9(5): p. 356-69.

476. Hong, H., et al., *Assessing batch effects of genotype calling algorithm BRLMM for the Affymetrix GeneChip Human Mapping 500 K array set using 270 HapMap samples.* BMC bioinformatics, 2008. 9 Suppl 9: p. S17.

477. Balding, D.J., *A tutorial on statistical methods for population association studies.* Nature reviews. Genetics, 2006. 7(10): p. 781-791.

478. Frazer, K.A., et al., *A second generation human haplotype map of over 3.1 million SNPs.* Nature, 2007. 449(7164): p. 851-61.

479. Mitry, D., et al., *SNP mistyping in genotyping arrays--an important cause of spurious association in case-control studies.* Genet.Epidemiol., 2011. 35(5): p. 423-426.

480. Price, A.L., et al., *Principal components analysis corrects for stratification in genome-wide association studies.* Nature genetics, 2006. 38(8): p. 904-9.

481. Campbell, C.D., et al., *Demonstrating stratification in a European American population.* Nature genetics, 2005. 37(8): p. 868-72.

482. Anderson, C.A., et al., *Data quality control in genetic case-control association studies.* Nature protocols, 2010. 5(9): p. 1564-73.

483. Hoggart, C.J., et al., *Genome-wide significance for dense SNP and resequencing data.* Genetic epidemiology, 2008. 32(2): p. 179-85.

484. Troendle, J.F. and J.L. Mills, *Correction for multiplicity in genetic association studies of triads: the permutational TDT.* Annals of human genetics, 2011. 75(2): p. 284-91.

485. Chanock, S.J., et al., *Replicating genotype-phenotype associations.* Nature, 2007. 447(7145): p. 655-660.

486. Hyman, L.G., et al., *Senile macular degeneration: a case-control study.* American journal of epidemiology, 1983. 118(2): p. 213-27.

487. Klein, M.L., W.M. Mauldin, and V.D. Stoumbos, *Heredity and age-related macular degeneration. Observations in monozygotic twins.* Archives of ophthalmology, 1994. 112(7): p. 932-7.

488. Hammond, C.J., et al., *Genetic influence on early age-related maculopathy: a twin study.* Ophthalmology, 2002. 109(4): p. 730-6.

489. Weeks, D.E., et al., *A full genome scan for age-related maculopathy.* Human molecular genetics, 2000. 9(9): p. 1329-49.

490. Stone, E.M., V.C. Sheffield, and G.S. Hageman, *Molecular genetics of age-related macular degeneration.* Human molecular genetics, 2001. 10(20): p. 2285-92.

491. Katta, S., I. Kaur, and S. Chakrabarti, *The molecular genetic basis of age-related macular degeneration: an overview.* Journal of genetics, 2009. 88(4): p. 425-49.

492. **Klein, R.J., et al., *Complement factor H polymorphism in age-related macular degeneration.* Science, 2005. 308(5720): p. 385-9.**

493. **Edwards, A.O., et al., *Complement factor H polymorphism and age-related macular degeneration.* Science, 2005. 308(5720): p. 421-4.**

494. **Haines, J.L., et al., *Complement factor H variant increases the risk of age-related macular degeneration.* Science, 2005. 308(5720): p. 419-21.**

495. **Laine, M., et al., *Y402H polymorphism of complement factor H affects binding affinity to C-reactive protein.* Journal of immunology, 2007. 178(6): p. 3831-6.**

496. **Gold, B., et al., *Variation in factor B (BF) and complement component 2 (C2) genes is associated with age-related macular degeneration.* Nature genetics, 2006. 38(4): p. 458-62.**

497. **Spencer, K.L., et al., *C3 R102G polymorphism increases risk of age-related macular degeneration.* Human molecular genetics, 2008. 17(12): p. 1821-4.**

498. **McKay, G.J., et al., *Further assessment of the complement component 2 and factor B region associated with age-related macular degeneration.* Investigative ophthalmology & visual science, 2009. 50(2): p. 533-9.**

499. **Richardson, A.J., et al., *Analysis of rare variants in the complement component 2 (C2) and factor B (BF) genes refine association for age-related macular degeneration (AMD).* Investigative ophthalmology & visual science, 2009. 50(2): p. 540-3.**

500. **Rivera, A., et al., *Hypothetical LOC387715 is a second major susceptibility gene for age-related macular degeneration, contributing independently of complement factor H to disease risk.* Human molecular genetics, 2005. 14(21): p. 3227-36.**

501. **Dewan, A., et al., *HTRA1 promoter polymorphism in wet age-related macular degeneration.* Science, 2006. 314(5801): p. 989-92.**

502. **Clausen, T., C. Southan, and M. Ehrmann, *The HtrA family of proteases: implications for protein composition and cell fate.* Molecular cell, 2002. 10(3): p. 443-55.**

503. **Tocharus, J., et al., *Developmentally regulated expression of mouse HtrA3 and its role as an inhibitor of TGF-beta signaling.* Development, growth & differentiation, 2004. 46(3): p. 257-74.**

504. **Tong, Y., et al., *LOC387715/HTRA1 gene polymorphisms and susceptibility to age-related macular degeneration: A HuGE review and meta-analysis.* Molecular vision, 2010. 16: p. 1958-81.**

505. **Kopplin, L.J., et al., *Genome-wide association identifies SKIV2L and MYRIP as protective factors for age-related macular degeneration.* Genes and immunity, 2010. 11(8): p. 609-21.**

506. **Klomp, A.E., et al., *Analysis of the linkage of MYRIP and MYO7A to melanosomes by RAB27A in retinal pigment epithelial cells.* Cell motility and the cytoskeleton, 2007. 64(6): p. 474-87.**

507. **Yang, Z., X. Qu, and C.Y. Yu, *Features of the two gene pairs RD-SKI2W and DOM3Z-RP1 located between complement component genes factor B and C4 at the MHC class III region.* Frontiers in bioscience : a journal and virtual library, 2001. 6: p. D927-35.**

508. **Kondo, N., et al., *Role of RDBP and SKIV2L variants in the major histocompatibility complex class III region in polypoidal choroidal vasculopathy etiology.* Ophthalmology, 2009. 116(8): p. 1502-9.**

509. **Schaumberg, D.A., et al., *A prospective study of 2 major age-related macular degeneration susceptibility alleles and interactions with modifiable risk factors.* Archives of ophthalmology, 2007. 125(1): p. 55-62.**

510. **Seddon, J.M., et al., *Prediction model for prevalence and incidence of advanced age-related macular degeneration based on genetic, demographic, and environmental variables.* Investigative ophthalmology & visual science, 2009. 50(5): p. 2044-53.**

511. **Chen, Y., et al., *Assessing susceptibility to age-related macular degeneration with genetic markers and environmental factors.* Archives of ophthalmology, 2011. 129(3): p. 344-51.**

512. **Tsuchihashi, T., et al., *Complement factor H and high-temperature requirement A-1 genotypes and treatment response of age-related macular degeneration.* Ophthalmology, 2011. 118(1): p. 93-100.**

513. **McKibbin, M., et al., *CFH, VEGF and HTRA1 promoter genotype may influence the response to intravitreal ranibizumab therapy for neovascular age-related macular degeneration.* Br J Ophthalmol, 2011.**

514. ***Trials.gov,* N.C.; Available from: http://clinicaltrials.gov.**

515. Stone, E.M., et al., *Identification of a gene that causes primary open angle glaucoma.* Science, 1997. 275(5300): p. 668-70.

516. Kwon, Y.H., et al., *Primary open-angle glaucoma.* N Engl J Med, 2009. 360(11): p. 1113-24.

517. Rezaie, T., et al., *Adult-onset primary open-angle glaucoma caused by mutations in optineurin.* Science, 2002. 295(5557): p. 1077-9.

518. Footz, T.K., et al., *Glaucoma-associated WDR36 variants encode functional defects in a yeast model system.* Human molecular genetics, 2009. 18(7): p. 1276-87.

519. Hewitt, A.W., J.E. Craig, and D.A. Mackey, *Complex genetics of complex traits: the case of primary open-angle glaucoma.* Clinical & experimental ophthalmology, 2006. 34(5): p. 472-84.

520. Nakano, M., et al., *Three susceptible loci associated with primary open-angle glaucoma identified by genome-wide association study in a Japanese population.* Proceedings of the National Academy of Sciences of the United States of America, 2009. 106(31): p. 12838-42.

521. Rao, K.N., I. Kaur, and S. Chakrabarti, *Lack of association of three primary open-angle glaucoma-susceptible loci with primary glaucomas in an Indian population.* Proceedings of the National Academy of Sciences of the United States of America, 2009. 106(44): p. E125-6; author reply E127.

522. Thorleifsson, G., et al., *Common variants near CAV1 and CAV2 are associated with primary open-angle glaucoma.* Nature genetics, 2010. 42(10): p. 906-9.

523. Kuehn, M.H., et al., *Chromosome 7q31 POAG locus: ocular expression of caveolins and lack of association with POAG in a US cohort.* Molecular vision, 2011. 17: p. 430-5.

524. Toda, N. and M. Nakanishi-Toda, *Nitric oxide: ocular blood flow, glaucoma, and diabetic retinopathy.* Progress in retinal and eye research, 2007. 26(3): p. 205-38.

525. Mishra, A., et al., *Genetic variants near PDGFRA are associated with corneal curvature in Australians.* Investigative ophthalmology & visual science, 2012. 53(11): p. 7131-6.

526. *The International HapMap Project.* Nature, 2003. 426(6968): p. 789-96.

527. Osman, W., et al., *A genome-wide association study in the Japanese population confirms 9p21 and 14q23 as susceptibility loci for primary open angle glaucoma.* Human molecular genetics, 2012. 21(12): p. 2836-42.

528. Burdon, K.P., et al., *Genome-wide association study identifies susceptibility loci for open angle glaucoma at TMCO1 and CDKN2B-AS1.* Nature genetics, 2011. 43(6): p. 574-8.

529. Zhang, Z., et al., *Molecular cloning, expression patterns and subcellular localization of porcine TMCO1 gene.* Mol Biol Rep, 2010. 37(3): p. 1611-8.

530. Ramdas, W.D., et al., *A genome-wide association study of optic disc parameters.* PLoS genetics, 2010. 6(6): p. e1000978.

531. Wiggs, J.L., et al., *Common variants at 9p21 and 8q22 are associated with increased susceptibility to optic nerve degeneration in glaucoma.* PLoS genetics, 2012. 8(4): p. e1002654.

532. Cao, D., et al., *CDKN2B polymorphism is associated with primary open-angle glaucoma (POAG) in the Afro-Caribbean population of Barbados, West Indies.* PloS one, 2012. 7(6): p. e39278.

533. Iwase, A., et al., *The prevalence of primary open-angle glaucoma in Japanese: the Tajimi Study.* Ophthalmology, 2004. 111(9): p. 1641-8.

534. Yu-Wai-Man, P., et al., *OPA1 increases the risk of normal but not high tension glaucoma.* Journal of medical genetics, 2010. 47(2): p. 120-5.

535. Mabuchi, F., et al., *The OPA1 gene polymorphism is associated with normal tension and high tension glaucoma.* American journal of ophthalmology, 2007. 143(1): p. 125-130.

536. Aung, T., et al., *A major marker for normal tension glaucoma: association with polymorphisms in the OPA1 gene.* Human genetics, 2002. 110(1): p. 52-6.

537. Toda, Y., et al., *Mutations in the optineurin gene in Japanese patients with primary open-angle glaucoma and normal tension glaucoma.* American journal of medical genetics. Part A, 2004. 125A(1): p. 1-4.

538. Fan, B.J., et al., *Association of polymorphisms of tumor necrosis factor and tumor protein p53 with primary open-angle glaucoma.* Investigative ophthalmology & visual science, 2010. 51(8): p. 4110-6.

539. Vickers, J.C., et al., *The apolipoprotein epsilon4 gene is associated with elevated risk of normal tension glaucoma.* Molecular vision, 2002. 8: p. 389-93.

540. Lam, C.Y., et al., *Association of apolipoprotein E polymorphisms with normal tension glaucoma in a Chinese population.* Journal of glaucoma, 2006. 15(3): p. 218-22.

541. Wiggs, J.L., *Genetic etiologies of glaucoma.* Archives of ophthalmology, 2007. 125(1): p. 30-7.

542. Mabuchi, F., et al., *Association between SRBD1 and ELOVL5 Gene Polymorphisms and Primary Open-Angle Glaucoma.* Investigative ophthalmology & visual science, 2011. 52(7): p. 4626-9.

543. Nakano, M., et al., *Common variants in CDKN2B-AS1 associated with optic-nerve vulnerability of glaucoma identified by genome-wide association studies in Japanese.* PloS one, 2012. 7(3): p. e33389.

544. Takamoto, M., et al., *Common variants on chromosome 9p21 are associated with normal tension glaucoma.* PloS one, 2012. 7(7): p. e40107.

545. Pasquale, L.R., et al., *CDKN2B-AS1 Genotype-Glaucoma Feature Correlations in Primary Open-Angle Glaucoma Patients From the United States.* American journal of ophthalmology, 2012.

546. Mabuchi, F., et al., *Association between genetic variants associated with vertical cup-to-disc ratio and phenotypic features of primary open-angle glaucoma.* Ophthalmology, 2012. 119(9): p. 1819-25.

547. Gottfredsdottir, M.S., et al., *Chronic open-angle glaucoma and associated ophthalmic findings in monozygotic twins and their spouses in Iceland.* Journal of glaucoma, 1999. 8(2): p. 134-9.

548. Damji, K.F., et al., *Familial occurrence of pseudoexfoliation in Canada.* Canadian journal of ophthalmology. Journal canadien d'ophtalmologie, 1999. 34(5): p. 257-65.

549. Krumbiegel, M., et al., *Exploring functional candidate genes for genetic association in german patients with pseudoexfoliation syndrome and pseudoexfoliation glaucoma.* Investigative ophthalmology & visual science, 2009. 50(6): p. 2796-801.

550. Thorleifsson, G., et al., *Common sequence variants in the LOXL1 gene confer susceptibility to exfoliation glaucoma.* Science, 2007. 317(5843): p. 1397-400.

551. Fan, B.J., et al., *DNA sequence variants in the LOXL1 gene are associated with pseudoexfoliation glaucoma in a U.S. clinic-based population with broad ethnic diversity.* BMC medical genetics, 2008. 9: p. 5.

552. Lemmela, S., et al., *Association of LOXL1 gene with Finnish exfoliation syndrome patients.* Journal of human genetics, 2009. 54(5): p. 289-97.

553. Mossbock, G., et al., *Lysyl oxidase-like protein 1 (LOXL1) gene polymorphisms and exfoliation glaucoma in a Central European population.* Molecular vision, 2008. 14: p. 857-61.

554. Aragon-Martin, J.A., et al., *Evaluation of LOXL1 gene polymorphisms in exfoliation syndrome and exfoliation glaucoma.* Molecular vision, 2008. 14: p. 533-41.

555. Mori, K., et al., *LOXL1 genetic polymorphisms are associated with exfoliation glaucoma in the Japanese population.* Molecular vision, 2008. 14: p. 1037-40.

556. Fuse, N., et al., *Evaluation of LOXL1 polymorphisms in eyes with exfoliation glaucoma in Japanese.* Molecular vision, 2008. 14: p. 1338-43.

557. Pasutto, F., et al., *Association of LOXL1 common sequence variants in German and Italian patients with pseudoexfoliation syndrome and pseudoexfoliation glaucoma.* Investigative ophthalmology & visual science, 2008. 49(4): p. 1459-63.

558. Chen, L., et al., *Evaluation of LOXL1 polymorphisms in exfoliation syndrome in a Chinese population.* Molecular vision, 2009. 15: p. 2349-57.

559. Liu, X., et al., *Elastic fiber homeostasis requires lysyl oxidase-like 1 protein.* Nature genetics, 2004. 36(2): p. 178-82.

560. Schlotzer-Schrehardt, U. and G.O. Naumann, *Ocular and systemic pseudoexfoliation syndrome.* American journal of ophthalmology, 2006. 141(5): p. 921-937.

561. Schlotzer-Schrehardt, U., et al., *Genotype-correlated expression of lysyl oxidase-like 1 in ocular tissues of patients with pseudoexfoliation syndrome/glaucoma and normal patients.* The American journal of pathology, 2008. 173(6): p. 1724-35.

562. Khan, T.T., et al., *LOXL1 expression in lens capsule tissue specimens from individuals with pseudoexfoliation syndrome and glaucoma.* Molecular vision, 2010. 16: p. 2236-41.

563. Urban, Z., et al., *Population differences in elastin maturation in optic nerve head tissue and astrocytes.* Investigative ophthalmology & visual science, 2007. 48(7): p. 3209-15.

564. Krumbiegel, M., et al., *Genome-wide association study with DNA pooling identifies variants at CNTNAP2 associated with pseudoexfoliation syndrome.* European journal of human genetics : EJHG, 2011. 19(2): p. 186-93.

565. Poliak, S., et al., *Caspr2, a new member of the neurexin superfamily, is localized at the juxtaparanodes of myelinated axons and associates with K+ channels.* Neuron, 1999. 24(4): p. 1037-47.

566. Horresh, I., et al., *Multiple molecular interactions determine the clustering of Caspr2 and Kv1 channels in myelinated axons.* The Journal of neuroscience : the official journal of the Society for Neuroscience, 2008. 28(52): p. 14213-22.

567. Liu, Y. and R.R. Allingham, *Molecular genetics in glaucoma.* Experimental eye research, 2011. 93(4): p. 331-9.

568. Awadalla, M.S., et al., *The association of hepatocyte growth factor (HGF) gene with primary angle closure glaucoma in the Nepalese population.* Molecular vision, 2011. 17: p. 2248-54.

569. Vithana, E.N., et al., *Genome-wide association analyses identify three new susceptibility loci for primary angle closure glaucoma.* Nature genetics, 2012. 44(10): p. 1142-6.

570. Krachmer, J.H., et al., *Corneal endothelial dystrophy. A study of 64 families.* Archives of ophthalmology, 1978. 96(11): p. 2036-9.

571. Biswas, S., et al., *Missense mutations in COL8A2, the gene encoding the alpha2 chain of type VIII collagen, cause two forms of corneal endothelial dystrophy.* Human molecular genetics, 2001. 10(21): p. 2415-23.

572. Vithana, E.N., et al., *SLC4A11 mutations in Fuchs endothelial corneal dystrophy.* Human molecular genetics, 2008. 17(5): p. 656-66.

573. Riazuddin, S.A., et al., *Missense mutations in TCF8 cause late-onset Fuchs corneal dystrophy and interact with FCD4 on chromosome 9p.* American journal of human genetics, 2010. 86(1): p. 45-53.

574. Baratz, K.H., et al., *E2-2 protein and Fuchs's corneal dystrophy.* N Engl J Med, 2010. 363(11): p. 1016-24.

575. Murre, C., et al., *Structure and function of helix-loop-helix proteins.* Biochimica et biophysica acta, 1994. 1218(2): p. 129-35.

576. Li, Y.J., et al., *Replication of TCF4 through association and linkage studies in late-onset Fuchs endothelial corneal dystrophy.* PloS one, 2011. 6(4): p. e18044.

577. Thalamuthu, A., et al., *Association of TCF4 Gene Polymorphisms with Fuchs Corneal Dystrophy in the Chinese.* Investigative ophthalmology & visual science, 2011.

578. Forstot, S.L., et al., *Familial keratoconus.* American journal of ophthalmology, 1988. 105(1): p. 92-3.

579. Edwards, M., C.N. McGhee, and S. Dean, *The genetics of keratoconus.* Clinical & experimental ophthalmology, 2001. 29(6): p. 345-51.

580. De Bonis, P., et al., *Mutational screening of VSX1, SPARC, SOD1, LOX, and TIMP3 in keratoconus.* Molecular vision, 2011. 17: p. 2482-94.

581. Li, X., et al., *A genome-wide association study identifies a potential novel gene locus for keratoconus, one of the commonest causes for corneal transplantation in developed countries.* Human molecular genetics, 2012. 21(2): p. 421-9.

582. Lu, Y., et al., *Genome-wide association analyses identify multiple loci associated with central corneal thickness and keratoconus.* Nature genetics, 2013. 45(2): p. 155-63.

583. Schluter, O.M., et al., *Localization versus function of Rab3 proteins. Evidence for a common regulatory role in controlling fusion.* The Journal of biological chemistry, 2002. 277(43): p. 40919-29.

584. Aligianis, I.A., et al., *Mutations of the catalytic subunit of RAB3GAP cause Warburg Micro syndrome.* Nature genetics, 2005. 37(3): p. 221-3.

585. Burdon, K.P., et al., *Association of polymorphisms in the hepatocyte growth factor gene promoter with keratoconus.* Investigative ophthalmology & visual science, 2011. 52(11): p. 8514-9.

586. Han, W., et al., *Family-based association analysis of hepatocyte growth factor (HGF) gene polymorphisms in high myopia.* Investigative ophthalmology & visual science, 2006. 47(6): p. 2291-9.

587. Wilson, S.E., et al., *Hepatocyte growth factor, keratinocyte growth factor, their receptors, fibroblast growth factor receptor-2, and the cells of the cornea.* Investigative ophthalmology & visual science, 1993. 34(8): p. 2544-61.

588. Taylor, H.R. and J.E. Keeffe, *World blindness: a 21st century perspective.* Br J Ophthalmol, 2001. 85(3): p. 261-6.

589. Hallman, D.M., et al., *Familial aggregation of severity of diabetic retinopathy in Mexican Americans from Starr County, Texas.* Diabetes Care, 2005. 28(5): p. 1163-8.

590. Hietala, K., et al., *Heritability of proliferative diabetic retinopathy.* Diabetes, 2008. 57(8): p. 2176-80.

591. Patel, S., et al., *Genetic susceptibility of diabetic retinopathy.* Current diabetes reports, 2008. 8(4): p. 257-62.

592. Grassi, M.A., et al., *Genome-wide meta-analysis for severe diabetic retinopathy.* Human molecular genetics, 2011. 20(12): p. 2472-81.

593. Huang, Y.C., et al., *Genome-wide association study of diabetic retinopathy in a Taiwanese population.* Ophthalmology, 2011. 118(4): p. 642-8.

594. Sandirasegarane, L. and M. Kester, *Enhanced stimulation of Akt-3/protein kinase B-gamma in human aortic smooth muscle cells.* Biochemical and biophysical research communications, 2001. 283(1): p. 158-63.

595. Grassi, M.A., et al., *Replication analysis for severe diabetic retinopathy.* Investigative ophthalmology & visual science, 2012. 53(4): p. 2377-81.

596. Looker, H.C., et al., *Genome-wide linkage analyses to identify Loci for diabetic retinopathy.* Diabetes, 2007. 56(4): p. 1160-6.

597. Wojciechowski, R., *Nature and nurture: the complex genetics of myopia and refractive error.* Clin.Genet., 2011. 79(4): p. 301-320.

598. Nakanishi, H., et al., *A genome-wide association analysis identified a novel susceptible locus for pathological myopia at 11q24.1.* PLoS.Genet, 2009. 5(9): p. e1000660.

599. Shi, Y., et al., *Genetic Variants at 13q12.12 Are Associated with High Myopia in the Han Chinese Population.* American journal of human genetics, 2011.

600. Mattingly, R.R. and I.G. Macara, *Phosphorylation-dependent activation of the Ras-GRF/CDC25Mm exchange factor by muscarinic receptors and G-protein beta gamma subunits.* Nature, 1996. 382(6588): p. 268-272.

601. McBrien, N.A., H.O. Moghaddam, and A.P. Reeder, *Atropine reduces experimental myopia and eye enlargement via a nonaccommodative mechanism.* Invest Ophthalmol Vis.Sci., 1993. 34(1): p. 205-215.

602. Chua, W.H., et al., *Atropine for the treatment of childhood myopia.* Ophthalmology, 2006. 113(12): p. 2285-2291.

603. Kiefer, A.K., et al., *Genome-wide analysis points to roles for extracellular matrix remodeling, the visual cycle, and neuronal development in myopia.* PLoS genetics, 2013. 9(2): p. e1003299.

604. Verhoeven, V.J., et al., *Genome-wide meta-analyses of multiancestry cohorts identify multiple new susceptibility loci for refractive error and myopia.* Nature genetics, 2013. 45(3): p. 314-8.

605. Verhoeven, V.J., et al., *Large scale international replication and meta-analysis study confirms association of the 15q14 locus with myopia. The CREAM consortium.* Human genetics, 2012. 131(9): p. 1467-80.

606. Hannon, G.J. and D. Beach, *p15INK4B is a potential effector of TGF-beta-induced cell cycle arrest.* Nature, 1994. 371(6494): p. 257-61.

607. Gallardo, M.E., et al., *Genomic cloning and characterization of the human homeobox gene SIX6 reveals a cluster of SIX genes in chromosome 14 and associates SIX6 hemizygosity with bilateral anophthalmia and pituitary anomalies.* Genomics, 1999. 61(1): p. 82-91.

608. Schmidt, W.M., et al., *Mutation in the Scyl1 gene encoding amino-terminal kinase-like protein causes a recessive form of spinocerebellar neurodegeneration.* EMBO reports, 2007. 8(7): p. 691-7.

609. Macgregor, S., et al., *Genome-wide association identifies ATOH7 as a major gene determining human optic disc size.* Human molecular genetics, 2010. 19(13): p. 2716-24.

610. Girkin, C.A., et al., *Differences in optic disc topography between black and white normal subjects.* Ophthalmology, 2005. 112(1): p. 33-9.

611. Khor, C.C., et al., *Genome-wide association studies in Asians confirm the involvement of ATOH7 and TGFBR3, and further identify CARD10 as a novel locus influencing optic disc area.* Human molecular genetics, 2011. 20(9): p. 1864-72.

612. Wang, L., et al., *Card10 is a novel caspase recruitment domain/membrane-associated guanylate kinase family member that interacts with BCL10 and activates NF-kappa B.* The Journal of biological chemistry, 2001. 276(24): p. 21405-9.

613. Tan, L., et al., *The Toll-->NFkappaB signaling pathway mediates the neuropathological effects of the human Alzheimer's Abeta42 polypeptide in Drosophila.* PloS one, 2008. 3(12): p. e3966.

614. Ramdas, W.D., et al., *Common genetic variants associated with open-angle glaucoma.* Human molecular genetics, 2011. 20(12): p. 2464-71.

615. Dueker, D.K., et al., *Corneal thickness measurement in the management of primary open-angle glaucoma: a report by the American Academy of Ophthalmology.* Ophthalmology, 2007. 114(9): p. 1779-87.

616. Toh, T., et al., *Central corneal thickness is highly heritable: the twin eye studies.* Investigative ophthalmology & visual science, 2005. 46(10): p. 3718-22.

617. Segev, F., et al., *Structural abnormalities of the cornea and lid resulting from collagen V mutations.* Investigative ophthalmology & visual science, 2006. 47(2): p. 565-73.

618. Brandt, J.D., L.A. Casuso, and D.L. Budenz, *Markedly increased central corneal thickness: an unrecognized finding in congenital aniridia.* American journal of ophthalmology, 2004. 137(2): p. 348-50.

619. Lu, Y., et al., *Common genetic variants near the Brittle Cornea Syndrome locus ZNF469 influence the blinding disease risk factor central corneal thickness.* PLoS genetics, 2010. 6(5): p. e1000947.

620. Berry, F.B., et al., *FOXC1 is required for cell viability and resistance to oxidative stress in the eye through the transcriptional regulation of FOXO1A.* Human molecular genetics, 2008. 17(4): p. 490-505.

621. Abu, A., et al., *Deleterious mutations in the Zinc-Finger 469 gene cause brittle cornea syndrome.* American journal of human genetics, 2008. 82(5): p. 1217-22.

622. Vitart, V., et al., *New loci associated with central cornea thickness include COL5A1, AKAP13 and AVGR8.* Human molecular genetics, 2010. 19(21): p. 4304-11.

623. Ormestad, M., et al., *Foxf1 and Foxf2 control murine gut development by limiting mesenchymal Wnt signaling and promoting extracellular matrix production.* Development, 2006. 133(5): p. 833-43.

624. Birk, D.E., et al., *Collagen type I and type V are present in the same fibril in the avian corneal stroma.* The Journal of cell biology, 1988. 106(3): p. 999-1008.

625. Fichard, A., J.P. Kleman, and F. Ruggiero, *Another look at collagen V and XI molecules.* Matrix biology : journal of the International Society for Matrix Biology, 1995. 14(7): p. 515-31.

626. Wenstrup, R.J., et al., *Murine model of the Ehlers-Danlos syndrome. col5a1 haploinsufficiency disrupts collagen fibril assembly at multiple stages.* The Journal of biological chemistry, 2006. 281(18): p. 12888-95.

627. Hoehn, R., et al., *Population-based meta-analysis in Caucasians confirms association with COL5A1 and ZNF469 but not COL8A2 with central corneal thickness.* Human genetics, 2012. 131(11): p. 1783-93.

628. Schache, M., et al., *The hepatocyte growth factor receptor (MET) gene is not associated with refractive error and ocular biometrics in a Caucasian population.* Molecular vision, 2009. 15: p. 2599-605.

629. Pellegata, N.S., et al., *Mutations in KERA, encoding keratocan, cause cornea plana.* Nature genetics, 2000. 25(1): p. 91-5.

630. Han, S., et al., *Association of variants in FRAP1 and PDGFRA with corneal curvature in Asian populations from Singapore.* Human molecular genetics, 2011. 20(18): p. 3693-8.

631. **Lassarre, C. and J.M. Ricort, *Growth factor-specific regulation of insulin receptor substrate-1 expression in MCF-7 breast carcinoma cells: effects on the insulin-like growth factor signaling pathway.* Endocrinology, 2003. 144(11): p. 4811-9.**

632. **Liu, Q., et al., *Implication of platelet-derived growth factor receptor alpha in prostate cancer skeletal metastasis.* Chin J Cancer, 2011. 30(9): p. 612-9.**

633. **Lei, H., et al., *Expression of PDGFR{alpha} Is a Determinant of the PVR Potential of ARPE19 Cells.* Investigative ophthalmology & visual science, 2011. 52(9): p. 5016-21.**

634. **Rabinowitz, Y.S., L. Dong, and G. Wistow, *Gene expression profile studies of human keratoconus cornea for NEIBank: a novel cornea-expressed gene and the absence of transcripts for aquaporin 5.* Investigative ophthalmology & visual science, 2005. 46(4): p. 1239-46.**

635. **Fan, Q., et al., *Genome-wide meta-analysis of five Asian cohorts identifies PDGFRA as a susceptibility locus for corneal astigmatism.* PLoS genetics, 2011. 7(12): p. e1002402.**

636. **Carbonaro, F., et al., *Heritability of intraocular pressure: a classical twin study.* Br J Ophthalmol, 2008. 92(8): p. 1125-8.**

637. **van Koolwijk, L.M., et al., *Common genetic determinants of intraocular pressure and primary open-angle glaucoma.* PLoS genetics, 2012. 8(5): p. e1002611.**

638. **Wiggs, J.L., et al., *Genome-wide scan for adult onset primary open angle glaucoma.* Human molecular genetics, 2000. 9(7): p. 1109-17.**

639. **Prokopenko, I., et al., *Variants in MTNR1B influence fasting glucose levels.* Nature genetics, 2009. 41(1): p. 77-81.**

640. **Zuk, O., et al., *The mystery of missing heritability: Genetic interactions create phantom heritability.* Proceedings of the National Academy of Sciences of the United States of America, 2012. 109(4): p. 1193-8.**

641. **Hindorff LA, J.H., Hall PN, Mehta JP and Manolio TA. . *A Catalog of Published Genome- Wide Association Studies.* . 2010 12/2010 [cited 2011 24/06/2011]; Available from: www.genome.gov/gwastudies.**

642. **Myles, S., et al., *Worldwide population differentiation at disease-associated SNPs.* BMC medical genomics, 2008. 1: p. 22.**

643. Frazer, K.A., et al., *Human genetic variation and its contribution to complex traits.* Nature reviews. Genetics, 2009. 10(4): p. 241-51.

644. Scherer, S.W., et al., *Challenges and standards in integrating surveys of structural variation.* Nature genetics, 2007. 39(7 Suppl): p. S7-15.

645. Costelloe, S.J., et al., *Gene-targeted analysis of copy number variants identifies 3 novel associations with coronary heart disease traits.* Circulation. Cardiovascular genetics, 2012. 5(5): p. 555-60.

646. Liu, M.M., C.C. Chan, and J. Tuo, *Genetic mechanisms and age-related macular degeneration: common variants, rare variants, copy number variations, epigenetics, and mitochondrial genetics.* Human genomics, 2012. 6: p. 13.

647. Ardlie, K., et al., *Lower-than-expected linkage disequilibrium between tightly linked markers in humans suggests a role for gene conversion.* American journal of human genetics, 2001. 69(3): p. 582-9.

648. Bodmer, W. and C. Bonilla, *Common and rare variants in multifactorial susceptibility to common diseases.* Nature genetics, 2008. 40(6): p. 695-701.

649. Keinan, A. and A.G. Clark, *Recent explosive human population growth has resulted in an excess of rare genetic variants.* Science, 2012. 336(6082): p. 740-3.

650. Cohen, J.C., et al., *Multiple rare alleles contribute to low plasma levels of HDL cholesterol.* Science, 2004. 305(5685): p. 869-72.

651. Frayling, I.M., et al., *The APC variants I1307K and E1317Q are associated with colorectal tumors, but not always with a family history.* Proceedings of the National Academy of Sciences of the United States of America, 1998. 95(18): p. 10722-7.

652. Gorlov, I.P., et al., *Shifting paradigm of association studies: value of rare single-nucleotide polymorphisms.* American journal of human genetics, 2008. 82(1): p. 100-12.

653. Bobadilla, J.L., et al., *Cystic fibrosis: a worldwide analysis of CFTR mutations--correlation with incidence data and application to screening.* Human mutation, 2002. 19(6): p. 575-606.

654. Schork, N.J., J. Wessel, and N. Malo, *DNA sequence-based phenotypic association analysis.* Advances in Genetics, 2008. 60: p. 195-217.

655. Wagner, M.J., *Rare-variant genome-wide association studies: a new frontier in genetic analysis of complex traits.* Pharmacogenomics, 2013. 14(4): p. 413-24.

656. Cortes, A. and M.A. Brown, *Promise and pitfalls of the Immunochip.* Arthritis Res Ther, 2011. 13(1): p. 101.

657. Talmud, P.J., et al., *Gene-centric association signals for lipids and apolipoproteins identified via the HumanCVD BeadChip.* American journal of human genetics, 2009. 85(5): p. 628-42.

658. Venter, J.C., et al., *The sequence of the human genome.* Science, 2001. 291(5507): p. 1304-51.

659. Majewski, J., et al., *What can exome sequencing do for you?* Journal of medical genetics, 2011. 48(9): p. 580-9.

660. Lehne, B., C.M. Lewis, and T. Schlitt, *Exome localization of complex disease association signals.* BMC genomics, 2011. 12: p. 92.

661. Duggal, P., G. Ibay, and A.P. Klein, *Current gene discovery strategies for ocular conditions.* Investigative ophthalmology & visual science, 2011. 52(10): p. 7761-70.

662. Liu, D.J. and S.M. Leal, *Replication strategies for rare variant complex trait association studies via next-generation sequencing.* American journal of human genetics, 2010. 87(6): p. 790-801.

663. Do, R., S. Kathiresan, and G.R. Abecasis, *Exome sequencing and complex disease: practical aspects of rare variant association studies.* Human molecular genetics, 2012. 21(R1): p. R1-9.

664. Feng, B.J., et al., *Design considerations for massively parallel sequencing studies of complex human disease.* PloS one, 2011. 6(8): p. e23221.

665. Mowatt, L., G. Shun-Shin, and N. Price, *Ethnic differences in the demand incidence of retinal detachments in two districts in the West Midlands.* Eye, 2003. 17(1): p. 63-70.

666. Sebag, J., *Ageing of the vitreous.* Eye, 1987. 1 (Pt 2): p. 254-62.

667. Pastor, J.C., *Proliferative vitreoretinopathy: an overview.* Survey of ophthalmology, 1998. 43(1): p. 3-18.

668. Satagopan, J.M. and R.C. Elston, *Optimal two-stage genotyping in population-based association studies.* Genet Epidemiol., 2003. 25(2): p. 149-157.

669. Mitry, D., et al., *Rhegmatogenous retinal detachment in Scotland: research design and methodology.* BMC ophthalmology, 2009. 9: p. 2.

670. Tenesa, A., et al., *Genome-wide association scan identifies a colorectal cancer susceptibility locus on 11q23 and replicates risk loci at 8q24 and 18q21.* Nature genetics, 2008. 40(5): p. 631-637.

671. Purcell, S., et al., *PLINK: a tool set for whole-genome association and population-based linkage analyses.* American journal of human genetics, 2007. 81(3): p. 559-75.

672. Wang, K., M. Li, and M. Bucan, *Pathway-based approaches for analysis of genomewide association studies.* American journal of human genetics, 2007. 81(6): p. 1278-83.

673. Franke, L., et al., *Reconstruction of a functional human gene network, with an application for prioritizing positional candidate genes.* American journal of human genetics, 2006. 78(6): p. 1011-25.

674. Thornblad, T.A., et al., *Prioritization of positional candidate genes using multiple web-based software tools.* Twin research and human genetics : the official journal of the International Society for Twin Studies, 2007. 10(6): p. 861-70.

675. Raychaudhuri, S., et al., *Identifying relationships among genomic disease regions: predicting genes at pathogenic SNP associations and rare deletions.* PLoS genetics, 2009. 5(6): p. e1000534.

676. Janse, M., et al., *Three ulcerative colitis susceptibility loci are associated with primary sclerosing cholangitis and indicate a role for IL2, REL, and CARD9.* Hepatology, 2011. 53(6): p. 1977-85.

677. Nalls, M.A., et al., *Multiple loci are associated with white blood cell phenotypes.* PLoS genetics, 2011. 7(6): p. e1002113.

678. Rye, M.S., et al., *Genome-wide association study to identify the genetic determinants of otitis media susceptibility in childhood.* PloS one, 2012. 7(10): p. e48215.

679. Jylhava, J., et al., *A genome-wide association study identifies UGT1A1 as a regulator of serum cell-free DNA in young adults: The Cardiovascular Risk in Young Finns Study.* PloS one, 2012. 7(4): p. e35426.

680. Ngwa, J.S., et al., *Pathway analysis following association study.* BMC proceedings, 2011. 5 Suppl 9: p. S18.

681. Hong, E.P. and J.W. Park, *Sample size and statistical power calculation in genetic association studies.* Genomics & informatics, 2012. 10(2): p. 117-22.

682. Iles, M.M., *What can genome-wide association studies tell us about the genetics of common disease?* PLoS.Genet, 2008. 4(2): p. e33.

683. Kim, D.S., et al., *Novel common and rare genetic determinants of paraoxonase activity: FTO, SERPINA12, and ITGAL.* Journal of Lipid Research, 2013. 54(2): p. 552-60.

684. Cox, A.J., et al., *Association of SNPs in the UGT1A gene cluster with total bilirubin and mortality in the Diabetes Heart Study.* Atherosclerosis, 2013.

685. Haimann, M.H., T.C. Burton, and C.K. Brown, *Epidemiology of retinal detachment.* Archives of ophthalmology, 1982. 100(2): p. 289-92.

686. Ivanisevic, M., M. Erceg, and D. Eterovic, *Rhegmatogenous retinal detachment and seasonal variations.* Acta medica Croatica : casopis Hravatske akademije medicinskih znanosti, 2002. 56(2): p. 49-51.

687. Mitry, D., et al., *The epidemiology and socioeconomic associations of retinal detachment in Scotland: a two-year prospective population-based study.* Investigative ophthalmology & visual science, 2010. 51(10): p. 4963-8.

688. Rowe, J.A., et al., *Retinal detachment in Olmsted County, Minnesota, 1976 through 1995.* Ophthalmology, 1999. 106(1): p. 154-9.

689. Hayreh, S.S. and J.B. Jonas, *Posterior vitreous detachment: clinical correlations.* Ophthalmologica. Journal international d'ophtalmologie. International journal of ophthalmology. Zeitschrift fur Augenheilkunde, 2004. 218(5): p. 333-43.

690. Weber-Krause, B. and C. Eckardt, *[Incidence of posterior vitreous detachment in the elderly].* Der Ophthalmologe : Zeitschrift der Deutschen Ophthalmologischen Gesellschaft, 1997. 94(9): p. 619-23.

691. **Shao, L., et al., *Prevalence and associations of incomplete posterior vitreous detachment in adult Chinese: the Beijing Eye Study.* PloS one, 2013. 8(3): p. e58498.**

692. **STATISTICS, O.F.N. 19 October 2011 31st May 2013]; Available from: http://www.ons.gov.uk/ons/dcp171778_238743.pdf.**

693. **Li, X., *Incidence and epidemiological characteristics of rhegmatogenous retinal detachment in Beijing, China.* Ophthalmology, 2003. 110(12): p. 2413-7.**

694. **Polkinghorne, P.J. and J.P. Craig, *Northern New Zealand Rhegmatogenous Retinal Detachment Study: epidemiology and risk factors.* Clinical & experimental ophthalmology, 2004. 32(2): p. 159-63.**

695. **Rosman, M., et al., *Retinal detachment in Chinese, Malay and Indian residents in Singapore: a comparative study on risk factors, clinical presentation and surgical outcomes.* International Ophthalmology, 2001. 24(2): p. 101-6.**

696. **Azad, R.V., H.K. Tewari, and P.K. Khosla, *Natural history of retinal detachment on the basis of the study of the fellow eye.* Indian Journal of Ophthalmology, 1983. 31(3): p. 170-3.**

697. **Algvere, P.V., P. Jahnberg, and O. Textorius, *The Swedish Retinal Detachment Register. I. A database for epidemiological and clinical studies.* Graefe's archive for clinical and experimental ophthalmology = Albrecht von Graefes Archiv fur klinische und experimentelle Ophthalmologie, 1999. 237(2): p. 137-44.**

698. **Minihan, M., V. Tanner, and T.H. Williamson, *Primary rhegmatogenous retinal detachment: 20 years of change.* Br J Ophthalmol, 2001. 85(5): p. 546-8.**

699. **Ducournau, D.H. and J.F. Le Rouic, *Is pseudophakic retinal detachment a thing of the past in the phacoemulsification era?* Ophthalmology, 2004. 111(6): p. 1069-70.**

700. **Boberg-Ans, G., J. Villumsen, and V. Henning, *Retinal detachment after phacoemulsification cataract extraction.* Journal of cataract and refractive surgery, 2003. 29(7): p. 1333-8.**

701. Das, B.N., et al., *The prevalence of age related cataract in the Asian community in Leicester: a community based study.* Eye, 1990. 4 (Pt 5): p. 723-6.

702. Tornquist, R., P. Tornquist, and S. Stenkula, *Retinal detachment. A study of a population-based patient material in Sweden 1971-1981. II. Pre-operative findings.* Acta ophthalmologica, 1987. 65(2): p. 223-30.

703. Guo, Y., et al., *Outdoor activity and myopia among primary students in rural and urban regions of Beijing.* Ophthalmology, 2013. 120(2): p. 277-83.

704. Foster, P.J., et al., *Refractive error, axial length and anterior chamber depth of the eye in British adults: the EPIC-Norfolk Eye Study.* Br J Ophthalmol, 2010. 94(7): p. 827-30.

705. Lahiri, S. and A.H. Futerman, *The metabolism and function of sphingolipids and glycosphingolipids.* Cellular and molecular life sciences : CMLS, 2007. 64(17): p. 2270-84.

706. Hannun, Y.A. and L.M. Obeid, *The Ceramide-centric universe of lipid-mediated cell regulation: stress encounters of the lipid kind.* The Journal of biological chemistry, 2002. 277(29): p. 25847-50.

707. Laviad, E.L., et al., *Characterization of ceramide synthase 2: tissue distribution, substrate specificity, and inhibition by sphingosine 1-phosphate.* The Journal of biological chemistry, 2008. 283(9): p. 5677-84.

708. Tomita, H., T. Abe, and M. Tamai, *Ceramide-induced cell death in cultured rat retinal pigment epithelial cells.* The Tohoku journal of experimental medicine, 2000. 190(3): p. 223-9.

709. Kannan, R., et al., *Ceramide-induced apoptosis: role of catalase and hepatocyte growth factor.* Free Radical Biology and Medicine, 2004. 37(2): p. 166-75.

710. German, O.L., et al., *Ceramide is a mediator of apoptosis in retina photoreceptors.* Investigative ophthalmology & visual science, 2006. 47(4): p. 1658-68.

711. Kim, J., M. Swee, and W.C. Parks, *Cytosolic SYT/SS18 isoforms are actin-associated proteins that function in matrix-specific adhesion.* PloS one, 2009. 4(7): p. e6455.

712. Eid, J.E., et al., *p300 interacts with the nuclear proto-oncoprotein SYT as part of the active control of cell adhesion.* Cell, 2000. 102(6): p. 839-48.

713. Zhao, Y., et al., *Deletion of core fucosylation on alpha3beta1 integrin down-regulates its functions.* The Journal of biological chemistry, 2006. 281(50): p. 38343-50.

714. Hu, P., et al., *E-cadherin core fucosylation regulates nuclear beta-catenin accumulation in lung cancer cells.* Glycoconjugate Journal, 2008. 25(9): p. 843-50.

715. Gelb, B.D., *Marfan's syndrome and related disorders--more tightly connected than we thought.* N Engl J Med, 2006. 355(8): p. 841-4.

716. Matt, P., et al., *Circulating transforming growth factor-beta in Marfan syndrome.* Circulation, 2009. 120(6): p. 526-32.

717. Habashi, J.P., et al., *Losartan, an AT1 antagonist, prevents aortic aneurysm in a mouse model of Marfan syndrome.* Science, 2006. 312(5770): p. 117-21.

718. Saito, M., et al., *ADAMTSL6beta protein rescues fibrillin-1 microfibril disorder in a Marfan syndrome mouse model through the promotion of fibrillin-1 assembly.* The Journal of biological chemistry, 2011. 286(44): p. 38602-13.

719. Juric, D., et al., *Differential gene expression patterns and interaction networks in BCR-ABL-positive and -negative adult acute lymphoblastic leukemias.* Journal of clinical oncology : official journal of the American Society of Clinical Oncology, 2007. 25(11): p. 1341-9.

720. Bein, K. and M. Simons, *Thrombospondin type 1 repeats interact with matrix metalloproteinase 2. Regulation of metalloproteinase activity.* The Journal of biological chemistry, 2000. 275(41): p. 32167-73.

721. De La Paz, M.A., et al., *Matrix metalloproteinases and their inhibitors in human vitreous.* Investigative ophthalmology & visual science, 1998. 39(7): p. 1256-60.

722. Symeonidis, C., et al., *Correlation of the extent and duration of rhegmatogenous retinal detachment with the expression of matrix metalloproteinases in the vitreous.* Retina, 2007. 27(9): p. 1279-85.

723. Wride, M.A., J. Geatrell, and J.A. Guggenheim, *Proteases in eye development and disease.* Birth defects research. Part C, Embryo today : reviews, 2006. 78(1): p. 90-105.

724. Stupka, N., et al., *Versican processing by a disintegrin-like and metalloproteinase domain with thrombospondin-1 repeats proteinases-5 and -15 facilitates myoblast fusion.* The Journal of biological chemistry, 2013. 288(3): p. 1907-17.

725. Mayer-Jochimsen, M., S. Fast, and N.L. Tintle, *Assessing the impact of differential genotyping errors on rare variant tests of association.* PloS one, 2013. 8(3): p. e56626.

726. Goldstein, J.I., et al., *zCall: a rare variant caller for array-based genotyping: genetics and population analysis.* Bioinformatics, 2012. 28(19): p. 2543-5.

727. International HapMap, C., *A haplotype map of the human genome.* Nature, 2005. 437(7063): p. 1299-1320.

728. Silverberg, M.S., et al., *Ulcerative colitis-risk loci on chromosomes 1p36 and 12q15 found by genome-wide association study.* Nature genetics, 2009. 41(2): p. 216-20.

729. Bansal, V., et al., *Statistical analysis strategies for association studies involving rare variants.* Nature reviews. Genetics, 2010. 11(11): p. 773-85.

730. Morgenthaler, S. and W.G. Thilly, *A strategy to discover genes that carry multi-allelic or mono-allelic risk for common diseases: a cohort allelic sums test (CAST).* Mutation Research, 2007. 615(1-2): p. 28-56.

731. Li, B. and S.M. Leal, *Methods for detecting associations with rare variants for common diseases: application to analysis of sequence data.* American journal of human genetics, 2008. 83(3): p. 311-21.

732. Price, A.L., et al., *Pooled association tests for rare variants in exon-resequencing studies.* American journal of human genetics, 2010. 86(6): p. 832-8.

733. Han, F. and W. Pan, *A data-adaptive sum test for disease association with multiple common or rare variants.* Human Heredity, 2010. 70(1): p. 42-54.

734. Lin, D.Y. and Z.Z. Tang, *A general framework for detecting disease associations with rare variants in sequencing studies.* American journal of human genetics, 2011. 89(3): p. 354-67.

735. Wu, M.C., et al., *Rare-variant association testing for sequencing data with the sequence kernel association test.* American journal of human genetics, 2011. 89(1): p. 82-93.

736. Adams, J.C. and R.P. Tucker, *The thrombospondin type 1 repeat (TSR) superfamily: diverse proteins with related roles in neuronal development.* Developmental dynamics : an official publication of the American Association of Anatomists, 2000. 218(2): p. 280-99.

737. Tan, K., et al., *Crystal structure of the TSP-1 type 1 repeats: a novel layered fold and its biological implication.* The Journal of cell biology, 2002. 159(2): p. 373-82.

738. Iruela-Arispe, M.L., et al., *Inhibition of angiogenesis by thrombospondin-1 is mediated by 2 independent regions within the type 1 repeats.* Circulation, 1999. 100(13): p. 1423-31.

739. Tang, B.L., *ADAMTS: a novel family of extracellular matrix proteases.* The international journal of biochemistry & cell biology, 2001. 33(1): p. 33-44.

740. Le Goff, C., et al., *ADAMTSL2 mutations in geleophysic dysplasia demonstrate a role for ADAMTS-like proteins in TGF-beta bioavailability regulation.* Nature genetics, 2008. 40(9): p. 1119-23.

741. Manabe, R., et al., *Transcriptome-based systematic identification of extracellular matrix proteins.* Proceedings of the National Academy of Sciences of the United States of America, 2008. 105(35): p. 12849-54.

742. Wlodawer, A., et al., *Protein crystallography for non-crystallographers, or how to get the best (but not more) from published macromolecular structures.* The FEBS journal, 2008. 275(1): p. 1-21.

743. Gerhardt, S., et al., *Crystal structures of human ADAMTS-1 reveal a conserved catalytic domain and a disintegrin-like domain with a fold homologous to cysteine-rich domains.* Journal of molecular biology, 2007. 373(4): p. 891-902.

744. Mosyak, L., et al., *Crystal structures of the two major aggrecan degrading enzymes, ADAMTS4 and ADAMTS5.* Protein science : a publication of the Protein Society, 2008. 17(1): p. 16-21.

745. **Akiyama, M., et al., *Crystal structures of the noncatalytic domains of ADAMTS13 reveal multiple discontinuous exosites for von Willebrand factor.* Proceedings of the National Academy of Sciences of the United States of America, 2009. 106(46): p. 19274-9.**

746. **Berman, H.M., et al., *The Protein Data Bank.* Acta crystallographica. Section D, Biological crystallography, 2002. 58(Pt 6 No 1): p. 899-907.**

747. **Marti-Renom, M.A., et al., *Comparative protein structure modeling of genes and genomes.* Annual Review of Biophysics and Biomolecular Structure, 2000. 29: p. 291-325.**

748. **Rose, P.W., et al., *The RCSB Protein Data Bank: new resources for research and education.* Nucleic acids research, 2013. 41(Database issue): p. D475-82.**

749. **Lesk, A.M. and C. Chothia, *How different amino acid sequences determine similar protein structures: the structure and evolutionary dynamics of the globins.* Journal of molecular biology, 1980. 136(3): p. 225-70.**

750. **Altschul, S.F., et al., *Gapped BLAST and PSI-BLAST: a new generation of protein database search programs.* Nucleic acids research, 1997. 25(17): p. 3389-402.**

751. **Kosinski, J., et al., *A "FRankenstein's monster" approach to comparative modeling: merging the finest fragments of Fold-Recognition models and iterative model refinement aided by 3D structure evaluation.* Proteins, 2003. 53 Suppl 6: p. 369-79.**

752. **Larkin, M.A., et al., *Clustal W and Clustal X version 2.0.* Bioinformatics, 2007. 23(21): p. 2947-8.**

753. **Laskowski R. A., M.M.W., Moss D. S., Thornton J. M, *PROCHECK: a program to check the stereochemical quality of protein structures.* J. Appl. Cryst., 1993. 26: p. 283-291.**

754. **Ramachandran, G.N., C. Ramakrishnan, and V. Sasisekharan, *Stereochemistry of polypeptide chain configurations.* Journal of molecular biology, 1963. 7: p. 95-9.**

755. **Brooks, B.R., et al., *CHARMM: the biomolecular simulation program.* Journal of computational chemistry, 2009. 30(10): p. 1545-614.**

756. **Abramoff, M.D., Magalhaes, P.J., Ram, S.J., *Image Processing with ImageJ.* Biophotonics International, 2004. 11(7): p. 36-42.**

757. Klenotic, P.A., et al., *Expression, purification and structural characterization of functionally replete thrombospondin-1 type 1 repeats in a bacterial expression system.* Protein Expression and Purification, 2011. 80(2): p. 253-9.

758. Gabriel L. A., H.J.G., Traboulsi E. I., Majors A. K., Apte S. S. A., *Characterization, Distribution and Putative Function of ADAMTSL4, an Extracellular Protein Mutated in Recessive Ectopia Lentis*, in *Association for Research in Vision and Ophthalmology*2010. p. E-Abstract 4771.

759. Gry, M., et al., *Correlations between RNA and protein expression profiles in 23 human cell lines.* BMC genomics, 2009. 10: p. 365.

760. Tsutsui, K., et al., *ADAMTSL-6 is a novel extracellular matrix protein that binds to fibrillin-1 and promotes fibrillin-1 fibril formation.* The Journal of biological chemistry, 2010. 285(7): p. 4870-82.

761. Pena, J.D., P.A. Mello, and M.R. Hernandez, *Synthesis of elastic microfibrillar components fibrillin-1 and fibrillin-2 by human optic nerve head astrocytes in situ and in vitro.* Experimental eye research, 2000. 70(5): p. 589-601.

762. Halfter, W., et al., *Origin and turnover of ECM proteins from the inner limiting membrane and vitreous body.* Eye, 2008. 22(10): p. 1207-13.

763. Cain, S.A., et al., *Proteomic analysis of fibrillin-rich microfibrils.* Proteomics, 2006. 6(1): p. 111-22.

764. Rossi, A., et al., *Human microvascular lymphatic and blood endothelial cells produce fibrillin: deposition patterns and quantitative analysis.* Journal of Anatomy, 2010. 217(6): p. 705-14.

765. Fujiwara, T., et al., *Enhanced depth imaging optical coherence tomography of the choroid in highly myopic eyes.* American journal of ophthalmology, 2009. 148(3): p. 445-50.

766. Raymond, S.M. and I.J. Jackson, *The retinal pigmented epithelium is required for development and maintenance of the mouse neural retina.* Current biology : CB, 1995. 5(11): p. 1286-95.

767. Low, S., et al., *Autosomal dominant Best disease with an unusual electrooculographic light rise and risk of angle-closure glaucoma: a clinical and molecular genetic study.* Molecular vision, 2011. 17: p. 2272-82.

768. Sundin, O.H., et al., *Developmental basis of nanophthalmos: MFRP Is required for both prenatal ocular growth and postnatal emmetropization.* Ophthalmic genetics, 2008. 29(1): p. 1-9.

769. Schwenk, J.M., et al., *Comparative protein profiling of serum and plasma using an antibody suspension bead array approach.* Proteomics, 2010. 10(3): p. 532-40.

770. Lesnik Oberstein, S.A., et al., *Peters Plus syndrome is caused by mutations in B3GALTL, a putative glycosyltransferase.* American journal of human genetics, 2006. 79(3): p. 562-6.

771. Sato, T., et al., *Molecular cloning and characterization of a novel human beta1,3-glucosyltransferase, which is localized at the endoplasmic reticulum and glucosylates O-linked fucosylglycan on thrombospondin type 1 repeat domain.* Glycobiology, 2006. 16(12): p. 1194-206.

772. Immonen, I., et al., *Proteinases in subretinal fluid.* Graefe's archive for clinical and experimental ophthalmology = Albrecht von Graefes Archiv fur klinische und experimentelle Ophthalmologie, 1996. 234(2): p. 105-9.

773. Jones, G.C. and G.P. Riley, *ADAMTS proteinases: a multi-domain, multi-functional family with roles in extracellular matrix turnover and arthritis.* Arthritis research & therapy, 2005. 7(4): p. 160-9.

774. Martin, A.C., M.W. MacArthur, and J.M. Thornton, *Assessment of comparative modeling in CASP2.* Proteins, 1997. Suppl 1: p. 14-28.

775. Wu, G., et al., *Convergent evolution of Trichomonas vaginalis lactate dehydrogenase from malate dehydrogenase.* Proceedings of the National Academy of Sciences of the United States of America, 1999. 96(11): p. 6285-90.

776. Xu, L.Z., et al., *Ligand specificity of brain lipid-binding protein.* The Journal of biological chemistry, 1996. 271(40): p. 24711-9.

777. Vakser, I.A., *Evaluation of GRAMM low-resolution docking methodology on the hemagglutinin-antibody complex.* Proteins, 1997. Suppl 1: p. 226-30.

778. Yu, H., et al., *Effects of Lysyl Oxidase Genetic Variants on the Susceptibility to Rhegmatogenous Retinal Detachment and Proliferative Vitreoretinopathy.* Inflammation, 2013.

779. Rojas, J., et al., *A genetic case-control study confirms the implication of SMAD7 and TNF locus in the development of proliferative vitreoretinopathy.* Investigative ophthalmology & visual science, 2013. 54(3): p. 1665-78.

9. CHAPTER 9: APPENDICES

9.1. APPENDIX I: QUESTIONNAIRE TO MEMBERS OF THE MARFAN TRUST (UK)

IF YOU HAVE MARFAN SYNDROME, PLEASE DO COMPLETE THIS FORM WHETHER OR NOT YOU HAVE HAD AN EYE PROBLEM

Retinal detachment is the most serious complication of Marfan Syndrome. However, it is unclear how frequently this condition affects those with this condition. We hope to clarify this and the nature of when it occurs with your help. Please take a few minutes to complete the questionnaire and return it in the enclosed envelope. All information will be confidential.

Name_____ Date of Birth_____

Address_____

Home Tel Number _____ Mobile number_____

1. Do you have Marfan Syndrome (MFS)? YES ☐ NO ☐

2. Have you ever had a retinal detachment?

YES ☐ (go to question 3) NO ☐ (go to question 8)

3. Which eye was affected? Tick all that apply

Right ☐ **Left** ☐ Date of any surgery (s): _____

Type of surgery: "buckle" ☐

"gas" ☐

"oil" ☐

Don't know ☐

Did you have the lens removed at the SAME time? YES ☐ NO ☐

4. Is there anyone in your family who has had a retinal detachment?

YES: ☐ HOW ARE THEY RELATED? _____

DO THEY HAVE MFS? YES: ☐ NO: ☐

NO: ☐

5. In which hospital did you have your eye surgery? (Hospital name and address)

_____

_____

6. What was the name of the consultant in charge of your care?

Operation 1: _____

Operation 2: _____

Operation 3: _____

Don't know ☐

7. Would you give us permission to contact your surgeon to get further information about your surgery?

YES ☐ NO ☐ (go to question 8)

If Yes: Please sign below:

I give my permission for Mr Aman Chandra to contact my consultant ophthalmologist to discuss my medical history.

SIGNED:

FULL NAME:

DATE:

8. Have you had dislocated lenses ("ectopia lentis")?

YES ☐ (go to question 9)

NO ☐ (END OF QUESTIONNAIRE)

9. Which eye was affected?

RIGHT: ☐ **LEFT** ☐

Have you had surgery for this?

YES: ☐ DATE: _____

NO: ☐

Have you had surgery for this?

YES: ☐ DATE: _____

NO: ☐

10. In which hospital did you have any surgery?

_____

11. What was the name of the consultant in charge of your care?

_____

12. Would you give us permission to contact your surgeon to get further information about your surgery?

YES: ☐ NO: ☐

If Yes: Please sign below:

I give my permission for Mr Aman Chandra to contact my consultant ophthalmologist to discuss my medical history.

SIGNED: _____

FULL NAME: _____

DATE: _____

Thank you very much for your help.

If you have any questions about this questionnaire, please contact

Mr Aman Chandra

Vitreoretinal Department

Moorfields Eye Hospital

City Road

London EC1V2PD

PLEASE RETURN IN THE SAE ENCLOSED.

9.2. APPENDIX II: REVISED GHENT CRITERIA (2010) FOR DIAGNOSIS OF MARFAN SYNDROME AND RELATED CONDITIONS

In the absence of family history:
(1) Ao (Z ≥2) AND EL=MFS*
(2) Ao (Z ≥2) AND *FBN1*=MFS
(3) Ao (Z ≥2) AND Syst (≥7pts)=MFS*
(4) EL AND *FBN1* with known Ao=MFS

EL with or without Syst AND with an *FBN1* not known with Ao or no *FBN1*=ELS
Ao (Z < 2) AND Syst (≥5 with at least one skeletal feature) without EL=MASS
MVP AND Ao (Z <2) AND Syst (<5) without EL=MVPS

In the presence of family history:
(5) EL AND FH of MFS (as defined above)=MFS
(6) Syst (≥7 pts) AND FH of MFS (as defined above)=MFS*
(7) Ao (Z≥2 above 20 years old, ≥3 below 20 years) +FH of MFS (as defined above)=MFS*

* Caveat: without discriminating features of SGS, LDS or vEDS (as defined in table 1) AND after *TGFBR1/2*, collagen biochemistry, *COL3A1* testing if indicated. Other conditions/genes will emerge with time.
Ao, aortic diameter at the sinuses of Valsalva above indicated Z-score or aortic root dissection; EL, ectopia lentis; ELS, ectopia lentis syndrome; *FBN1*, fibrillin-1 mutation (as defined in box 3); *FBN1* not known with Ao, *FBN1* mutation that has not previously been associated aortic root aneurysm/dissection; *FBN1* with known Ao, *FBN1* mutation that has been identified in an individual with aortic aneurysm; MASS, myopia, mitral valve prolapse, borderline (Z<2) aortic root dilatation, striae, skeletal findings phenotype; MFS, Marfan syndrome; MVPS, mitral valve prolapse syndrome; Syst, systemic score (see box 2); and Z, Z-score.

- Wrist AND thumb sign — 3 (wrist OR thumb sign — 1)
- Pectus carinatum deformity — 2 (pectus excavatum or chest asymmetry — 1)
- Hindfoot deformity — 2 (plain pes planus — 1)
- Pneumothorax — 2
- Dural ectasia — 2
- Protrusio acetabuli — 2
- Reduced US/LS AND increased arm/height AND no severe scoliosis — 1
- Scoliosis or thoracolumbar kyphosis — 1
- Reduced elbow extension — 1
- Facial features (3/5) — 1 (dolichocephaly, enophthalmos, downslanting palpebral fissures, malar hypoplasia, retrognathia)
- Skin striae — 1
- Myopia > 3 diopters - 1
- Mitral valve prolapse (all types) — 1

Maximum total: 20 points; score ≥7 indicates systemic involvement; US/LS, upper segment/lower segment ratio.

J Med Genet. 2010 Jul;47(7):476-85

9.3. APPENDIX III: BEIGHTON SCORE

The Beighton score is a simple system to quantify joint laxity and hypermobility. It uses a simple 9 point system, where the higher the score the higher the laxity. The threshold for joint laxity in a young adult is ranges from 4-6.

Joint	**Finding**	**Points**
left little (fifth) finger	passive dorsiflexion beyond 90°	1
	passive dorsiflexion <= 90°	0
right little (fifth) finger	passive dorsiflexion beyond 90°	1
	passive dorsiflexion <= 90°	0
left thumb	passive dorsiflexion to the flexor aspect of the forearm	1
	cannot passively dorsiflex thumb to flexor aspect of the forearm	0
right thumb	passive dorsiflexion to the flexor aspect of the forearm	1
	cannot passively dorsiflex thumb to flexor aspect of the forearm	0
left elbow	hyperextends beyond 10°	1
	extends <= 10	0
right elbow	hyperextends beyond 10°	1
	extends <= 10	0
left knee	hyperextends beyond 10°	1
	extends <= 10	0
right knee	hyperextends beyond 10°	1
	extends <= 10	0
forward flexion of trunk with knees full extended	palms and hands can rest flat on the floor	1
	palms and hands cannot rest flat on the floor	

9.4. APPENDIX IV: PRIMERS, AMPLIMER SIZE AND ANNEALING TEMPERATURES FOR *ADAMTSL4*

Number of Exons	Primer Sequence	Given Name	PCR Size in bp	Tm (^{0}C)
Ex1	GAGGTTGCCTGGAGAGAGC	ADAMTSL4 Ex1F	534	57
Ex2	CACCCCAACAGGTGTCTTTC	ADAMTSL4 Ex2R		
Ex3	CCAGATGCCTGCGTAGTTTT	ADAMTSL4 Ex3F	433	57
Ex4	GGAGATGAAAGGGTGGCA	ADAMTSL4 Ex4R		
Ex5	TTGGTCTACATGGACACTCTGG	ADAMTSL4 Ex5F	495	57
	CTCCCCTTTCCTTCATGCTA	ADAMTSL4 Ex5R		
Ex6	TCAGAGGGCTTGTCTTTGGT	ADAMTSL4 Ex6(A)F	574	57
	ACCGAAGGAAAAGGATCAGG	ADAMTSL4 Ex6(A)R		
	CTACGGCATCACCCCAGA	ADAMTSL4 Ex6(B)F	515	57
	TGCCCTGAGGTGGTCAGAT	ADAMTSL4 Ex6(B)R		
Ex7	TTGGCATCTGACCACCTCA	ADAMTSL4 Ex7AF	626	57
	ATGAAGCGGATGGTAACCTG	ADAMTSL4 Ex7R		
Ex8	GAATGATGCACCCACCTC	ADAMTSL4 Ex8F	415	57
	GTATGCATATGGGGGCATGT	ADAMTSL4 Ex8R		
Ex9	GGCACAAAAAGCAGGGTAGT	ADAMTSL4 Ex9F	451	57
	CCCTCTCAGCTTCCTCACTC	ADAMTSL4 Ex9R		
Ex10	CTCGTGGAAGGAGTGAGGAA	ADAMTSL4 Ex10F	484	57
	TGGGTTTTCCTCCTGAAAGA	ADAMTSL4 Ex10R		
Ex11	CTGTGGTTGTCAAGATGGGA	ADAMTSL4 Ex11F	460	57
	ATGCAGAGTGTCCCACTCGT	ADAMTSL4 Ex11R		
Ex12	TTCACCTCCTCCAATCCTTG	ADAMTSL4 Ex12F	468	57
	TAGAGCCCAAGCTCAGTGGT	ADAMTSL4 Ex12R		
Ex13	GAGACATCACAGTGCGTTCC	ADAMTSL4 Ex13F	442	57
	TTTCTTGCTGCCTACCGAAT	ADAMTSL4 Ex13R		
Ex14	CAGCCCCACACATCTCATC	ADAMTSL4 Ex14F	319	57

	GTTGTTCACCTGTGCCCAT	ADAMTSL4 Ex14R		
Ex15	CCACGAAGCCATGTGACTG	ADAMTSL4 Ex15F	462	57
	GCCCCTCATGGAAGTTGTT	ADAMTSL4 Ex15R		
Ex16	AAGTGAGAACAACTTCCATGAGG	ADAMTSL4 Ex16F	568	57
	CGTCCCCAGTTTGGATACAC	ADAMTSL4 Ex16R		
Ex17	CACTTGGGGTGCTCTCTGTC	ADAMTSL4 Ex17F	355	57
	GCTTGGCTGGGCTTATTCT	ADAMTSL4 Ex17R		
Ex18	CCAAGCGTTACCACTGTCCT	ADAMTSL4 Ex18F	408	57
	TCCCACTGGTCCTTTCTCAT	ADAMTSL4 Ex18R		
Ex19	CTCTCCCCAATCCCCAATAC	ADAMTSL4 Ex19F	509	57
	AGTCCCAAAAGCACACCTGA	ADAMTSL4 Ex19R		

9.5. APPENDIX V: PCR MIX FOR *ADAMTSL4* AMPLIFICATION

Constituent	Volume	Concentration
PCR buffer	2µl	10x
MgCl2	1.2µl	25mM
dNTP	2µl	2mM
Taq polymerase	0.1µl	5U/µl
H2O	11.3µl	
Forward Primer	0.4µl	10mM
Reverse Primer	0.4µl	10mM
DMSO	1.6µl	8%
DNA	1µl	50ng/µl

$MgCl_2$: Magnesium Chloride

dNTP: Deoxyribonucleotide triphosphate

H20: Water

DMSO: Dimethyl sulfoxide

9.6. APPENDIX VI: PRIMERS FOR *FBN1* PCR AND SEQUENCING

1-FN	GCAAGAGGCGGCGGGAG
1-RP	GAAACTTGGGAGACCCACA
2-FN	TCTGCCAGGATTCATCTTGC
2-RN	CAACACAACAAAAGAAGGAC
3-FN	TCGTGTTCCAAATCCATGTG
3-RN	TGGGTATAACCACATAAAATAAT
4-FN	AACTCCTGTGAGCTGTTGC
4-RN	GCTGTGTCCCAGGTAATCG
5-FP	TTTCAGGTAAAGCGTCTCAG
5-RP	CCGGGTACCAGCATGTCTT
6-FN	TCTGCATGATGGTTCCTGC
6-RN	CCAGAGCAAATAAGATTAATCC
7-FP	TTCTGCAATGAATTTCATATGAG
7-RP	CTACACCCCCCAACTGCAA
8-FN	ACTGACGAATGGTTTTATATTG
8-RN	TACACAAACCATGCATGCTG
9-FN	GTTACAAGTATTATCTCAGCG
9-RN	GCTGGGATGGGATATTCTG
10-FN	CAGCTGTTGTGTTTTGTTTTG
10-RN	ATGTTAACTTGAACAATGCAAG
11-FN	ACTGATGAAAGATACCATAGTT
11-RN	AGGAACAGAATTACAACAGAC
12-FN	AGAATTATGAGGTATTGCTATG
12-RN	CAGTTAGCATATATGTCCCAC
13-FP	CTCCCCCAAATAAAGCTATTTC
13-RP	TTGAAACTGCAATGGAAGGAG
14-FN	TCAGGTCATAAGAAAATGTATG
14-RN	GGAGGAGAAAAGGCACGTG

15-FN	TGTCACTTCATTTTTAATAAGTG
15-RN	GTGACAGAGGCTGAACCTC
16-FN	CTCATCTGTTTGAAGTGACAG
16-RN	GGTGGCAGAAGGCTGGC
17-FN	GATCTACCTGTTCTGCAAAC
17-RN	GTAAATTTTGAAAGGAATCCTTA
18-FP	TAGCTCCTAAGGTCATTACATT
18-RP	ATTATGCAGGCAATGTTTCAG
19-FN	AAAGTTTGGGCCCTTTTTAAG
19-RN	ATAGCAAAGTACACAGTATAAG
20-FN	CCCAGACTAGATTTTAGCAG
20-RN	TTAAGTATAACAACATTGATAAAC
21-FN	GTGTATGTTTGAATTTTTATATAG
21-RN	CTCATGTGAGCCTAGATAAATG
22-FN	CTACTTCATGCTCCAGGTC
22-RN	CTGTTCCGTTTTGTAGTTCTC
23-FN	GTTTTATGAACTTACCAGGTTC
23-RN	ACCGAAGCTAAGTGCTCAG
24-FN	CAGCAAATTATTATGTGTGCAG
24-RN	ATCAAGTAGAGTGCTGAGATC
25-FN	CAAGAACTTCCAACCTTCATG
25-RN	TTAAAGGACGTCCCCTCTC
26-FN	AATTAAGGCTGTCCTGAGAC
26-RN	CATGGAATCCTTCTCTTTCTG
27-FP	GCCCCCACCTTTAACATGG
27-RN	GAAAGTCTTTGCTCCTTAC
28-FP	GCCAAAGTTGGAAGCTTATGT
28-RP	ATAACATAACATAACATAAAATAAAG
29-FN	CAGACATCCAAACCATATCAG
29-RN	GAACCTACTGAGAGATTCAAC

30-FN	AATAGTCTTATGCTAGTAGGC
30-RN	ACAGTGCTTATGACTAACAAG
31-FN	GTACTCAATGATATCAAATAGC
31-RN	ACCAATCTCTTAACTACTTAATA
32-FN	CCAAAAGACATTTGTGCTGAG
32-RN	GTGTAATCTATGCAGTCCTTG
33-FN	GGTTTTAAATACCACCCTTTC
33-RN	CTGGCTTCTCTGACTAGTG
34-FN	CGAGGAAGAGTAACGTGTG
34-RN	TCAAGCCCAGCAAGGCTC
35-FP	GTTAAGTTTTTGCTTTTTCTCC
35-RP	GACACCAGGGAGCTGATTTT
36-FN	GAGATAACTCCACTACTCAC
36-RN	AATACACAGTATGCTTGCTTC
37-FN	GTAGAAAGATTCTGCCTGATG
37-RN	GAACTGGCTGGAGTTGAAAT
38-FN	AAACTTTAGATTCAAAACAACTC
38-RN	TCAAGTTGTGTGTGCTTTAAG
39-FN	ATTTACAATGCTAAAGGAATGC
39-RP	TTCTTGATATCTGCAAGACCTT
40-FN	AAATGTGAAGTTTTCATATTCAC
40-RN	CATGCATTACTGAGAAAAGCT
41-FN	GCTTGTTGAGTATCCACTTAG
41-RN	GCTTCCTTCGCTAAGACTG
42-FP	TCCGGTCCCACCTTTGTTTA
42-RP	AAACCAGAAAGTTCTGACAATG
43-FP	TGTCACTCATGAATGACTACT
43-RN	CTCTTTTCTGGATATGATAAAG
44-FN	CTGTTCTCCTTCAAATTCAGT
44-RN	GTAGGCATGTCCAGCCTG

45-FN	GAGCTAGGATTACTCCTGAG
45-RP	TGAAGCTTTCAACAGCATATG
46-FN	AAGTTCTCAGCCTATGGATG
46-RN	TGGTTCACTAGAGATGATGC
47-FN	GACATCTTTGGAATATATTAAAG
47-RP	CCAGGTCTTTCTAAGTCCTGT
48-FP	AACCTCTTCCTTATTTTTCCC
48-RP	CCTCATTTGCTACAACTGATA
49-FN	TGATGTCTCCATCGTGTTTG
49-RP	GACCACCACAAATAAACATGC
50-FP	GGACTCAGTAGGAAAGCAAC
50-RP	CCAGTCTGCACCCTGCAT
51-FP	AGCTTGTAATGAATTGCTATTG
51-RP	GAAGCAGATTGAGAATACTGA
52-FP	GATTAAACACTGAAATGATCATAA
52-RP	AATTTGTAAAGTTCCTATGGAAG
53-FN	CTCAATTCATCATGTTTTGGAC
53-RN	CCATCAGGCCTAGATGATC
54-FN	CTTTGTTGCTGTCCATGATC
54-RN	CTCACAGATAAAGCTTCCTG
55-FN	GCAGATATATGCATTTTCTTTG
55-RN	GTCCACTGTCACTTCTGATG
56-FN	TGGTCAGATGACTCTTCTTG
56-RN	GTGTGGAGGCTGAGGTTAG
57-FN	ATTTCCTGACATCCCCTTTG
57-RN	CAAATAAATAGATTCCCTGTAAG
58-FII	GTTGTCAATTTTATGATATATTTCT
58-RII	ATTTCCACTTGAGGATAAGCC
59-FN	GCGTGTACACATCATTTTTAG
59-RN	ATGTGTCAGGAGCTAGGTG

60-FN	ATCCTGTTTTGTTGGCTGAC
60-RN	GAATCGCTACAATCCATGTAG
61-FN	GTATGTGTGAGCACACCTG
61-RN	CTCCACAAGGATTCACCAG
62-FN	AGAGATGTTGAGTTGGCATC
62-RN	TAGGACCTGATAGCCATGC
63-FN	CAAGTGGCCAGATCCAATG
63-RN	GGTTCTCCTCTGCTAGGAC
64-FP	TACCTTGTCTTCCCATTCTAA
64-RH	AGGAGACATCAGGAGAAACTA
65a-FP	GCTAAGTGGCATATGTACATT
65a-RP	GCTGATCCCTTCCTTTTGG
65b-FP	AGATACTTGATCGAATCTGGA
65b-RP	GTTCTACCTATCTATATTTGTTT

9.7. APPENDIX VII. PCR MIX FOR *FBN1*.

dNTP: Deoxyribonucleotide triphosphate, $MgCl_2$: Magnesium Chloride, Taq: Taq Polymerase, F; Forward Primer, R: Reverse Primer, FV: Final Volume

Next three pages.

EXONS	**1**	**4**	**6**	**8**	**9**	**10**	**11**	**12**
	Plat					Plat		
dH_20	**331**	319	319	319	319	319	319	319
10x Buffer	60	60	60	60	60	60	60	60
dNTPs	60	60	60	60	60	60	60	60
$MgCl_2$	**24**	36	36	36	36	36	36	36
Taq	4.8	4.8	4.8	4.8	4.8	4.8	4.8	4.8
F	36	36	36	36	36	36	36	36
R	36	36	36	36	36	36	36	36
DNA	4	4	4	4	4	4	4	4
FV	50	50	50	50	50	50	50	50

EXONS	**13**	**14**	**16**	**17**	**18**	**19**	**22**	**23**
	Plat							
dH_20	319	319	319	319	319	319	319	319
10x Buffer	60	60	60	60	60	60	60	60
dNTPs	60	60	60	60	60	60	60	60
$MgCl_2$	36	36	36	36	36	36	36	36
Taq	4.8	4.8	4.8	4.8	4.8	4.8	4.8	4.8
F	36	36	36	36	36	36	36	36
R	36	36	36	36	36	36	36	36
DNA	4	4	4	4	4	4	4	4
FV	50	50	50	50	50	50	50	50

EXONS	**24**	**25**	**26**	**29**	**30**	**32**	**33**	**34**
			Plat					Plat
dH_20	319	319	319	319	319	319	319	319
10x Buffer	60	60	60	60	60	60	60	60
dNTPs	60	60	60	60	60	60	60	60
$MgCl_2$	36	36	36	36	36	36	36	36
Taq	4.8	4.8	4.8	4.8	4.8	4.8	4.8	4.8
F	36	36	36	36	36	36	36	36
R	36	36	36	36	36	36	36	36
DNA	4	4	4	4	4	4	4	4
FV	50	50	50	50	50	50	50	50

Plate 4

EXONS	36	37	39	40	41	42	44	45
	Plat		Plat	Plat		Plat		
dH_20	319	319	319	319	319	319	319	319
10x Buffer	60	60	60	60	60	60	60	60
dNTPs	60	60	60	60	60	60	60	60
$MgCl_2$	36	36	36	36	36	36	36	36
Taq	4.8	4.8	4.8	4.8	4.8	4.8	4.8	4.8
F	36	36	36	36	36	36	36	36
R	36	36	36	36	36	36	36	36
DNA	4	4	4	4	4	4	4	4
FV	50	50	50	50	50	50	50	50

Plate 5

EXONS	46	48	50	51	53	54	55	56
	Plat		Plat	Plat				
dH_20	319	319	319	319	319	319	319	319
10x Buffer	60	60	60	60	60	60	60	60
dNTPs	60	60	60	60	60	60	60	60
$MgCl_2$	36	36	36	36	36	36	36	36
Taq	4.8	4.8	4.8	4.8	4.8	4.8	4.8	4.8
F	36	36	36	36	36	36	36	36
R	36	36	36	36	36	36	36	36
DNA	4	4	4	4	4	4	4	4
FV	50	50	50	50	50	50	50	50

Plate 6

EXONS	58	59	60	61	62	63	64	65
	Plat		Plat	Plat				Plat
dH_20	319	319	319	319	319	319	319	319
10x Buffer	60	60	60	60	60	60	60	60
dNTPs	60	60	60	60	60	60	60	60
$MgCl_2$	36	36	36	36	36	36	36	36
Taq	4.8	4.8	4.8	4.8	4.8	4.8	4.8	4.8
F	36	36	36	36	36	36	36	36
R	36	36	36	36	36	36	36	36
DNA	4	4	4	4	4	4	4	4
FV	50	50	50	50	50	50	50	50

Plate 7

EXONS	2	3	5	7	15	21	27	35
	Plat	Plat	Plat	Plat		Plat	Plat	Plat
dH_20	319	319	319	319	319	319	319	319
10x Buffer	60	60	60	60	60	60	60	60
dNTPs	60	60	60	60	60	60	60	60
$MgCl_2$	36	36	36	36	36	36	36	36
Taq	4.8	4.8	4.8	4.8	4.8	4.8	4.8	4.8
F	36	36	36	36	36	36	36	36
R	36	36	36	36	36	36	36	36
DNA	4	4	4	4	4	4	4	4
FV	50	50	50	50	50	50	50	50

Plate 8

EXONS	38	43	47	49	57
	Plat	Plat	Plat	Plat	Plat
dH_20	**199**	319	319	319	319
10x Buffer	60	60	60	60	60
dNTPs	60	60	60	60	60
$MgCl_2$	36	36	36	36	36
Taq	4.8	4.8	4.8	4.8	4.8
F	**96**	36	36	36	36
R	**96**	36	36	36	36
DNA	4	4	4	4	4
FV	50	50	50	50	50

Plate 9

EXONS	20	28	31	52
	Plat	Plat	Plat	Plat
dH_20	319	319	319	319
10x Buffer	60	60	60	60
dNTPs	60	60	60	60
$MgCl_2$	36	36	36	36
Taq	4.8	4.8	4.8	4.8
F	36	36	36	36
R	36	36	36	36
DNA	4	4	4	4
FV	50	50	50	50

9.8. APPENDIX VIII: PRIMERS USED TO AMPLIFY AND SEQUENCE *ADAMTS18*

EXON	PRIMERS (F and R)	Amplicon (bp)
1-2	CCCTCCCTCAGAGCTGGA GGGAAGGAAGGGTCAAAGTG	803
3	ATTTGGAATTGTGGGCTCTG GAGTTGGCTGGAAGAGCATT	425
4	TTAGCTCCTGTGCCCACAT AGGGTAGCCCCATTTTGACT	460
5	GGATTGGTGGTGTGTTGGTT ACCTGCTATTCAACCCATGC	355
6	TGATTCCCCCTAAGGTTTTG ATTCTGAACGGCAGACTGAA	455
7	TTCAGCATTCTCATCTCTGTG GGGCTATCCATCATCCATAGAA	256
8	AAATCATCATCATGTATCTGTGTGTG CAACGGTTAGAGGAACACCAA	197
9	AATGGGTTCACAAAGCAGGA GGAGCACAATTCTGTCATCA	203
10	CAGAAGTGTGTTGTCGTAAATGG CTTCTGTTAGGGACACAGACACA	247
11	TTTATTGTATATCACCATTAACAGCA GCATTCACCCTAAGGTCACAA	186
12	CTGTTACTGTGCAGGTGTTGG GCGTGTTACAGGCTGAAGGT	250
13	CACTGTGGCAGTGCTCATCT	360

	GGTCTGGGGAGTGAAAGGTA	
14	TTTTGACAATCCTATCATTTTTCC TCTCTCACACCACTGTTCACG	240
15	GAGGGATTTGAACCCCAAGT AACCACATTTGGCGTGACTC	334
16	CATGTCGGGCCATTTCTAGT GGAGTTCTGGCTCAAATTGC	360
17	TCCTGGGAAAGCTTTAAGTCA AGACGCCTGGAGTGAAAGAA	338
18	CAATGCTGGTAAATCAGAAGC CACAGTGAGCTTTCATCATCTCA	255
19	CATGGCTTCCATAGGTGGTT TAAACTGCCAAGAGCCCAGT	355
20	TTTTTAATGTGGCTACTGAAACC CAGCCTCCCCAGTAGATCAG	341
21	ATTTCATGTGGATGGTGCAA GTTTGCAGAACGCCTCATTT	339
22	GGGAATTCCTTCTGTTTGATG GCTGCACTACTAACAAAGTAGCC	256
23	AGACACCCTAGCCAACATGC CAAAGGCAGCTGGTCTCTCT	190

9.9. APPENDIX IX: PRIMERS USED TO AMPLIFY AND SEQUENCE *PAPILIN*

EXON	Primer Sequence (F and R)	Amplicon (bp)
2	CTGTGGGCCATAGGGAGAGA CTGACATCGCCCCTTTCCTG	261
3	TCCTTGATGGGTAGGGGAGG CCCCTGCTCCTGCTTTAACA	265
4-5	GAGAGTCCCGCAGAAGTTGG ACTGTGGCATCAACGTAGGT	697
6	ACCCATGCTTTCCTGTTGCT AAGCTCATGGCAGCTACCTG	328
7	CCTGATGTGGCCATGATGC GACAGGCAAGGAAGGGACAG	242
8-9	AGGGTTAGGTCCTAGGCAGG ACTTGTCCATCTCCCCAGGA	683
10	GAACGCGCTTGGTGAATGTT TGGGCCTCATCATGGGTAGA	224
11	TGTGAGTGAGGGCAGAAACC CTCGGTTTCCACAGCAGAGA	379
12-13	CTAGCTGTCCGAACTGGCG GGACATGCTTGCTGGGTTTG	650
14-15	CAGTGGGGTAGAAGCCAGTG ATTCCTGAGCTCTGCACACC	785
16-17	ACCATGGGGAGCCTCAGAG GGAAGGTCTTTGGTCCTGGG	762
18	GGATGGAGGGTGCAGCTTTA	609

	TAGCTCCAACTGGCATGCTC	
19	GCTTAGGGTGGTTCTGGTCC TGTCACACACACCTGTCAGG	276
20-21	AGACTCACTGTTGCCCTTGG AGCAGACGTTCCCCTCCTTA	661
22	AGAGGTGCCCATGGGAGTAG CAGGACTGGCCATGACCATG	316
23-24	CTTGTGTTCCCTCCCTGACC GGTGACAGTGACATCCCTGG	519
25	TGTCTCCCAGACCTCCAGAG CAGGGTGAGCCAGGATTCAA	337
26	GGCAGGTGAGAATTTTCAGCA TAACTCCCTTTGCCAGCCAG	340

9.10. APPENDIX X: PRIMERS USED TO AMPLIFY AND SEQUENCE *LTBP2* [203]

EXON	Primer Sequence (F and R)	Amplicon (bp)
1a	GCCGACCACAAAGCTCTTC GAGTGCTTCTCCGGGTCTG	434
1b	TGCAGCCAAGGTGTACAGTC CCCCTCTGTACCCTCCAAAC	342
2	TGCAGCCAAGGTGTACAGTC GCGGAGTGTCTGCTACTGGT	286
3	AGAGTGGCTTCCTGCTTGAG CTTCACCAAACGGTCCAAAG	476
4	GCAGCCAGAGAGCATTTTTC AACTCAGCCCCTCTGTGAGA	403
5	AATGCCCTTGAGATGAATGC CTGGCTCTCTGGCCATCTAC	349
6	GCCTGTTTCTCTGTGGTGGT CAGCTTCCCTATCCCTGTCA	386
7	TGGTGGATACCCTTCAGAGG GAGGAGGAGAAGGGCAGACT	441
8	AATGTGGGGAGTGAGCTCTG AAGGCAGGTCTGGGAAGTCT	351
9	AGGTGGGCTGAGAGGAGTCT TAGTCCCCTGGAATCAGCAG	415
10	CGGGCACTTGGTCATCTCCT GTGATCAGGTCTGGGGAAAA	262
11	GCTCCAAACTTCCCAACTGA	444

	GGTTGGGATAAGCACGTGAG	
12	TCACGTGCTTATCCCAACCT AGGGACCCAGGATTAACACC	447
13	CAGAGGAGCCAAAAGTGACC TCCTTCTCACCCTCCTCTGA	206
14	GTCTGAGCACCAGGGAAGAG GAGGGACCCTGTGTTCTTTG	370
15	CACCCTGCCATAACCTCTGT TGCTTGGACCTTCTGCTTCT	271
16	GGCTGACTTTATGGCTTCCA CAGGCTGGAGTTCTGGTCTC	457
17	ATCCTTTGTCCTTGGCCTCT GAATGTCACTGAGGGGATGG	406
18	AGGGACAAGGATTTGCTGTG ACCTCTTTCCCTTTCCGTGT	287
19	CCCTGGCCTCATAACTGAGA GGATGTGTTGGGTCAGTGTG	350
20	CTGCAGAGTCCCACACAGAA TATTCTGTCCCCTTCCACCA	202
21	TCCCCAAGTTCAGAGTGAGG AGCTTGTGAGCGACTCTTGG	466
22-23	GGAGACTTCCCCCTTGACTC GCTGGCTTCCCATGCTCCTG	475
24	GCCCAGAGGAAGCTACACAG GAGCTAAGGACCAGGCAGTG	273
25	GGAAATCGTCCTGACCTTGA TGAAAAGCAGCCTCTCAACC	492

26	GTGCATGCGTGTGAGAGAGT CAGGACCAGTTGAGGAGGAG	298
27	AAGGCCTAGCCTGCTTCTTT CCTGTAGCTCCTGGTTTTGC	447
28-29	CCTTAGAGGGTCATGAACAGACA CCCACTCAGGTGAAGGAGTT	489
30	CCCTCATACTGCCTCTCACC TCCTGGGGACAATCTCTGAC	356
31-32	TGATAGGCAAACACCCTTCC CCTGCAGGGTATCCCCTTTG	499
33	CAGAGGGTACCAGTCCTTGC CTAGCAGGTGGAGGAGATGG	455
34	AGTCTGGACACAGCCCTCAG TCTTCCAGCCTTCCTGAGTT	279
35	CTTGGGCATGGTATGAGCTT AACCTCTGGCCTGATGTCAC	450

9.11. APPENDIX XI: PRIMERS USED TO AMPLIFY AND SEQUENCE *ADAMTS17*

EXON	Pimers Sequence (F and R)	**Amplicon (bp)**
1	TCCGCAGCGCTAATTACTTT ACCCGATTCCCGTACTCC	353
2	CTGACGCGTCTCCTCTCTCC TGCCTATAGAGGGTACCGAAGG	579
3	CAAATCACAGCAAGGTGGTC TTCTCACTCATGTGGCTTCAGT	359
4	CTGACCACTCTCTCGGGC ACCCAGCGTCTTCCTCACT	383
5	TTTCTGTGTCCCAAGTTCCC AGAGAGTGACGGAGACTGGC	290
6	GCCTCCACCTTAACGTCCTT GTGGCCCAAGGTCTGATTT	362
7	TTGCAGGATGACTACTTGAGG GCTTGTTTGAGGACAGCTCC	237
8	TTGATTGTGCATGACGTTGA CAGATGCAGCAAAGGCATAG	314
9	AAGACTTGATTTACCTTAGCATGG TTCTCCACTTCACACTTGCTG	329
10	GGAGGTGCCCTCTTCTCAGT GTGCTGAGTGTGAATGCCC	361
11	ATTTGAAACAGTGGTTGGGC TGTTTCAGGGGCTCCTAAGT	304
12	TGGCAGCACGGCATTTT CTTCTAATGCTCAGCGGGAG	342
13	CCCTTCCTCTCCTCCCC CTGGGTTGGTTTGGGAAAG	369
14	CTTCCTCAGGGTTTCCCTCT CCTGAGACCTCTGCTCTACCC	315
15	TATGCTGCACCTCATGGAAA TCCACTACCATCTAGCCCTTAAA	331
16	CTGTGGAAGGGAGACCTCTG	361

	GAGGTCCCAGGCAGAAGTAA	
17	AAAGAGCTGGTTACCCCTCA ATGTCTCACACTCTGCGTGC	370
18	GCACCCAAACATGCTTTCAT GCATAGAGCAGTACTGTGGCA	331
19	AGGGCAGCAATTCCAGGAT CAACTTCAAGCTGACCTGGG	415
20	GCACCTGGCACATTGGA GCCTAGTTACGCTGGGACTG	357
21	CCTGGGCATGACACACAGT TGTCAGCCTTATGTGACAAGTGA	565
22	AGTGCAAAGGGTTGACGTGT CCAAGTCCACGCTCATGTT	429

9.12. APPENDIX XII: PRIMERS USED TO AMPLIFY *ADAMTS17* cDNA

Primers	Expected amplicon size (bp)
Ex 1F: CTGCCTCCGCTCGTCCTG Ex3R: AGCTGAATGAGGCCAACCAG	449
Ex2F: GAGCTGTGCTTCTACTCGGG Ex10R: GGTGCTGACTTTTGACTTGAGG	972
Ex10F: AGATGACCTTGAAAACTTCCTCA Ex16R: GTCTTTGAGAGCTGTCCCCC	850
Ex15F: AAGGGCGACTTCAGCCAC Ex20R: GCAGAGCACTGTGACCACTC	698
Ex19F: ATCTGGGAGGCGTCTGAGT Ex22R: GACTGCGTGTCACGAGTTCG	528